THESIS

This is to certify that the

thesis entitled

SOLAR WATER HEATING FOR THE FOOD INDUSTRY
IN THE UNITED STATES

presented by

Petros Z. Mintzias

has been accepted towards fulfillment
of the requirements for

Ph.D. degree in Agr. Engineering

Fred W. Bakker-Arkema

Major professor

Date 11/12/80

O-7639

SOLAR WATER HEATING FOR THE FOOD INDUSTRY IN THE UNITED STATES

by

Petros Z. Mintzias

A DISSERTATION

Submitted to
Michigan State University
in partial fulfillment of the requirements
for the degree of

DOCTOR OF PHILOSOPHY

Agricultural Engineering

1980

ABSTRACT

SOLAR WATER HEATING FOR THE FOOD INDUSTRY IN THE UNITED STATES

by

Petros Z. Mintzias

The engineering and economic potential of solar water heating in the food industry in the United States has been the subject of this study. The energy consumption in selected meat and dairy plants was analyzed and five energy use patterns which take into consideration the variability of the energy usage encountered in food processing plants were obtained.

Based on the energy consumption and distribution at the Michigan State University milk processing plant a pilot plant solar water heater was built to supply approximately fifty percent of the total energy demand in the plant. The daily energy use in the dairy plant was found to be about 2,000,000 KJ.

The experience gained by operating the pilot plant solar water heater was useful in the design and simulation of a wide variety of solar systems for the food industry. The Transient Simulation Program (TRNSYS) and the f-chart program, both developed at the University of Wisconsin, were used. Experimental results from the pilot plant solar water heater were utilized to verify TRNSYS. The agreement between experimental and numerical data was found to be excellent.

Petros Z. Mintzias

The f-chart program was modified in order to be used in the design and evaluation of industrial type solar water heaters. The MAIN program and subroutine CALC of the f-chart were modified to account for the variability of the yearly energy usage in various foods processing plants. Results from f-chart were checked against those obtained by TRNSYS and the agreement was found to be satisfactory.

The daily energy use pattern in a food processing plant and the time at which the plant starts operation during the day does not affect the long-run performance of a solar water heater. Solar collectors exhibit higher efficiencies in food processing plants operating seven days per week than in plants with six or five work day weekly schedules.

The effect of the geographic location on solar system thermal output and life-cycle costing of solar water heating was investigated. A series of sensitivity tests of various economic parameters was performed to demonstrate the significance of each parameter on the economics of solar water heating. Annual fuel price escalation and annual nominal discount rate were identified as the most sensitive parameters for the economic analyses of solar water heaters. A solar water heater with an optimized collector area results in positive savings for most of the locations in the United States. Positive savings will be realized when the alternative is oil and electricity, the solar system costs 150 $\$/m^2$ of collector area, the annual inflation rate is eight percent and price of the conventional fuel escalates at an annual rate of ten percent over the period of the

economic life of the solar system which was assumed to be twenty years.

The amount of the yearly hot water needs in a food processing plant which can be economically supplied by solar is thirty to ninety percent depending on the location under consideration. Solar water heating shows higher potential in the western states of the United States than the eastern and midwestern states.

Dedicated to my wife, Katherine

and to our children --

Zacharias and Elena

ACKNOWLEDGMENTS

The author is grateful to Alvin L. Rippen and Pericles Markakis, Professors of Food Science and Human Nutrition; James Beck, Professor of Mechanical Engineering; and James Steffe, Assistant Professor of Agricultural Engineering, for serving on his Ph.D. committee.

Special appreciation is due to the United States Department of Energy for its financial support of this study.

The encouragement, enthusiastic support and constructive criticism during the course of this study by Dr. Lloyd E. Lerew, colleague, once academic advisor, and friend are gratefully recognized by the author.

The completion of this study has been greatly encouraged by the courteous help and brilliant counsel of Dr. Fred W. Bakker-Arkema, Professor of Agricultural Engineering and academic advisor to the author. It was the special relationship the author developed with Fred W. Bakker-Arkema that made this work possible.

TABLE OF CONTENTS

LIST OF TABLES

LIST OF FIGURES

LIST OF SYMBOLS

A	Area, m^2
B	Control function with value of zero or unity
C_1	Constant in Eq. 4.5.3, 0.595×10^{-14} W-cm^2
C_2	Constant in Eq. 4.5.3, 1.438 cm-°K
C_b	Bond conductance, KJ/h-m-°C
c_p	Specific heat, KJ/Kg-°C
D	Tube diameter, m
$e_{\lambda b}$	Spectral distribution of hemispherical emissive power, KJ/h-m^2-λm
f	Fraction of total heating load supplied by solar energy
F_R	Collector heat removal factor defined in Eq. 5.20, dimensionless
F'	Collector efficiency factor defined in Eq. 5.17, dimensionless
F'_R	Collector-heat exchanger efficiency factor, dimensionless
G	Flow rate per unit area, Kg/h-m^2
H	Rate of direct or diffuse radiation per unit area, KJ/h-m^2
I	Instantaneous solar radiation incident on the collector surface per unit area, KJ/m^2
k	Thermal conductivity, KJ/h-m-°C
L	Total load, KJ
m	Water mass, Kg
$\dot{m}$	Flow rate, Kg/h
N	Number of glass covers
Q_L	Rate at which energy is delivered to load, KJ/h

Q_u	Rate at which useful energy is collected, KJ/h
R	Factor to convert total radiation to that on the plane of the collector, dimensionless
S	Collector incident radiation over a finite period of time, KJ/m^2
t	time
T_a	Ambient temperature, °C
T_A	Absolute temperature, °K
T_c	Collector temperature, °C
$T_{1,r}$	Temperature of make up water entering the tank, °C
T_m	Water mains temperature, °C
T_s	Storage tank water temperature, °C
$T_{s,n}$	Stratified tank temperature with n-sections, °C
T_w	Water set temperature, °C
TX1	Temperature ratio defined in Eq. 10.3
U_L	Over all loss coefficient, $KJ/h\text{-}m^2\text{-}°C$
U_b	Collector bottom loss coefficient, $KJ/h\text{-}m^2\text{-}°C$
U_{up}	Collector upper loss coefficient, $KJ/h\text{-}m^2\text{-}°C$
V	Wind speed, m/s
X	Dimensionless group defined in Eq. 4.9.5
X'	Dimensionless group defined in Eq. 4.10
Y	Dimensionless group defined in Eq. 4.9.6

Greek

α'_λ	Directional spectral absorbance
β	Cone angle, degrees
ε'_λ	Directional spectral emittance
ε	Absorber plate effective emittance
θ	Circumferential angle, degrees
η	Fin efficiency
λ	Wavelength, time
η_f	Collector efficiency
σ	Stefan-Boltzmann constant, 5.279×10^{-12} W/cm^2-°K
τ	Glass transmittance
ϕ	Dimensionless temperature ratio

Subscripts

a	Ambient
b	Bottom
c	Collector
in	Inlet
L	Load
l	Loss
o	Outlet
s	Storage
u	Useful
up	Upper
w	Wind

CHAPTER 1

INTRODUCTION

For the last ten years the energy problem has absorbed the attention of the public. In the early 1970's economists, legislators and decision makers realized that there are physical and economic limits on the world's supply of oil, the most versatile and widely used energy source. As a result of this awareness, research efforts to substitute fossil fuels by renewable and essentially inexhaustible sources of energy have been considerably increased. Among the new energy technologies investigated, solar energy is widely expected to contribute substantially to the future energy needs (Gustaffero, 1979).

In the mid-1970's the Energy Research Development Administration established a program to demonstrate the potential of solar energy in agricultural and industrial processes. The areas included in the program were (ERDA, 1977):

1. agricultural food processing
2. grain drying
3. crop drying
4. heating of livestock shelters
5. heating and cooling of greenhouses.

A simulation study by Thomas (1977) indicated that a significant solar energy contribution can be made by replacing up to 90 percent of the electric and 20 percent of the fossil fuel energy consumption for most food processing plants over a 20-year payback period. Similar work by Singh et al. (1978) indicated that a solar water heater would be able to supply about 29 to 34 percent of the total processing energy demand in a food processing plant. The Transient Simulation Program (TRNSYS) was used in both studies.

While solar water heaters have been successfully modeled by the above investigators, the numerical results were not verified experimentally. In addition, operational characteristics of solar systems and the effect of the daily energy usage pattern in the processing plant on solar system performance were not considered.

This research investigates the application of solar water heating in food processing plants in the United States. A pilot scale solar water heater has been built for the Michigan State University dairy plant. Experimental results from the pilot scale system are used to verify the results of the TRNSYS and f-chart simulation programs. The performance and thermal output of solar water heaters is investigated under various daily energy use scheduling encountered in food processing plants.

CHAPTER 2

OBJECTIVES

The primary objective of this study is to investigate the potential of solar water heating in the United States food industry from an engineering and economic point of view. The specific objctives are:

1. To compare simulation results obtained by the Transient Simulation Program (TRNSYS) with experimental data from the Michigan State University dairy plant solar water heater and determine the engineering behavior of solar systems for the food processing industry.
2. To identify daily energy use profiles encountered in the food processing industry and to investigate the effect of the energy use pattern on the long- and short-run performance of solar water heaters.
3. To examine the effect of the work schedule and energy demand in food processing plants on the performance of solar hot water systems.
4. To modify the f-chart program in order to investigate the long-run engineering and economic performance of industrial type solar water heaters.

5. To evaluate the economic feasibility of solar retrofit in the food industry.

CHAPTER 3

JUSTIFICATION OF THE STUDY

The objective of thermal food processing is to destroy pathogenic and toxin-forming microorganisms and food enzymes. In addition to microorganism and enzyme destruction, heat is also detrimental to organoliptic and nutritive properties of foods as well. These observations emphasize the principle that no more heat should be applied or required by regulation than the minimum necessary to free foods of mircoorganisms which may deteriorate the foods or endanger the consumer.

In practice very few food processes occur at temperatures above 121°C (250°F). Most food products are thermally processed below 100°C. This is illustrated in Table 3.1 where various food processing temperatures are listed.

In a food processing plant heat is typically generated in a central power station (boiler) at temperatures higher than those required by the processes in the plant. The heat is then distributed as 99°C water or steam at 90 psia (125°-170°C) to the individual processes, most of which operate at lower temperatures. Such heat generation and distribution systems are convenient and assure adequate heat to specific operations.

TABLE 3.1.--Processing temperatures of various food process operations.

Operation	Temperature, °C
Milk pasteurization	
- Batch	63
- HTST	72
Juice pasteurization	77-87
Cheese manufacture	
- Milk pasteurization	28-31
- Curd cooking	38-50
Beer manufacture	
- Mashing	38-77
- Pasteurization	60
Meat processing	
- Scalding	60
- Smoking	125-135
Canning	115-130
Sanitation	
- Hand washing	66
- Equipment cleaning	60-82

From an energy efficiency point of view, the above practice has serious disadvantages. A typical boiler efficiency for many plants is about 75 percent (Casper, 1977). Heat losses to the environment from steam pipes and process equipment are increased significantly with increasing temperatures. Finally, steam can lose as much as 68 percent of its heat because of improper condensation (Singh, 1979).

Nwude et al. (1975) investigated the energy consumption and supply at the Campbell Soup Plant 2. The conclusions of the study could be summarized as follows: (1) 65 percent of the energy needed by the plant is at temperatures below 93°C (200°F) and 20 percent at temperatures between 121°-132°C (250°-270°F); (2) 75 percent of the energy supplied is at a temperature above 121°C; (3) 43 percent of the energy supplied by the boiler (or 52 percent of fuel oil energy) to the processes is wasted in the form of hot water from the processes.

A more detailed study of an Australian Coca-Cola plant showed that over 40 percent of the total heat required was in the form of hot water at 60°-80°C (140°-176°F) (Proctor and Morse, 1977). Percentages of the heat used at different temperatures in the plant are shown in Table 3.2.

TABLE 3.2.--Percentage of process heat required at different temperature ranges in an Australian Coca-Cola plant.

Temperature Range, °C	Percent of Total Heat Consumed
0 - 20	0.5
20 - 40	7
40 - 60	13
60 - 80	43
80 - 100	8
100 - 125	20
125 - 150	8
150	0.5

SOURCE: Proctor and Morse (1977).

A similar work by Singh et al. (1978) in a Wisconsin milk processing plant indicated that more than 75 percent of the processing energy requirements in the plant is at 80°C. Energy requirements in the dairy plant at different temperatures are listed in Table 3.3.

TABLE 3.3.--Total energy requirements in a dairy plant: one week (average).

Load	Energy Requirements, GJ	Percent of Total
Boiler feed make-up (100°C)	2.41	0.33
Pasteurization make-up water (81°C)	546.20	75.35
Case water and rinsing (49°C)	82.50	11.38
Clean-up (71°C)	54.00	7.45
HTST clean-up (79°C)	0.87	0.12
Bottle washer (93°C)	39.90	5.37

SOURCE: Singh et al. (1978).

Meat processing plants utilize large amounts of hot water at temperatures between 60° and 72°C (140°-160°F). To heat and maintain the temperature of the water at 60°C in scald and dehairing tanks in an Indiana Meat plant, a daily amount of energy equal to 50×10^6 KJ is required (Wilson et al., 1978).

Evaluation of various research and demonstration programs has revealed that solar water heating is one of the most promising solar energy technologies (Anonymous, 1978a).

Among the various types of solar collectors, flat plate collectors are the least expensive devices. They also are simple, require little maintenance and can be easily installed into retrofit designs. The efficiency of a flat plate collector below 100°C is about 50 percent. Further, at moderate temperatures (<60°C) flat plate collectors could be as efficient as evacuated tube collectors (Grimmer and Moore, 1977).

Preliminary simulation work by the author has shown that solar systems operating at a temperature range of 60°-80°C and assisted by a conventional water heater can supply a substantial amount of the energy needs in most food processing plants.

For these reasons the author felt that a study of solar water heating will be beneficial to the food industry in overcoming future difficulties related to energy cost and availability.

CHAPTER 4

LITERATURE REVIEW

4.1 Energy as a Global and Multidimensional Problem

Assuming a balance between births and deaths, the United Nations (1979) projects the global population in 2075 to be about 11.5 billion. To maintain such a population at a reasonable standard of living with present practiced technologies, the petroleum-oriented societies must undergo major changes (Ridker and Cecelsky, 1979). Changes such as slow-down in population and economic growths are not sufficient to maintain long-run sustenance of life on earth (Ridker and Watson, 1980).

The side effects of the skyrocketing prices and predicted shortages in the near future are difficult to evaluate, particularly when the problem is viewed as a global rather than a regional one. Industrial and oil importing nations such as the United States have lost their freedom of political maneuvering due to oil imports (The Rockefeller Foundation, 1978). Because of a sluggish world economy and oil price increases, the developing Third World countries have fallen $258 billion in debt (World Bank, 1979). Furthermore, petroleum exporting countries have begun exercising their energy related power in different directions (Corradi, 1979).

To delay and further avert a tight energy supply and shortage situation, conservation and development of new energy alternatives is urgent and essential. Conservation itself is a very complex and controversial case. The complexity arises from the fact that its potential and constrains vary widely among countries and among sectors (WAES, 1977). Within the business and the industrial world it is also feared that conservation might slowdown growth and destroy economic balance (Meador, 1978). One of the main reasons conservation has not yet made an impact, is because of the short payback time private energy consumers demand from cost saving measures (Beijdorff, 1979).

While the urgency for developing new energy technologies is widespread, the direction of a new energy policy has to follow is at issue. Shale and tart sands, which are found in large quantities around the world, could extend the role of oil considerably longer, assuming their adverse environmental problems can be solved (Ridker and Cecelsky, 1979). Coal liquefaction technology might prove too costly and environmentally degrading if improper planning and management prevail over comprehensive and well-coordinated objectives (Lewis and Muller, 1979). Renewable energy sources such as nuclear fusion, solar energy and wind power appear to be associated with minimal environmental constraints. However, the economic cost of utilizing the renewable energy sources is difficult to evaluate (Ridker and Cecelsky, 1979).

4.2 The United States Energy Situation

Since the Arab oil embargo of 1973, the United States energy outlook has become a major public and governmental issue. The embargo, associated with indigenous factors such as declining production of gas and oil, diminishing mine productivity and environmental legislation, has drastically affected domestic energy costs. For the period 1973 to 1975, the cost of energy in the United States increased much faster than the overall inflation rate. While the consumer price index has increased 21 percent, the price of energy increased by 84 percent (Decker, 1977). The price of oil has been constantly rising since 1973 and it is estimated that the price increase of petroleum adopted by OPEC in December, 1979 will add at least $25 billion to the 1980 oil import bill, thus increasing the total value of the imported oil to $76 billion (Anonymous, 1979).

A broad breakdown of the energy distribution usage in the United States is shown in Table 4.1 and indicates that the industrial sector is the largest energy user. For the period from 1900 to 1970, the energy consumption in the United States has grown at a rate of about 3 percent per year (Dorf, 1978). In Figure 4.1, the growth of the energy consumption in the United States is shown for the 1900-1975 period. Extrapolation of the curve to the year 2020 yields a total of 316×10^{15} KJ energy consumed. The case for linear and zero growth is also shown in Figure 4.1.

The strong dependence of the United States on petroleum products and natural gas is evident in Figure 4.2, where the total U.S. energy consumption is presented (U.S. Department of Commerce,

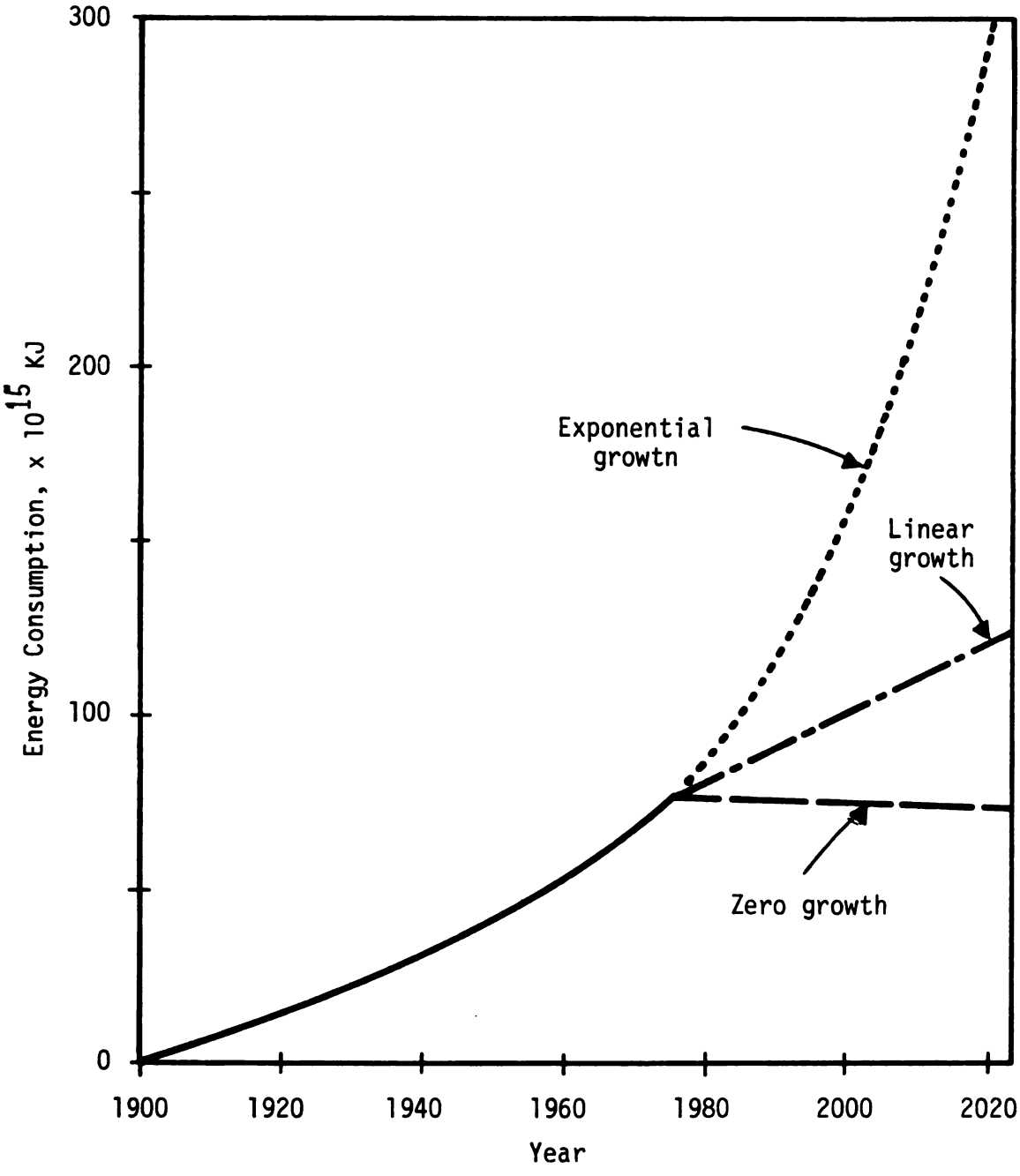

Figure 4.1.--Historical growth of energy consumed in the United States and several projections for the period 1975 to 2000 (Dorf, 1978).

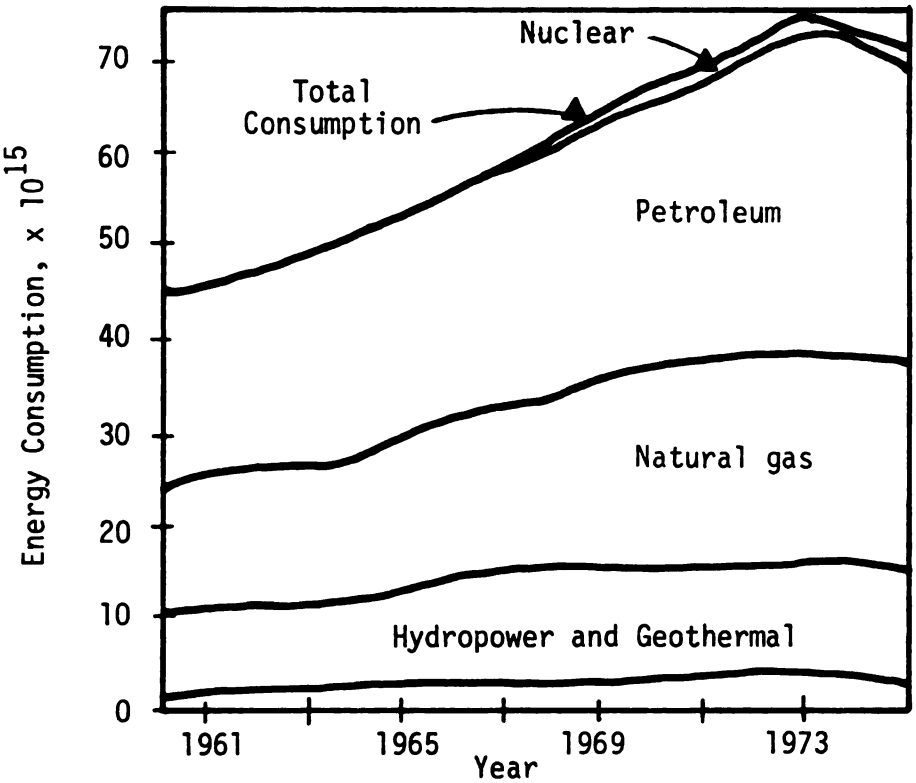

Figure 4.2.--Total United States energy consumption (U.S. Department of Commerce, 1976).

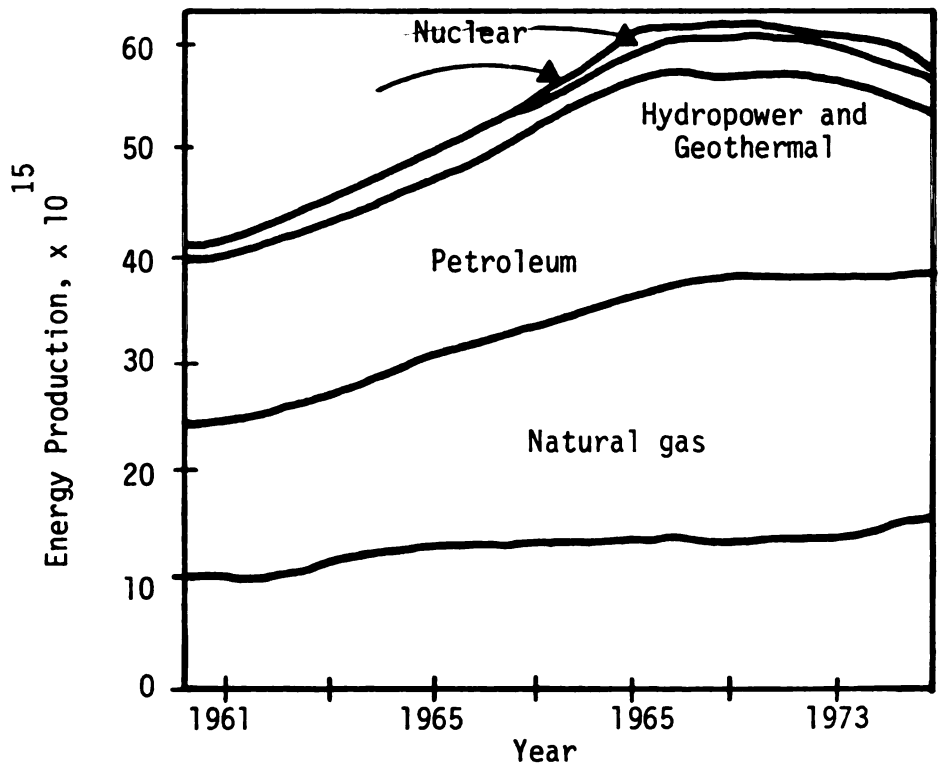

Figure 4.3.--Total United States gross energy production (U.S. Department of Commerce, 1976).

TABLE 4.1.--Energy distribution usage in the United States.

Sector	Energy Percent Usage
Industry	32
Generation of electricity	27
Transportation	24
Residential & Commercial	17

SOURCE: Quillman, 1977.

1976). Disturbances related to the supply and availability of those two energy sources is expected to cause deleterious effects on the economic and social status of the United States, since their contribution to the total energy supply is well over 70 percent. The relationship which exists between standard of living and energy consumption is one of the reasons the United States has become a large oil importer. The United States' total energy production, shown in Figure 4.3, started lagging behind consumption during the beginning of the 1960's, the period which also produced an all time high industrial output (Dorf, 1978). Although a large energy importer, the United States is far less dependent on foreign oil than Western Europe and Japan (Table 4.2).

4.3 The Solar Energy Option

Approximately 25 percent of the total energy consumed world-wide comes from solar resources such as windpower, waterpower,

TABLE 4.2.--Consumption, production, and net imports of energy in the United States and the rest of the world x 10^{15} Btu.

Region	Consumption	Production	Imports	% Imports
United States	74	63	11	15
Western Europe	53	19	34	64
Japan	14	2	13	86
Sino-Soviet Block	67	70	--	--
Rest of the World	40	100	--	--

SOURCE: U.S. Department of Commerce, 1976.

biomass and direct sunlight; by 2025, solar energy could possibly account for about 75 percent of the energy used in the world (Hayes, 1977). The transition to a solar era will probably be associated with social changes and certainly with yet undetermined economic efforts, but its benefits will far outweigh the costs and sacrifices.

A sharp decrease of the oil consumption in the United States will occur sometime between 1985 and 2000 (Gustaffero et al., 1979). The direct involvement of the federal government in the promotion of solar energy research and development indicates that solar technology is expected to make a significant contribution to the future energy needs. The national solar budget has risen from $1 million in 1971 to approximately $600 million in 1980 (Rice, 1979). The evolution of the United States' solar budget is shown in Figure 4.4. The six basic areas where solar research and development is active are (Gilman, 1978):

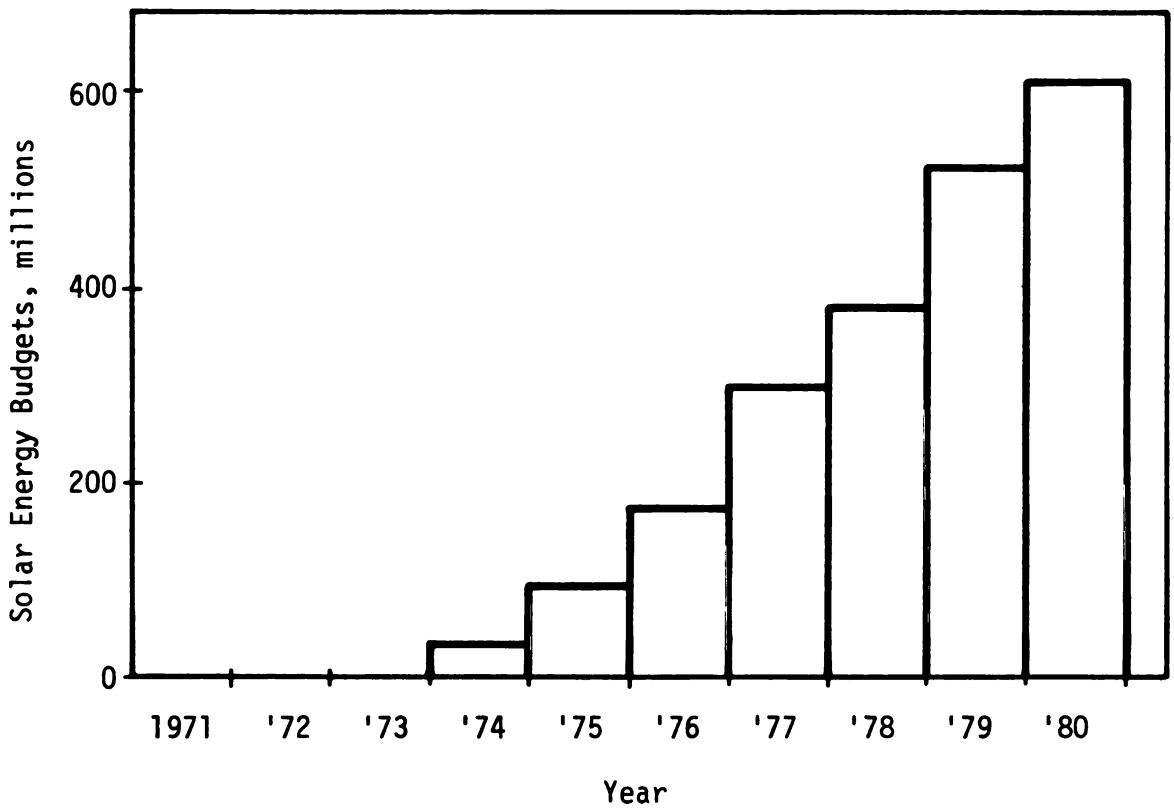

Figure 4.4.--Evolution of solar energy budgets.

1. Heating and cooling buildings
2. Solar thermal conversion
3. Photovoltaic conversion
4. Biomass conversion
5. Wind conversion, and
6. Ocean thermal conversion.

Evaluation of federal research, development and demonstration programs has shown that solar heating of buildings, biomass, wind power and photovoltaics are the most promising solar energy technologies (Anonymous, 1978a).

For solar energy to emerge as a significant energy alternative, a consolidated national solar policy is necessary. On June 20, 1979, the White House announced that the nation should commit itself to a goal of meeting 20 percent of its energy needs with solar and renewable resources by the end of the century. The formation of a national solar bank to provide interest subsidies has also been proposed. These announcements do not constitute a well-defined solar policy. The solar acts of 1974 which encourage and support development and demonstration of practical means to employ solar energy on a commercial scale, still remain the only coherent energy policy (Rice, 1979).

The projection of the future energy supply in the United States (shown in Figure 4.5) indicates that a 20 percent contribution by solar is attainable by 2000. The rapid increase of solar installations shown in Figure 4.6 also indicates the possibility of a significant solar output in the near future.

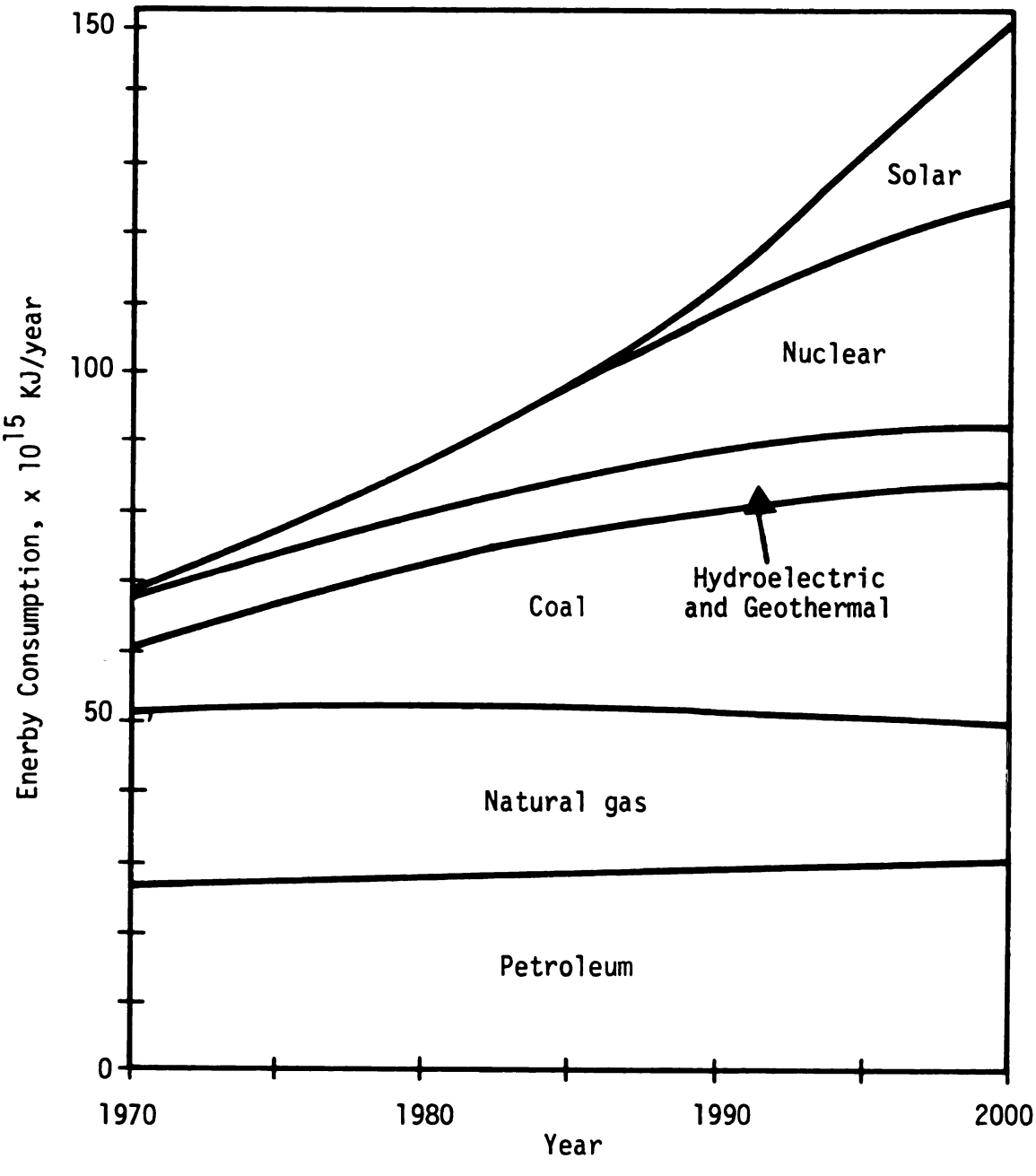

Figure 4.5.--Possible projection for the supply of energy in the United States during the period 1970-2000 (Dorf, 1978).

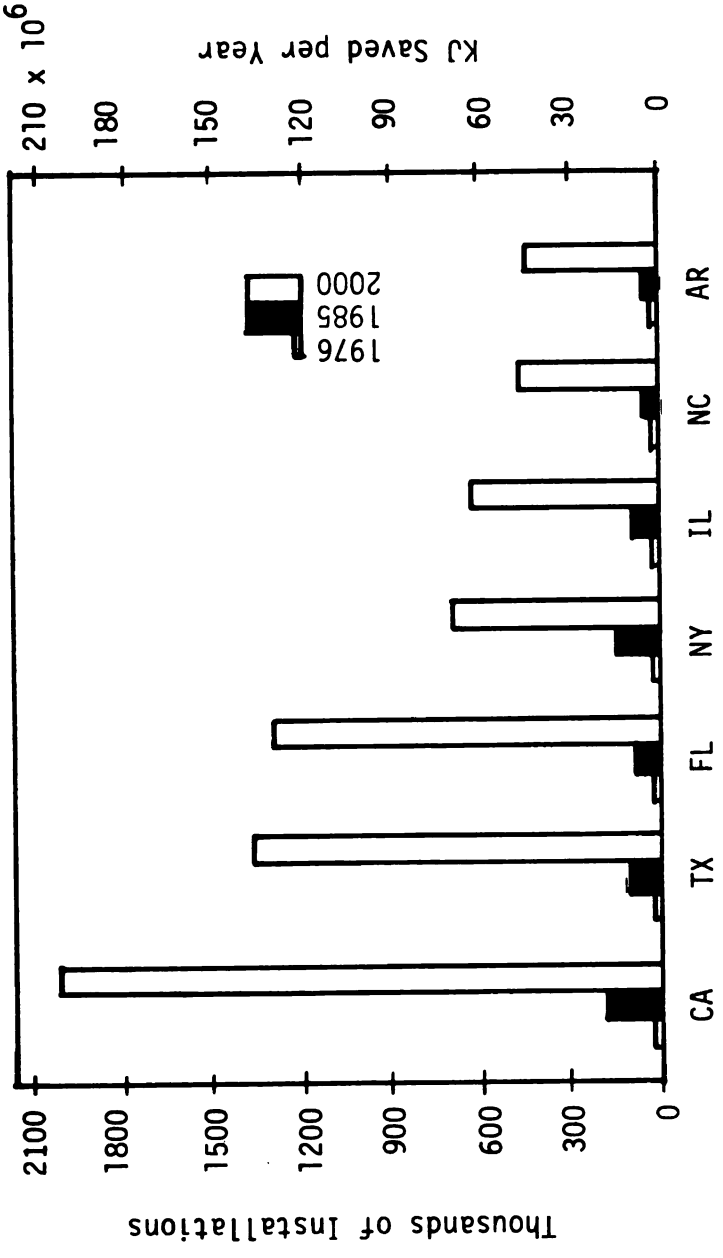

Figure 4.6.--Solar installations for the seven highest states by the year 2000 (Gustaffero et al., 1979).

4.4 Collection of Solar Energy

4.4.1 Solar Radiation Fundamentals

The energy generated in the interior of the sun by fusion is transferred to its surface and then radiated into space. The amount of solar radiation intercepted in space by a surface perpendicular to the radiation at the earth's mean distance from the sun, is called the solar constant. Its value is 1353 W/m^2 (Thekaekara, 1971) and varies by ±3 percent due to the elliptical sun-earth orbit and the variations in the total energy emitted by the sun. The solar energy reaching the earth is greatly reduced compared to the rate of the extraterrestrial solar constant. Air molecules, water vapor and dust particles present in the atmosphere cause the attenuation of the sun's radiation. A detailed analysis of the various factors contributing to the reduction of the solar intensity has been presented by Thekaekara (1974).

Radiation is classified as direct and/or diffuse. Direct radiation is received from the sun without change of direction. Diffuse radiation reaches the earth after its direction has been changed inside the atmosphere. The pyranometer and the pyrheliometer are the instruments most commonly used to measure solar radiation. The pyranometer measures total radiation while the pyrheliometer measures normal incident direct radiation. In the absence of radiation data, meteorological data on percent of possible sunshine can be used to estimate radiation. For design purposes, an hour by hour system performance is often required. Availability of solar radiation data on an hourly basis exists for only a few locations in

the United States. As a result, hourly values have to be estimated from daily values. A description of the methods used to calculate hourly solar radiation is presented by Duffie and Beckman (1974) and Kreith and Kreider (1978). Thomas (1977) investigated the models available to predict solar radiation and found the ASHRAE weekly model to be the best for simulating long-term performance of solar systems.

Measured and estimated insolation is reported as data on horizontal surfaces. However, radiation incident on surfaces of various orientation is often required. Duffie and Beckman (1974) describe the various equations used to convert solar radiation on a horizontal surface to radiation on a tilted surface.

4.5 Flat Plate Collectors

4.5.1 General Description

The present principal applications of flat plate collectors are in water heating systems and in building heating/air conditioning. Flat plate collectors are distinguished by their low cost, simplicity, low maintenance and ability to capture both direct and diffuse radiation. These features make flat plate collectors attractive devices from an engineering and economic point of view. This is especially true when energy is desired up to 100°C above ambient temperatures. Flat plate collectors have a high net energy yield. A conventional collector returns the energy utilized in its manufacture in less than one year.

Flat plate collectors are simple in concept. An absorber plate acts to absorb the solar energy and to convert it into heat. One or more covers are placed over the absorber to reduce the convective and reflective heat losses. The heat collected from the absorber is transferred to a working fluid which is either gas or liquid. In liquid systems, tube-like channels are thermally bonded to the absorber to conduct heat from the plate to the tube wall. Conductive heat losses through the back are reduced by means of thermal insulation.

Because of diurnal and seasonal motions, a solar collector should face south (or north in the southern hemisphere). In addition, the collector must be tilted from the horizontal so that a maximum amount of absorbed solar radiation is intercepted. The present practice is to specify the collector slope as a function of latitude only. In cases where a solar system is designed to supply a fraction of the yearly heating load, the surface should be inclined at an angle of about 0.9 times the latitude (Morse and Czarnecki, 1958). If a solar system is designed to supply the total heating load during the year it should be inclined at 1.5 times the latitude angle (Lof and Close, 1967). Although the collector tilt has a significant effect on hourly system performance, deviations of latitude ±20° have a small effect on the annual system performance (Duffie and Beckman, 1974).

4.5.2 Absorber Plates and Selective Surfaces

The main functional part of a collector is the absorber plate. In Table 4.3 a comparison is made of the most common metals used in manufacturing absorbers.

TABLE 4.3.--Collector material comparison.

Material	Modulus of Elasticity, psi	Cost $/lb	Energy to Produce BTU/lb
Mild steel	29×10^6	0.12	7,500
Copper	16×10^6	0.29	42,000
Aluminum	10×10^6	0.47	64,000

SOURCE: Grimer and Moore, 1977.

The absorber efficiency of a collector is greatly increased by painting the metal plate black. Common black paints have a high absorbance. According to Kirchhoff's law, the directional spectral absorbance is equal to the directional spectral emittance:

$$\varepsilon'_\lambda (\lambda,\beta,\theta,T_A) = \alpha'_\lambda (\lambda,\beta,\theta,T_A) \qquad [4.5.1]$$

where ε'_λ and α'_λ are the directional spectral emittance and absorbance, respectively, λ the wavelength, β the cone angle measured from the directional normal to the surface, θ the circumferential angle and T_A the surface absolute temperature.

The heat losses due to radiation and convection from an absorber can be considerable:

$$q_{\ell} = h(T - T_s) + \varepsilon_e \sigma (T^4 - T_s^4) \qquad [4.5.2]$$

where q_{ℓ} is the heat loss between the absorber and the nearest glass cover, T and T_s are the absolute temperature of the absorber and the nearest cover, h is the convective heat transfer coefficient, σ the Stephan-Boltzmann constant, and ε_e the effective emittance of the absorber.

The functional properties of spectrally selective surfaces can be explained by the equations described in detail by Siegel and Howell (1972). The distribution of the emissive power of a black body is governed by Plank's law:

$$e_{\lambda b}(\lambda) = \frac{C_1 \lambda^{-5}}{e^{C_2/\lambda T} - 1} \qquad [4.5.3]$$

where $e_{\lambda b}(\lambda)$ is the spectrial emissive power, C_1 and C_2 are constants, λ is the wavelength and T the absolute surface temperature.

Equation [4.5.3] is a humped curve with a peak value at λ_{max} given by Wien's displacement law:

$$\lambda_{max} = \frac{2898}{T} \qquad [4.5.4]$$

where λ is given in microns and T in °K.

For calculation purposes, the sun can be considered a black body emitting energy at about 5500°K. Its peak intensity is at 0.52 micron. Allowing for absorption in the atmosphere, the solar radiation is almost entirely confined to wavelengths between 0.3 and 2.0 microns. Objects emitting radiation at earth temperatures exhibit their peak radiation at about 8.0 microns. Thus, the solar spectrum and that of an object on the earth do not overlap. If a material can be manufactured which differentiates its absorption, reflection or transmission characteristics between wavelengths above two microns and below two microns, the absorption of solar energy would be maximized and its emission minimized. Such surfaces have been designed. They are called spectral selective surfaces.

A comprehensive discussion on selective surfaces has been presented by Tabor (1967). Until a few years ago selective surfaces were too costly to be used for inexpensive solar applications. Recent technological improvements in synthesizing the materials has considerably reduced their cost. Today selective paints have the same price as common black paints (Schreyer, 1979).

4.6 Evacuated Tube and Concentrating Collectors

Evacuated tube collectors are a compromise between flat plate collectors and concentrators. They collect both direct and diffuse radiation like the flat plate collectors and operate at high

temperatures like the concentrators without tracking the sun. At moderate temperatures (i.e., less than 60°C) flat plate collectors are as efficient as evacuated tube collectors.

Tubular collectors are not as easily incorporated into retrofit designs (Grimer and Moore, 1977). In addition, they require sophisticated controls and higher initial capital investments (Graham, 1979). Although their applicability has been demonstrated (Louie and Miller, 1978; Trice, 1979), tubular collectors have not yet penetrated the solar market (Graham, 1979).

The basic design concepts of flat plate collectors also apply to tracking concentrators or focusing collectors. Additional problems such as stacking the sun, higher optical losses and possible structural damages from high winds complicate the design process from an engineering point of view. Most of the concentrating collector designs can only use beam radiation. A family of compound parabolic concentrators developed by Winston (1975) and Rabl (1976) collect both beam and diffuse radiation.

With focusing collectors temperatures as high as 1500°C can be achieved (Dorf, 1978). Operating problems and high maintenance and initial costs have restricted the application of concentrating collectors for purposes other than furnaces and experimental studies (Duffie and Beckman, 1974).

4.7 Solar System Analysis: Components

A schematic diagram of a typical solar water heater is shown in Figure 4.7. The performance of the collector is only the first

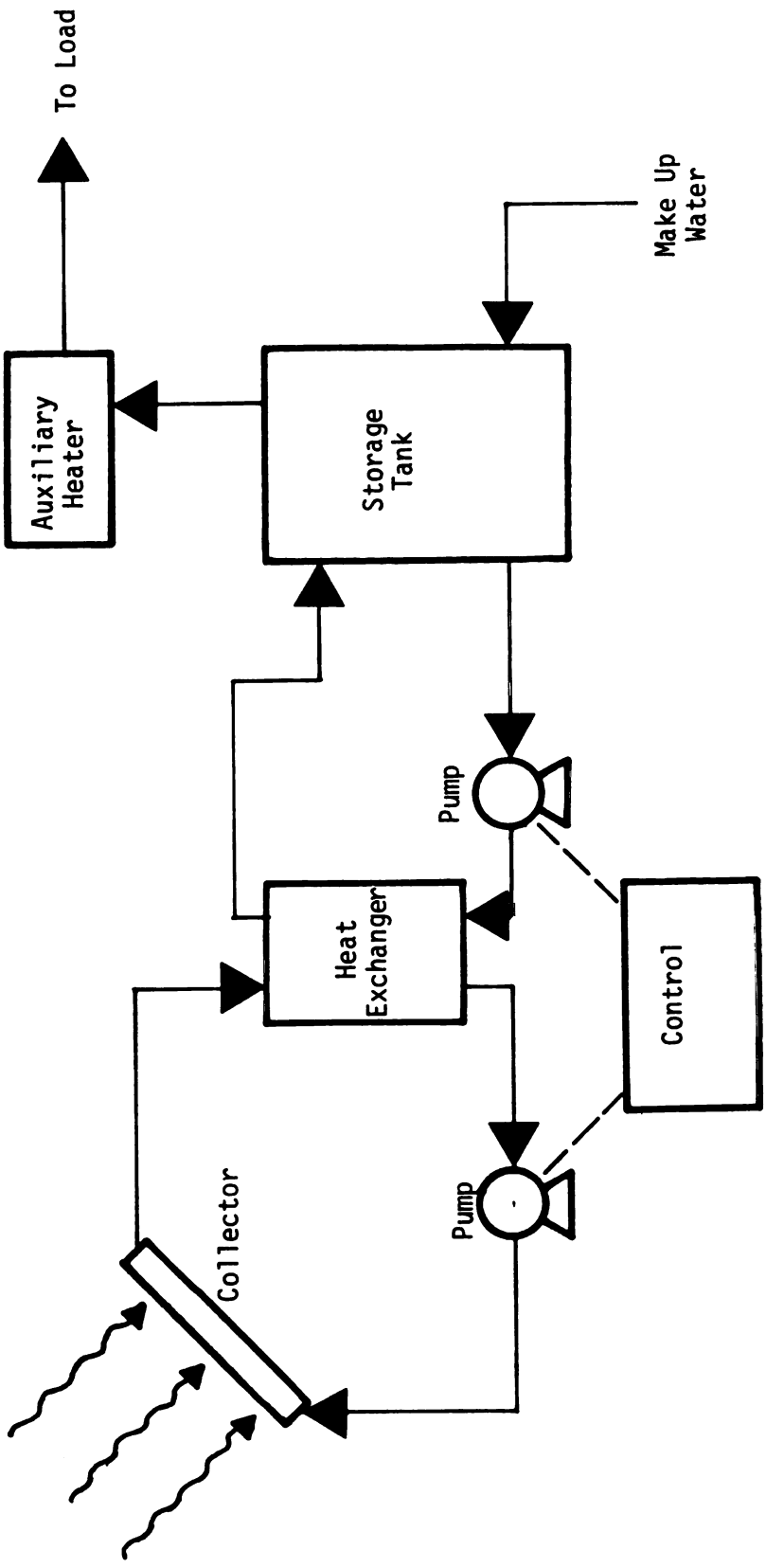

Figure 4.7.--Schematic diagram of a solar water heater.

step of the design process as evidenced by the additional system components shown in Figure 4.7. The long-term performance and the reliability of solar systems depends upon properly coupling a collector with the other components.

4.7.1 Energy Storage and Controls

Energy can be stored by utilizing phase change materials (Telkes, 1974), rock beds (Lof et al., 1964), and hot water storage (Duffie and Beckman, 1974). Water is non-toxic, has a high specific heat and is readily available.

The water in a storage tank is heated by the working fluid that circulates through the collector. The hot water from the storage tank is used to supply the load at various flow rates. An energy balance for a nonstratified tank gives (Duffie and Beckman, 1974):

$$Mc_p \frac{dTs}{dt} = Qu - L - (UA)_s (T_s - T_a) \qquad [4.7.1]$$

where M is the mass of water in the tank, T_s and T_a are the tank and environmental temperatures, Qu is the rate of energy added to the collector, L is the load, U is the tank loss coefficient and A is the area of the tank.

The rate of energy added by the collector, Qu in equation [4.7.1] can be expressed as:

$$Q_u = B(\dot{m}\, c_p)\ (T_o - T_s) \qquad [4.7.2]$$

where $\dot{m}$ is the flow rate of the working fluid, T_o is collector outlet temperature and B is a control in a function equal to unity when the pumps operate and zero at other time.

One of the targets of solar system design is to maintain a high degree of stratification inside the tank. The efficiency of the collector in a stratified tank system is greatly improved. The ratio of tank height to tank diameter (L/D) strongly effects the maintenance of stratification. The higher the ratio, the more stable the stratification. Structural and costs constraints limit the value of L/D. An L/D between 3 and 4 is a reasonable compromise between cost and performance (Lavai and Thompson, 1977).

The objective of the control strategy, is to maximize the value of Qu in Equation [4.7.1]. A control device senses and compares the temperatures of the tank, T_s, and the collector, T_c, whenever $T_c > T_s$ the working fluid is allowed to circulate through the collector. Schlesinger (1977) has described the type of controls used in solar applications. By properly choosing and installing a control device, the area of the collector required for a specific process can be reduced by 35 to 40 percent (Newton, 1978).

In a stratified tank, the water temperature is not uniform over the vertical dimension of the tank. Under stratification conditions energy balances as in Equation [4.7.1] can be written for several sections in the tank. Each section is assumed to be at

uniform temperature. A two section tank is shown in Figure 4.8. An energy balance for the upper section ($T_{s,1}$) can be rewritten as (Duffie and Beckman, 1974):

$$\frac{dT_{s,1}}{dt} = \frac{1}{(\dot{m}C_p)_{s,1}} [F_1(\dot{m}C_p)_c (T_{c,o} - T_{s,1}) + (\dot{m}C_p)_L (T_{s,2} - T_{s,1}) - (UA)_{s,1} (T_{s,1} - T_a)] \quad [4.7.3]$$

where

$$F_1 = \begin{cases} 1 \text{ if } T_{c,o} > T_{s,1} \\ 0 \text{ if } T_{s,1} > T_{c,o} \quad T_{,s,2} \end{cases} \quad [4.7.4]$$

For the lower section ($T_{s,2}$) the energy balance is

$$\frac{dT_{s,2}}{dt} = \frac{1}{(mC_p)_{s,2}} [F_1(\dot{m}Cp)_c (T_{s,1} - T_{s,2}) + (1 - F_1)(\dot{m}C_p)_c (T_{c,o} - T_{s,2}) + (\dot{m}C_p)_L (T_{L,r} - T_{s,2}) - (UA)_{s,2}(T_{s,2} - T_a)] \quad [4.7.5]$$

Depending on the nature of the application, predicted system performance using Equations [4.7.3] and [4.7.5] may be significantly higher than the performance of an unstratified tank system (Equation

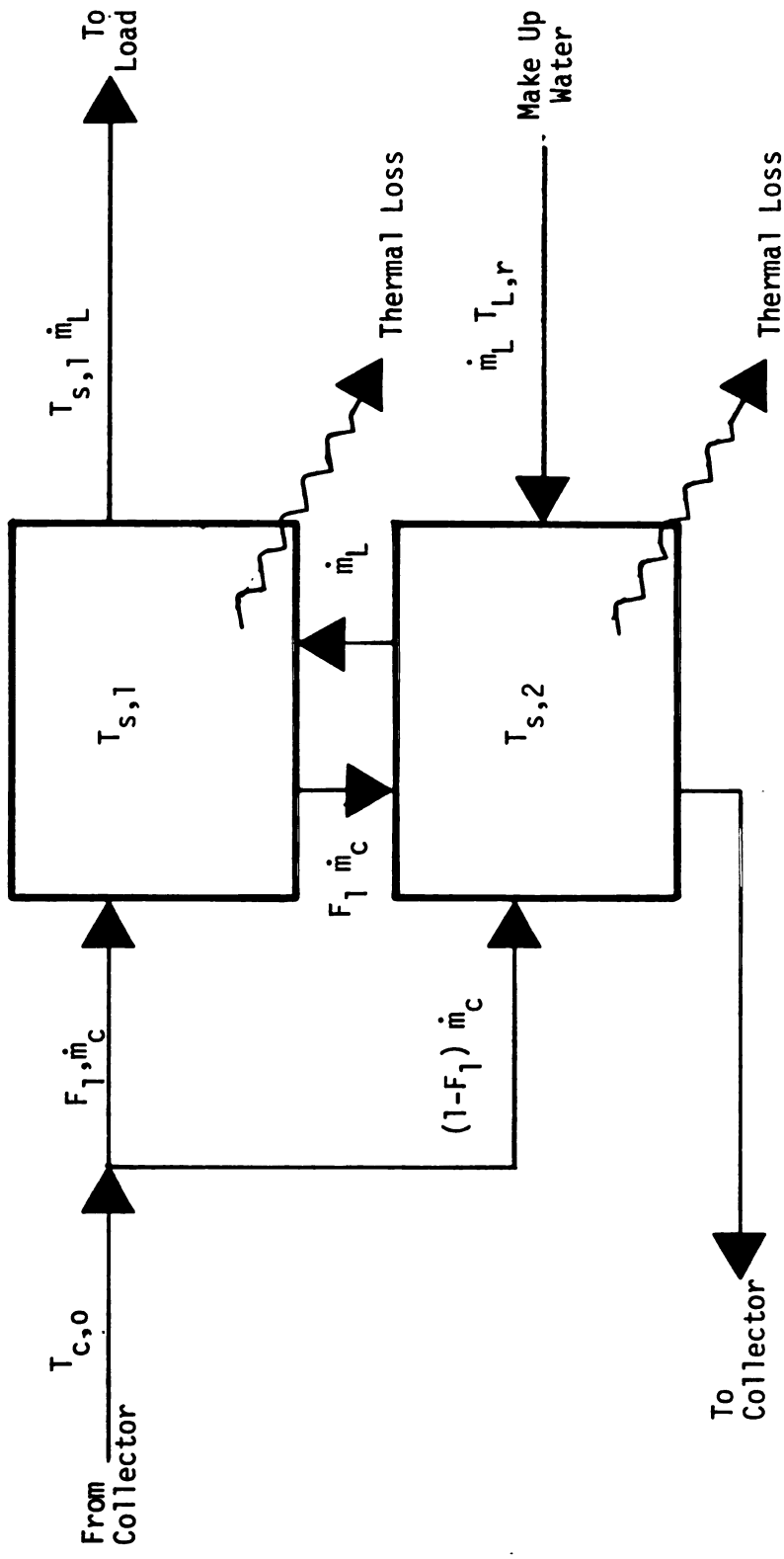

Figure 4.8.--Stratified water storage tank with each section at uniform temperature (Duffie, J.A. and Beckman, W.A., 1974, pp. 224).

[4.7.1]) (Duffie and Beckman, 1974). This is more evident when a two or three section tank is substituted for a one-section tank.

4.8 Economics

4.8.1 The Present Value Concept

Once a capital investment has been implemented, its consequences cannot be altered. Capital commitments, particularly those that influence the long-run flexibility and earning power of an investor, should be based on sound economic indices and criteria. Judging the economic desirability of a capital expenditure on the payback period fails to recognize the time value of money and investment profitability (Bierman and Smidt, 1970).

The time values of money arise from the fact that because of uncertainty, inflationary trends and alternative uses of money, a dollar in hand today is more valuable than a dollar to be received sometime in the future (Nelson et al., 1973). The interest rate charged by financial institutions represents the time value of money since the speculative motive is one of the principles behind a money lending process (Keynes, 1936).

When an accumulated amount of money under compound interest is determined, the present sum of money is known. The amount of money received sometime in the future by investing and allowing compound interest to accrue is determined by advancing forward in time. When the present value has to be determined, the sum of money to be received in the future is known. The objective of discounting is to determine the present worth of that future sum by retreating in time (Aplin and Casler, 1973).

The practice of discounting incorporates the time value of money. The discount rate is cost related to the value of money with respect to the timing of its receipt and disbursement. This cost is established during a normal investment activity based on both debt and equity sources of capital. Usually, a company sets a minimum discount rate which is between 10 and 15 percent (Horwitz, 1980). In a discounting process cash flow receipts and disbursements are adjusted by the discount rate for the period of time funds are in use. The result of discounting is called the present value which is expressed as:

$$PV = C_o + \frac{C_1}{(1+i)} + \frac{C_2}{(1+i)^2} + \ldots + \frac{C_n}{(1+i)^n} + \frac{SV}{(1+i)^n} \qquad [4.8.1]$$

where

PV = present value of net cash inflows

C_o = investment

C_1, C_2, C_n = cash inflow after taxes in years 1,2,...n,

i = the discount rate

n = expected economic life of asset

SV = salvage value of the asset in year n

The present value is a powerful technique to judge several cash flow alternatives in terms of today's dollars (Aplin and Casler, 1973).

4.8.2 The Life-Cycle Costing Method

In general, solar systems require higher initial and lower operating costs than conventional electric or fossil fuel fired systems. As a result, a solar system financially examined on a basis of short-term return of investment will be put at a disadvantage. Solar systems are more attractive if the life-cycle costing method is used (Hayes, 1977).

The objective of the life-cycle costing method is to minimize the present values of a summation of costs arising both now and in the future (Corcoran, 1978). The method is an evaluation process suitable for the economic comparison of alternative projects and for the selection of the most cost-effective design for a specified application. The federal government is employing life-cycle costing in the Federal Energy Management Programs. The National Energy Conservation Policy Act (NECPA), passed in the fall of 1978, requires that "practical and effective" life-cycle costing methods and procedures are to be used in evaluating energy conservation and solar energy programs for federal buildings and facilities (Ruegg, 1978).

Reynolds et al. (1976) provided guidelines for the application of the life-cycle method as a decision making process. The following components comprise the fundamental considerations of the method.

1. Initial capital investment cost
2. Annual operating and routine maintenance costs
3. Major repairs and component replacements

4. Complete item or system replacement
5. Residual values
6. Time.

The time factor is used to determine when costs or benefits occur and when replacements are required. Reynolds et al. expressed the economic viability of a life-cycle optimized solar system in terms of the following statistics: (1) savings/investment ratios, (2) discounted payback period, and (3) BTU savings/investment dollar.

Although life-cycle costing is accepted by most economists as the soundest approach in a decision making process (Ruegg, 1975), its application involves some serious assumptions. The method assumes a period of study equal to the life of equipment under investigation. However, for solar systems this life is unknown. As a result, an equipment life must be assumed. An erroneous assumption can lead to serious miscalculations (Boer, 1978).

Fuel cost, term of mortgage, collector area cost and annual nominal discount rate were found to be the more sensitive economic parameters of an optimized solar system (Singh et al., 1979). Another study indicated that duel escalation and maintenance are the most critical factors (ERDA, 1976). Solar hot water and space heating were found to be economically attractive when the alternative is electric energy (Butt, 1976). For a payback of 20 years, it was shown that solar energy could replace 30 to 40 percent of the electric energy demand for water heating in milk processing plants (Thomas et al., 1977). Assuming a constant fuel cost equal to $\$13/10^6$ BTU, a solar water heater in Lansing, Michigan will pay for

itself in 9.5 years, if the capital is borrowed at 7 percent and the collectors cost $\$300/m^2$ (Zapp, 1979).

4.9 Computer Models for Solar System Design

Solar systems operate in a transient fashion subject to time changes in all forcing functions. In addition, many solar component models are non-linear. Therefore, computerized models are necessary tools for solar system design.

Various solar simulation models and their status were discussed by Graven (1974). Buchber and Roulet (1968), Lof and Tybout (1972), and Butz et al. (1974) have developed quasi steady-state solar system models which are the predecessors of the widely used simulation model TRNSYS.

4.9.1 The TRNSYS Program

The transient system simulation, TRNSYS, has been developed at the University of Wisconsin Solar Energy Lab for the design and simulation of a wide variety of solar energy systems. The computer program has been thoroughly described by Klein et al. (1979). A typical solar system consists of interconnected components such as solar collector, energy storage unit, heat exchanger, pumps and temperature sensing collectors. TRNSYS models the transient behavior of a solar system by collectively simulating the performance of the interconnected components.

TRNSYS is written in FORTRAN and is composed of a main program and various subroutines which model the function of a specific solar system component. Additional subroutines are used to perform

tasks such as data reading, printing, plotting and numerical integration. The flow of information in TRNSYS is either of acyclic or recyclic type. Recyclic flow occurs whenever information is flowing from a component to one or more other components of the system and then back to the starting component. In acyclic flow the information does not return to the starting component. The recyclic type flow necessitates a numerical integration algorithm which in TRNSYS is the Modified-Euler method. Predicted values of the dependent variables are corrected by the trapezoid rule. In the recycle loop, simultaneous differential and algebraic equations are solved by successive substitution iteration until all the outputs converge to within tolerance limits specified by the user.

TRNSYS will best model solar systems if hourly isolation and temperature data is used. For locations where hourly data is unavailable, the ASHRAE weekly insolation model is satisfactory for determine long-term solar system performance (Thomas, 1977). Experimental results have indicated that simulating systems with average meteorological data, the performance of the system tends to be too optimistic (Klein et al., 1975). Such a performance overestimation was stated to be the result of the nonlinear operation of solar systems. The negative contribution of cloudy days is not proportional to the positive contribution of sunny days.

Oonk et al. (1975) used TRNSYS to model the Colorado State University heating and cooling system. The efficiency of the system was found to be lower in the summer than in the winter but both seasons exhibited higher efficiencies than in the spring and fall.

TRNSYS was used to model the demonstration solar systems described by Rippen et al. (1978) and Key (1979). At the present time, the systems are in operation and the validity of the TRNSYS program is being investigated in both cases.

4.9.2 The f-chart Design Method

The f-chart program is a fast simulation program for solar heating systems. The method correlates two dimensionless variables of a solar system to its long-term performance. It was developed at the University of Wisconsin Solar Lab by correlating hundreds of simulations of solar heating systems. A complete description of the program is presented by Hughest et al. (1978). The authors also discuss the assumptions under which the design procedure is valid.

The identification of the dimensionless variables in f-chart has been described in Beckman et al. (1977). Assuming the energy change in the storage tank to be small, the fraction of the monthly total heating load supplied by solar energy, f, is

$$f = Q_u/L \qquad [4.9.1]$$

where L is the monthly total load.

The useful energy, Q_u, collected during the month is

$$Q_u = F'_R A_c [S - U_L (T_{in} - T_a)] \Delta t \qquad [4.9.2]$$

where Δt is the number of days in a month.

A dimensionless temperature, ϕ, can be defined:

$$\phi \equiv (t_{in} - T_a) / (T_{ref} - T_a) \qquad [4.9.3]$$

where T_{ref} is a reference temperature equal to 100°C.

Equation [4.9.1] can be written as:

$$f = \frac{F_R' A}{L} [I_t (\overline{\tau\alpha}) - U_L (T_{ref} - T_a) \phi \Delta t] \qquad [4.9.4]$$

where I_t is the instantaneous solar radiation incident on the collector surface per unit area and $(\overline{\tau\alpha})$ is the monthly average transmittance absorbance product.

In Equation [4.9.4], f may be determined using the following two dimensionless parameters:

$$X \equiv \frac{F_R' U_L A (T_{ref} - T_a) \Delta t}{L} \qquad [4.9.5]$$

$$Y \equiv \frac{F_R' (\overline{\tau\alpha}) I_T A}{L} \qquad [4.9.6]$$

Equations [4.9.5] and [4.9.6] are the basis of the f-chart method design technique.

The f-chart program is written in FORTRAN for use in interactive mode. It can be used to determine annual performance of resiential type solar systems for approximately 270 cities in the United States. Besides the thermal analysis, the program also

performs an economic assessment of a specified or an economically optimized collector area for a given location. The optimized area is the one which minimizes the present value of cumulative costs with the solar-assisted system over the period of analysis. The life-cycle costing method is used for the economic analysis.

The economics of solar water and space heating for thirteen cities has been examined by the f-chart method (ERDA, 1976). For the same values of X and Y air heating systems outperformed liquid systems, particularly for systems designed to supply a large fraction of the heating load (Klein et al., 1977).

A more detailed description of TRNSYS and f-chart will appear in Chapter 6.

4.10 The Food Industry from an Energy Point of View

4.10.1 Energy Utilization

Approximately 16 percent of the total United States' energy consumption is attributed to the food system (Pierotti et al., 1977). This accounts for food production, processing, distribution and food preparation. The percentage distribution of the energy used among different stages in the food system is listed in Table 4.10.1.

The Food and Kindred Products industrial group, SIC 20 (Standard Industrial Classification 20) ranks sixth among all major industries (Table 4.10.2) and as such, it has been the subject of numerous energy related studies. After the oil embargo of 1973, the United States food industry has become energy cautious. The result of this cautiousness is shown in Table 4.10.3. Table 4.10.3 indicates

TABLE 4.10.1.--Percentage distribution of the energy used in the United States food system.

Functional State	Percent
Production	18
Processing	33
Transportation	3
Wholesale and retail trade	16
Households	30

SOURCE: Hirst, 1973.

TABLE 4.10.2.--Consumption of purchased fuels and electric energy in the United States industrial sector in 1976.

SIC	Description	Quantity Trillion KJ	Percent of Total
	All Industries	13,320	100
28	Chemicals and Allied Products	3,183	23.9
33	Primary Metals	2,511	18.8
26	Paper and Allied Products	1,366	10.2
29	Petroleum and Coal Products	1,362	10.2
32	Stone, Clay and Glass Products	1,287	9.6
20	Food and Kindred Products	989	7.4
	All Other Industries	2,622	19.9

SOURCE: Annual Survey of Manufacturers, 1976.

TABLE 4.10.3.--Energy consumed for heat and power in the United States food industry and value of shipments of food products for 1972, 1974, 1975, and 1976.

Code	Industry Group and Industry	Energy Consumed $X 10^{12}$ KJ				Value of Shipments $X 10^{9}$ $			
		1972	1974	1975	1976	1972	1974	1975	1976
20	Food and Kindred Products	1100.5	1011.5	964.0	989.0	106.7	150.5	160.6	168.0
201	Meat Products	134.4	121.3	197.4	109.4	29.2	36.7	40.8	42.7
202	Dairy Products	116.0	105.8	100.2	97.5	14.4	18.4	29.1	21.9
203	Preserved Fruits and Vegetables	132.2	135.4	133.8	131.8	10.7	14.7	16.0	18.8
204	Grain and Mill Products	155.2	157.2	150.7	157.5	11.5	19.3	19.8	20.4
205	Baker Products	71.2	57.2	55.2	54.3	6.9	9.2	10.3	10.7
206	Sugar Confectionary Products	172.3	159.7	160.8	167.1	6.5	12.0	11.2	10.2
207	Fats and Oils	123.9	109.4	102.2	111.0	6.6	13.7	12.3	12.2
208	Beverages	129.3	110.9	103.5	106.2	12.9	16.5	19.1	19.5
209	Miscellaneous Foods	65.8	53.3	50.2	54.2	7.9	10.0	11.0	13.8

SOURCE: Annual Survey of Manufacturers, 1976

that despite the increasing value of shipments of food products from 1972 to 1976, the amount of energy consumed in the same period declined steadily.

Beet sugar is the largest energy user among the food industries utilizing about 10.4 percent of the total energy consumed within the food sector. The twenty energy leading food industries are listed in Table 4.10.4 where each industry is ranked on a gross KJ basis. The energy efficiency improvement with respect to the base year of 1972 which each industry estimated meeting by 1980 is also presented in Table 4.10.4.

Of all the fuels used to supply heat and power in the food industry, natural gas is the dominant energy source (Table 4.10.5). This is generally true for all but three food industries, namely, Fluid Milk, Frozen Fruits and Vegetables, and Manufactured Ice, where electricity is the prevailing energy source (Unger, 1975).

4.10.2 Energy Conservation in Food Processing

In general, processing requires about 33 percent of the total energy utilized in the food system (Table 4.10.1). However, Table 4.10.6 indicates that processing could account fof from 18.7 to 83.4 percent of the total energy depending on the food processing industry.

Energy conservation techniques in the food industry have been described in detail by a team of researchers (Casper, 1977). Energy conservation techniques and procedures applicable to the food industry were identified in the study as follows:

TABLE 4.10.4.--Energy consumed, energy use rank for 1976 and energy efficiency improvement goals for 1980 among twenty energy leading food industries.

Sic	Industry	Rank	Energy Used x 10^{12} KJ	Percent of Total	Improvement Goal for 1980 (%)
2063	Beet sugar	1	97.8	10.43	21
2046	Wet corn mills	2	87.7	9.43	7
2011	Meat packing	3	68.4	7.29	12
2082	Malt beverages	4	49.4	5.26	7
2075	Soybean oil mills	5	49.3	5.25	17
2033	Canned fruit & vegetables	6	47.4	5.08	11
2051	Bread, cake	7	42.8	4.57	19
2026	Fluid milk	8	41.1	4.38	15
2062	Cane sugar refineries	9	35.5	3.79	13
2037	Frozen fruits & vegetables	10	31.7	3.38	11
2099	Food preparation	11	30.8	3.28	14
2048	Prepared feeds	12	28.1	3.00	24
2079	Shortenings	13	27.2	2.90	14
2077	An.&mar. fats & oils	14	24.9	2.65	12
2022	Cheese	15	23.6	2.52	10
2086	Soft drinks	16	22.0	2.36	14
2023	Cond. & evap., milk	17	21.4	2.28	14
2016	Poultry dressing	18	18.7	1.99	14
2013	Saus. & prepared meats	19	18.3	1.96	11
2085	Distilled liquor	20	15.8	1.69	11

SOURCE: Casper, 1977.

TABLE 4.10.5.--Food industry fuel usage.

Fuel Used	Percent of Total (by Year)	
	1972	1976
Natural gas	62.0	53.7
Fuel oil	13.0	18.9
Electricity	11.6	12.7
Middle distillates	3.9	6.3
Liquified petroleum gas	0.4	0.6
Other	0.4	0.8

SOURCE: Anonymous, 1978b.

1. waste energy recovery
2. improved electical energy usage
3. increased boiler and steam efficiency
4. use of insulation
5. refrigeration and space conditioning
6. dryers, evaporators and other process equipment, and
7. general energy management.

Preventable heat losses in the food processing plants can be easily identified by writing simple energy balances of processes and operations encountered in various food processing plants. Computer programs such as CNSRV greatly faciltate the quantitative determination of heat losses in food processing operations (Rao and Katz, 1976).

TABLE 4.10.6.--Total energy used for selected processed foods (input).

Food Product	Total Energy Finished Product (KWH/lb)	Processing Energy (KWH/lb)	Processing in Total (percent)
Butter	6.18	1.90	30.7
Cheese	6.62	1.69	25.5
Condensed & evaporated milk	3.58	1.38	38.5
Fluid milk	1.28	0.24	18.7
Canned fruit & vegetables	1.29	0.67	51.9
Frozen fruit & vegetables	2.05	0.97	47.3
Dehydrated foods	2.62	1.87	71.4
Cereals	3.03	1.26	41.6
Bread and cake	2.13	0.73	34.3
Distilled liquor	40.86 (gal.)	34.06	83.6
Meat products	11-16	1.6-6.0	--

SOURCE: Pieroti, 1977.

The energy included in steam condensate can be recovered by means of heat exchangers or by direct condensate injection to heat water used in food plants (Rippen and Mintzias, 1977). Rao et al. (1978) discussed the significance of properly insulating steam pipes and process equipment and the recovery of heat from discard hot water. The optimum insulation thickness was found to depend on the type of fuel considered, surface temperature of the equipment and

the duration of heat loss. The authors recommended application of the lifecycle method to calculate the economics of an energy conservation procedure.

To determine the efficient use of energy, proper identification and measurement of energy inputs and outputs in food processing operations must be accomplished. Singh (1978) outlined the procedures for energy accounting in food processing and proposed the use of special symbols to denote the different inputs and outputs in a food operation. In-plant energy flows can be successfully measured by selecting the suitable metering devices for a particular quantity (Knoph et al., 1978; Wilson et al., 1978).

Inefficient steam utilization in food processing has been of great concern even before the present energy crisis. An atmospheric retort in a canary in California was found to utilize only 30.5 percent of the incoming steam to heat the food containers (Singh, 1979). The author also reported that indirect heating of the cans by means of a heat exchanger installed outside the retord improved the efficiency of the stem by 15 percent. Similar observations about the boiler and steam efficiency were made by Nwude et al. (1975) at a Campbell Soup Plant.

Chen et al. (1979) examined the utilization of energy in commercial citrus evaporators and investigated the energy savings resulting from the introduction of an additional effect and stage in a 4-effect, 7-stage evaporator. The new design was found to save 16.5 billion BTU per season and depending on the energy cost, the

payback period of the process modification was estimated at 1 to 2.5 seasons.

4.10.3 Applications of Solar Energy in Food Processing

Solar energy applications in the area of food processing are at the present time in an experimental stage. Drying of fruits and vegetables, solar water heating and the economics of solar applications are the subjects which draw most of the attention of the researchers.

Solar drying of food products such as fish, peaches, potatoes, nectarines, peppers, apricots, prunes and mushrooms have been accomplished in the laboratory (Berry et al., 1979; Deng et al., 1979; Smith et al., 1979; and Bolin et al., 1977). Because of the low temperatures of the drying air, solar dehydration is substantially prolonged and as a result enzymatic browning and mold formation is highly possible and frequently occurs in solar dryed products. The problem can be satisfactorily solved if a greater concentration of SO_2 is used in solar drying than in conventional hot air drying. Retention of Vitamin C and reconstituted properties were reported to be the same as in conventional drying (Smith et al., 1979).

Miller (1979) studied solar regeneration of solid desiccants used in fresh fruit drying. The optical, physical and thermal properties of commercially available desiccants were determined before the regeneration process. Activated alumina and silica gel

showed the greatest potential for solar regeneration, both exhibiting more than 87 percent regeneration at 75°C.

A simulation and feasibility study of solar water heating for the food processing industry in the Midwestern United States indicated that solar water heating can supply up to 90 to 100 percent of the total hot water demand (Thomas, 1977). The economics of solar water heating was also examined in the study and it was concluded that solar can replace up to 90 percent of the electric and 20 percent of the fossil fuel energy consumption for most plants over a 20-year payback period.

Singh et al. (1978) investigated the compatibility of solar energy collection, storage and supply with the energy demand in a dairy plant in Wisconsin. The TRNSYS and f-chart programs were used. Simulation results showed that solar energy can supply up to 34 percent of the processing energy but the economics under 1976 fuel prices was not favorable for solar water heating.

Pasteurization of fruit juices by passing them through a solar collector is another option for utilizing solar energy in the area of food processing, since the process occurs at moderate temperatures (76°-87°C). This application is presently being investigated by Davis et al. (1979). Selection of a suitable solar collector, pasteurization temperature and determination of radiation absortivities of different fruit juices within the solar spectrum are a few of the important considerations in a solar juice pasteurization process.

The energy required to concentrate liquid foods using membrane techniques is much less than that used by conventional evaporation systems. Reverse osmosis and ultrafiltration membranes have temperature limits of 40° to 100°C, respectively, which are within the efficient flat plate collector range. Limited studies by Puri et al. (1979) have shown that for a given membrane, an increase in concentration rate of between 20 and 50 percent per 10°C is realized for reverse osmosis and ultrafiltration. At the present time, the above authors are developing a pilot plant which will be used to demonstate the feasibility of solar membrane concentration of liquid foods.

Concentrated $CaCl_2$ brines readily absorb water and can be used to dry and concentrate foods and to drive water-absorption based refrigeration and heat pump systems which can be used in food processing. Methods for concentrating $CaCl_2$ brines by solar driven evapoartion and means for using such brines for concentrating liquid foods and drying solid foods are being investigated by Schwartzberg and Rosenau (1979).

CHAPTER 5

FLAT PLATE COLLECTOR HEAT TRANSFER ANALYSIS AND PERFORMANCE

An energy balance on a flat plate solar collector results in the following equation:

$$A_c S = q_u + q_L + \frac{de_c}{dt} \qquad [5.1]$$

where $S = [HR(\tau\alpha)]_b + [HR(\tau\alpha)]d$

A_c is the collector area, H is the rate of direct and diffuse radiation, R is a factor to convert the solar radiation to that of the plane of the collector, $(\tau\alpha)$ is the absorbance-transmittance product, q_u is the rate of useful energy transferred to the working fluid, and $\frac{de_c}{dt}$ is the rate of internal energy stored in the collector.

Assuming the magnitude of $\frac{de_c}{dt}$ to be small in comparison to the other terms, Equation [5.1] yields:

$$q_u = A_c S - q_L \qquad [5.2]$$

The heat lost to the surroundings is determined by:

$$q_L = U_L A_c (T_c - T_a) \qquad [5.3]$$

where U_L is the overall heat transfer coefficient,

T_c is the average temperature of the absorber, and

T_a is the ambient temperature.

Combination of Equations [5.2] and [5.3] results in:

$$q_u = A_c[S - U_L (T_c - T_a)] \qquad [5.4]$$

For the collector shown in Figure 5.1, the rate of heat loss is

$$q_L (x,y) = U_L [T_c (x,y) - T_a] \, dxdy \qquad [5.5]$$

If conduction in the x direction is negligible, a heat blanace at x_o per unit length in the x direction is given by

$$Sdy - U_L (T_c - T_a) \, dy + q|_{y,x_o} - q|_{y + dy,xo} \qquad [5.6]$$

where $q|_{y+dy,x_o} = q_{y,x_o} + \frac{dq}{dy}|_{y,x_o} \, dy$

Assuming uniform plate thickness (t) and constant thermal conductivity (k), Equation [5.6] can be written as

$$Sdy - U_L (T_c - T_a) \, dy - [Kt \frac{d^2 t_c}{dy^2}|_{y,x_o}] \, dy = 0$$

or

$$\frac{d^2 T_c}{dy^2} = \frac{U_L}{Kt} [T_c - (T_a + \frac{S}{U_L})] \qquad [5.7]$$

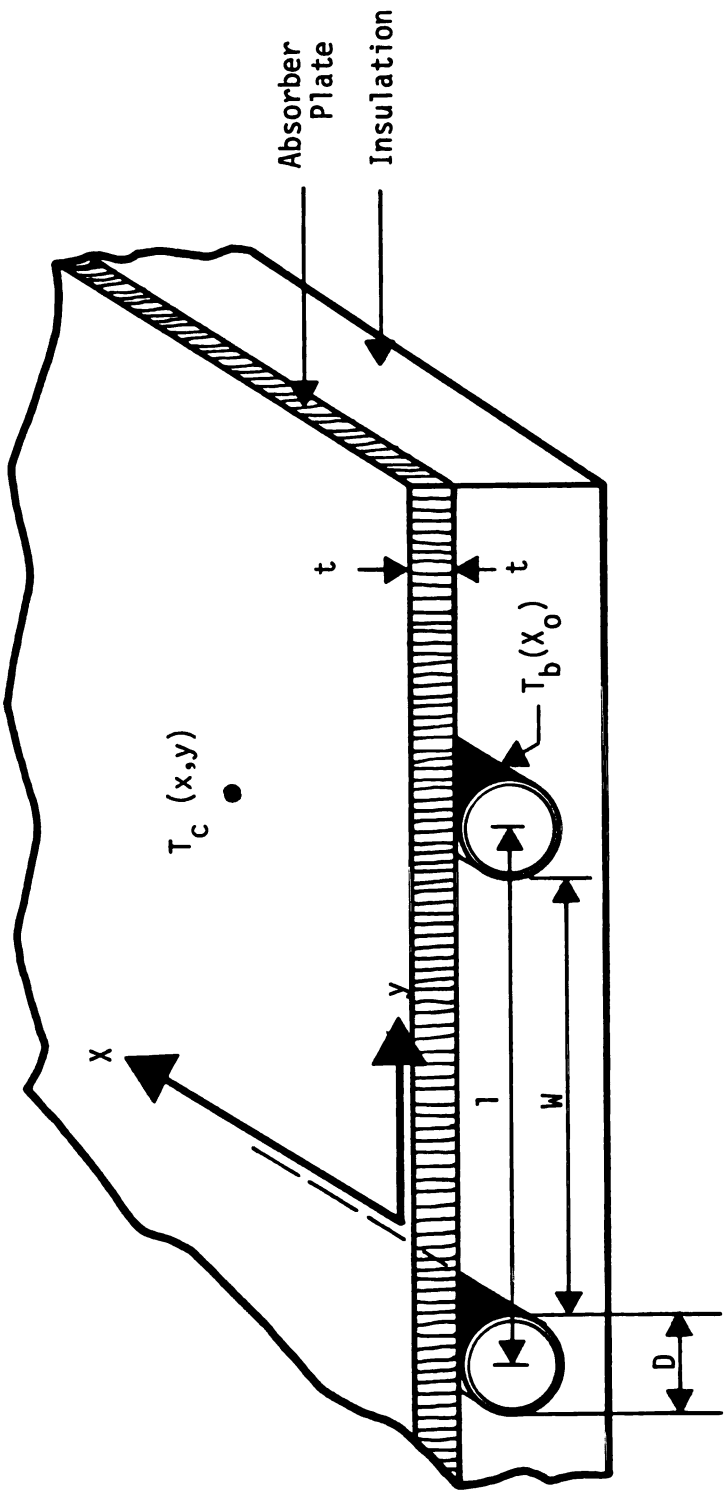

Figure 5.1.00Cross section of a solar collector.

The boundary conditions for the system shown in Figure 5.1 at fixed x_o are:

$$\frac{dT_c}{dy} = 0 \qquad \text{at} \quad y = 0$$

and

$$T_c = T_b\,(x_o) \qquad \text{at} \quad y = w$$

letting

$$m^2 = \frac{U_L}{Kt} \quad \text{and} \quad \xi = T_c - \left(T_a + \frac{S}{U_L}\right)$$

Equation [5.7] becomes

$$\frac{d^2\xi}{dy^2} = m^2\,\xi \qquad [5.8]$$

subject to boundary conditions

$$\frac{d\xi}{dy} = 0 \quad \text{at} \quad y = 0$$

$$\text{and } \xi = T_b\,(X_0) - \left(T_a + \frac{S}{U_L}\right) \quad \text{at } y = w$$

Equation [5.8] is linear in ξ and also homogenous. Its solution is

$$\xi = a_1 e^{my} + a_2 e^{-my} \qquad [5.9]$$

Using the two boundary conditions and substituting for ξ, Equation [5.9] yields

$$\frac{T_c - (T_a + \frac{S}{U_L})}{T_b(x) - (T_a + \frac{S}{U_L})} = \frac{\cosh my}{\cosh mw} \qquad [5.10]$$

Therefore, the energy conducted to both sides of the tube is

$$q_t(x_o) = 2w\,[S - U_L\,(T_b(x_o) - T_a)]\,\frac{\tanh mw}{mw} \qquad [5.11]$$

Defining fine efficiency, η_f, as (Meyers, 1971)

$$\eta_f = \frac{\tanh mw}{mw}$$

Equation [5.11] in terms of fin efficiency can be written as

$$q_t(x_o) = 2w\eta_f\,[S - U_L\,(T_b(x_o) - T_a])) \qquad [5.12]$$

In addition, heat is transferred from above the tube region which is

$$q_d(x_o) = D\,[S - U_L\,(T_b(x_o) - T_a)] \qquad [5.13]$$

Combinations of Equations [5.12] and [5.13] results in the useful energy gain per unit length in the direction of the flow

$$q_u(x_o) = (D + 2w\eta_f)\,[S - U_L\,(T_b(x_o) - T_a)] \qquad [5.14]$$

The useful energy in Equation [5.14] must be transferred to the working fluid. If the thermal resistance of the metal wall of the tube is negligible, the rate of heat transfer to the fluid is

$$q_u\ (x_o) = \frac{T_b(x_o) - T_f(x_o)}{1/h_{f,i}\pi D_i + 1/C_b} \qquad [5.15]$$

where $h_{f,i}$ is the heat transfer coefficient between the tube wall and the fluid, D_i is the inside tube diameter, C_b the bond conductance, and $T_f(x_o)$ is the fluid temperature.

Solving for $T_b(x_o)$ in Equation [5.15] and substituting this relation in Equation [5.14] results in

$$q_u\ (x_o) = \ell F' \left[S - U_L(T_f\ (x_o) - T_a)\right] \qquad [5.16]$$

where F' is called the collector efficiency factor given by

$$F' = \frac{1/U_L}{\ell\left[\frac{1}{U_L\ (D + 2\ w\eta_f)} + \frac{1}{C_b} + \frac{1}{\pi D_i h_{f,i}}\right]} \qquad [5.17]$$

The collector efficiency factor was first discussed by Hottle and Whillier (1958). It is dependent on U_L, $h_{f,i}$, and η_f and slightly dependent on temperature. For practical purposes F' can be treated as a design parameter.

Equation [5.16] gives the rate of heat transfer at a given point x. Considering the temperature variation with x as shown in Figure 5.2 and writing an energy balance for a small section dx gives

$$\dot{m}\, c_p\, (T_{f|x+dx} - T_{f|x}) = q_u\, (x)\, dx \qquad [5.18]$$

Combinations of Equations [5.16] and [5.18] and integration with respect to $T_f(x)$ yields

$$q_u = A_c F_R\, [S - U_L\, (T_{f,in} - T_a)] \qquad [5.19]$$

where F_R is the heat removal factor defined by

$$F_R = \frac{G\, C_p}{U_L} [1 - \exp\, (\frac{U_L\, F'}{G\, c_p})] \qquad [5.20]$$

Where $G = \dot{m}/A_c$

Equations [5.19] and [5.4] are the same with the only difference, $T_{f,in}$ in [5.19] is known, whereas T_c in [5.4] cannot be determined.

Double-loop solar systems are often employed in climates with subfreezing winter temperatures. In addition, most collectors require use of corrosion inhibitors because corrosion-proof metals are expensive. In situations where antifreeze solutions are used in the place of water as working fluids, a heat exchanger is introduced to heat the water in the storage tank. Under these circumstances, a new efficiency factor, F_R', is applied instead of F_R in

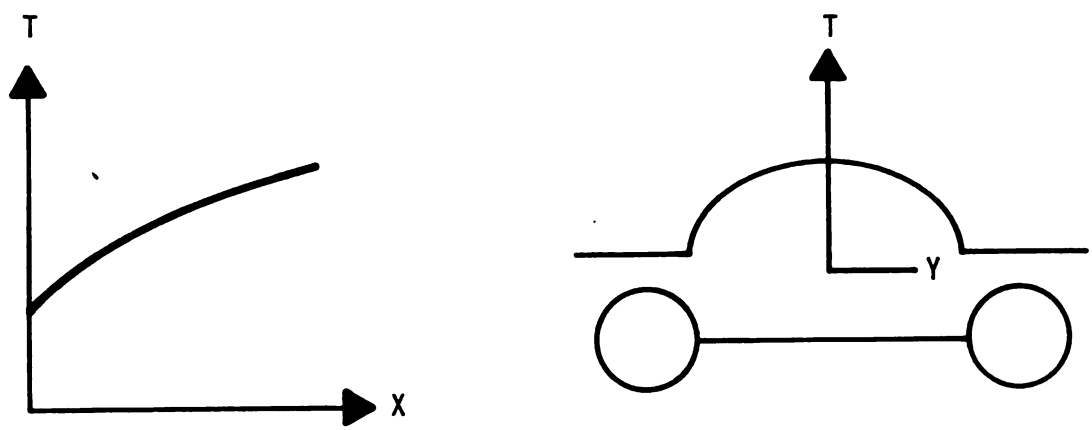

Figure 5.2.--Temperature distribution of absorber plate.

Equation [5.19]. The effectiveness of a heat exchanger, ε, defined by Keys and London (1958) as

$$\varepsilon = \frac{1}{1 + \frac{\dot{m}c_p}{U_A}}$$

together with the collector heat removal factor, F_R, dictate the value of F_R'.

DeWinter (1975) discussed the optimum size of the heat exchanger which maximizes the value of F_R' in double-loop solar systems.

The overall heat transfer coefficient, U_L, is the result of conductive losses from the back and radiative and convective losses from the top of the collector. The back loss coefficient, U_b, is easily calculated as a function of insulation thickness, l, and thermal conductivity, k;

$$U_b = k/l \qquad [5.21]$$

Calculation of the upward loss coefficient, U_{up}, is more complicated. Since it is the result of radiative and convective effects, factors such as wind speed, radiative properties of the materials, collector tilt and the number of glass covers must be taken into account. The following relationship is accurate within $\pm$ 0.2 W/m^2 - °C for plate temperatures between 40° and 130°C (Klein, 1973).

$$U_t = \left(\frac{N}{(344/T_p)[(T_p - T_a)/(N + f)]^{0.31}} + \frac{1}{h_w}\right)^{-1}$$

$$+ \frac{\sigma(T_p + T_a)(T_p^2 + T_a^2)}{[\varepsilon_p + 0.0425\ N\ (1 - \varepsilon_p)]^{-1} + [(2N + f - 1)/\varepsilon_g] - N} \qquad [5.22]$$

where N = number of glass covers;

$f = (1.0 - 0.04\ h_w + 5.0 \times 10^{-4}\ h_w^2)(1 + 0.058\ N)$;

εg = emittance of glass (0.88);

εp = emittance of plate;

T_a = ambient temperature (°K);

T_p = plate temperature (°K)

h_w = wind heat transfer coefficient = 5.7 + 3.8V

V = wind speed

Addition of Equations [5.21] and [5.22] yields

$$U_L = U_b + U_{up} \qquad [5.23]$$

The instantaneous efficiency of a collector, η, is defined as the ratio of the useful energy delivered to the total incident radiation

$$\eta = q_u/A_c\ HR \qquad [5.24]$$

For design purposes, the efficiency as a measure of collector performance must be calculated over a finite time period. Under these circumstances, the average efficiency is calculated by

$$\bar{\eta} = \frac{\int_0^t q_u \, dt}{\int_0^t A_c \, HR \, dt} \qquad [5.25]$$

Equation [5.19] indicates that U_L, F_R, and $(\tau\alpha)$ are the parameters with the strongest effect on collector performance. F_R is slightly effected by temperature while the angular dependence of $(\tau\alpha)$ is small for incident angles less than 45° (Duffie and Beckman, 1974). U_L can be either calculated from Equation [5.23] or a single value for U_L can be chosen.

Various design factors influencing flat plate collector performance are discussed by Whillier (1967), Duffie and Beckman (1974), and Kreith and Kreider (1978).

CHAPTER 6

SOLAR SYSTEM DESIGN

The potential of solar water heating in the food industry has been investigated by combining experimental and simulation work. A pilot plant solar water heater was built. The system was designed to supply a substantial amount of the energy needs of the dairy plant of Michigan State University. Preliminary findings regarding the operation and the performance of the solar water heater were used to examine specific solar water heaters for various processing plants in the United States. The TRNSYS and f-chart programs were used to model different sizes of solar systems and to determine their long-run performance.

6.1 Energy Audit

The first step of the solar system was to audit the MSU dairy plant from an energy point of view. Daily hot water needs, fuel price, and space availability are the main factors determining the size of a solar water heater.

In the dairy plant, various types of cheese, yogurt, and ice cream are manufactured. Operations identified in the plant are illustrated in Figures 6.1.1 through 6.1.3.

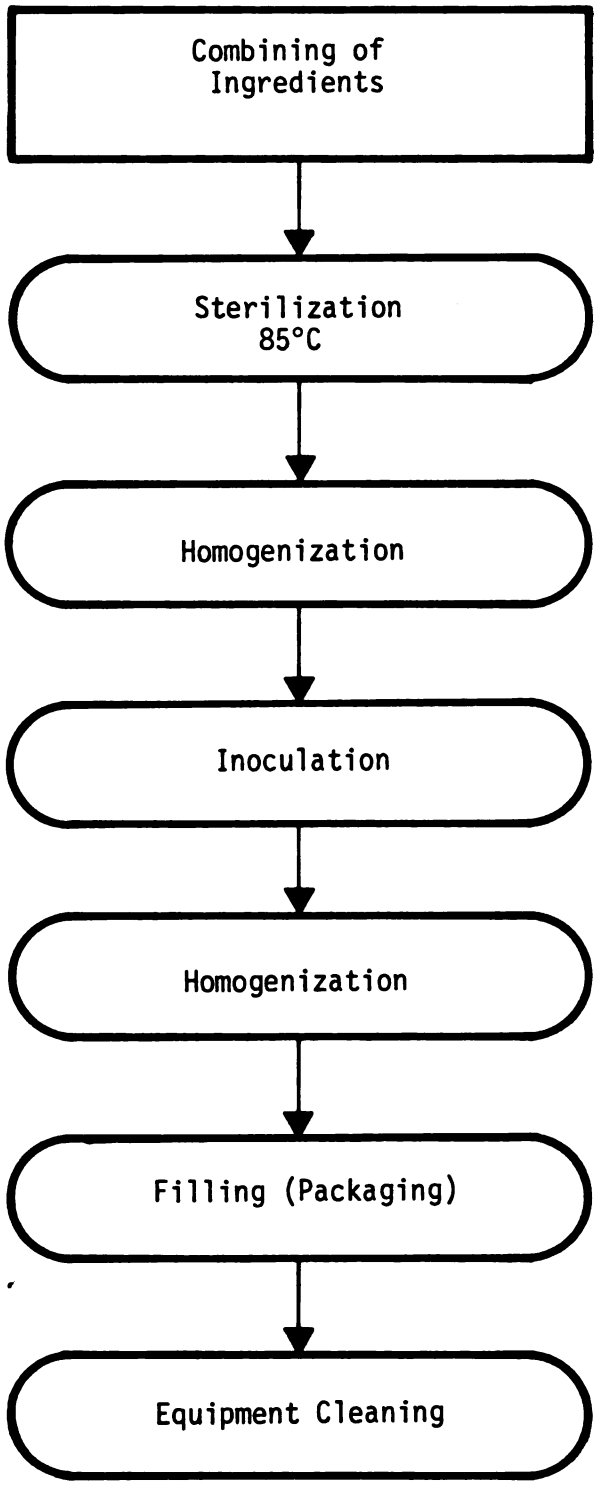

Figure 6.1.1.--Flow chart for yogurt manufacture in the MSU dairy plant.

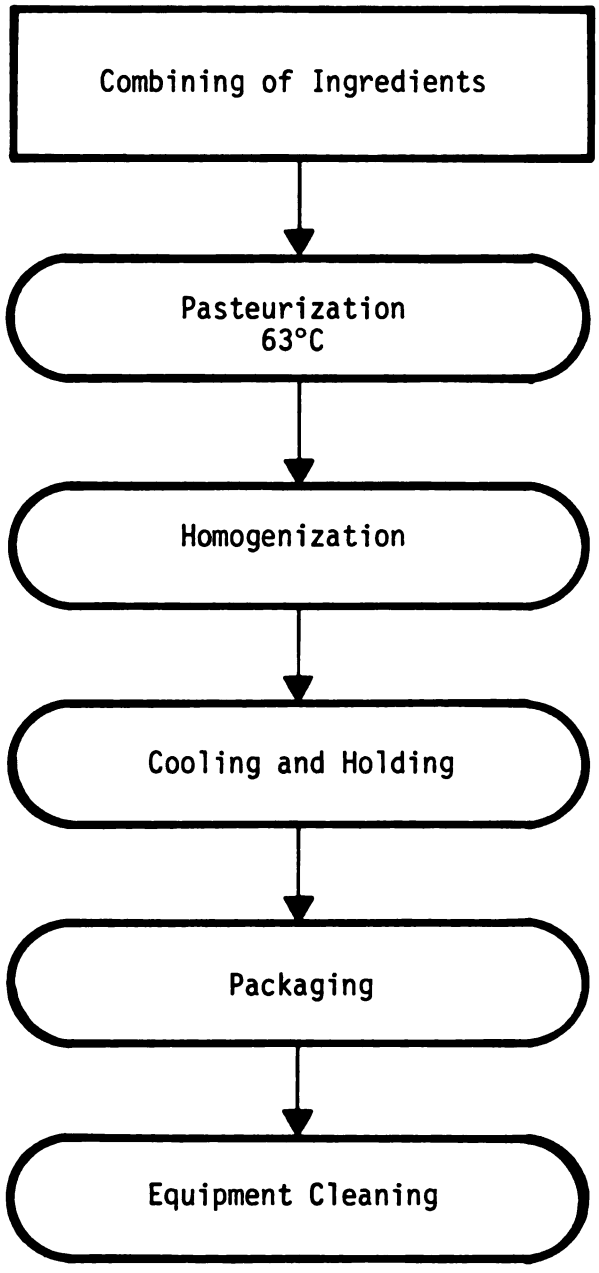

Figure 6.1.2.--Flow chart for ice cream manufacture in the MSU dairy plant.

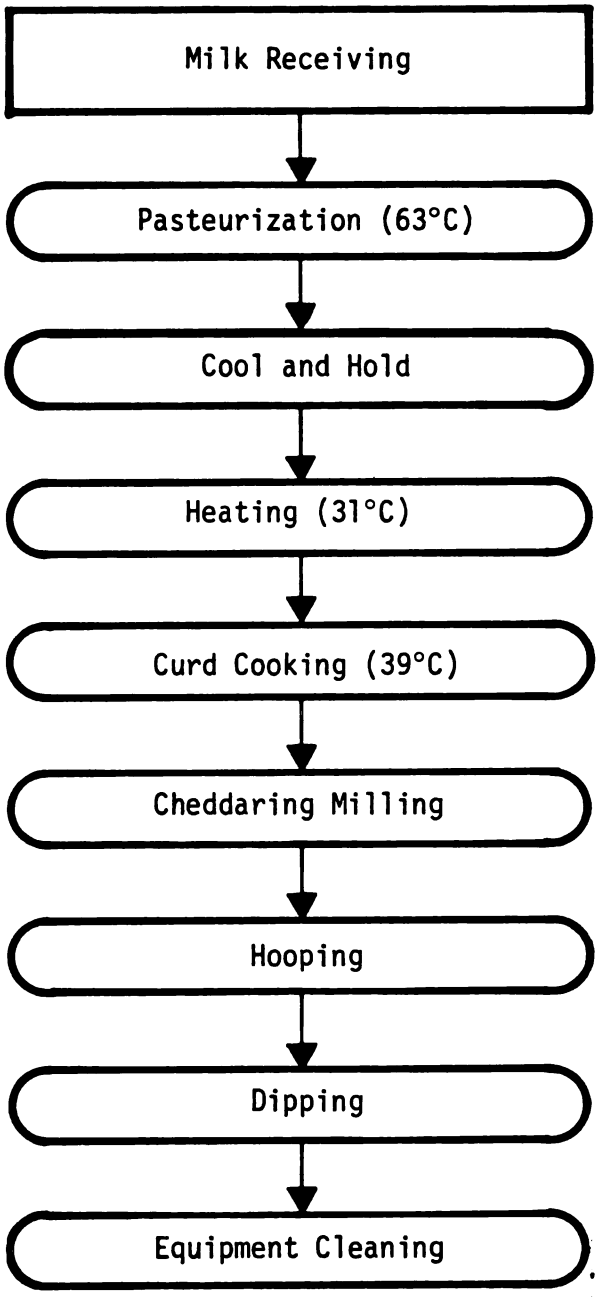

Figure 6.1.3.--Flow chart for cheese manufacture in the MSU dairy plant.

The weekly energy consumption in the plant is presented in Tables 6.1.1, 6.1.2 and 6.1.3. The energy consumed per Kg of finished product is also shown in the tables. Live steam generated

TABLE 6.1.1.--Weekly energy consumption for cheese processing at MSU Dairy Plant.

Energy Input	KJ/Week	KJ/KG Finished Product
Electrical	2,513,300	1950
Processing	2,658,700	2310
Cleaning	4,123,100	3190
TOTAL	9,295,100	7450

SOURCE: Dansburry, 1978.

TABLE 6.1.2.--Weekly energy consumption for ice cream processing at MSU Dairy Plant.

Energy Input	KJ/Week	KJ/KG Finished Product
Electrical	203,620	490
Processing	92,840	224
Cleaning	397,330	960
TOTAL	693,790	1674

SOURCE: Dansburry, 1978.

TABLE 6.1.3.--Weekly energy consumption for yogurt processing at MSU Dairy Plant.

Energy Input	KG/Week	KJ/KG Finished Product
Electrical	88,620	220
Processing	118,170	290
Cleaning	323,480	795
TOTAL	530,270	1305

SOURCE: Dansburry, 1978.

at the MSU Power Plant is used as the heat source for all food processing operations. The steam arrives at the dairy plant at 85 psi (Rippen, 1977). Heat losses in the plant were calculated by Dansbury (1978). The solar water heater is designed to supply hot water for processing and sanitation. The daily distribution of the hot water to be supplied by the solar system is shown in Figures 6.14, 6.15, and 6.16. The peaks in the figures represent hot water used for cleaning floors and processing equipment. The water is supplied at 74°C (165°F) at a daily rate of approximately 7600 Kg (2000 gal.). The plant does not operate during weekends.

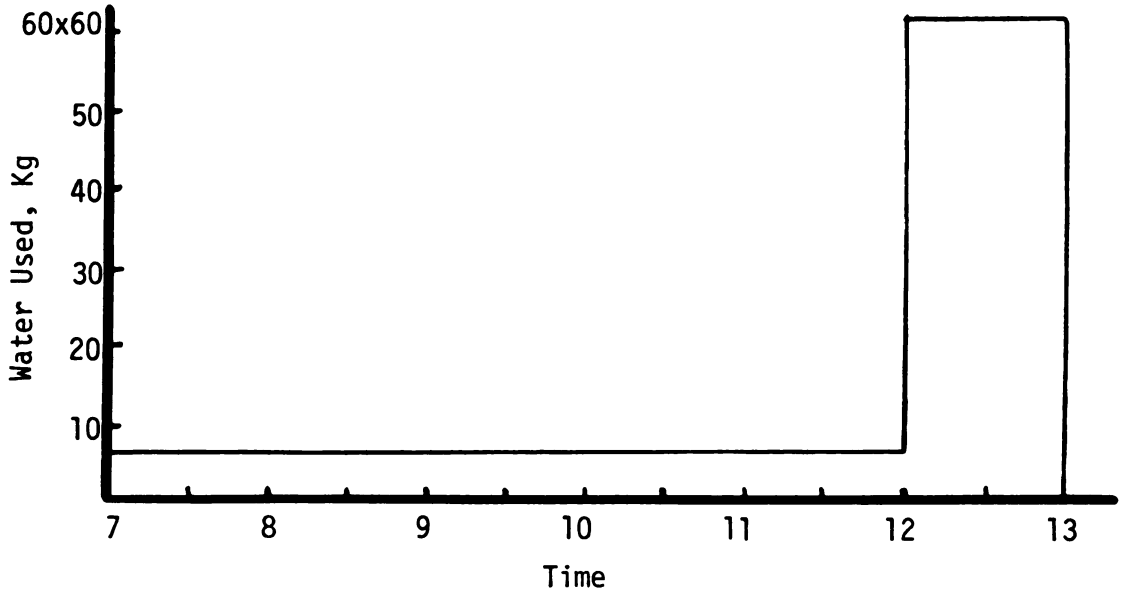

Figure 6.1.4.--Hot water consumption during cheddar cheese processing.

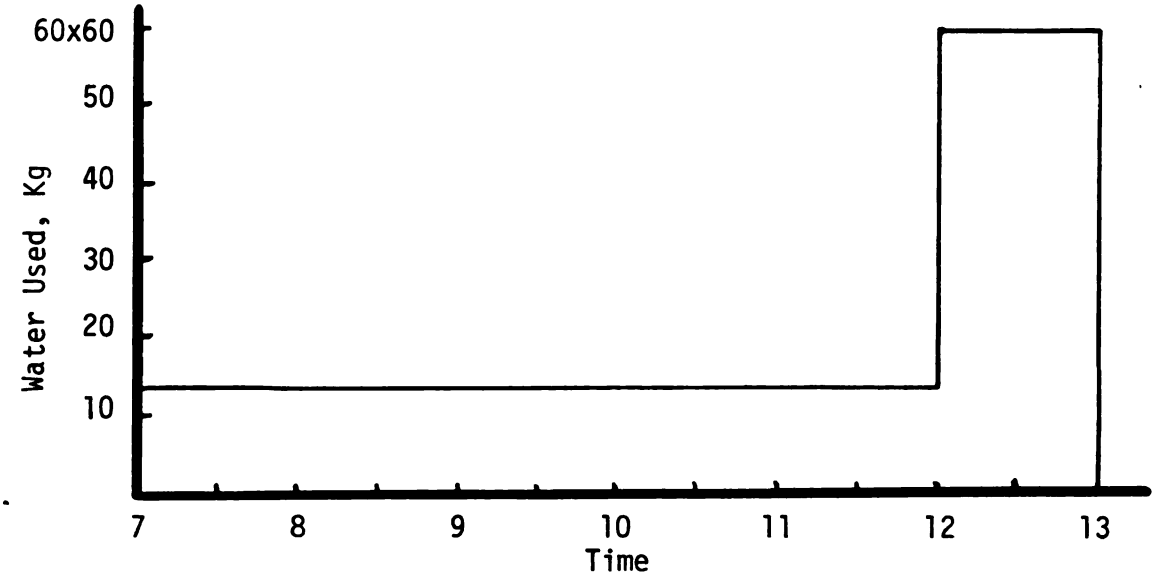

Figure 6.1.5.--Hot water consumption during acid cheese processing.

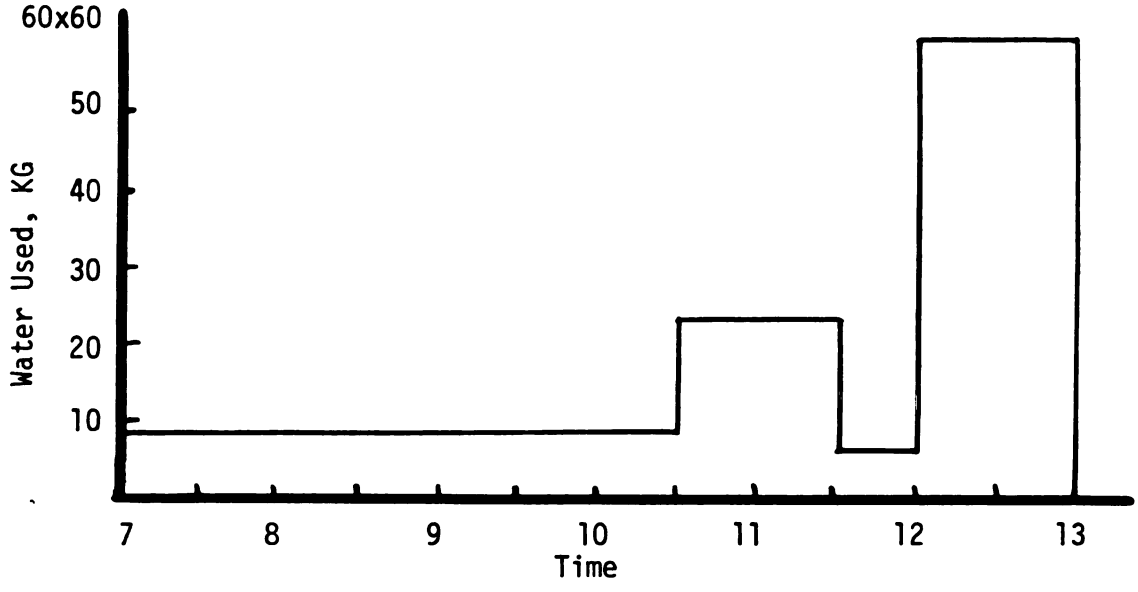

Figure 6.1.6.--Hot water consumption during cheese or ice cream processing.

6.2 Solar System Sizing

The optimum size of the solar system was assumed to be the one which will meet the hot water requirements in the dairy plant established by the energy audit. However, economic constraints may limit the size of the system to a point where only a fraction of the hot water could be attributed to solar energy. Further increase of the system size would be financially unjustifiable. Based on the parameters determined by the energy audit and the economic scenario presented in Table 6.2.1, the f-chart program was used to obtain the size of the solar system.

TABLE 6.2.1.--Economic criteria used to size the solar system.

Period of economic analysis	20 years
Collector cost	200 $/m^2
Collector indepencent cost	2000 $
Down payment (percent of original)	10 percent
Interest rate of mortgage	8 percent
Discount rate	8 percent
Inflation rate	6 percent
Fuel cost	10 $/GJ
Annual fuel rise	20 percent

6.2.1 Application of the f-chart Program

The f-chart program is programmed to be used in an interactive mode program. The computer asks the user yes or no questions followed by a branch point. The user answers with "Y" or "N", followed by a branch point. The nature of the questions asked are presented in Table 6.2.2.

At the branch point the user has the following options:

A. To list the parameter values which describe the solar system under investigation. By typing "L" the parameters presented in Table 6.2.3 are listed.

B. To change the value of the parameters. The value of a parameter will change by typing the parameter code followed by a comma and the new value. Table 6.2.4 shows change of value of various parameters.

C. Entering "R" the program performs a thermal analysis like the one shown in Table 6.2.5 and unless the user specified otherside, an economic analysis will follow.

D. Execution of the program is terminated by entering "S".

Other options such as listing weather data, adding weather data, returning to the beginning of the program and changing units are also offered.

f-Chart is composed of a MAIN program and the subroutines CALC, ECON, YESNO RADIN, TAUALF, RBAR, CYREAD, and DATAIN. Weather and location data used by the program are in the form of five data

TABLE 6.2.2.--Questions asked by the f-chart program.

```
DO YOU NEED INSTRUCTIONS(Y,N OR X)?N
YOU MAY USE EITHER SI OR ENGLISH UNITS.
DO YOU WISH TO USE SI UNITS?Y
WOULD YOU LIKE A LISTING OF LOCATIONS FOR WHICH CALCULATIONS CAN BE
MADE?N
YOU MAY MODEL THE SPACE HEATING LOAD USING THE DEGREE-DAY CONCEPT
OR YOU MAY TYPE IN A SPACE HEATING LOAD FOR EACH MONTH.
DO YOU WISH TO USE THE DEGREE-DAY CONCEPT?Y
YOU MAY EITHER HAVE THE GROUND REFLECTANCE SET TO 0.2 FOR ALL MONTHS
OR YOU MAY TYPE IN A VALUE FOR EACH MONTH.
DO YOU WISH TO HAVE THE GROUND REFLECTANCE SET TO 0.2 FOR ALL MONTHS?Y
WOULD YOU LIKE THE PROGRAM TO PERFORM AN ECONOMIC ANALYSIS?Y
IS THIS AN INCOME PRODUCING BUILDING (NOT A RESIDENCE)?Y
TYPE IN CODE NUMBER AND NEW VALUEL
```

TABLE 6.2.3.--Description of parameters used by f-chart.

CODE	VARIABLE DESCRIPTION	VALUE	UNITS
1	AIR SH+WH=1,LIQ SH+WH=2,AIR OR LIQ WH ONLY=3.	2.00	
2	IF 1,WHAT IS (FLOW RATE/COL.AREA)(SPEC.HEAT)?	12.23	W/C-M2
3	IF 2,WHAT IS (EPSILON)(CMIN)/(UA)?.....	2.00	
4	COLLECTOR AREA.....	50.00	M2
5	FRPRIME-TAU-ALPHA PRODUCT(NORMAL INCIDENCE)..	.70	
6	FRPRIME-UL PRODUCT.....	4.72	W/C-M2
7	INCIDENCE ANGLE MODIFIER (ZERO IF NOT AVAIL.)	0.00	
8	NUMBER OF TRANSPARENT COVERS.....	2.00	
9	COLLECTOR SLOPE.....	43.00	DEGREES
10	AZIMUTH ANGLE (E.G. SOUTH=0, WEST=90).....	0.00	DEGREES
11	STORAGE CAPACITY.....	315.00	KJ/C-M2
12	EFFECTIVE BUILDING UA.....	24000.00	KJ/C-DAY
13	CONSTANT DAILY BLDG HEAT GENERATION.....	0.00	KJ/DAY
14	HOT WATER USAGE.....	300.00	L/DAY
15	WATER SET TEMP.(TO VARY BY MONTH,INPUT NEG.#)	60.00	C
16	WATER MAIN TEMP(TO VARY BY MONTH,INPUT NEG.#)	11.00	C
17	CITY CALL NUMBER.....	132.00	
18	THERMAL PRINT OUT BY MONTH=1, BY YEAR=2.....	2.00	
19	ECONOMIC ANALYSIS ? YES=1, NO=2.....	1.00	
20	USE OPTMZD. COLLECTOR AREA=1, SPECFD. AREA=2.	2.00	
21	SOLAR SYSTEM THERMAL PERFORMANCE DEGRADATION.	0.00	PERCENT/YR
22	PERIOD OF THE ECONOMIC ANALYSIS.....	20.00	YEARS
23	COLLECTOR AREA DEPENDENT SYSTEM COSTS.....	100.00	$/M2 COLL.
24	CONSTANT SOLAR COSTS.....	1000.00	$
25	DOWN PAYMENT(PERCENT OF ORIGINAL INVESTMENT).	10.00	PERCENT
26	ANNUAL INTEREST RATE ON MORTGAGE.....	8.00	PERCENT
27	TERM OF MORTGAGE.....	20.00	YEARS
28	ANNUAL NOMINAL(MARKET) DISCOUNT RATE.....	8.00	PERCENT
29	EXTRA INSUR.,MAINT. IN YEAR 1(PCT ORIG.INV.)	1.00	PERCENT
30	ANNUAL PERCENT INCREASE IN ABOVE EXPENSES....	6.00	PERCENT
31	PRESENT COST OF SOLAR BACKUP FUEL (BF).....	6.00	$/GJ
32	BF RISE: PERCENT/YR=1,SEQUENCE OF VALUES=2...	1.00	
33	IF 1, WHAT IS THE ANNUAL RATE OF BF RISE.....	10.00	PERCENT
34	PRESENT COST OF CONVENTIONAL FUEL (CF).....	6.00	$/GJ
35	CF RISE: PERCENT/YR=1,SEQUENCE OF VALUES=2...	1.00	
36	IF 1, WHAT IS THE ANNUAL RATE OF CF RISE.....	10.00	PERCENT
37	ECONOMIC PRINT OUT BY YEAR=1, CUMULATIVE=2...	2.00	
38	EFFECTIVE FEDERAL-STATE INCOME TAX RATE.....	35.00	PERCENT
39	TRUE PROP. TAX RATE PER $ OF ORIGINAL INVEST.	2.00	PERCENT
40	ANNUAL PERCENT INCREASE IN PROPERTY TAX RATE.	6.00	PERCENT
41	CALC.RT. OF RETURN ON SOLAR INVTMT?YES=1,NO=2	2.00	
42	RESALE VALUE (PERCENT OF ORIGINAL INVESTMENT)	0.00	PERCENT
43	INCOME PRODUCING BUILDING? YES=1,NO=2.....	1.00	
44	DPRC.: STR.LN=1,DC.BAL.=2,SM-YR-DGT=3,NONE=4.	1.00	
45	IF 2, WHAT PCT OF STR.LN DPRC.RT.IS DESIRED?.	150.00	PERCENT
46	USEFUL LIFE FOR DEPREC. PURPOSES.....	20.00	YEARS

TYPE IN CODE NUMBER AND NEW VALUE

TABLE 6.2.4.--Value change of various parameters of the f-chart.

```
TYPE IN CODE NUMBER AND NEW VALUE1,3.
TYPE IN CODE NUMBER AND NEW VALUE5,.75
TYPE IN CODE NUMBER AND NEW VALUE6,3.5
TYPE IN CODE NUMBER AND NEW VALUE11,275.
TYPE IN CODE NUMBER AND NEW VALUE14,532000.
TYPE IN CODE NUMBER AND NEW VALUE15,72.
TYPE IN CODE NUMBER AND NEW VALUE17,69.
TYPE IN CODE NUMBER AND NEW VALUE18,1.
TYPE IN CODE NUMBER AND NEW VALUE20,1.
TYPE IN CODE NUMBER AND NEW VALUE23,200.
TYPE IN CODE NUMBER AND NEW VALUE24,2000.
TYPE IN CODE NUMBER AND NEW VALUE31,10.
TYPE IN CODE NUMBER AND NEW VALUE34,10.
TYPE IN CODE NUMBER AND NEW VALUE37,1.
TYPE IN CODE NUMBER AND NEW VALUE41,1.
TYPE IN CODE NUMBER AND NEW VALUER
WHAT IS THE COLLECTOR MODULE SIZE(FT2 OR M2)?2
```

TABLE 6.2.5.--Thermal and economic analysis performed by f-chart.

****THERMAL ANALYSIS****

TIME	PERCENT SOLAR	INCIDENT SOLAR (GJ)	HEATING LOAD (GJ)	WATER LOAD (GJ)	DEGREE DAYS (C-DAY)	AMBIENT TEMP (C)
JAN	24.8	54.62	0.00	62.19	730.	-5.0
FEB	50.1	78.23	0.00	56.17	638.	-4.0
MAR	64.4	106.78	0.00	62.19	553.	0.0
APR	63.4	98.70	0.00	60.18	308.	8.0
MAY	77.4	123.10	0.00	62.19	156.	13.0
JUN	84.2	127.50	0.00	60.18	27.	19.0
JUL	86.1	133.32	0.00	62.19	5.	21.0
AUG	83.5	127.88	0.00	62.19	15.	20.0
SEP	79.3	117.74	0.00	60.18	74.	16.0
OCT	65.5	101.55	0.00	62.19	234.	10.0
NOV	31.7	57.34	0.00	60.18	443.	3.0
DEC	23.3	51.53	0.00	62.19	653.	-2.0
YR	61.2	1178.30	0.00	732.25	3836.	

****ECONOMIC ANALYSIS****

OPTIMIZED COLLECTOR AREA = 218.0 M2
INITIAL COST OF SOLAR SYSTEM = $ 45600.
THE ANNUAL MORTGAGE PAYMENT FOR 20 YEARS = $ 4180.

YR	INTRST PAID	END OF YR PRINC	DEPRC DEDUCT	PROP TAX PAID	INC TAX SAVED	BACKUP FUEL COST	INSUR, MAINT COST	COST WITH SOLAR	SAVNGS WITH SOLAR	PW OF SOLAR SAVNGS
0	0	41040	0	0	0	0	0	4559	-4559	-4559
1	3283	40143	2280	911	3420	2841	455	4969	-209	-194
2	3211	39174	2280	966	3523	3126	483	5232	3	2
3	3133	38128	2280	1024	3636	3438	512	5519	239	190
4	3050	36998	2280	1086	3759	3782	543	5832	503	369
5	2959	35778	2280	1151	3894	4160	575	6173	795	541
6	2862	34461	2280	1220	4042	4576	610	6545	1120	706
7	2756	33037	2280	1293	4204	5034	646	6950	1481	864
8	2643	31500	2280	1371	4381	5537	685	7393	1881	1016
9	2520	29840	2280	1453	4575	6091	726	7876	2325	1163
10	2387	28048	2280	1540	4787	6700	770	8404	2818	1305
11	2243	26112	2280	1633	5020	7371	816	8980	3365	1443
12	2088	24021	2280	1731	5275	8108	865	9609	3970	1576
13	1921	21762	2280	1835	5555	8918	917	10295	4641	1706
14	1741	19323	2280	1945	5862	9810	972	11046	5385	1833
15	1545	16689	2280	2061	6198	10791	1030	11866	6208	1957
16	1335	13844	2280	2185	6567	11871	1092	12761	7120	2078
17	1107	10772	2280	2316	6972	13058	1158	13741	8129	2197
18	861	7454	2280	2455	7416	14364	1227	14811	9246	2313
19	596	3870	2280	2603	7903	15800	1301	15981	10481	2428
20	309	0	2280	2759	8438	17380	1379	17261	11848	2542

THE RATE OF RETURN ON THE SOLAR INVESTMENT(PER CENT)= 23.8
YRS UNTIL UNDISC. FUEL SAVINGS = INVESTMENT 10.
YRS UNTIL UNDISC. SOLAR SAVINGS = MORTGAGE PRINCIPAL 13.
UNDISCOUNTED CUMULATIVE SOLAR SAVINGS = $ 76797.
PRESENT WORTH OF YEARLY TOTAL COSTS WITH SOLAR = $ 84032.
PRESENT WORTH OF YEARLY TOTAL COSTS W/O SOLAR = $ 105515.
PRESENT WORTH OF CUMULATIVE SOLAR SAVINGS = $ 21484.

TYPE IN CODE NUMBER AND NEW VALUES
GOOD-BYE
STOP
1.117 CP SECONDS EXECUTION TIME

blocks, namely CITYDATA, SOLDATA, DDDATA, TADATA, and TEXT. The data contain city labels and latitudes, monthly average total radiation on a horizonatal surface, monthly average degree days, and monthly average ambient temperature. Data is available for 266 cities in the United States and Canada.

Notations and symbols used by the original program had to be changed to a certain extent to be recognized by the MSU CDC 6500 computer, since the program was originally developed to run on a UNIVAC 1110 computer. The core requirement of f-chart is 32,000 words decimal (Hughes et al., 1978). For thermal analysis the execution time is 1.044 CP sec and the cost is $1.90. If economic analysis is performed, the time is 1.111 CP sec and the cost is $2.27 (1980 MSU rate).

Tables 6.2.2 through 6.2.5 represent the run made to size the solar water heater for the dairy plant. In Table 6.2.5 an optimized area of 218 m^2 is shown. The thermal analysis of this size system indicated that 61.2 percent of the hot water needs in the plant could be supplied by solar.

6.2.2 Space Requirements

The roof of the plant was considered the original site to install the solar collector. Its area is large enough for installing a 218 m^2 solar collector. Evaluation of the roof strength revealed that reinforcement was necessary. Solar retrofit, under these circumstances, was rejected on the basis of economics. The collector was finally installed on the ground approximately 60 m (200 ft) away from the dairy plant.

Space availability limited the area of the collector fo 116 m^2. The area of the proposed solar collector was about 100 m^2 smaller than the optimum area (218 m^2) determined by f-chart.

6.3 Solar System Modeling

6.3.1 Description of TRNSYS

Modeling of the solar system shown in Figure 6.3.1 was conducted by developing a simulation model where the system and its components were sized in accordance to the energy requirements in the dairy plant. The model together with measured hourly weather data were combined with the TRNSYS program to form an executable element.

The functional properties of TRNSYS are explained in the diagram shown in Figure 6.3.2. The MAIN program contains the alsorithm for solving differential equations. Subroutines PROC, CLOCK, EXEC, and PRINT are called by MAIN. PROC reads and processes the user's model. Subroutine CLOCK contains the time clock and the print/reset timers for the output producing components. Subroutine EXEC calls the component subroutines and checks the input/output connections for convergence. Subroutine PRINT handles the output producing components. The BLOCK DATA is a non-executable subroutine and it is used to initialize variables in common.

The TRNSYS deck, consisting of control and data cards, contains the information required to simulate a solar system. A description of each card can be found in the TRNSYS manual (Klein et al., 1979). A sample TRNSYS deck is listed in Appendix A.

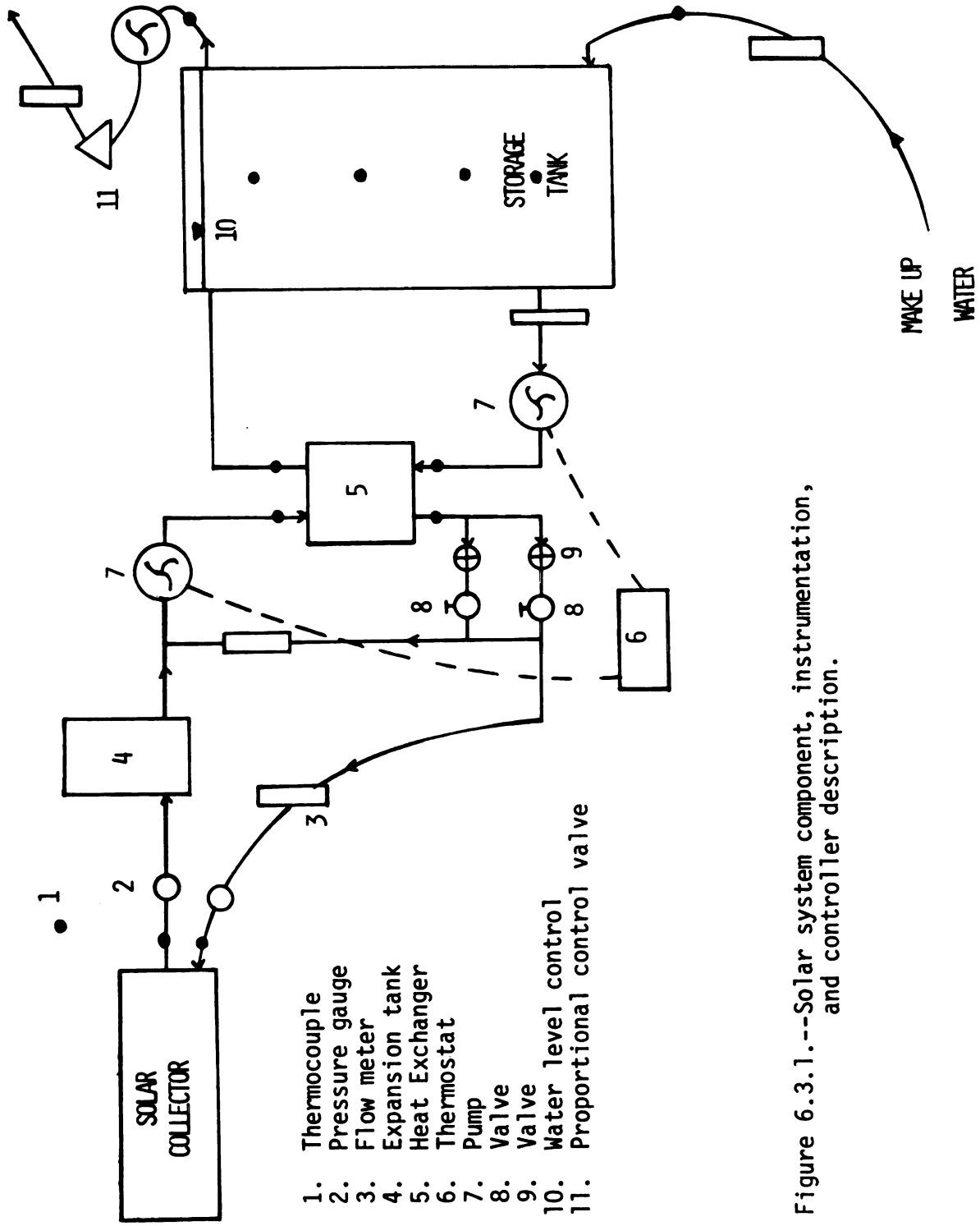

1. Thermocouple
2. Pressure gauge
3. Flow meter
4. Expansion tank
5. Heat Exchanger
6. Thermostat
7. Pump
8. Valve
9. Valve
10. Water level control
11. Proportional control valve

Figure 6.3.1.--Solar system component, instrumentation, and controller description.

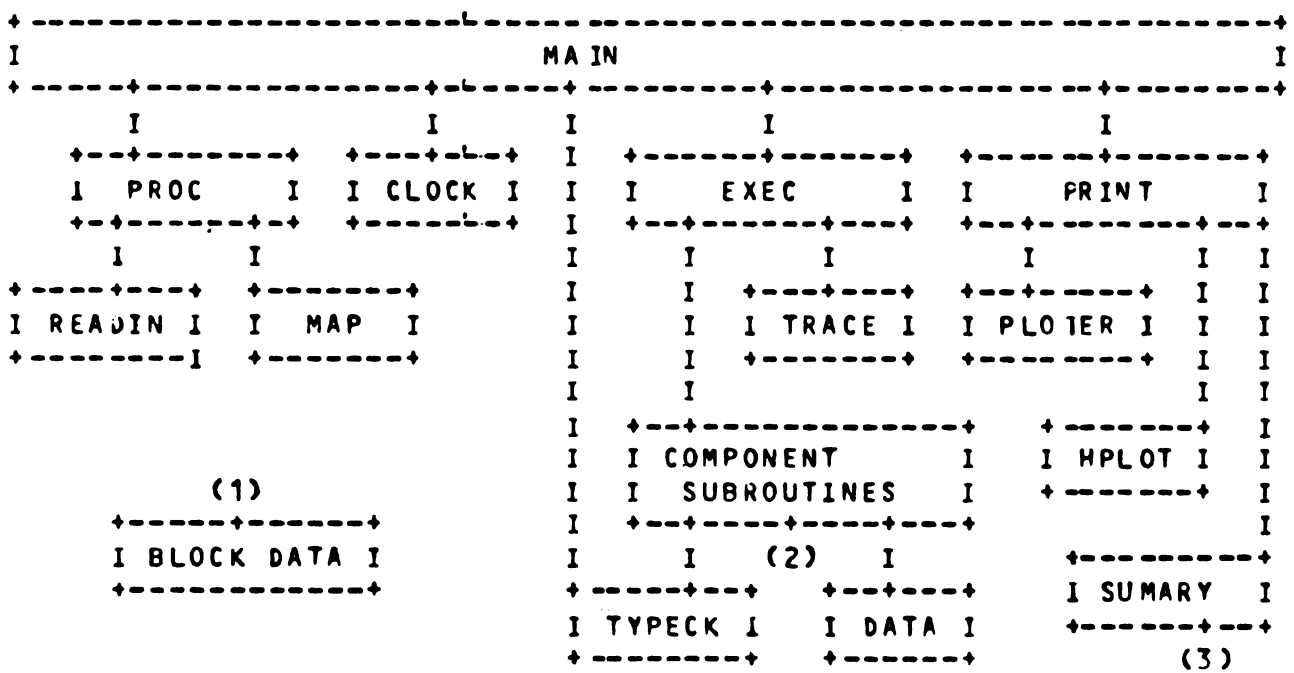

Figure 6.3.2.--Block diagram of TRNSYS subroutines and MAIN program.

Each component subroutine is identified by a UNIT and TYPE number. Two components may have the same TYPE number but the UNIT number must be unique for each component.

Each component has a fixed number of inputs, outputs, and parameters and they can be identified by consulting the TRNSYS manual.

The latest TRNSYS version (v. 10.1) contains 38 component subroutines. The user, however, most likely will not use all of them within one system. It is advisable to eliminate the unnecessary ones to decrease the core requirements and the simulation cost.

TRNSYS requires 12.244 sec at a cost of $17.48 at RG3. The core requirements for the run is about 120,000 words.

6.3.2 System Modeling

The overall behavior of a solar system is determined by TRNSYS by solving a set of algebraic and/or differential equations. The time step and the tolerance limits used by the numerical integration algorithm were specified such that accuracy and minimum computing costs were met. Preliminary runs revealed that a time step of 0.25 hours and a tolerance of 0.01 were found to satisfy the above objectives. A maximum number of 40 iterations per step was allowed.

Knowledge of the specific task of each component of the solar system is necessary to generate a flow chart such as the one shown in Figure 6.3.3. Information presented in Figure 6.3.3 simplifies the development of the TRNSYS deck.

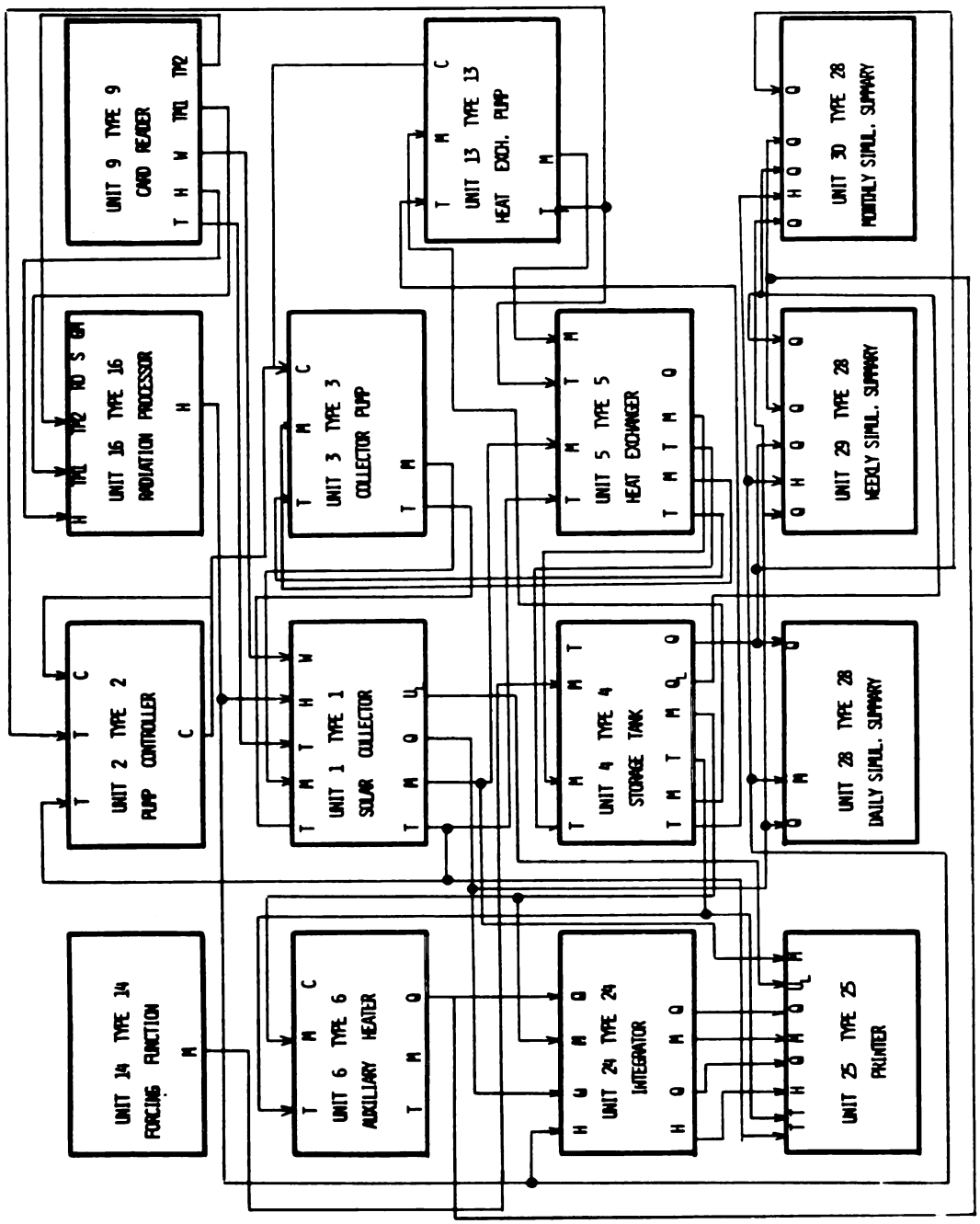

Figure 6.3.3.--Subroutine and information flow diagram of the TRNSYS solar water heating model.

Design parameters already established during system sizing, which was discussed earlier, were used to determine the value of the remaining parameters. The objective was to achieve operating conditions which wuld allow a temperature rise across the solar collector of 8° to 10°C (15°-20°F). This temperature range is recommended for maximum thermal output from a solar system (U.S. Department of Commerce, 1977).

Hourly weather data for the year 1974 in East Lansing was used by the program.

A number of preliminary runs were conducted to determine the value of the parameters used by TRNSYS. Their numerical values are presented in Table 6.3.1.

Based on the parameter values, a TRNSYS run resulted in solar system performance as shown in Table 6.3.2.

6.4 Solar Water Heater Characteristics

The solar collector array was built in the Department of Agricultural Engineering at MSU. It has an effective collective area of 116 m^2 (1250 ft^2).

The two transparent covers of the collectors are tempered glass with low iron content and with reflectivity and transmissivity values of 0.08 and 0.80, respectively, at normal incident.

The absorber plates are manufactured by Tranter, Inc. (Lansing, Michigan). The plates are full-flooded with a 90 percent internally wetted surface. The size of each plate is 209 cm by 87 cm (82.2 x 34.2 in.) providing an effective surface area of 1.83 m^2

TABLE 6.3.1.--Parameter Values Used in Solar System Design.

RADIATION PROCESSOR UNIT 16 TYPE 16			
	1.	Mode	1
	2.	Day of year of start of the simulation	1
	3.	Latitude	42.7°C
	4.	Solar constant	4871 KJ/m^2-hr
	5.	Shift of solar time angle	0
SOLAR COLLECTOR UNIT 1 TYPE 1			
	1.	Mode	1
	2.	Area	116 m^2
	3.	F'	0.95
	4.	Specific heat of fluid	3.64 KJ/Kg-C
	5.	Collector absorbance	0.90
	6.	Number of glass covers	2
	7.	Collector plate emittance	0.10
	8.	Back loss coefficient	0.5 KJ/hr-min^2-C
	9.	Transmittance of glass	0.82
PUMP CONTROLLER UNIT 2 TYPE 2			
Parameter:	1.	NSTK	4
	2.	Upper dead band difference	10°C
	3.	Lower dead band difference	3°C
COLLECTOR PUMP UNIT 3 TYPE 3			
Parameter:	1.	Maximum flow rate	15000 Kg/hr
HEAT EXCHANGER UNIT 5 TYPE 5			
Parameter	1.	Mode 2	counterflow
	2.	US	12000 KJ/hr-C
	3.	Specific heat of hot fluid	3.64
	4.	Specific heat of cold fluid	4.186
HEAT EXCHANGER PUMP UNIT 13 TYPE 3			
Parameter:	1.	Maximum flow rate	15000 Kg/hr
STORAGE TANK UNIT 4 TYPE 4			
Parameter:	1.	Tank volume	7.6 m^2
	2.	Tank height	3
	3.	Specific heat of fluid	4.186
	4.	Fluid density	1000 Kg/m^3
	5.	Loss coefficient	1
AUXILLARY HEATER UNIT 6 TYPE 6			
Parameter:	1.	Maximum heating rate	10^6 KJ/hr
	2.	Set temperature	74°C
	3.	Specific heat of fluid	4.186

TABLE 6.3.2.--Solar system monthly performance.

Month	Efficiency	Percentage of Load Supplied by Solar
January	43.1	22.0
February	43.3	37.5
March	43.1	40.4
April	46.5	55.3
May	45.0	44.5
June	48.6	57.4
July	48.8	66.0
August	50.0	62.0
September	48.0	56.5
October	48.7	45.4
November	46.9	25.9
December	43.4	22.5
YEAR	47.0	44.7

(19.6 ft^2). The plates are constructed of 18 gauge (0.048 psia) carbon steel. The pressure drop through one plate is 2 psia at a flow rate of 2.3 Kg of water per minute (0.6 gpm), which assures satisfactory uniform flow distribution over the plate.

The spacing between the glass cover directly above the adsorber of each collector is 2.54 cm (1 in.), with another inch between the lower glass plate and the top cover glass. Six inches of fiberglass insulation (R19) is placed under the absorber plates. The absorber plate, glass covers, and insulation are assembled as a module into a wooden frame box with a total depth of 16.5 cm (6.5 in.).

Black silicone paint constitutes the non-selective absorber plate coating. The solar absorbance of the coating is 0.92, the emittance is 0.86.

The total set of collector plates is 64. Four plates are assembled in one large module. The modules are assembled side by side to form an array of south facing collectors. The tilt of the collector is variable. Figure 6.4.1 is a schematic diagram of the collector array.

Ethylene glycol at a concentration of 30 percent is used as the collector fluid. A nitrate base corrosion inhibitor is added.

The collector modules are mounted on A frames and the system is designed to withstand a maximum of 100 mph wind.

A 2200 gallon cylindrical fiberglass storage tank functions as the energy storage device. This results in 1.8 gal per ft^2 collector (73.3 kg/m^2). The maximum design water temperature of the

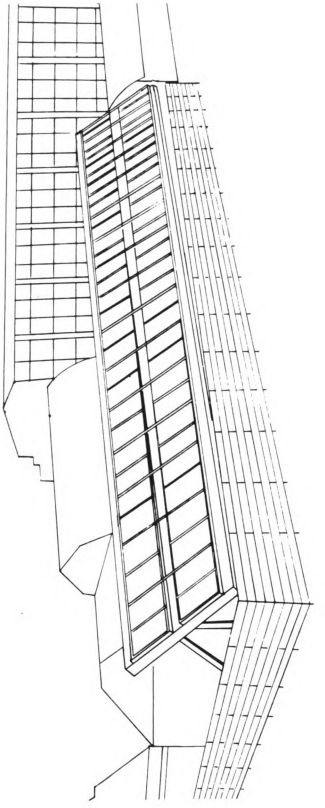

Figure 6.4.1.--Schematic diagram of the collector array.

tank is 82.2°C (180°F). The dimensions of the tank are 1.82 m (72 in.) diameter by 3.05 m (120 in.). The tank is insulated by cellulose insulation (R20). The storage tank is not pressurized. A float valve provides make-up water.

The solar water heater is a dual liquid system, employing a heat exchanger for the transferring of energy from the working fluid to the service water. One pump (1.5 HP) circulates the solution from the solar collectors to the liquid-to-liquid heat exchanger and back. A second pump (0.5 HP) circulates water from the storage tank through the heat exchanger and back to the tank. A 0.5 HP pump supplies the load requirements. A small make-up water tank with a vent to the atmosphere is placed in the collector loop to allow steam escape in case of power failure.

A plate type heat exchanger manufactured by Tranter, Inc., is used in the system. The exchanger consists of 16 plates fabricated of 316SS and has a total heat transfer area of 5.3 m^2 (56.5 ft^2). At a flow rate of 190 l/min (50 gpm) of glycol and 190 l/min water, the rated heat exchange (at a ΔT of 11.1°C between the solar heated glycol solution and the water) is about 242,000 KJ (230,000 BTU) per hour. The pressure drop under these circumstances is 9 psia in each loop.

Figure 6.3.1 is a schematic presentation of the solar system. It shows the location of system components, controls, valves, meters, and other instrumentation.

The controllers are solid-state with thermistor inputs and solid state switches and relays producing the electric impulses to

the motors and valves. A differential thermostat is used to sense the difference in temperature between the collector array outlet and the bottom of the storage tank. The sensor which measures the fluid temperature at the collector is located on the manifold pipe which collects the heated fluid from the collector array. The sensor in the storage tank is located in the bottom fourth inside the tank.

The differential thermostat will eventually be replaced by a Dynabyte microprocessor (Model 280). The unit is designed to act as a control, data acquisition, and load simulation device. The microprocessor contains 4K of RAM, 4K of EPROM, a keyboard input port, 300 BAUD audio cassette interface with file handling capabilities. The Dynabyte is programmed in BASIC.

Temperatures, pressure and flow rates are measured and checked as it is shown in Figure 6.3.1. Six additional thermocouples not shown in the figure have been attached to the collector array. The temperature recording system consists of an Esterline Angus digital thermocouple recorder (Model PD 2064, Key programmable system) and a paper tape puncher. The temperatures at 22points on the solar system are being recorded at hourly intervals.

Storage tank, heat exchanger, pumps, controllers, and temperature recorder, are all located in a specially built storage house. The arrangement inside the house is shown in Figure 6.4.2.

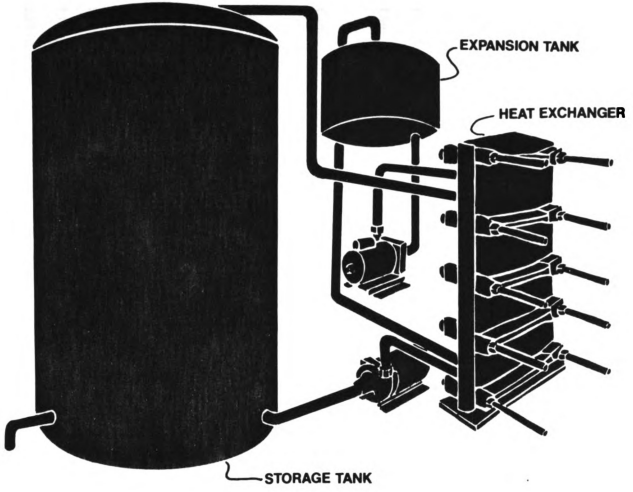

Figure 6.4.2.--Component arrangement in the storage house.

CHAPTER 7

ESTABLISHMENT OF HOT WATER DEMAND IN FOOD PROCESSING PLANTS

In general, load requirements in food processing plants are variable. Two or more operations of different temperature and flow rate can likely occur at the same time in a plant. Examination of the load requirement of a number of processing plants indicated that the load distribution is unique for each plant.

To generate representative energy demands, four selected food processing plants will be investigated: a milk plant in Wisconsin (Lund, 1977), a milk plant in Lansing, Michigan (Rippen and Mintzias, 1977), a meat plant in Indiana (Wilson et al., 1978), and the Michigan State University Dairy Plant.

Processes and energy requirements for the Wisconsin milk plant are shown in Table 3.3. Expressing the daily energy demand in the plant in terms of flow rate and temperature the daily energy demand distribution shown in Figure 7.1.1 is obtained. Each line in Figure 7.1.1 corresponds to a specific process. For example, the solid line is the energy consumed in the pasteurizer. To input the information of Figure 7.1.1 in TRNSYS is a time consuming process. In addition, a representative total energy demand is difficult to obtain from Figure 7.1.1. Expressing the energy demand in KJ/hr

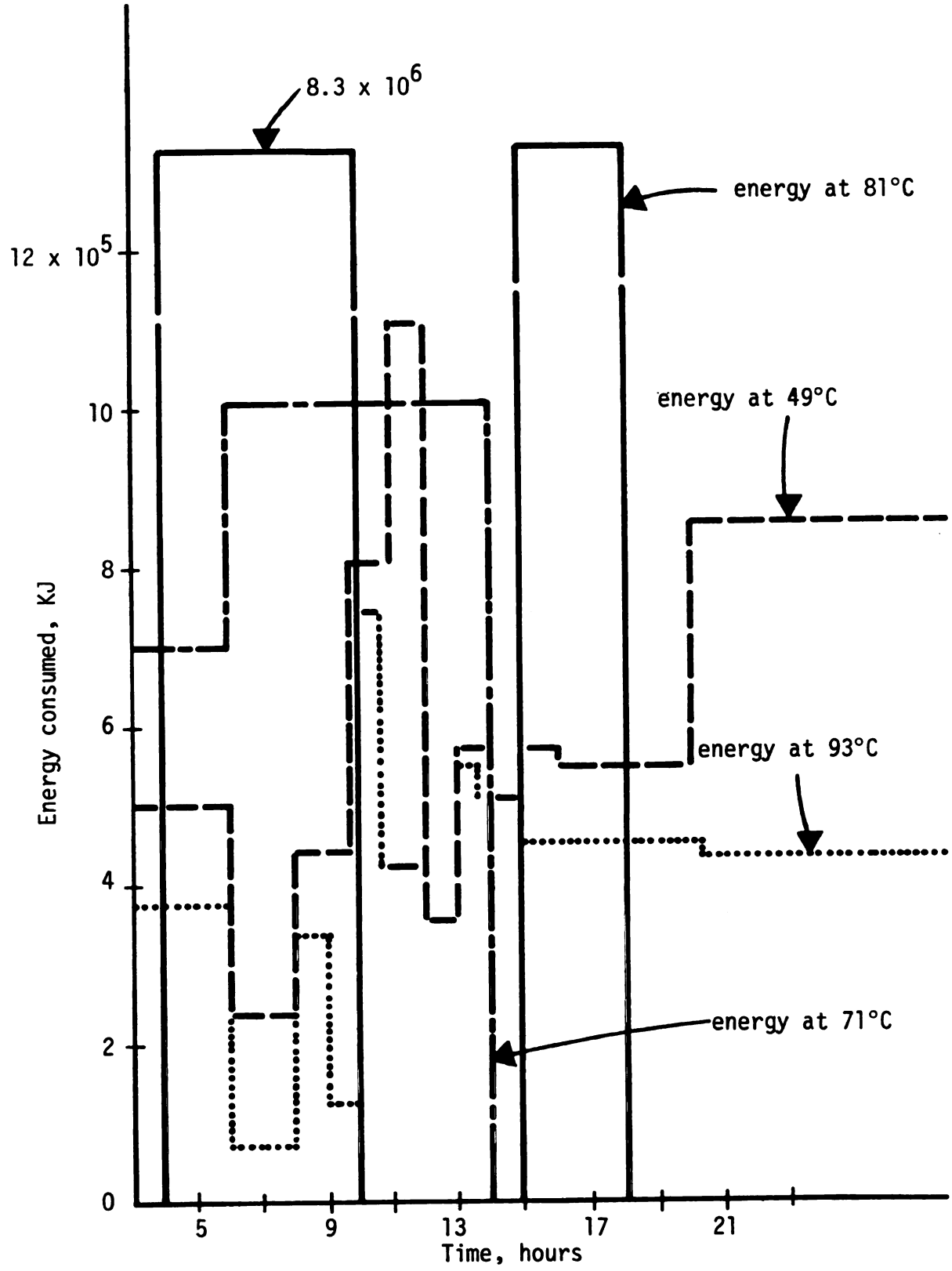

Figure 7.1.1.--Distribution of the daily energy consumed in the Wisconsin dairy plant.

instead of in terms of flow rate and temperature, the daily energy demand shown in Figure 7.1.2 is obtained. The demand in Figure 7.1.2 was approximated for the TRNSYS runs by Figure 7.1.3.

Similarly, the energy demand in the Lansing, Michigan milk plant was approximated as shown in Figure 7.1.4. It should be noted that the Wisconsin and Lansing, Michigan plants are both pasteurizing milk and orange juice, but their daily energy demand distribution show no similarity (see Figures 7.1.3 and 7.1.4).

In the meat processing plant the steam consumed to heat a 11,190 gallon dehairing tank was analyzed. The daily energy demand and distribution for the two processes are shown in Figure 7.1.5. The solid line in the Figure is the total energy. The load in Figure 7.1.5 was approximated by the graph (histogram) of Figure 7.1.6. This corresponds well with the relatively constant demand common in meat processing plants (Thomas, 1977; Lund, 1977).

The energy demand in the Michigan State University dairy plant (see Figures 6.1.4 and 6.1.5) was approximated as shown in Figure 7.1.7. This type of demand is common in small food processing plants with one working shift where cleaning floors and equipment is the last operation of the day.

The investigated plants resulted in five representative loads encountered in the food industry. The approximated loads are summarized in Figure 7.1.8 (Case A-d). Case E is assumed to account for a load with variable daily energy distribution.

Canning plants are not considered in this study. Canaries show seasonal operations and as a result a solar water heater does

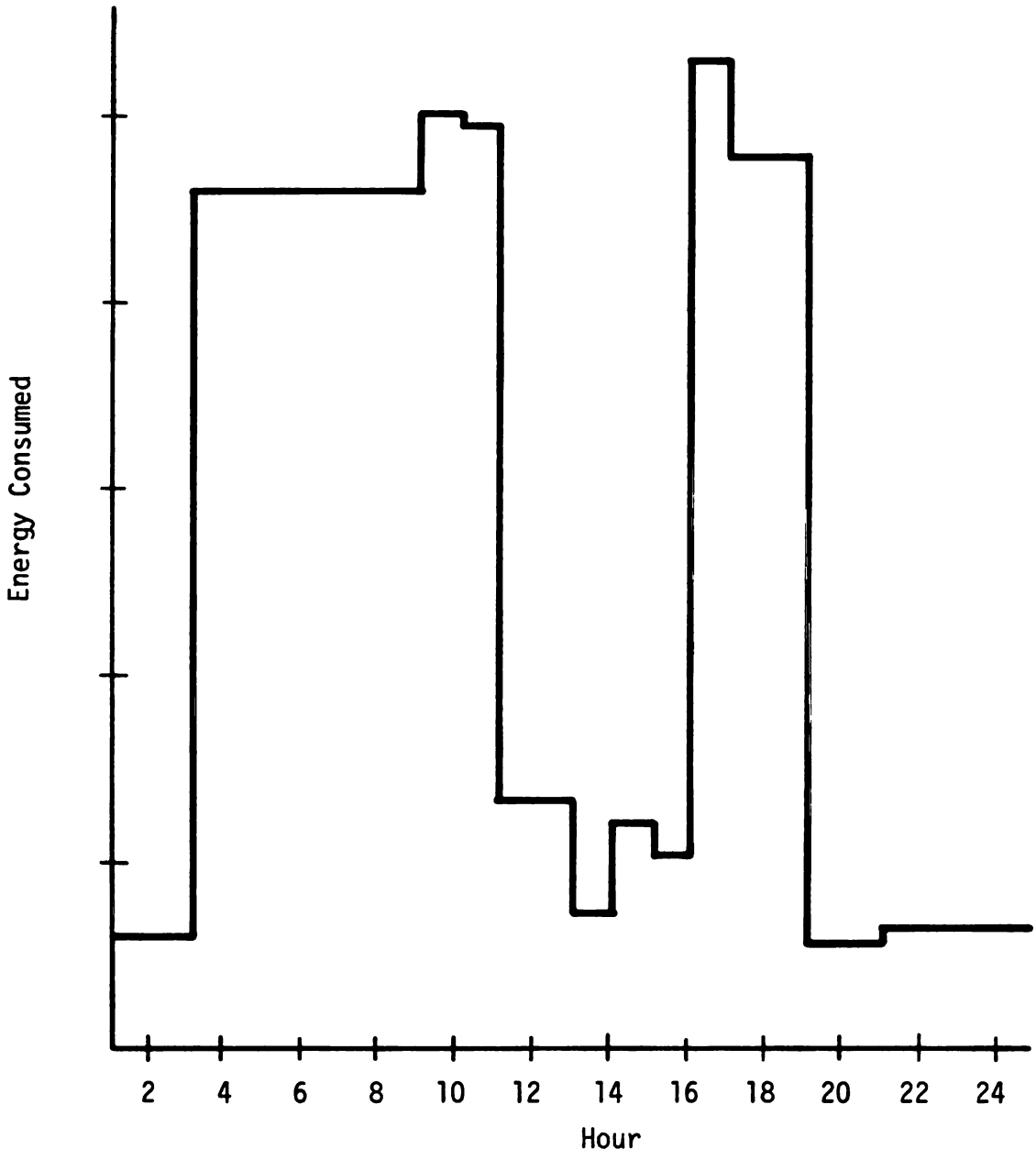

Figure 7.1.2.--Distribution of the daily energy consumed in the Wisconsin dairy plant.

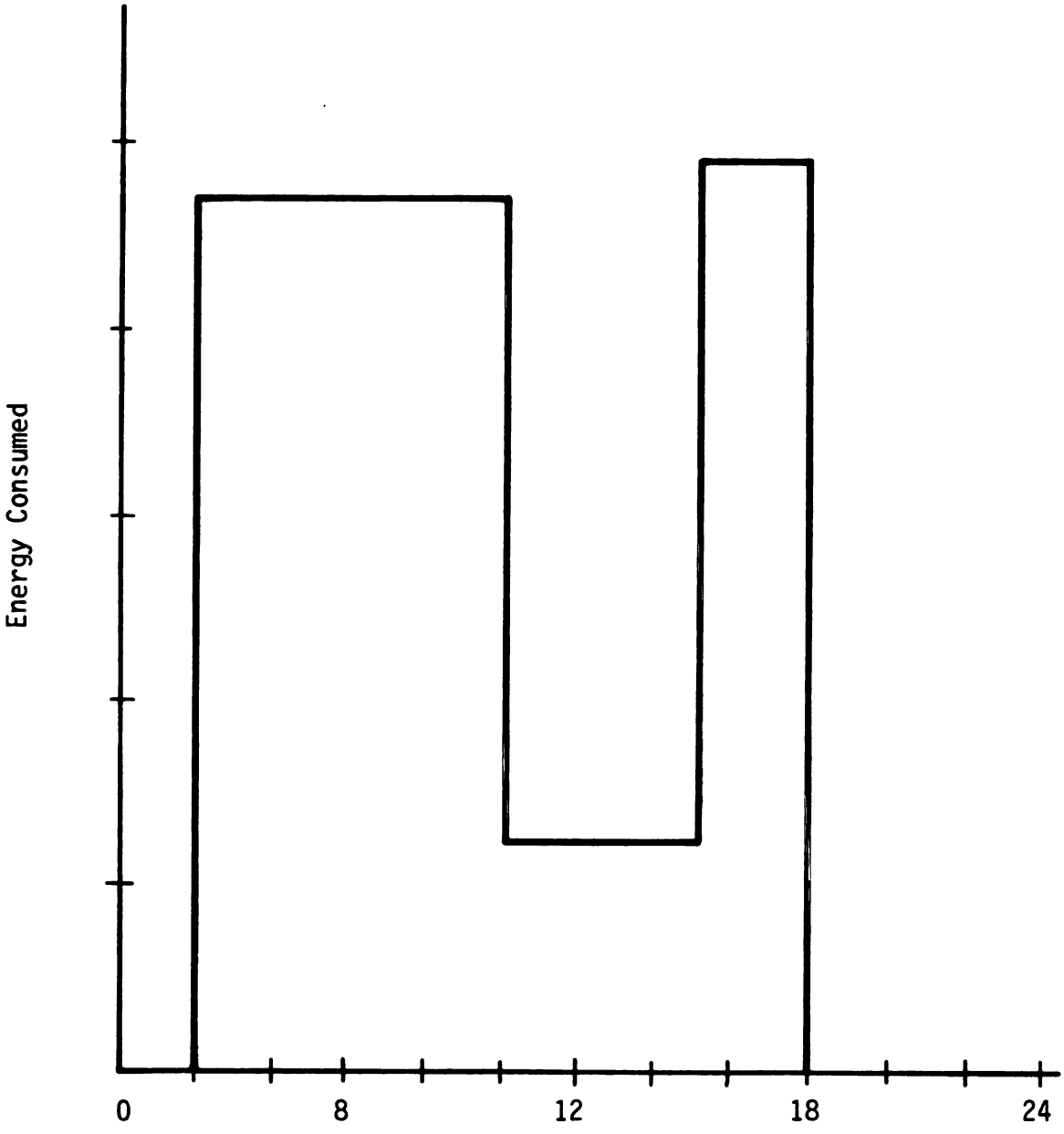

Figure 7.1.3.--Approximated distribution of the daily energy consumed in the Wisconsin dairy plant.

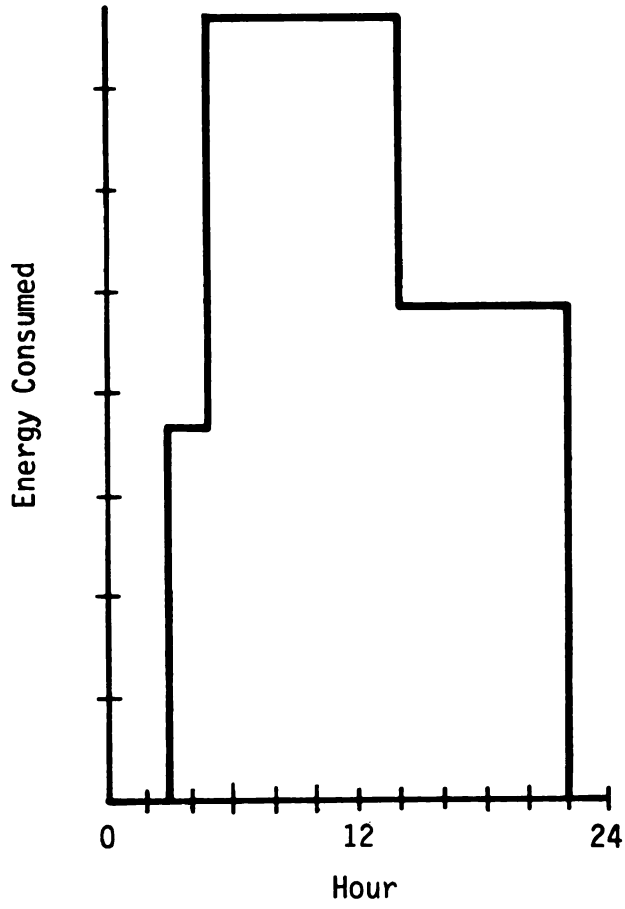

Figure 7.1.4.--Approximated distribition of the daily energy consumed in the Lansing, Michigan dairy plant.

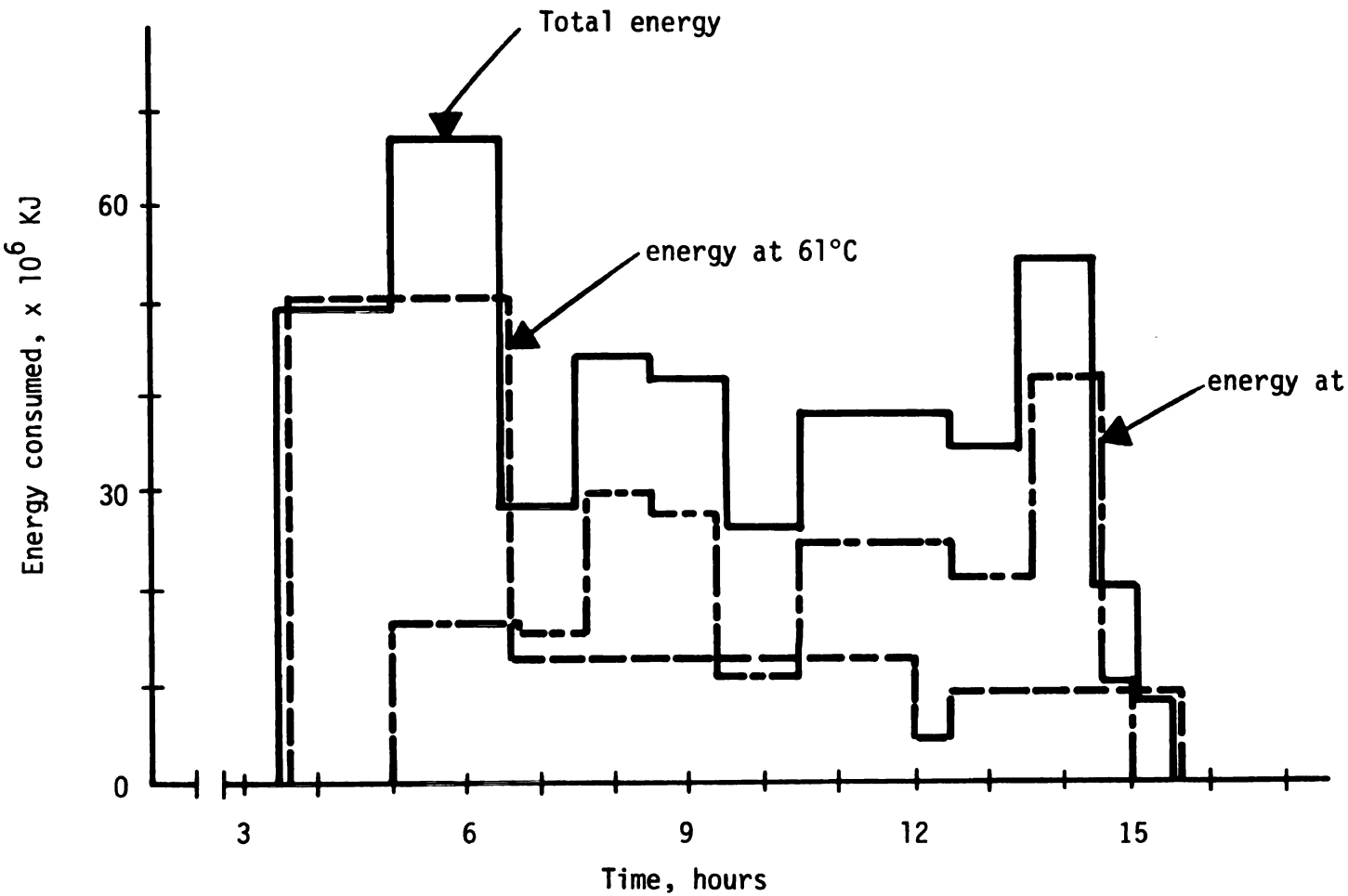

Figure 7.1.5.--Distribution of the daily energy consumed in the Indiana meat processing plant.

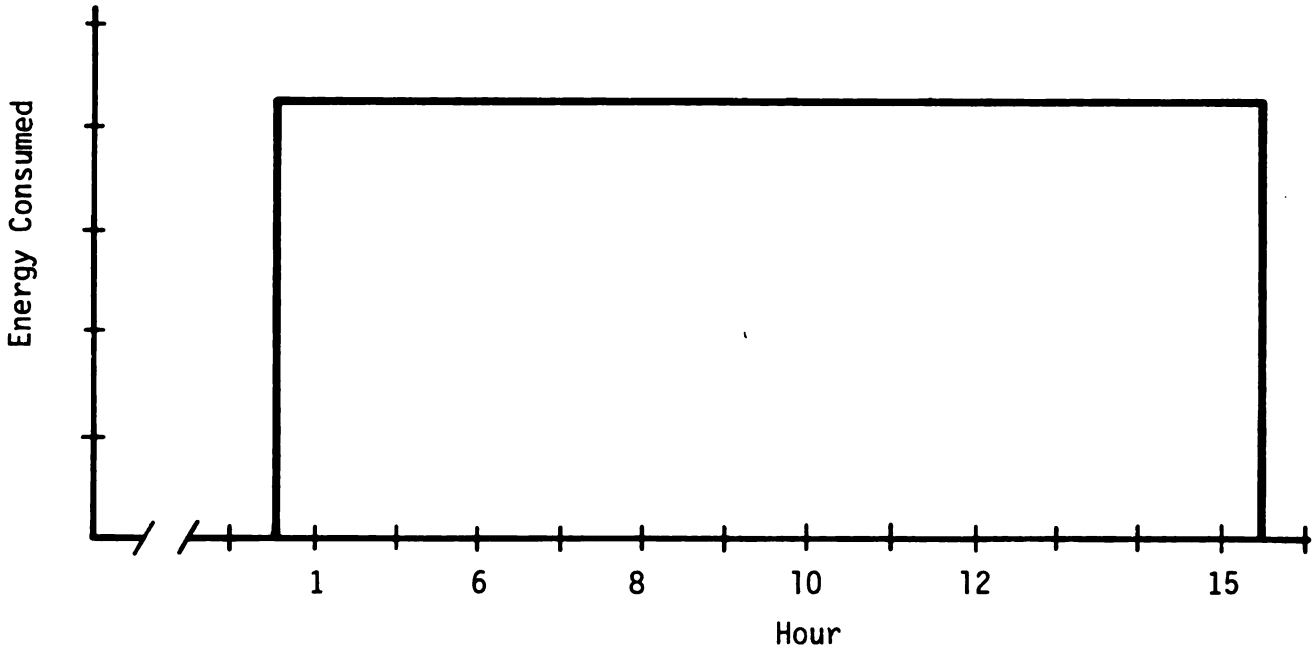

Figure 7.1.6.--Approximated distribution of the daily energy consumed in the Indiana meat processing plant.

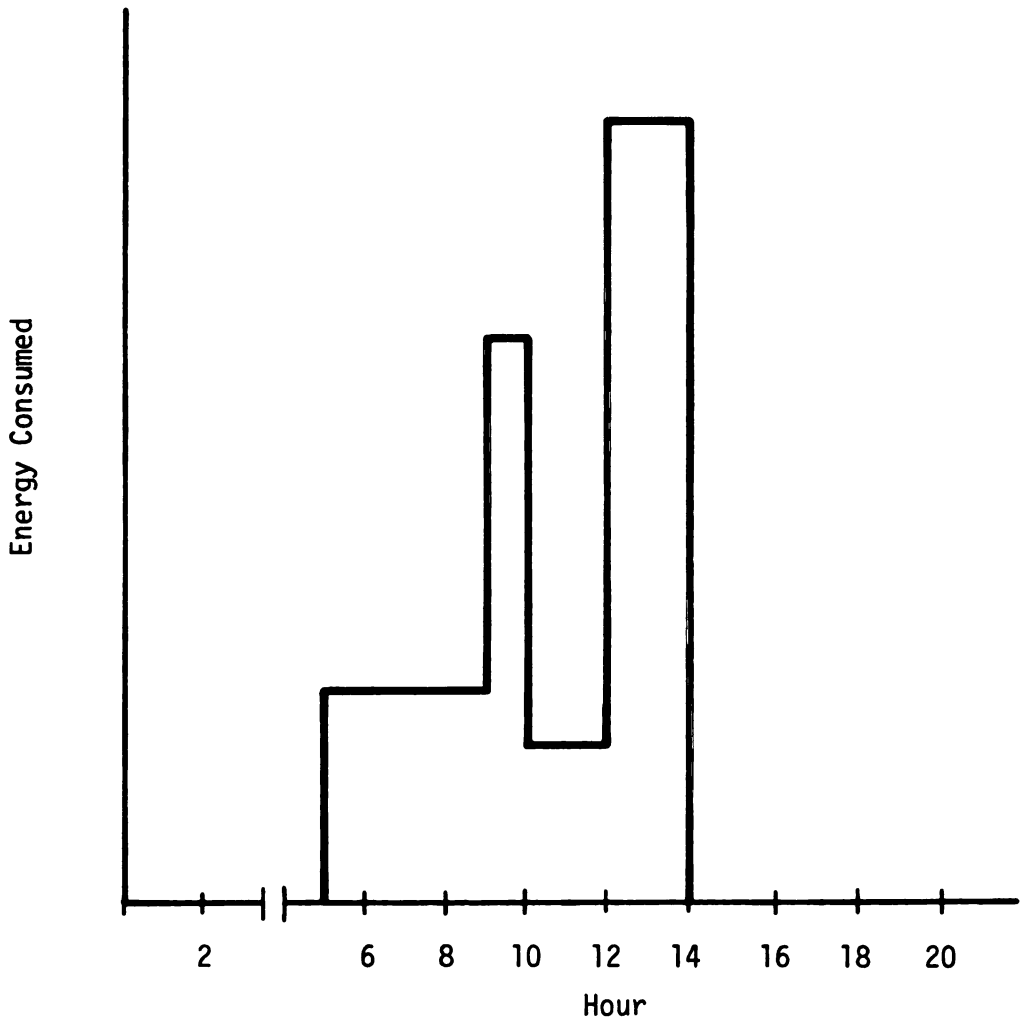

Figure 7.1.7.--Approximated distribution of the daily energy consumed in the Michigan State University dairy plant.

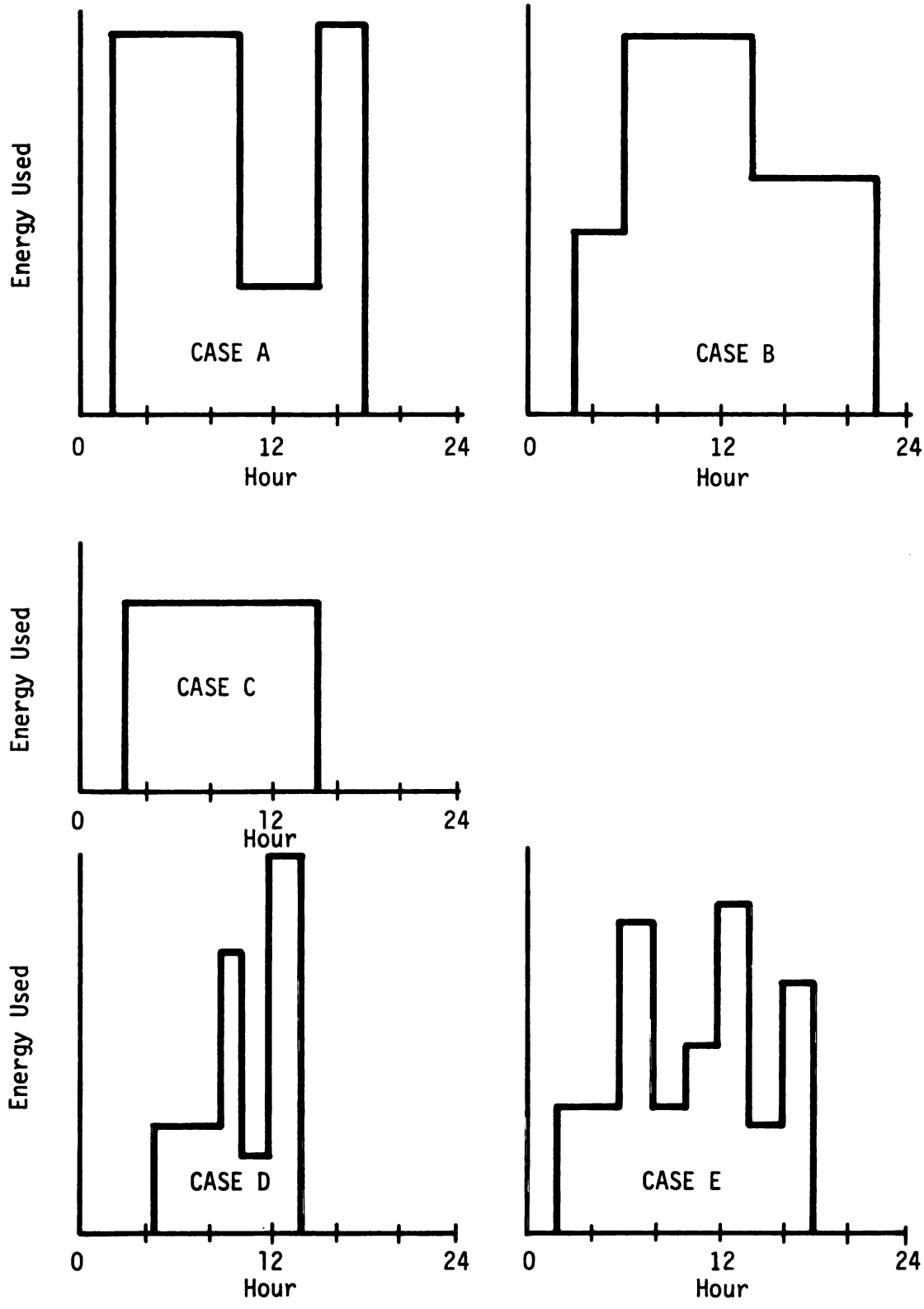

Figure 7.1.8.--Representative hot water demand distribution in the food industry.

not seem compatible with a canning operation. In canaries a solar heating system could be used for water heating during the operating season and for space heating the rest of the year.

CHAPTER 8

VERIFICATION OF THE TRNSYS PROGRAM

To demonstrate the validity of TRNSYS, the MSU dairy plant solar water heater was simulated under various hot water loads and weather conditions. The ambient temperature was measured at the site of the solar system. Solar radiation was measured at the MSU weather station with an EPPLY Pyronometer. The instrument records total radiation on a horizontal plane. A sample of solar radiation recorded is shown in Figures 8.1 and 8.2. The average hourly radiation was estimated by calculating the area under the curve. The wind speed was measured at the Lansing city airport which is located less than 10 miles from Michigan State University.

The temperature of the water in the storage tank was chosen as the criterion for the reliability of the TRNSYS results. Four thermocouples were installed at various depths inside the tank (see Figure 6.3.1) to measure the tank water temperature.

Three TRNSYS runs were made. The first run was for September 27 and 28, 1979, the second for September 30 - October 2, 1979 and the third for October 29-31, 1979. October 2 was a day with low solar radiation. On October 30 the solar system operated under zero load conditions.

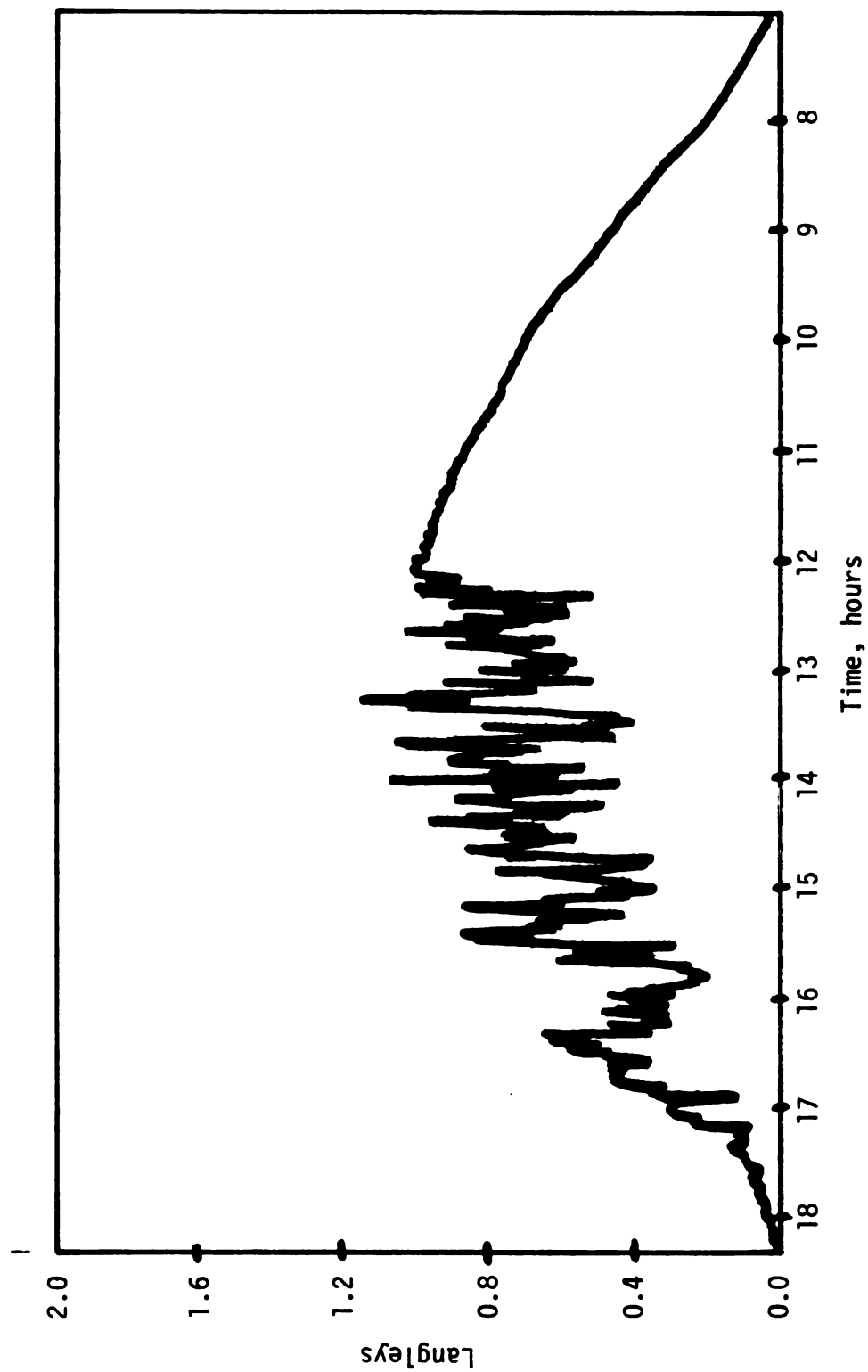

Figure 8.1.--Total radiation on a horizontal plane in East Lansing, Michigan in September 27, 1979.

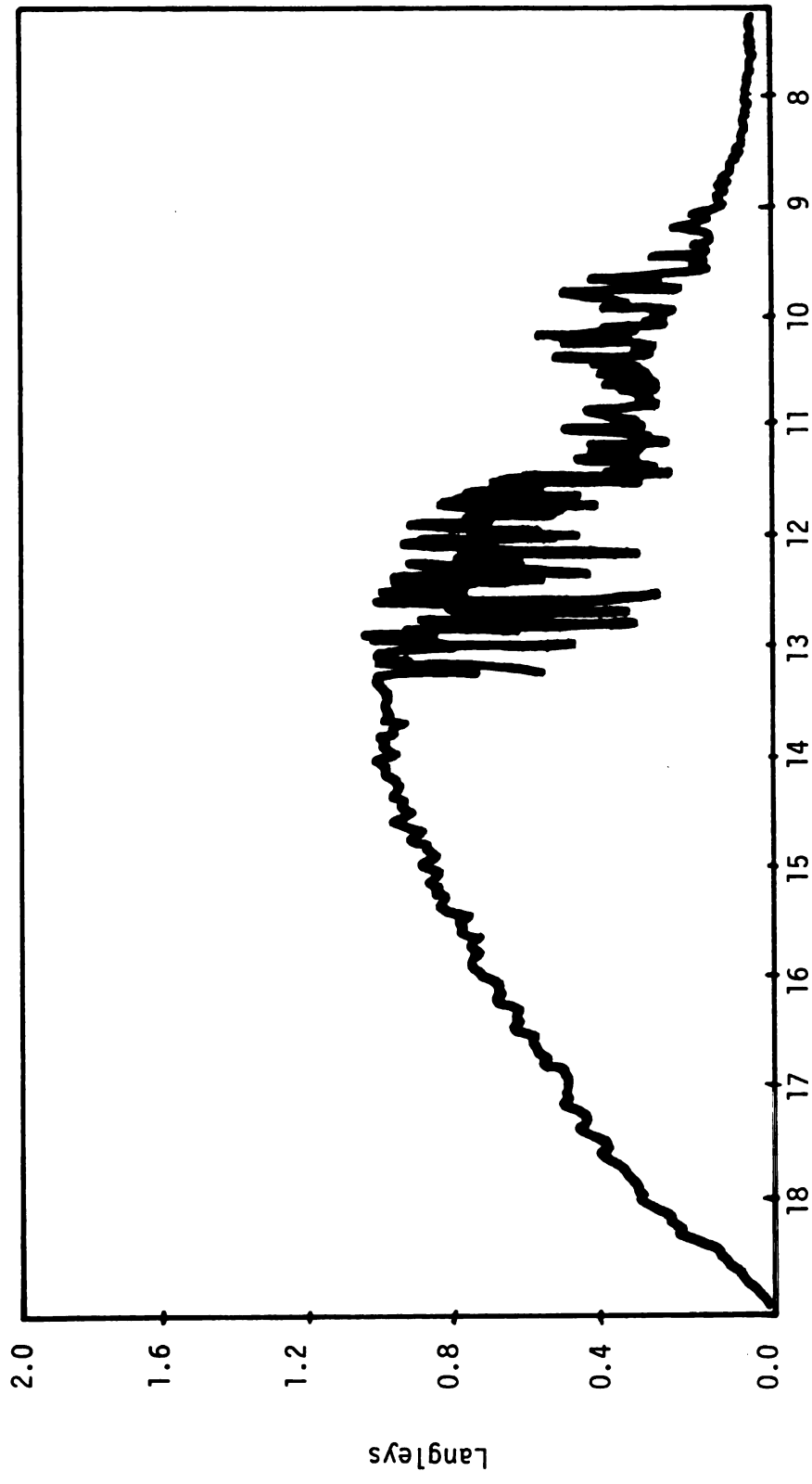

Figure 8.2.--Total radiation on a horizontal plane in East Lansing, Michigan in September 28, 1979.

In Tables 8.1 through 8.7 the hourly experimental and theoretical tank water temperature are presented. The experimental temperature was measured by the four thermocouples inside the tank. Since the tank of the MSU solar system is fully mixed, the four thermocouples were recording the same temperature. The difference between numerical and experimental values (ΔT) is shown in column four of each table, the TRNSYS temperatures are sometimes higher and sometimes lower than the measured ones. A small disagreement between the two temperatures was expected because the simulated solar system and the MSU solar water heater operated under slightly different circumstances.

Equation (4.7.1) for a finte period in time can be written as:

$$T_{s,new} = T_{s,old} + \frac{\Delta\tau}{(mc)_s} [q_u - L - (UA)_s (T_{s,old} - T_a)$$

[8.1]

TRNSYS estimates the tank temperature numerically according to the above equation. In TRNSYS, the energy collected by the solar collector (q_u) is calculated assuming a constant value of collector incident solar radiation for a finite time increment (one hour). Under experimental conditions, however, q_u will change according to the total radiation shown in Figures 8.1 and 8.2. The deviation of the instantaneous radiation, about the averaged hourly value, is sometimes substantial. For example, at 14-15 on September 27 (Figure 8.1) the average radiation is 1.15 langleys (1 langley =

TABLE 8.1.--Storage tank water temperature of the MSU solar water heater on September 27, 1979.

Hour	Tank Temperature, °C		ΔT°C	Measured Solar Radiation KJ/m^2	Load Kg
	Measured	Simulated			
0- 1	58.0	58.0	0.0	--	--
1- 2	58.0	58.0	0.0	--	--
8- 9	57.8	57.0	-0.8	251.0	--
9-10	57.9	58.4	1.5	853.7	960.0
10-11	59.4	55.8	-3.6	1456.0	970.0
11-12	54.8	56.5	1.7	1958.0	760.0
12-13	49.7	55.0	5.3	2310.0	1650.0
13-14	49.4	51.6	2.2	1506.0	2433.0
14-15	42.2	44.7	2.5	1908.0	
15-16	45.6	47.0	1.4	1757.0	
16-17	49.2	49.0	-0.2	1205.0	
17-18	50.0	49.3	-0.7	954.0	
18-19	50.0	49.3	-0.7	301.0	
23-24	49.5	49.1	+0.4		

TABLE 8.2.--Storage tank water temperature of the MSU solar water heater on September 28, 1979.

Hour	Tank Temperature, °C		ΔT°C	Measured Solar Radiation KJ/m^2	Load Kg
	Measured	Simulated			
0- 1	49.5	49.1	0.4	--	--
1- 2	49.5	49.1	0.4	--	--
8- 9	48.9	49.0	0.1	100.0	--
9-10	45.7	41.6	-4.1	630.0	2300.0
10-11	39.4	40.6	1.2	900.0	700.0
11-12	37.7	41.0	3.3	1506.0	850.0
12-13	37.2	39.9	2.7	1760.0	2000.0
13-14	42.5	44.6	2.1	2410.0	--
14-15	48.9	48.7	-0.2	2270.0	--
15-16	53.0	51.2	-1.8	1958.0	--
16-17	54.0	52.0	-2.0	1506.0	--
17-18	54.0	52.0	-2.0	803.0	--
18-19	54.0	52.0	-2.0	401.0	--
23-24	53.7	51.9	-1.8	--	--

TABLE 8.3.--Storage tank water temperature of the MSU solar water heater on September 30, 1979.

Hour	Tank Temperature, °C		ΔT°C	Measured Solar Radiation KJ/m^2	Load Kg
	Measured	Simulated			
0- 1	71.5	71.5	0.0	--	--
1- 2	71.5	71.5	0.0	--	--
8- 9	71.1	71.3	0.2	301.3	--
9-10	71.0	71.3	0.2	752.2	950.0
10-11	68.3	66.6	-1.7	1355.8	950.0
11-12	59.6	60.4	0.8	703.8	950.0
12-13	57.0	54.0	-3.0	577.5	950.0
13-14	54.7	49.7	-6.0	828.6	950.0
14-15	47.2	45.7	-1.5	1130.0	950.0
15-16	45.6	45.2	-0.4	1581.0	950.0
16-17	46.1	44.0	-2.1	703.0	950.0
17-18	45.5	44.2	-1.3	125.0	--
23-24	44.5	44.0	-0.5	--	--

TABLE 8.4.--Storage tank water temperature of the MSU solar water heater on October 4, 1979.

Hour	Tank Temperature, °C		ΔT°C	Measured Solar Radiation KJ/m^2	Load Kg
	Measured	Simulated			
0- 1	44.5	44.0	-0.5	--	--
1- 2	44.5	44.0	-0.5	--	--
8- 9	43.3	44.0	0.7	276.0	760.0
9-10	44.4	42.1	-2.1	753.2	450.0
10-11	41.7	42.9	1.2	1481.4	450.0
11-12	40.3	45.6	5.3	2008.7	450.0
12-13	42.6	48.0	4.4	2058.9	2044.0
13-14	41.1	44.5	3.4	2008.7	1703.0
14-15	41.0	41.2	0.2	1556.7	--
15-16	45.0	43.3	-1.7	1531.7	--
16-17	48.0	45.0	-3.0	828.6	--
17-18	48.0	45.0	-3.0	703.0	--
23-24	48.0	45.0	-3.0	--	--

TABLE 8.5.--Storage tank water temperature of the MSU solar water heater on October 29, 1979.

Hour	Tank Temperature, °C		T°C	Measured Solar Radiation KJ/m^2	Load Kg
	Measured	Simulated			
0- 1	25.0	25.0	0.0	--	--
1- 2	25.0	25.0	0.0	--	--
8- 9	24.8	24.7	-0.1	502.0	--
9-10	24.7	33.5	8.8	1255.4	2040.0
10-11	25.5	34.1	8.6	1556.7	1470.0
11-12	28.0	37.0	9.0	1858.0	910.0
12-13	33.3	40.0	6.7	2109.0	1470.0
13-14	35.1	38.0	2.9	1757.6	2044.0
14-15	35.0	39.0	4.0	1456.3	970.0
15-16	34.5	38.0	3.5	853.0	970.0
16-17	32.4	35.1	2.7	376.0	970.0
17-18	31.7	32.4	0.7	--	970.0
18-19	31.6	30.0	-1.6	--	--
23-24	31.6	30.0	16.	--	--

TABLE 8.6.--Storage tank water temperature of the MSU solar water heater on October 30, 1979.

Hour	Tank Temperature, °C		ΔT°C	Measured Solar Radiation KJ/m^2	Load Kg
	Measured	Simulated			
0- 1	31.6	30.0	1.6	--	--
1- 2	31.6	30.0	1.6	--	--
8- 9	32.0	31.0	-1.0	1004.3	--
9-10	32.7	33.1	0.4	1506.5	--
10-11	35.8	36.1	0.3	1757.6	--
11-12	40.5	41.5	1.5	1858.0	--
12-13	46.1	46.5	0.4	1757.6	--
13-14	50.0	51.4	1.4	1858.0	--
14-15	55.3	55.5	0.2	1757.6	--
15-16	57.9	57.9	0.0	1781.0	--
16-17	57.9	58.3	0.4	753.0	--
17-18	57.9	58.2	0.3	301.0	--
23-24	57.1	58.2	1.1	--	--

TABLE 8.7.--Storage tank water temperature of the MSU solar water heater on October 31, 1979.

Hour	Tank Temperature, °C		ΔT°C	Measured Solar Radiation KJ/m^2	Load Kg
	Measured	Simulated			
0-1	57.1	58.2	1.1	--	--
1- 2	57.1	58.2	1.1	--	--
8- 9	56.4	60.0	3.6	502.0	--
9-10	57.0	61.6	4.6	828.6	1610.0
10-11	53.3	56.6	3.3	1355.8	1930.0
11-12	44.4	51.2	6.8	1632.0	2044.0
12-13	44.0	46.0	2.0	1556.0	1022.0
13-14	40.0	45.0	5.0	1456.3	1533.0
14-15	38.9	42.0	3.1	1130.0	510.0
15-16	39.4	40.0	0.6	470.0	--
16-17	39.1	40.0	0.9	276.0	--
17-18	39.1	40.0	0.9	--	--
23-24	39.0	40.0	1.0	--	--

4.186 J/cm^2). At 14:15 the radiation is 1.15 langleys, whereas at about 14:28 it is 0.4 langleys. To what extent the change of the instantaneous q_u will affect the average over the hour q_u is not known. Since over a finite period of time both, experimental and numerical results will be based on approximately the same amount of solar radiation, the effect of the instantaneous change of solar radiation on the tank temperature is not expected to be serious.

The disagreement between the numerical and experimental results is at least partially due to different hourly load conditions. The hourly load used in TRNSYS is shown in columns 6 of Tables 8.1 through 8.7. In actuality, the hourly load distribution was different than the one shown in the tables. During the experiments the load distribution was changing according to the water demand in the dairy plant. Most of the time the hot water supply was not changing hourly. For example, on September 27 the actual daily load distribution (see Figure 8.3) shows zero load between 10:20 and 11:20. In TRNSYS the amount of water from 10:00 to 10:20 was distributed over a 60-minute period (10:00 - 11:00) because changes occurring at time intervals of less than one hour are not recognized by TRNSYS under circumstances of hourly data input. The two parts of Figure 8.3 demonstrate the differences between the actual load distribution is different for the experimental and the simulated cases, the total daily load is the same for both. In Tables 8.1 through 8.7 it can be seen that in the beginning and the end of each day the temperature differences are not as great as during the day. This indicates that the energy supplied by the system to the load is approximately the

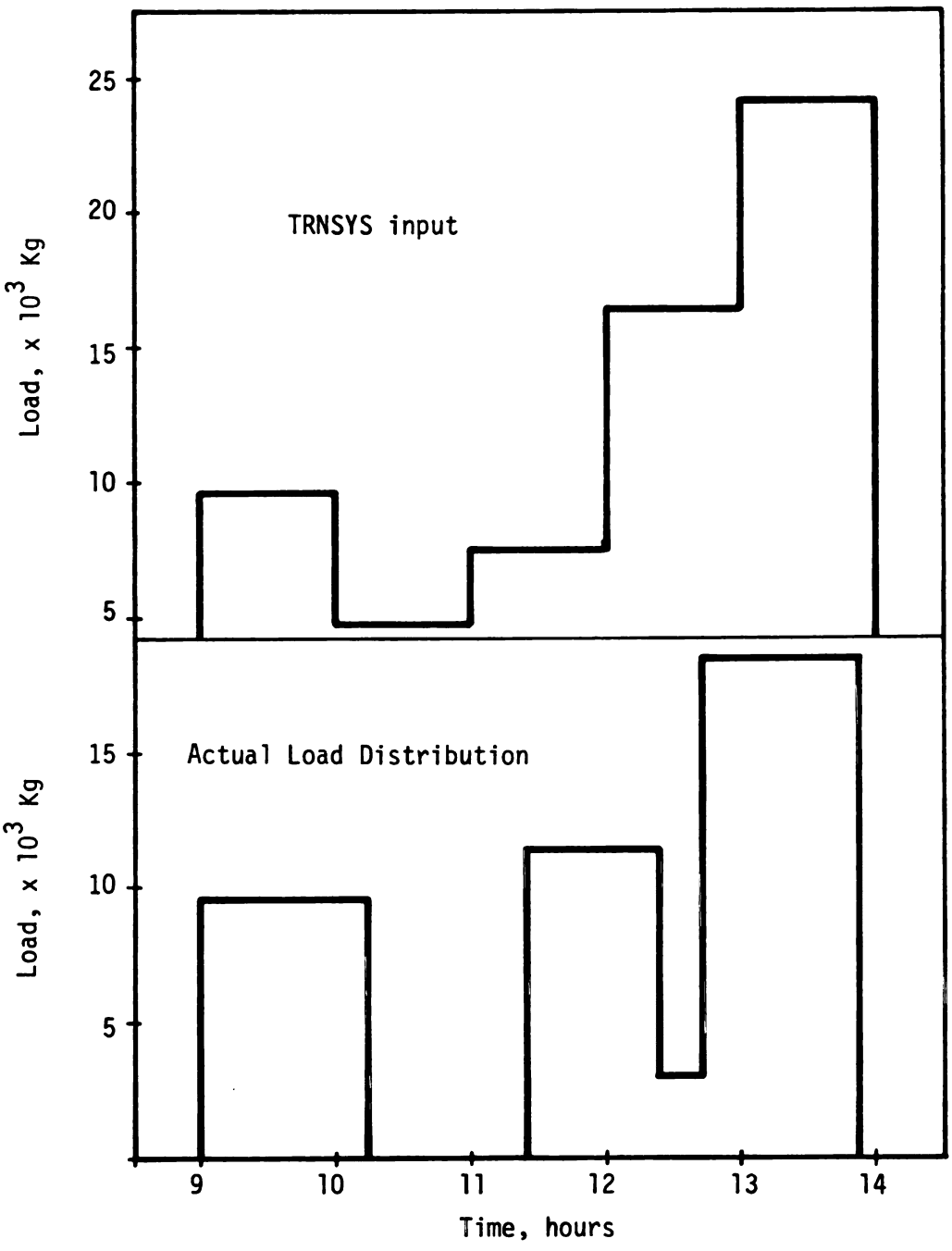

Figure 8.3.--Daily load distribution for the experimental and simulated case on September 27, 1979.

same in both the experimental and the simulated situations. The effect of the load distribution is better shown in Table 8.6 where the two temperatures are very similar. On October 30 (Table 8.6) the system operated under zero load conditions.

The temperatures in the tank on October 2 are shown in Figure 8.4. An important phenomenon is shown in Figure 8.4. October 2, 1979 was a rainy day. The solar radiation was very low. The temperature in the tank was considerably higher than that of the collector (see Figure 8.4). Therefore, no energy had been supplied to the tank from the collector. At 8:30 a.m. removal of hot water from the tank began in order for the load to be met (see upper part of Figure 8.4). In the meantime, cold city water started replacing the hot water removed. Because of the higher density of the cold water, the cold water remained in the lower sections of the tank. Under these circumstances, a cold water front developed close to the bottom of the tank. The solid lines in Figure 8.4 represent temperatures measured at different depths in the tank. At approximately 9:00 a.m. the thermocouples nearest to the bottom of the tank indicated a sudden temperature drop (from 47° to 13°C). The same is observed for the next nearest thermocouple at 10:00 a.m. Finally, at 1:00 p.m. the temperature of the upper tank section began to drop. At about 4:00 p.m. the temperature in the tank became uniform (12°C). Each of the four lines representing the sudden temperature drop inside the tank, indicates the position of the cold water front at various times during the day. The front moves to the top of the tank as time advances.

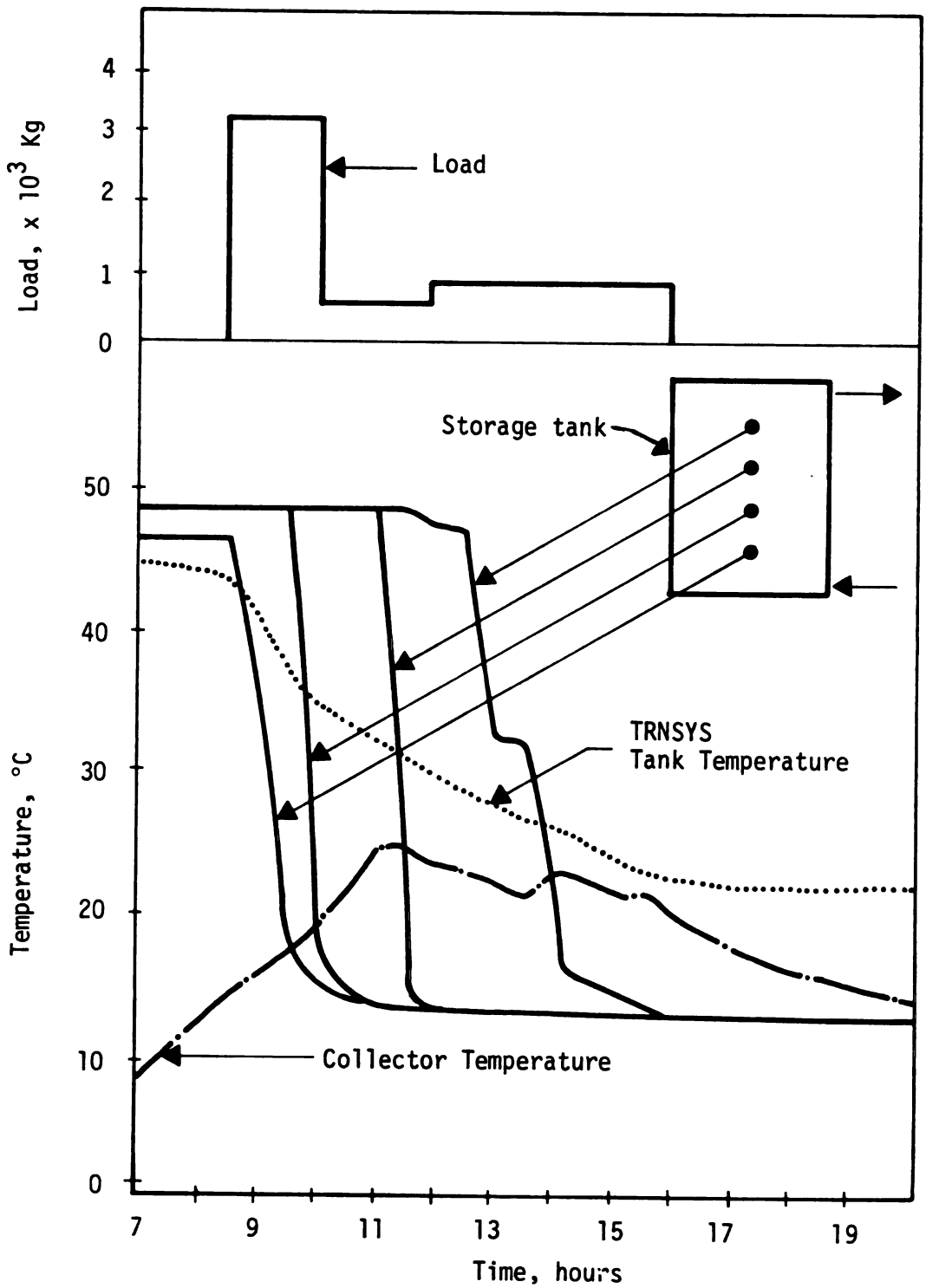

Figure 8.4.--Tank temperature and load distribution on October 2, 1979.

In Figure 8.4 it can be seen that despite the low temperature in the lower tank sections, most of the water removed to meet the load was at a much higher temperature (48°C).

The dotted line in Figure 8.4 is the temperature of the tank from the TRNSYS run. It can be seen that TRNSYS underestimated the temperature in the tank. Under these conditions, Equation [8.1], which is used by the TRNSYS algorithm, cannot describe the temperature in the tank. The energy of the load (L) in the equation is based on a temperature which corresponds to the total water mass $(M)_s$ in the tank. From Figure 8.4 it can be seen that this is not true.

The behavior of the water temperature inside the tank, shown in Figure 8.4, can be explained by assuming a stratified tank with four sections (see Chapter 4). By this assumption, Equation [8.1] will be replaced by four differential equations. Figure 4.8 and Equation [4.7.3] and [4.7.5] are an example of a stratified tank with two sections. For a four section tank with zero energy supplies from the colar collector, the tank will be as in Figure 8.5. An energy balance for section 1 will result in:

$$T_{1,new} = T_{1,old} = \frac{\Delta\tau}{(m_1 c)} [-\dot{m}_L (T_1 - T_2) - \dot{m}_1 (T_1 - T_2)$$

$$+ \dot{m}_6 (T_2 - T_1) - (UA)_{s,1} (T_1 - T_a)] \qquad [8.2]$$

Similar equations can be written for the other tank sections.

A stratified tank was not assumed during the verification of TRNSYS because the tank of the MSU solar system was fully mixed for all days indicated in Tables 8.1 through 8.7, except for October 2, 1979.

If a stratified tank would have been assumed, then, as will be discussed in Chapter 9, the long-run performance of the solar system would have been substantially overestimated.

The energy supplied to the load by the solar system is presented in Table 8.8. The relative percent error of the numerical results indicates that with the exception of October 2, the error is relatively small. As was explained above, on October 2 TRNSYS could not describe the temperature in the tank.

Modeling a solar system is a complex procedure. The transient behavior of the various components of a solar system is determined by solving simultaneously sets of algebraic and/or differential equations. Accounting for the complexity of solar water heating from a system modeling point of view, the differences observed in Tables 8.1 through 8.8 can be considered small.

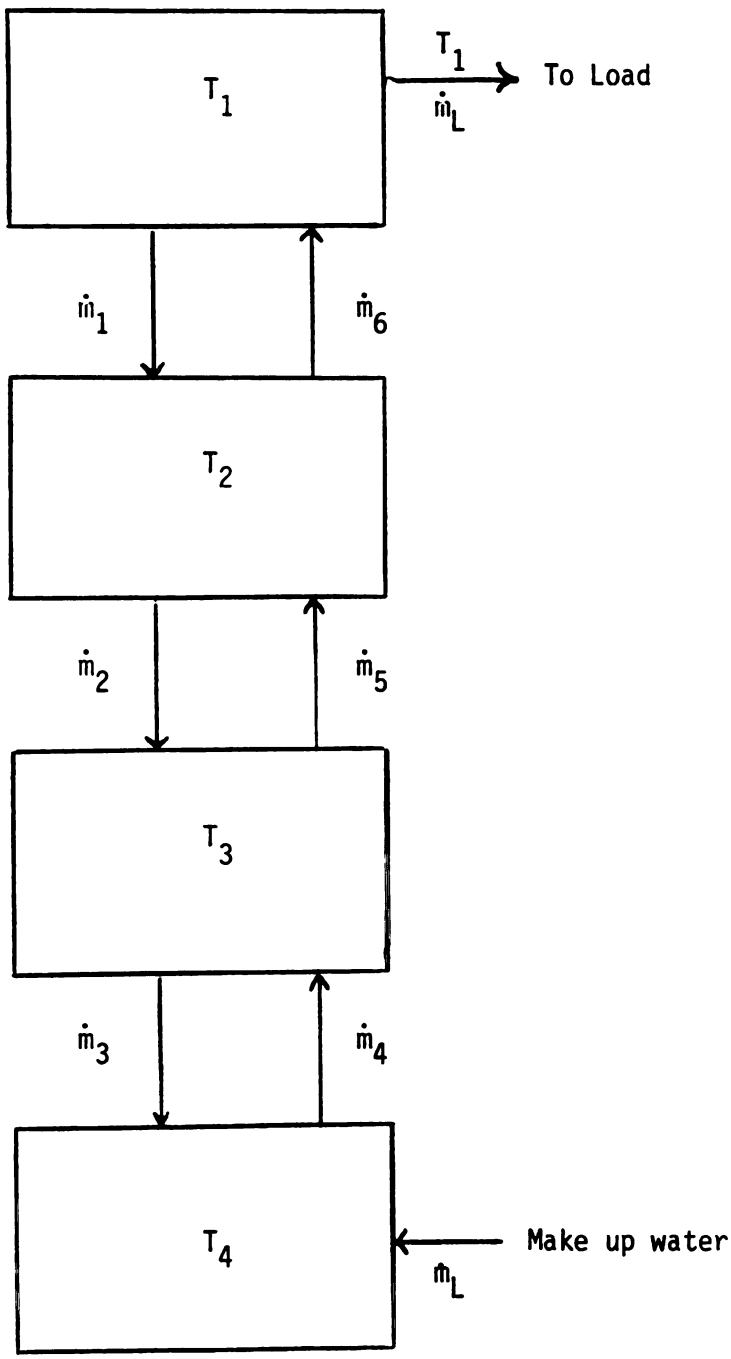

Figure 8.5.--Stratified storage tank with four sections which can be used to estimate the four tank temperatures on October 2, 1979.

TABLE 8.8.--Comparison of the energy delivered to the delivery load calculated by TRNSYS to that calculated from the measured temperatures and flow rates of the MSU solar water heater and relative percentage error of the numerical results.

Date	Energy Delivered to the Daily Load, KJ		Relative Error Percent
	Actual	TRNSYS	
September 27	1,040,581	1,101,411	5.84
September 28	727,978	695,036	-4.40
September 30	1,411,111	1,387,409	-1.63
October 1	810,060	844,223	4.19
October 2	1,251,148	750,219	-39.96
October 29	1,083,104	1,356,147	6.74
October 31	1,356,870	1,449,560	6.85

CHAPTER 9

TRNSYS RUNS

The purpose of the FORCING-FUNCTION subroutine (unit 14 type 14) in TRNSYS is to generate a time dependent forcing function which has a behavior characterized by a repeated pattern. The pattern is established by a set of discrete data points indicating its values at various times through a cycle. Generation of continuing forcing functions is obtained by linear interpolation between the discrete data points.

The forcing function in the TRNSYS runs is the hot water consumed inthe processing plants. Cases A-E in Figure 7.1.8 are the repeated patterns characterizing the forcing functions used in this study. Each function was repeated 5, 6 or 7 times per week depending on the time schedule in a plant. In Figure 7.1.8 each discrete data point represents a fixed percentage of the daily load. Determination of this percentage value allows calculation of the flow rate of the water being supplied to the plant at various times during the day.

To scale-up the Michigan State University dairy plant solar water heater, the parameters related to the size of the solar system were generated according to the figures presented in Table 9.1. By assuming the volume of the storage tank to be equal to the daily hot

TABLE 9.1.--Relationships used in TRNSYS to estimate the size of a solar system.

Collector area/storage volume [1]	19.8 m^2/m^3 (0.805 ft^2/gal)
Flow rate/collector area [2]	64 lt/hr-m^2 (1.57 gal/hr-ft^2)
(UA) H.E./collector area [3]	130 KJ/hr-°C-m^2 (83 BTU/hr-°F-ft^2
Tank height	5.4 (17.4 ft)
Storage volume	Daily hot water load

[1], [2] U.S. Department of Commerce, 1977.

[3] Used in the Michigan State University Solar Collector.

water consumed in a processing plant, the size of the solar collector, the flow rate through the collector and the head exchanger size are determined based on the information of Table 9.1. The value of the parameters which are independent of the system size are presented in Table 9.2.

Another objective during the TRNSYS run was to maintain the ratio of tank height to the diameter L/D to values between 3-4. For most food processing plants the floor to ceiling distance is about 6 m (20 ft) (Lopez, 1975). As a result, a maximum tank height of 5.4 m (17.7 ft) was assumed. Values of L/D for various size solar systems are shown in Table 9.3.

Experimental results from the Michigan State University Dairy Plant solar water heater have indicated that for L/D equal to 1.16 and tank height equal to 3 m the storage tank was unstratified. Since the height of the tank (5.4 m) in the various solar system simulated by TRNSYS is approximately twice as big as the Michigan State University solar system tank, a stratified tank with two sections was assumed in the TRNSYS runs.

Nine sizes of solar water heaters for each Case in Figure 7.8 were investigated. The collector area and storage tank volume for each size are presented in Table 9.3.

In Table 9.4 the size of the heat exchanger of the solar systems studied is shown. The estimated heat exchanger area, shown in the second column of Table 9.4, is the one calculated according to the relationship in Table 9.1. An overall heat transfer coefficient equal to 4100 KJ/hr-m^2-°C was assumed. As will be discussed

TABLE 9.2.--Parameter values independent of the size of the solar system used in solar system simulation with TRNSYS.

Parameter	Value
F'	0.95
Specific heat of fluid	3.64 KJ/Kg-°C
Collector absorbance	0.90
Number of glass covers	2
Collector plate emittance	0.10
Collector back loss coefficient	0.5 KJ/hr-m^2-m^2-°C
Collector tilt	43°
Transmittance of glass	0.82
Tank loss coefficient	1.0 KJ/hr-m^2-°C
Service water temperature	74°C

TABLE 9.3.--Solar system sizes used per CASE in solar water heating simulation by TRNSYS.

Collector Area m^2 (ft^2)	Storage Tank Volume m^2 (gal)	Tank Height m (ft)	Tank Height Diameter Ratio
150 (1614)	7.6 (2000)	5.4 (17.7)	4.03
250 (2690)	12.8 (3400)	5.4 (17.7)	3.13
500 (5380)	26.5 (7000)	5.4 (17.4)	2.16
1000 (10760)	53.0 (14000)	5.4 (17.4)	1.53
2000 (21520)	106 (28000)	5.4 (17.4)	1.08
3000 (32280)	151.4 (40000)	5.4 (17.4)	0.90
4000 (43040)	202.9 (54000)	5.4 (17.4)	0.78
5000 (53800)	265.0 (70000)	5.4 (17.4)	0.68
6000 (64560)	303.0 (80000)	5.4 (17.4)	

TABLE 9.4.--Heat exchanger sizes used in solar system simulation with TRNSYS.

Collector Area m^2	Heat Exchanger Area	
	Estimated m^2	Used m^2
150	4.8	4.9
250	7.9	8.2
500	15.8	15.9
1000	31.7	31.7
2000	63.4	48.8
3000	95.0	48.8
4000	127.0	61.0
5000	158.5	73.2
6000	190.2	73.2

in Chapter 11, reducing the area of heat exchanger by a factor of two decreases the collector efficiency by about 2 percent. For large collector areas ($\geq$ 2000 m^2) the heat exchanger was not sized according to the relationship in Table 9.1. A smaller area was assumed as is shown in column three of Table 9.4 and it is a compromise between cost and collector efficiency.

The simulation period per TRNSYS run was one year (8760 hrs). Outputs on hourly, daily, weekly, monthly, and yearly basis were obtained. At the end of every day, month, week and year a simulation summary was made and various quantities were printed out. Hourly weather data was used in the TRNSYS runs. The data was measured in East Lansing, MI in 1974.

A sample of an hourly simulation output is shown in Appendix A2. Appendix A3 and A4 represent samples of daily, weekly, monthly and yearly outputs.

CHAPTER 10

MODIFICATION OF THE f-CHART PROGRAM

The assumptions under which the f-chart design procedure of solar water heaters is valid, are the following (Hughes et al., 1978):

1. The useful energy transferred to the working fluid, is described by Equation [5.19];
2. The control system will operate the collectors whenever there is useful energy to be collected;
3. The over-all loss coefficient (U_L) is constant;
4. The water tank is not pressurized so that the maximum temperature allowed is the boiling point of water (100°C);
5. The system load can extract energy from the tank as long as the tank temperature is above 20°C;
6. The distribution of the daily water demand is assumed to be the average residential distribution, described by Mutch (1974) as in Figure 10.1;
7. The loss coefficient for the storage tank and piping is assumed to be 0.48 W/m^2-°C;
8. The ratio of $\varepsilon C_{min}/UA$ in the heat exchanger is 2, if different, f-chart uses a correction factor;
9. The storage tank is fully mixed.

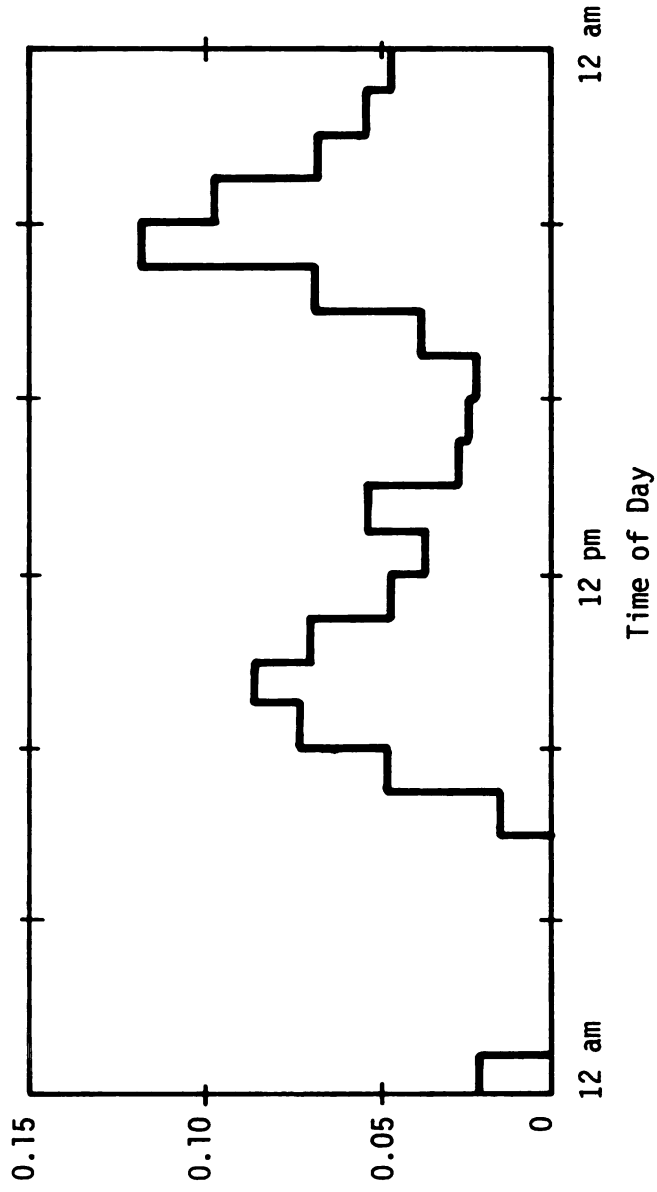

Figure 10.1.--Average residential water heating demand distribution (Mutch, 1974).

Under the above conditions, f, which is the fraction of the monthly space and water heating load supplied by solar, is given by (Klein et al., 1976):

$$f = 1.04\ Y - 0.065\ X - 0.159\ Y^2 + 0.00187\ X^2 - 0.0095\ Y^3 \qquad [10.1]$$

where X and Y are defined in equations [4.9.5] and [4.9.6]

Equation [10.1] calculates f for cases where the solar system is used for space and water heating. The f-chart method has been developed for residential type solar water and space heating systems. If water heating constitutes the total load, X is given by

$$X = TX1 * F_R' U_L A_c \Delta\tau / L \qquad [10.2]$$

where

$$TX1 + \frac{11.6 + 1.18\ Tw + 3.86\ Tm - 2.32\ Ta}{(100 - Ta)} \qquad [10.3]$$

where Tw is the minimum acceptable hot water temperature, Tm is the make-up water temperature, and Ta is the ambient temperature.

For an individual type solar water heater the temperature in the storage tank may exceed 100°C. Then the tank must be pressurized. The dimensions of the storage tank may also be such

that a certain degree of stratification is obtained. The water demand distribution in a processing plant is considerably different than the one shown in Figure 10.1. As a result, assumptions (3), (5), (6) and (9) are violated when f-chart is used for the design of an industrial type solar water heater and thus equation (10.1) is not applicable. Thus, a new "f equation" needs to be developed for food processing plants.

The incident radiation on a flat plate collector, S, is partially transferred to the working fluid and partially lost to the environment due to convetive, conductive and radiation losses. The amount of energy stored in the collector has been neglected, since it is small compared to the other terms. Therefore,

$$S = Q_u + Q_L \qquad [10.4]$$

where Q_u is the energy transferred to the working fluid and Q_L is the energy lost.

Division of Equation [10.4] by the energy of the load, L, yields

$$\frac{S - Q_u}{L} = \frac{Q_L}{L} = X' \qquad [10.5]$$

Equation [10.5] is related to the definition of X in the f-chart program (p. 57, Beckman et al., 1977).

The average efficiency, $\bar{\eta}$, of a collector is defined by

$$\bar{\eta} = Q_u/S \qquad [10.6]$$

Equation [10.5] can then be written as

$$\frac{S\ (1 - \bar{\eta})}{L} = X' \qquad [10.7]$$

Industrial solar water heaters, designed as in Chapter 9, of different size and hot water use patterns have been simulated by the author with TRNSYS. The results (to be discussed in Chapter 11) reveal that the average monthly collector efficiency varies within a narrow range (Table 11.2.2). Equation [10.7] indicates that X is directly related to the efficiency of the solar collector and to the ratio S/L.

A simple regression analysis for the following model can be made:

$$X' = A\ (S/L) \qquad [10.8]$$

Both X' and S/L were calculated from TRNSYS outputs. The collector area of the simulated solar systems was between 150 m^2 and 6000 m^2. The simulation was made for East Lansing, Michigan weather conditions. X' was calculated as the ratio of $(S - Q_u)/_L$.

The values of A from the regression analysis was found to be 0.55342; the coefficient of determination (r^2) 0.99819 and the coefficient of variation 4.5 percent. Then the model becomes

$$X' = \frac{Q_L}{L} = 0.55348\ S/L \qquad [10.9]$$

which is a good relationship between X' and S/L. The results were based on 324 data points. The regression line of the above analysis is shown in Figure 10.2.

The new "f-equation," derived by applying regression analysis, is:

$$f = A_0 + A_1X' + A_2Y + A_3X^2 + A_4Y^2 + A_5X'^3 + A_6Y^3 + A_7X'^4 + A_8Y^4 \qquad [10.10]$$

X' and Y were calculated by TRNSYS as in Equations [10.9] and [4.9.6], respectively.

A regression analysis based on 540 data points and using the statistical package for Social Sciences (SPSS) resulted in the following new "f-equation":

$$f = 29.56\ X' - 23.238\ Y - 64.554\ X'^2 + 41.774\ Y^2 + 57.688\ X'^3 - 29.822\ Y^3 - 18.121\ X'^4 + 7.447\ Y^4 \qquad [10.11]$$

The regression line in the analysis was forced through the origin because for X' = Y = 0, f ix zero.

The goodness of fit of Equation [10.11] is satisfactory. Its squared multiple correlation coefficient was found to be 0.99777 and the coefficient of variation 5.0 percent.

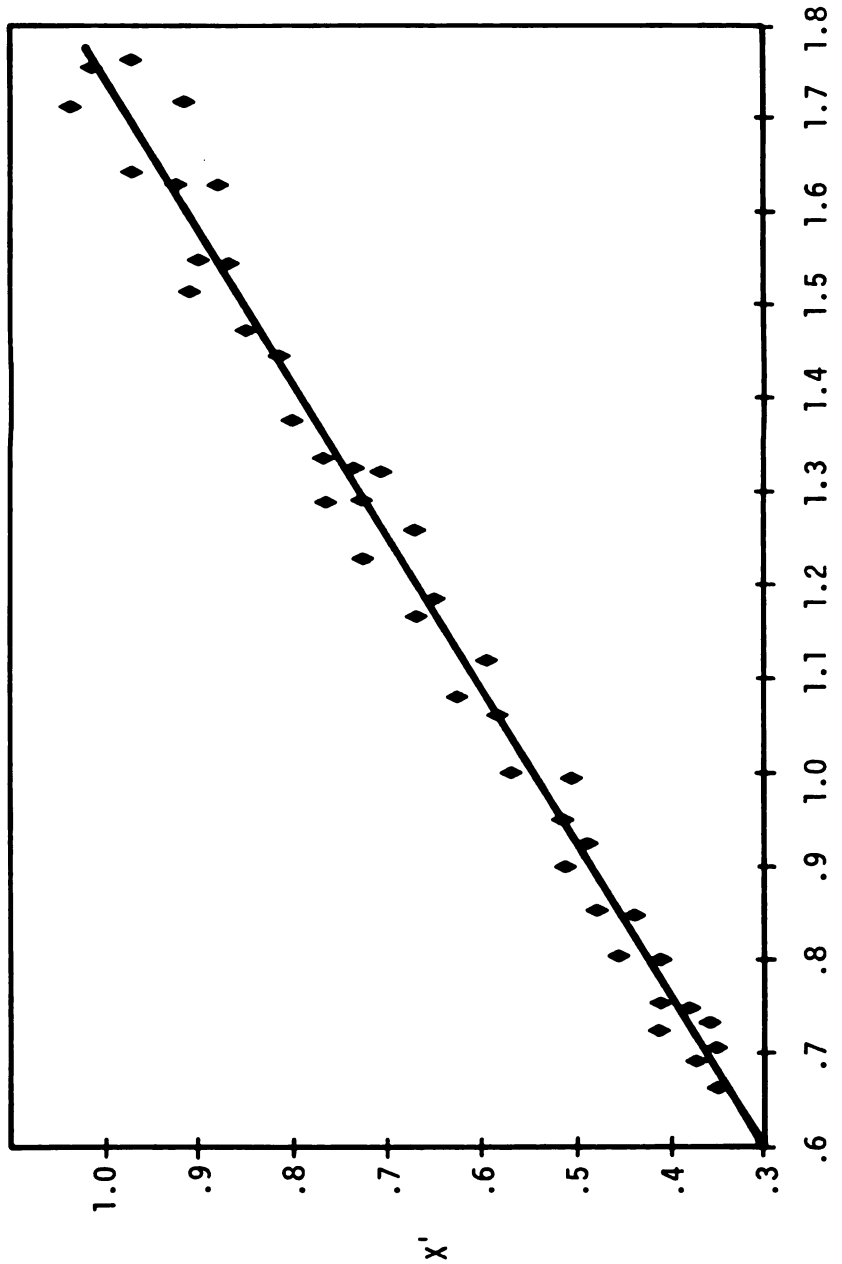

Figure 10.2.--Data points and regression line for Equation [10.8].

The modification of the f-chart program mainly serves two purposes. First, the MAIN program and subroutine CALC of the program had to be modified to accept weekly instead of daily loads. This approach allows the user to investigate solar systems for processing plants with various working schedules. Second, Equation [10.1] was replaced by Equation [10.11]. Assumptions

3. The over-all loss coefficient (U_L) is constant;
4. The water tank is not pressurized so that the maximum temperature allowed is the boiling point of water (100°C);
5. The system load can extract energy from the tank as long as the tank temperature is above 20°C;
6. The distribution of the daily water demand is assumed to be the average residential distribution, described by Mutch (1974) as in Figure 10.1;
7. The loss coefficient for the storage tank and piping is assumed to be 0.48 W/m^2-°C;
9. The storage tank is fully mixed

were not used to derive Equation [10.11].

CHAPTER 11

RESULTS AND DISCUSSION

11.1 Solar Water Heater Performance

The performance of the solar water heaters investigated in this study is expressed in terms of colelctor efficiency. The degree of compatibility of solar water heating with specific food processing plants is expressed by the percentage of the hot water supplied by the solar water heater.

11.1.1 Hourly Performance

Solar water heaters operating in a certain food processing plant with different energy use profiles are expected to perform differently. The difference arises from the fact that hot water is removed from the storage tank according to the energy use schedule. Since the hot water removed is automatically replaced by cold water of fixed temperature, the temperature of the water in the storage tank will change according to the energy use profile in the processing plant.

In Figure 11.1.1 the temperature of the water in the storage tank during a typical Michigan day in July is shown. The five solar systems in the figure are of equal size (collector area 1000 m^2, and tank volume 14,000 gal.) and deliver the same amount of hot water (53,000 Kg/day).

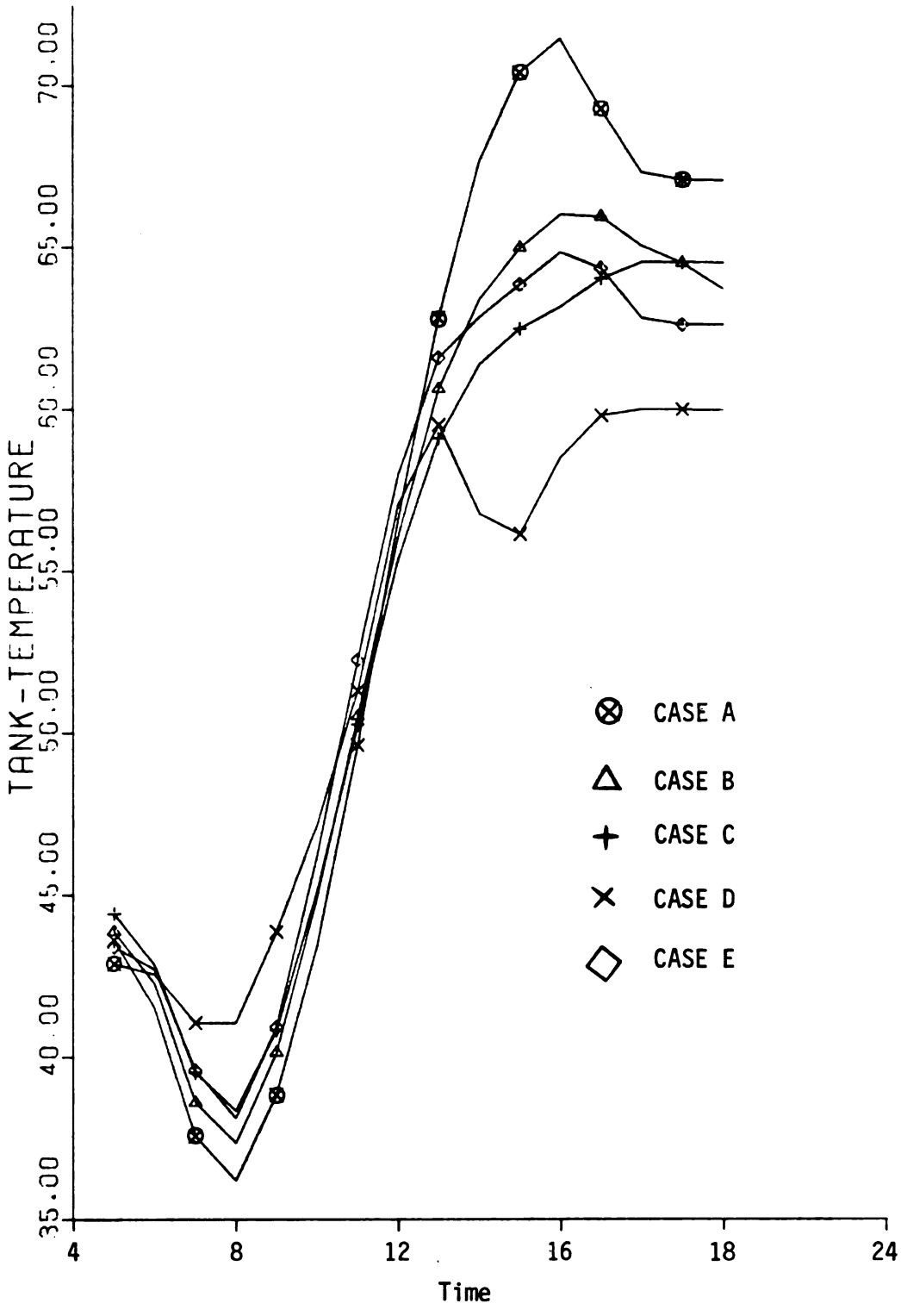

Figure 11.1.1.--Non-stratified tank temperature change during a typical day in July in Michigan

The hourly supply of hot water, however, varies in the five systems according to the energy use profiles established in Chapter 7 (Figure 7.1.8). In Figure 11.1.1 can be seen that before any solar energy is collected the temperature in the storage tank drops due to hot water usage. As soon as the sun strikes the solar collector the hot water temperature increases.

The water temperature in the tank in Case A reaches the lowest point. This is because at 7 a.m. when the temperature begins to rise approximately 20,000 Kg of hot water is supplied to the processing plant. During the same period the processing plant of Case D has used only approximately 5,000 Kg of hot water.

The water temperature rise in the tank stops either because of decreased insolation (late in the afternoon) or because of the energy removed from the tank becomes greater than that absorbed by the solar collector. In Figure 11.1.1 the temperature of the tank in Case D begins to decrease around noon due to the fact that approximately 50 percent of the daily water delivery occurs between 12 and 2 p.m.

Figures 11.1.2 through 11.1.6 represent the daily variation of the tank temperature for the five use patterns in July in Michigan (Lansing). The distribution of the daily hot water supply is also shown in the figures. Figures 11.1.7 through 11.1.11 show the tank temperature and the same loads during a day in December. As expected, the water temperature in December remains considerably lower than in July.

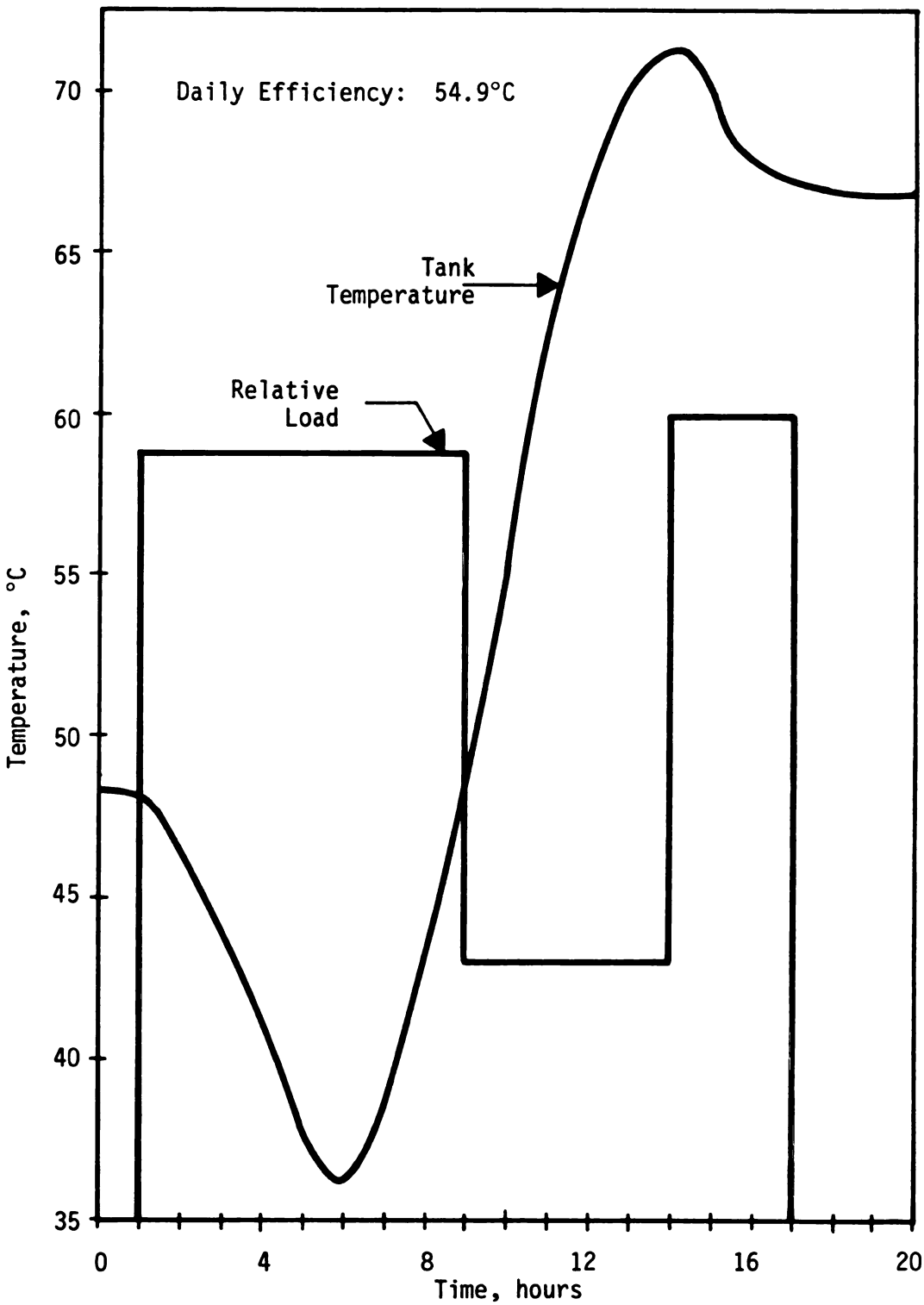

Figure 11.1.2.--Tank temperature change during a typical day in July (Case A).

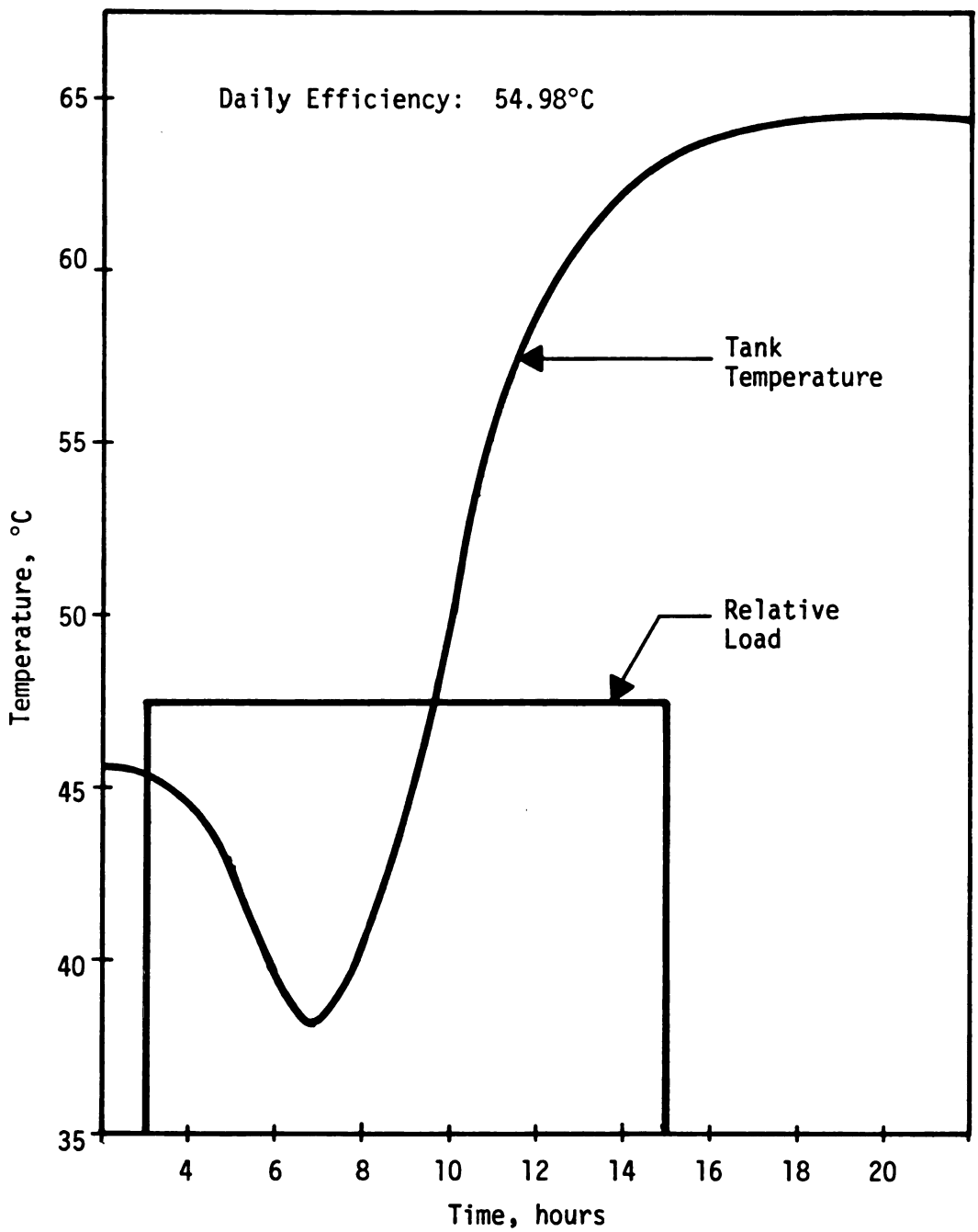

Figure 11.1.3.--Tank temperature change during a typical day in July.

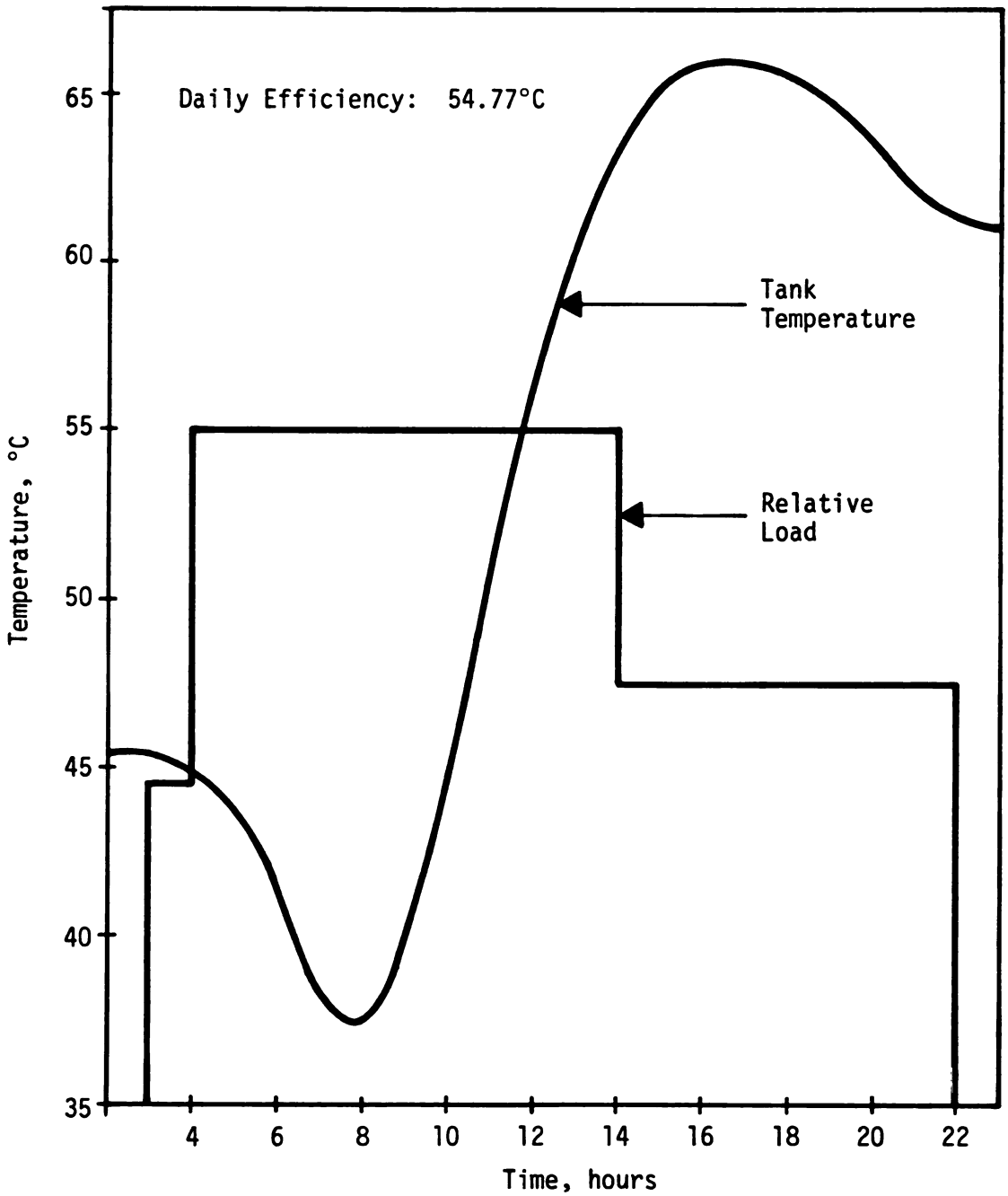

Figure 11.1.4.--Tank temperature change during a typical day in July (Case B).

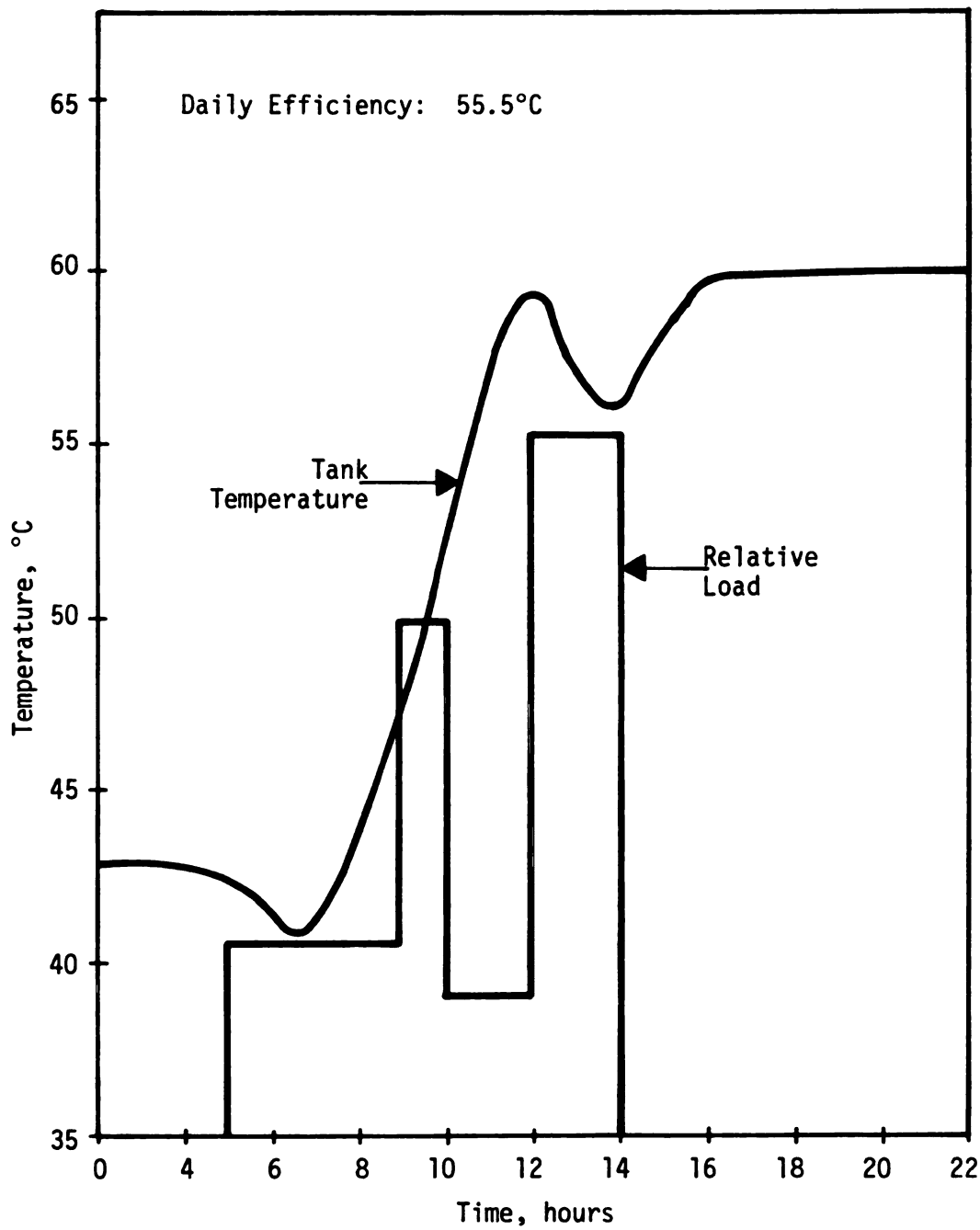

Figure 11.1.5.--Tank temperature change during a typical day in July (Case D).

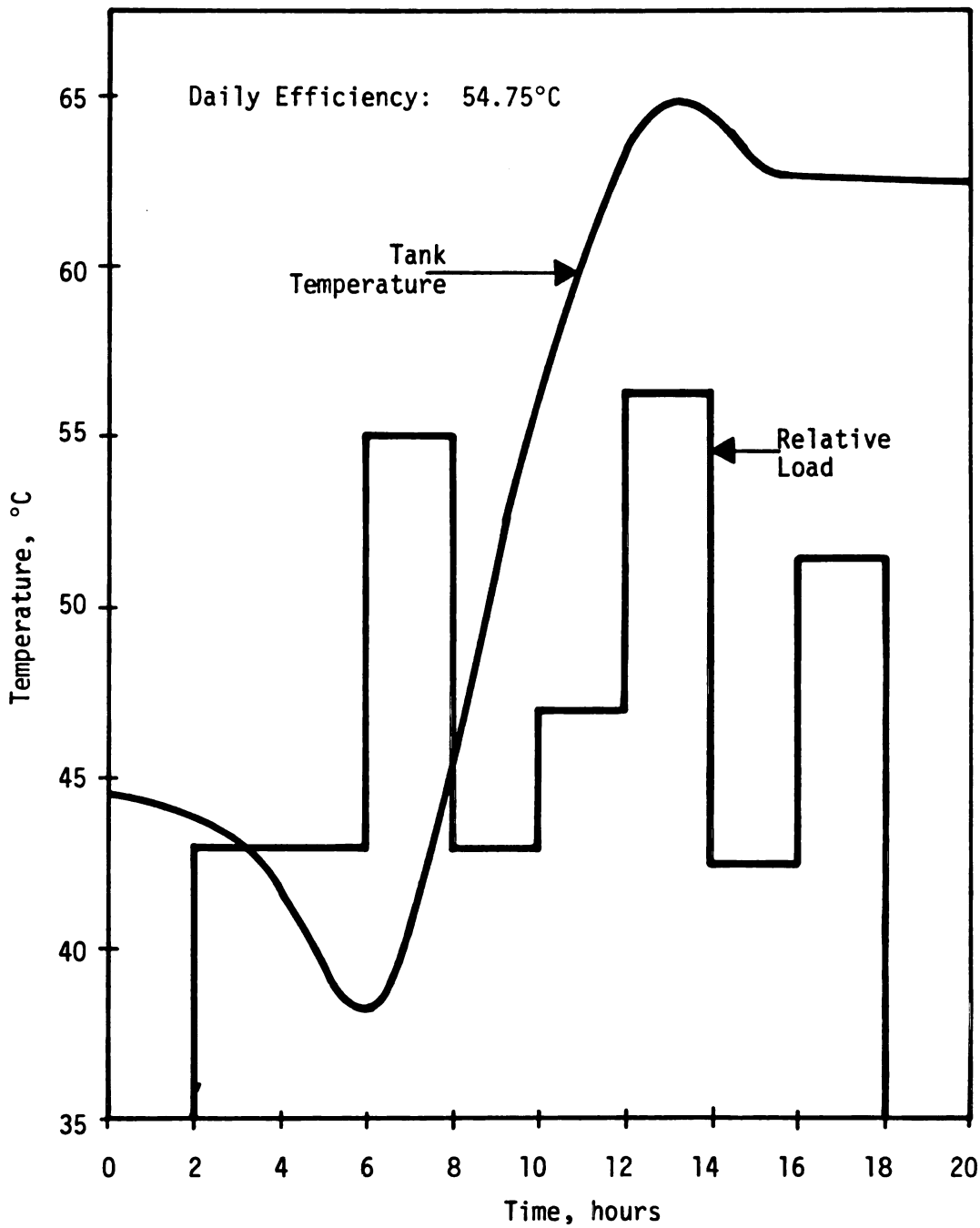

Figure 11.1.6.--Tank temperature change during a typical day in July (Case E).

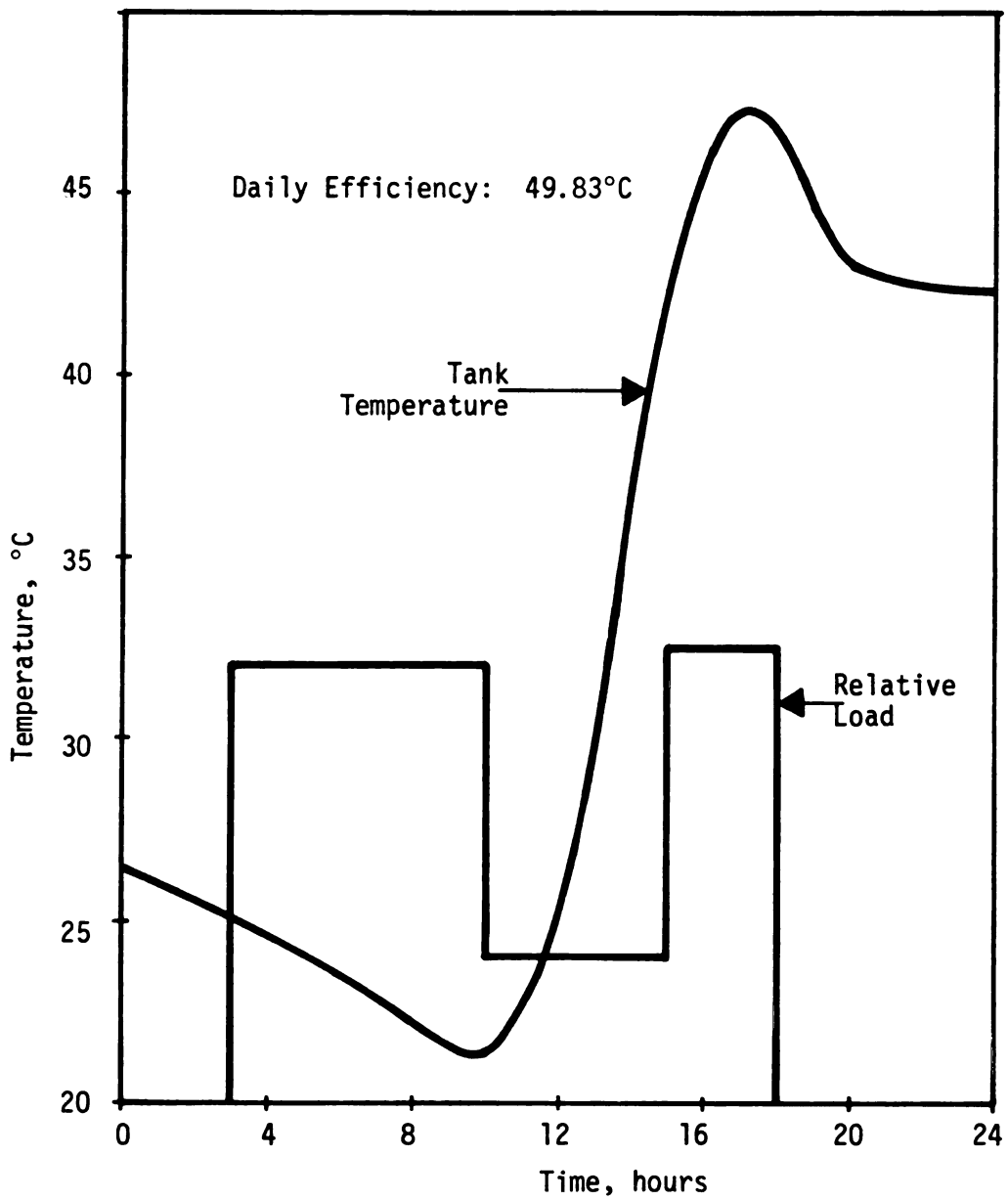

Figure 11.1.7.--Tank temperature change during a typical day in December (Case A).

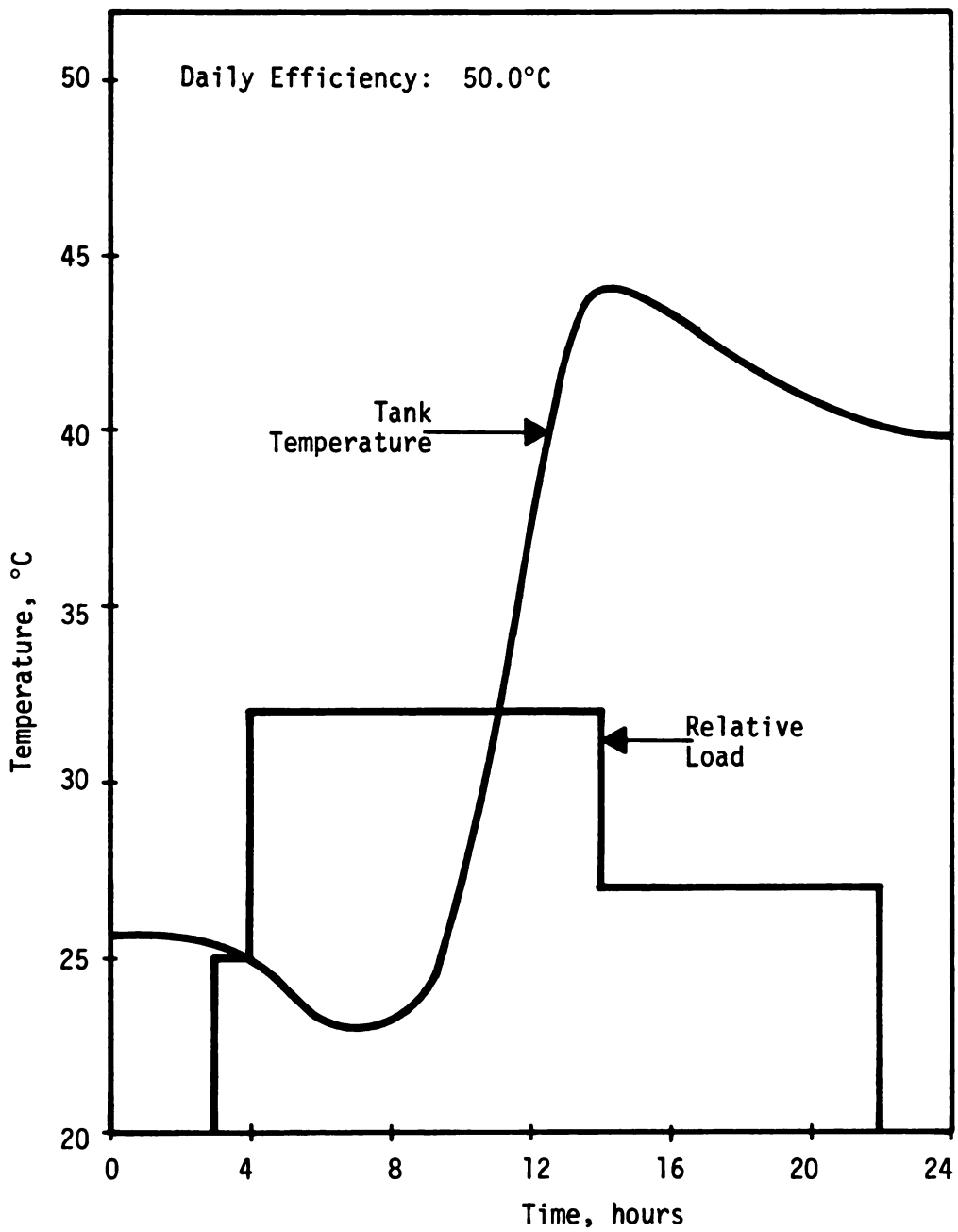

Figure 11.1.8.--Tank temperature change during a typical day in December (Case B).

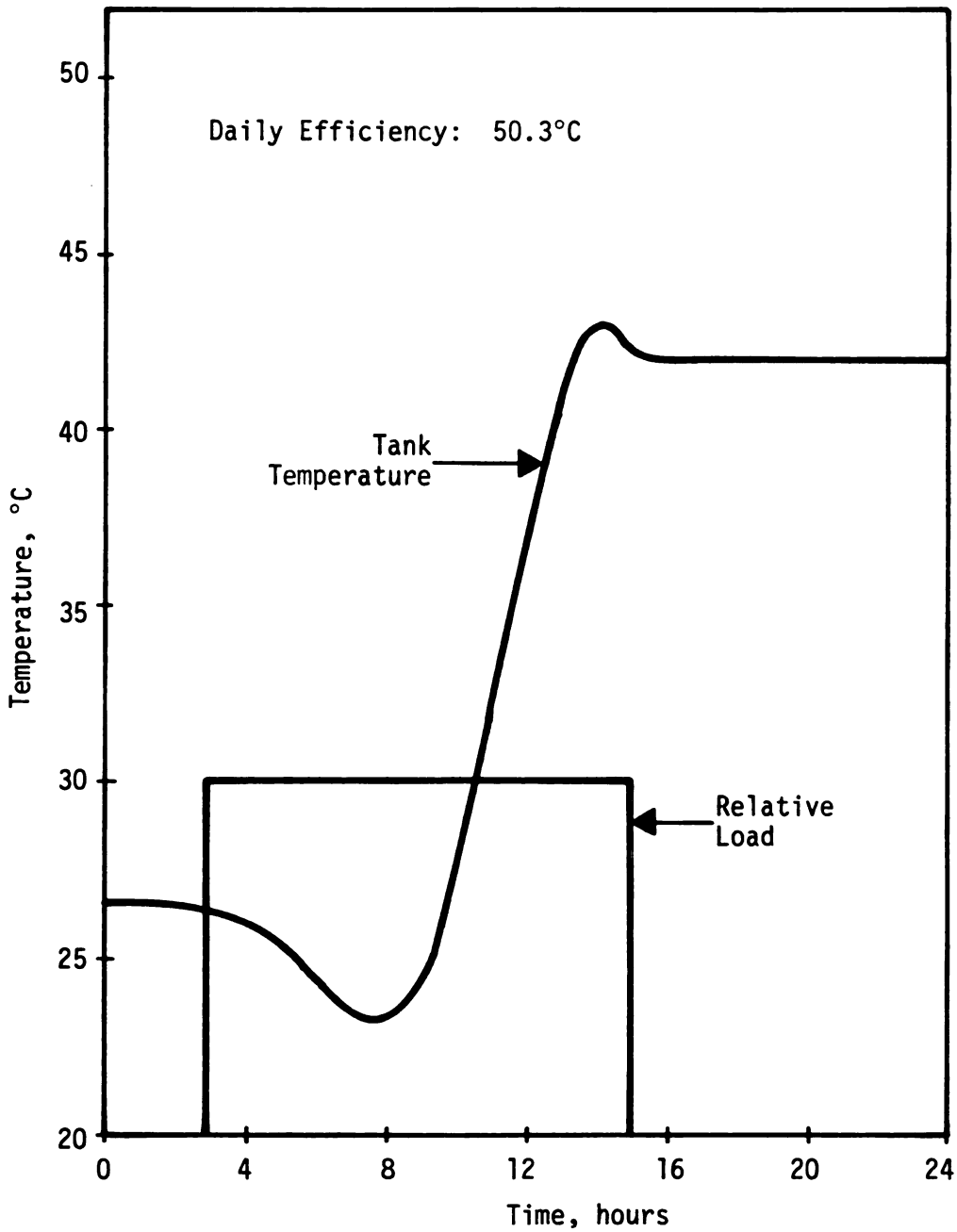

Figure 11.1.9.--Tank temperature change during a typical day in December (Case C).

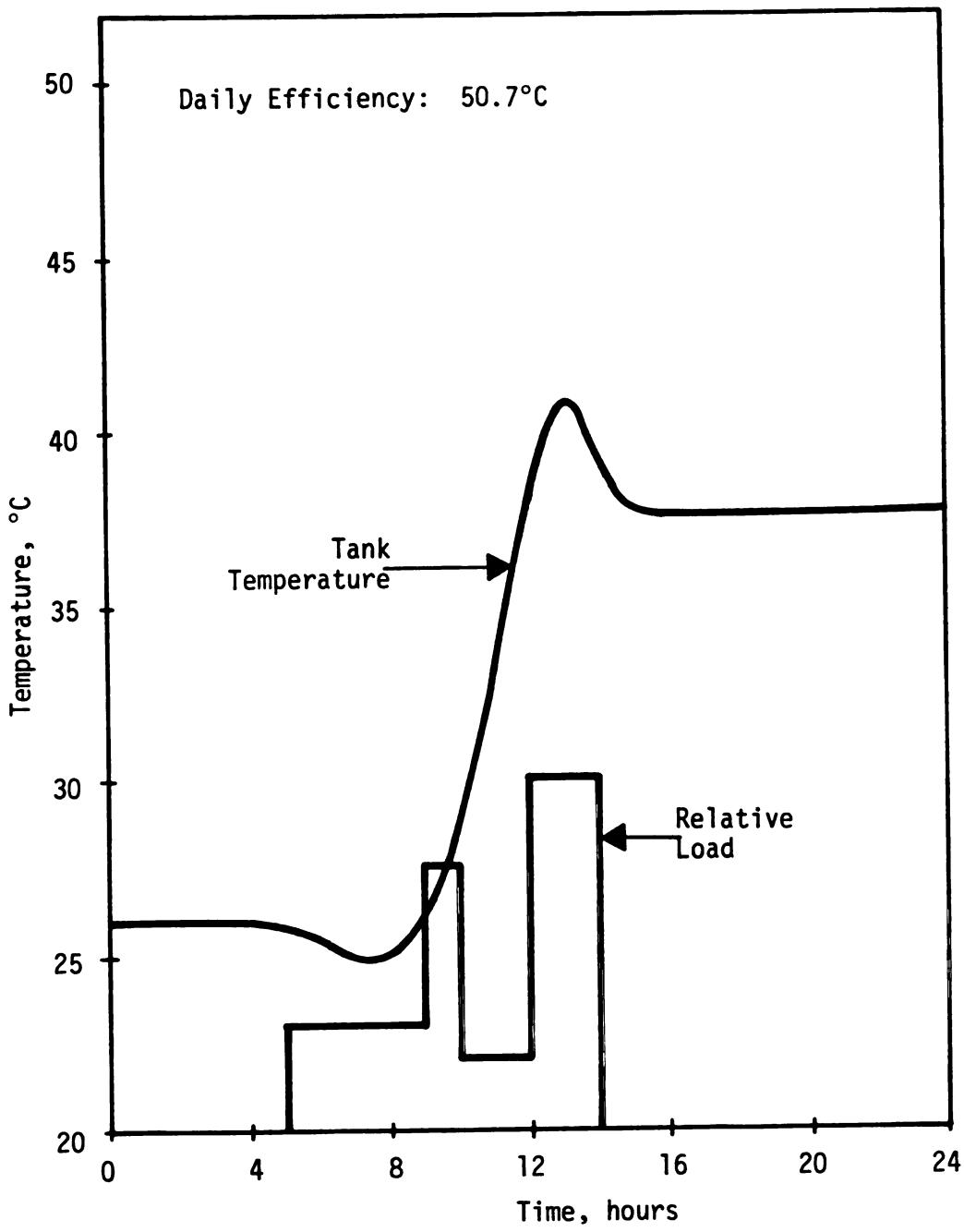

Figure 11.1.10.--Tank Temperature change during a typical day in December (Case D).

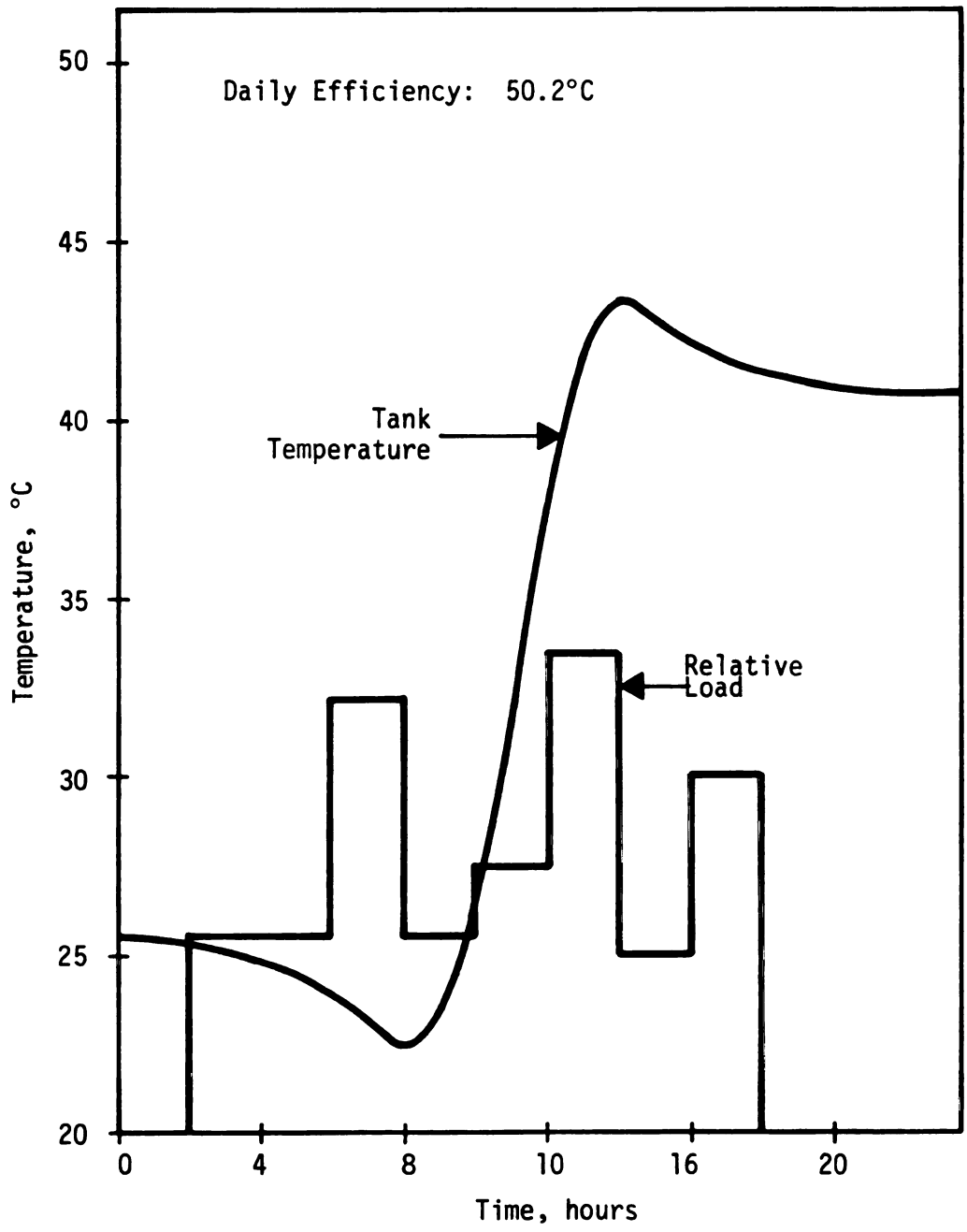

Figure 11.1.11.--Tank temperature change during a typical day in December (Case E).

The temperature rise in the water tank of a solar water heater system exhibits an exponential profile. The nature of the exponential profile appears to be a function of the amount of hot water removed from the tank (see Figures 11.1.2 through 11.1.11). Other factors such as amount of insulation and degree of mixing in the storage tank will also affect the temperature profile.

The hourly efficiency of a solar system cannot be determined by TRNSYS. This is because at times of zero incident radiation the TRNSYS run will terminate since a division by zero will be performed. As was discussed in Chapter 5, efficiency is calculated by dividing the energy absorbed by the total incident radiation (see Equation 5.25).

The hourly performance of the solar systems is expressed in terms of the over-all heat loss coefficient of the collector, the temperature rise across the collector, and the collector inlet and ambient temperature differences. As was discussed in Chapter 5, collector efficiency, thermal losses and thermal output of the collector are directly related to the above quantities (see Equations 5.19 and 5.25).

In Appendix B1 and B2 the simulated collector inlet and outlet temperature for the five solar systems during the same day of July and December in Lansing, Michigan is presented. The collector inlet temperature varies for the five systems. For an individual system the hourly variation is in accordance to the temperature in the tank. A similar variation in the collector outlet temperature is observed. Despite the above differences, the temperature rise

across the collector, presented in Tables 11.1.1 and 11.1.2, is approximately the same for all solar systems. As was mentioned previously, each system represents a certain food processing plant with characteristic energy use profile. A significant difference in the temperature rise across the collector during the day is observed, but there is little variation among the five systems during a specific time interval (i.e., 10-11 a.m. in July). This indicates that the thermal output of the solar collector is hardly affected by the hourly amount of hot water removed from the tank. It seems that considerably larger differences in inlet temperature among the five systems than the ones which occurred during the two days investigated, are required for a significant difference in thermal output to be noticed.

The overall heat loss coefficient of the collector for the five solar systems is shown in Figures 11.1.12 and 11.1.13. The variation of the loss coefficient among the five systems is small. According to Equation [5.22] for the same ambient temperature a 20°C rise of the plate temperature will increase the loss coefficient about 0.5 KJ/hr-m^2-°C. In the figures it can be seen that the range of change is relatively narrow (6.7 to 8.4 KJ/gr-m^2-°C). The loss coefficient is mostly dependent on characteristics such as number of glass covers, absorbance, and emittance of the plate, transmittance of the glass and amount of insulation. For a simulation period equal to one year the maximum and minimum values observed are 6.1 and 9.2 KJ/hr-m^2-°C. The majority of the values are about 8 KJ/hr-m^2-°C. Thus, it seems that by treating the overall loss

TABLE 11.1.1.--Difference between collector outlet and inlet temperature during a typical day in July.

Hour	$(T_{out} - T_{in})$, °C				
	Case A	Case B	Case C	Case D	Case E
7- 8	1.8	1.7	0.7	1.5	1.7
8- 9	3.7	3.6	3.6	3.5	3.6
9-10	5.6	5.5	5.5	5.4	5.5
10-11	7.1	7.0	7.0	7.0	6.9
11-12	8.0	8.0	8.0	8.0	8.0
12-13	8.2	8.2	8.3	8.2	8.2
13-14	7.5	7.7	7.7	7.8	7.7
14-15	6.2	6.4	6.5	6.8	6.5
15-16	4.9	5.0	5.2	5.2	5.0
16-17	3.0	3.2	3.3	3.4	3.2
17-18	1.3	1.4	1.4	1.6	1.5

TABLE 11.1.2.--Difference between collector outlet and inlet temperature during a typical day in December.

Hour	$(T_{out} - T_{in})$, °C				
	Case A	Case B	Case C	Case D	Case E
8- 9	4.6	4.6	4.6	4.5	4.6
9-10	3.0	3.0	3.0	2.9	3.0
10-11	4.5	5.0	4.4	4.4	4.4
11-12	6.2	6.2	6.2	6.2	6.2
12-13	5.5	5.6	5.6	5.5	5.6
13-14	6.8	6.9	6.9	7.0	6.9
14-15	4.3	4.4	4.4	4.7	4.4
15-16	1.3	1.5	1.5	1.7	1.5

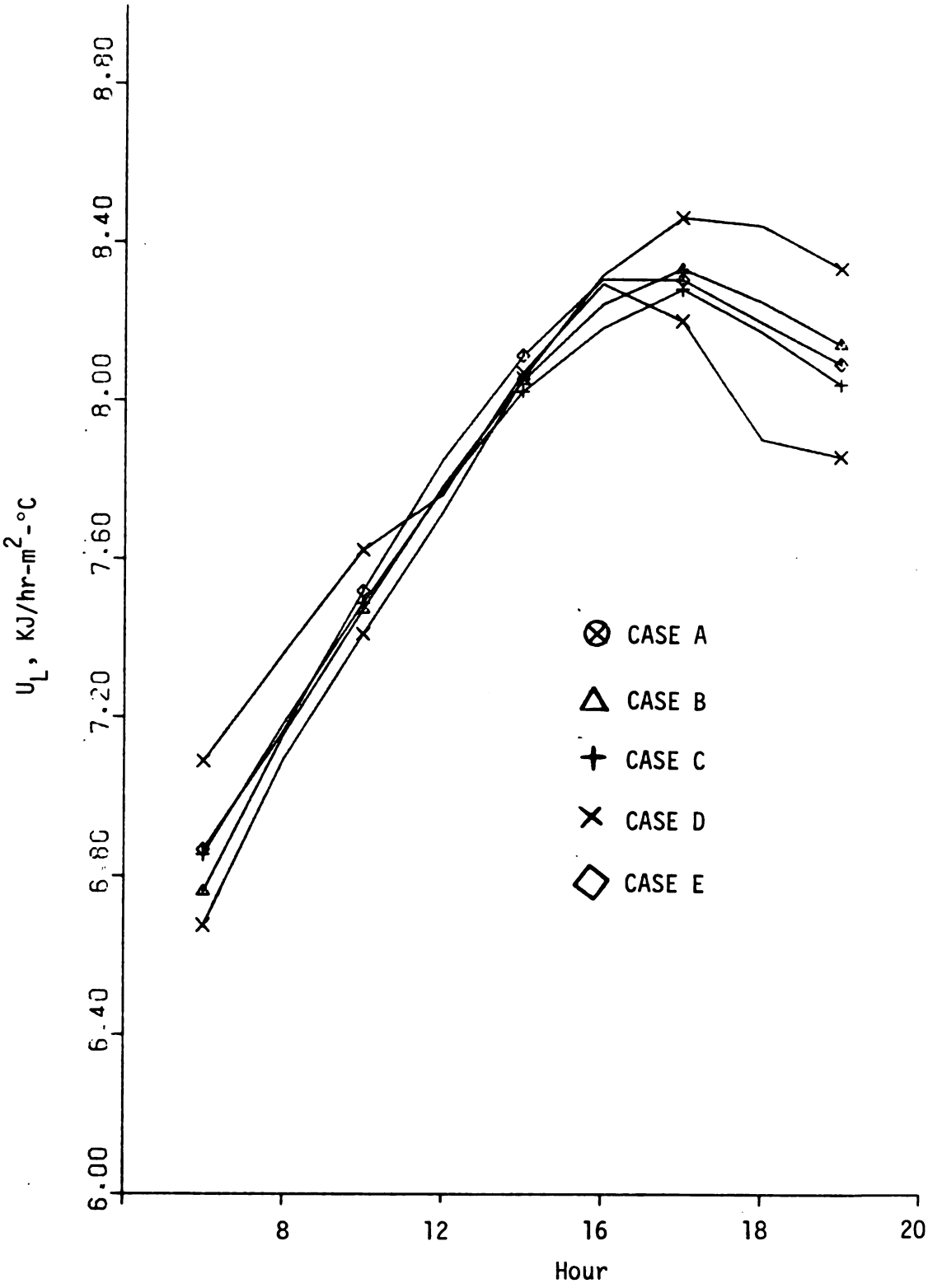

Figure 11.1.12.--Overall heat loss coefficient change during a typical day in July in Michigan.

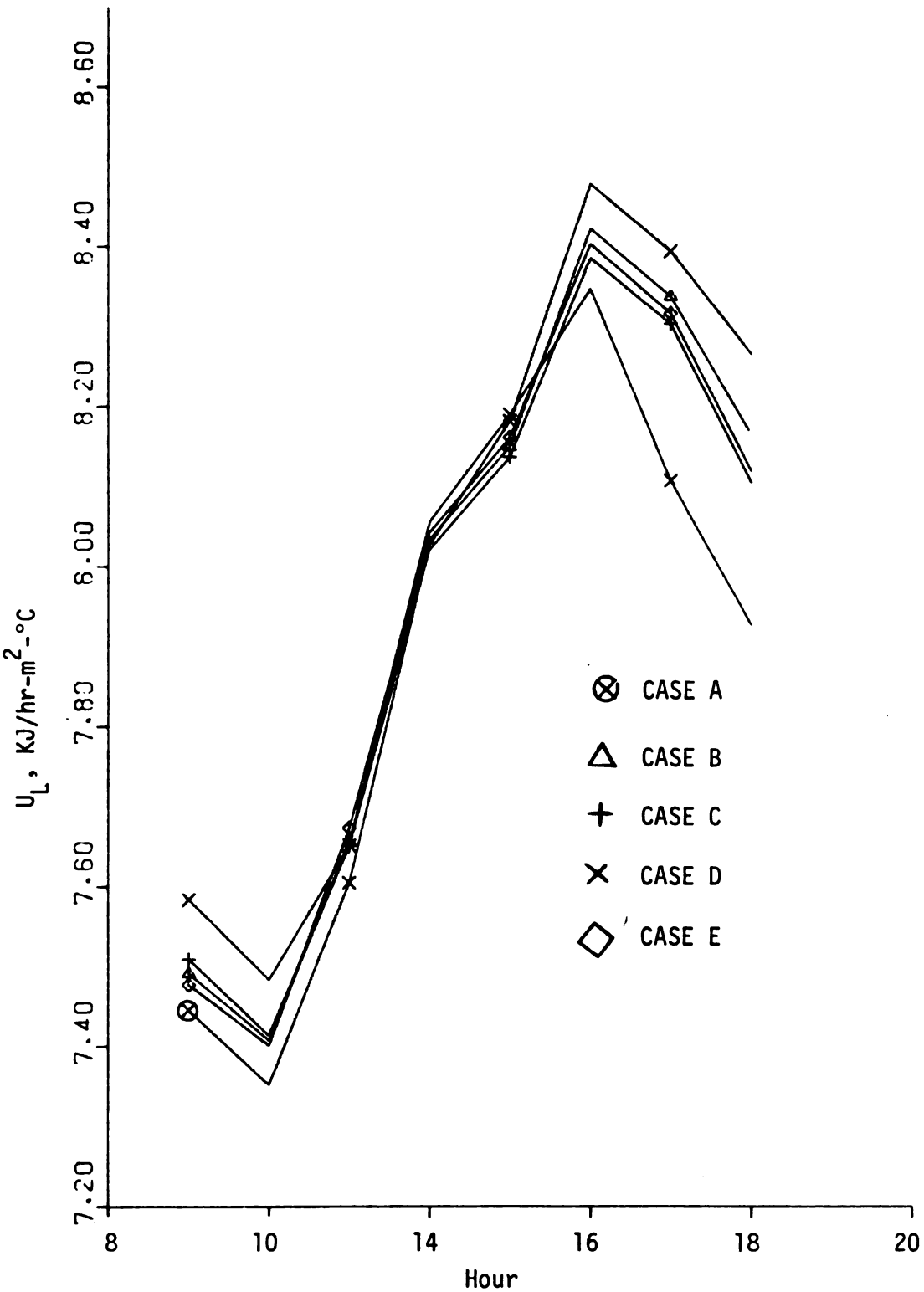

Figure 11.1.13.--Overall heat loss coefficient change during a typical day in December in Michigan.

coefficient as a design parameter rather than an operational characteristic, the error introduced in determining the long run performance of a solar system is relatively small.

The difference between the collector inlet and ambient temperature for two days in July and December is presented in Tables 11.1.3 and 11.1.4. As was explained in Chapter 5, the heat losses of a solar collector are calculated based on this temperature difference since the plate temperature is difficult to estimate. From Tables 11.1.1 and 11.1.3 and Figures 11.1.1 and 11.1.12 it can be seen that higher tank temperatures will result in a higher loss coefficient, a higher difference between the collector inlet and ambient temperature and a lower temperature rise across the collector.

The difference in magnitude of the above quantities among the five systems is not large enough to result in significant variation of the daily solar system performance. The daily collector efficiency shown in Figures 11.1.2 through 11.1.11 does not vary significantly among the five systems. In December a slightly smaller daily efficiency is observed because of the higher differences of collector inlet and ambient temperature observed in December (Table 11.1.4) compared to July. As will be discussed in the next pages, the long-term performance of a solar system is slightly better in the summer than in the winter because of the higher differences between collector inlet and ambient temperature observed in the winter than in summer (Tables 11.1.3 and 11.1.4).

TABLE 11.1.3.--Difference between collector inlet and ambient temperature during a typical day in July.

	(Ti - Ta), °C				
Hour	Case A	Case B	Case C	Case D	Case E
7- 8	17.1	18.5	20.2	24.8	20.4
8- 9	22.2	23.5	24.0	27.9	23.7
9-10	26.4	27.8	28.2	31.5	28.9
10-11	31.0	32.6	32.5	32.1	34.4
11-12	38.3	38.1	37.3	38.6	39.9
12-13	44.2	42.0	40.3	43.6	43.9
13-14	47.6	43.6	42.1	39.8	42.8
14-15	49.9	44.0	41.7	34.2	42.4
15-16	50.2	44.3	41.4	36.2	42.9
16-17	48.5	44.0	41.0	37.1	42.5
17-18	43.6	42.4	41.0	37.1	29.4

TABLE 11.1.4.--Difference between collector inlet and ambient temperature during a typical day in December.

	(Ti - Ta), °C				
Hour	Case A	Case B	Case C	Case D	Case E
8- 9	32.0	33.2	33.7	35.6	32.8
9-10	30.2	31.6	31.7	33.4	31.4
10-11	35.4	36.2	36.7	36.7	37.3
11-12	44.0	44.2	43.9	44.9	44.5
12-13	46.7	45.7	45.3	46.9	46.0
13-14	53.9	52.0	50.8	49.5	51.4
14-15	52.2	50.3	49.2	43.2	49.6
15-16	50.3	47.1	45.3	40.2	45.7

11.1.2 Daily Performance

In Table 11.1.5 the daily collector efficiency of solar systems operating in food processing plants with different energy use profiles is presented. A small variation of the efficiency among the various processing plants is observed. The table is divided in weekly sections. The processing plants were assumed to operate five days per week. The last two rows of each weekly section represent days at which the plants do not operate. During such days the temperature in the tank constantly increases, reaching its peak the last day of the week. The result of this operational characteristic of food processing plants is expressed directly in lower collector efficiencies for the last two days of the week. The first operating day of the week in the plant which follows the two idle days is also exhibiting lower efficiencies because of the relatively high water temperature in the storage tank. During this day the effect of the energy profile on collector efficiency is more pronounced than during the rest of the days.

Table 11.1.6 contains the same information as Table 11.1.5 for the month of December. For reasons mentioned previously, lower efficiency values are observed in December than in July.

11.1.3 Weekly Performance

The weekly collector efficiency in December and July for various food processing plants is presented in Table 11.1.7. There is no significant effect of the energy use profile on the efficiency

TABLE 11.1.5.--Daily efficiency of a 150 m^2 solar collector for food processing plants exhibiting various energy use profiles (July) in Michigan.

Day	Efficiency, percent				
	Case A	Case B	Case C	Case D	Case E
1	40.1	38.4	42.4	39.8	40.9
2	30.1	29.4	31.5	30.2	30.3
3	44.1	47.6	40.8	45.4	43.3
4	54.4	55.4	54.0	54.3	54.4
5	46.9	47.9	46.9	47.8	47.7
6	53.6	54.7	54.4	55.1	54.4
7	52.6	53.5	53.3	53.4	53.4
8	42.3	41.5	44.9	42.7	42.9
9	28.8	28.1	30.4	29.2	29.8
10	43.8	45.3	40.9	43.3	42.6
11	47.5	45.2	44.1	45.3	45.0
12	54.0	54.8	54.4	55.0	54.4
13	52.5	53.2	52.9	53.1	52.8
14	52.7	53.0	52.8	53.4	53.1
15	44.2	42.9	46.9	44.5	44.9
16	31.2	31.0	32.7	31.6	32.0
17	43.8	44.5	41.3	42.6	42.1
18	49.3	47.6	46.9	45.4	47.1
19	56.0	56.4	56.0	56.0	56.0
20	54.9	55.3	55.0	55.2	55.0
21	53.0	53.1	53.0	53.0	53.6
22	43.0	42.1	45.2	43.2	44.0
23	0.0	0.0	0.0	0.0	0.0
24	42.4	43.5	40.4	41.8	41.3
25	52.9	53.1	51.6	52.7	52.4
26	48.1	47.9	48.0	42.8	43.4
27	54.6	55.5	55.2	56.2	55.6
28	43.5	42.9	45.7	44.6	44.4
29	28.9	28.5	29.9	29.2	29.2
30	38.9	40.4	36.7	38.4	37.6
31	45.0	44.9	45.1	45.0	44.7

TABLE 11.1.6.--Daily efficiency of a 150 m^2 solar colelctor for food processing plants exhibitng various energy use profiles (December) in Michigan.

Day	Efficiency, percent				
	Case A	Case B	Case C	Case D	Case E
1	27.4	27.4	27.3	28.0	26.2
2	7.9	5.4	8.5	7.7	8.1
3	50.4	49.9	50.7	50.2	50.5
4	28.0	32.8	27.9	28.1	30.3
5	50.7	52.0	51.2	52.1	51.5
6	33.9	34.2	34.4	31.3	34.0
7	51.6	51.5	51.1	51.9	51.6
8	0.0	12.1	0.0	18.3	0.0
9	29.4	30.9	32.0	29.8	29.7
10	45.3	43.8	45.6	44.7	45.5
11	47.5	48.0	46.7	47.4	46.6
12	36.5	36.0	35.9	34.1	35.9
13	18.8	14.0	15.1	13.2	15.1
14	25.0	25.2	25.1	25.1	25.0
15	33.6	34.7	33.8	34.9	34.6
16	0.0	0.0	0.0	0.0	0.0
17	26.7	26.4	27.4	27.0	27.1
18	43.1	46.5	44.4	45.1	44.8
19	41.7	42.6	41.1	42.0	42.4
20	40.1	41.4	40.1	41.6	41.4
21	43.9	45.6	45.5	44.4	43.8
22	30.0	29.1	29.0	28.6	29.1
23	42.8	42.1	43.2	42.6	42.9
24	48.2	48.0	48.4	48.2	48.2
25	34.9	34.3	29.3	30.4	31.4
26	38.7	39.8	39.1	39.9	40.1
27	49.7	50.1	49.9	50.6	50.0
28	20.9	27.5	27.7	29.4	28.7
29	29.7	28.9	28.8	27.1	28.5
30	35.0	35.3	36.1	35.8	35.4
31	50.1	49.9	50.1	50.0	50.1

TABLE 11.1.7.--Weekly efficiency of 150 m^2 solar collector for food processing plants with different energy use profiles.

	Efficiency, percent				
Month	Case A	Case B	Case C	Case D	Case E
July	46.6	46.6	46.9	46.6	46.8
	46.7	47.3	47.3	47.4	47.2
	46.6	46.7	46.8	46.8	46.7
	48.3	48.3	48.1	47.8	48.0
	46.2	46.6	46.4	46.5	46.5
December	45.0	45.3	45.0	44.9	44.9
	43.3	44.4	43.7	44.3	43.8
	38.3	38.2	37.6	37.6	37.6
	43.2	43.7	43.5	43.5	43.5

of the collector. The efficiency in December is slightly lower than in July.

Table 11.1.8 shows the percentage of the weekly hot water load supplied by a solar system. The processing plants have been supplied by the same amount of solar heated water. There is a difference among the various weeks and among the two seasons but not between cases. As will be explained in later pages, this is due to the seasonal variation of the solar radiation available.

11.1.4 Monthly and Yearly Performance

The monthly collector efficiency of a solar system operating in a food processing plant is shown in Figure 11.1.14. The minimum and maximum efficiency is reached in December (42%) and August (49%), respectively. The lower efficiency of the winter months shown in Figure 11.1.14 is the result of the low ambient temperature in the winter (Figure 11.1.15).

In Table 11.1.9 the monthly collector efficiency for various size solar systems operating in food processing plants exhibiting energy use profile as in Case A is presented. Collector areas up to 4000 m^2 show no change in efficiency because each solar system has been scaled according to the procedure described in Chapters 6 and 9. For collector areas larger than 3000 m^2 the efficiency is slightly lower. Lower efficiency for these sizes was expected since the heat exchanger of the systems was considerably smaller than the one determined by the scaling procedure (see Table 9.1).

TABLE 11.1.8.--Percentage of weekly load delivered by a 150 m^2 solar collector system for food processing plants for different energy use profiles.

	Percent of Load Supplied by Solar				
Month	Case A	Case B	Case C	Case D	Case E
July	83.6	82.2	84.7	85.5	85.2
	78.5	76.9	79.1	79.8	80.2
	81.3	81.1	82.5	83.3	83.1
	78.7	78.5	79.4	81.3	80.3
	73.4	78.9	74.4	75.1	74.7
December	31.6	33.0	32.0	32.7	32.4
	38.7	39.5	30.0	40.4	39.4
	23.1	24.2	23.2	24.1	23.6
	14.0	14.2	14.4	14.8	14.4

TABLE 11.1.9.--Monthly efficiency for various size solar collectors for food processing plants exhibiting energy use profile as in Case A in East Lansing, Michigan.

Month	Efficiency, percent Collector Size, m^2								
	150	250	500	1000	2000	3000	4000	5000	6000
January	41.6	41.8	41.9	41.9	41.5	40.1	39.9	39.9	39.0
February	42.3	42.8	42.7	42.7	42.0	40.6	40.3	40.3	39.4
March	42.4	42.9	42.9	42.9	42.3	41.2	40.6	40.6	39.7
April	45.0	45.4	45.4	45.3	44.8	43.4	43.1	43.0	42.1
May	45.3	45.6	45.6	45.6	45.1	43.7	43.4	43.3	42.4
June	46.8	47.4	47.3	47.3	46.7	45.2	44.9	44.9	44.0
July	46.2	46.6	46.7	46.7	46.1	44.7	44.4	44.3	43.4
August	48.7	49.2	49.2	49.2	48.5	46.8	46.6	46.5	45.6
September	46.5	47.0	46.9	46.9	46.4	44.8	44.6	44.5	43.7
October	46.9	47.3	47.3	47.3	46.6	45.1	44.8	44.7	43.8
November	45.6	46.0	46.1	46.1	45.5	44.0	43.7	43.7	42.7
December	42.5	43.0	43.0	43.0	42.4	41.2	41.0	40.9	40.0

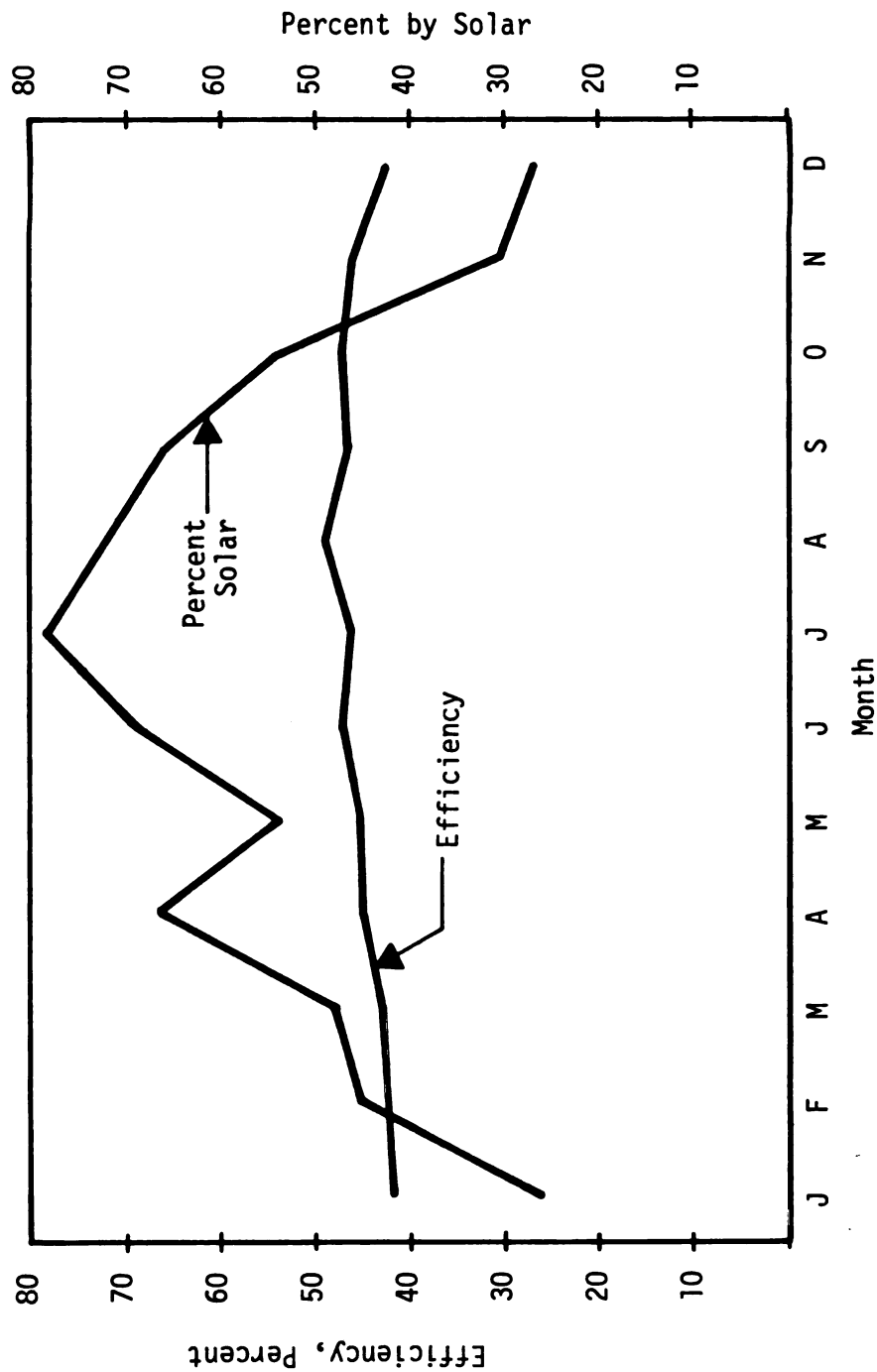

Figure 11.1.14.--Monthly efficiency and percent of load supplied by solar.

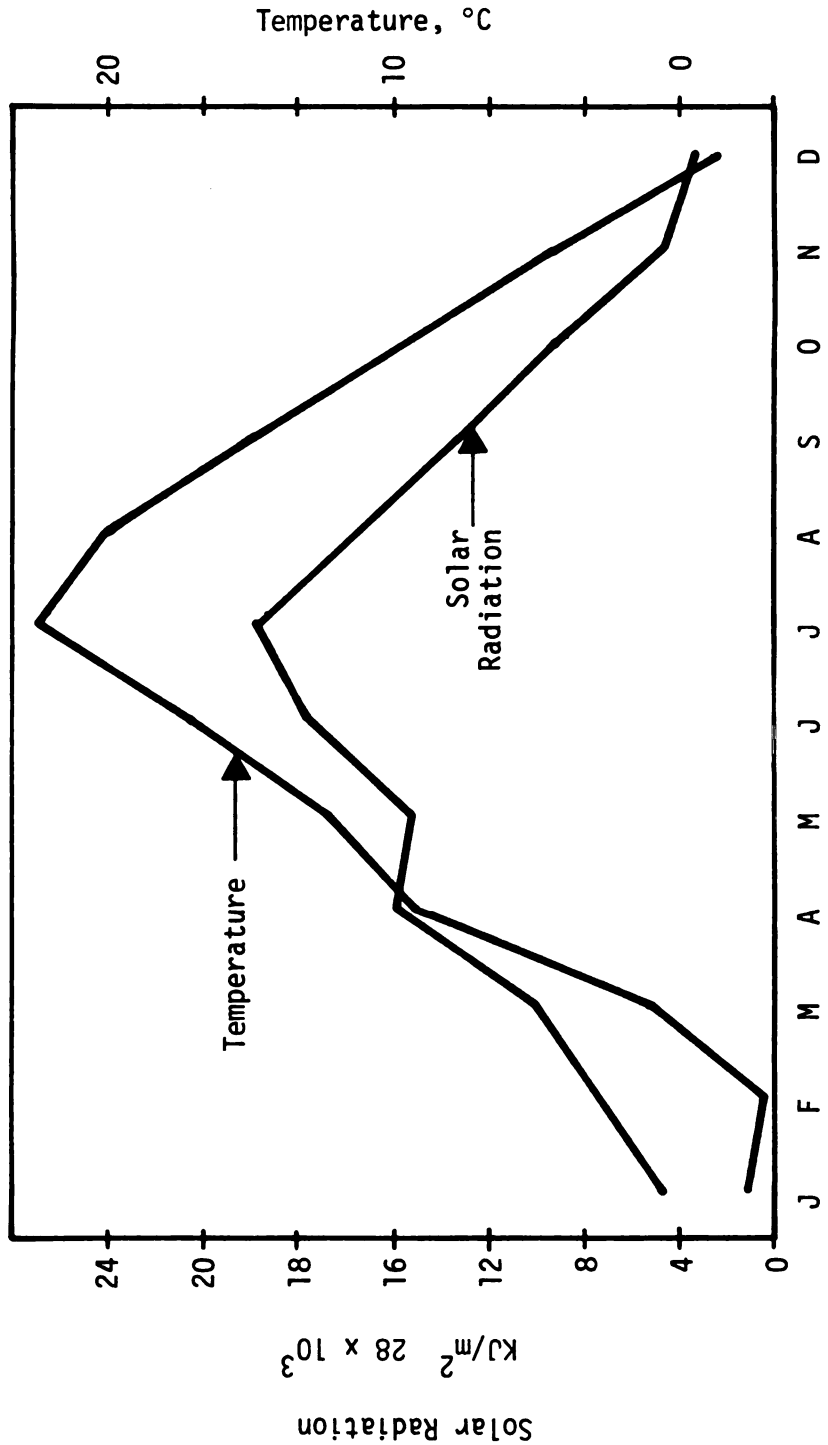

Figure 11.1.15.--Monthly average daily total radiation on a horizontal plane and average temperature in East Lansing, Michigan.

The monthly collector efficiency for other type food processing plants is tabulated in Appendices B3-B6.

The yearly collector efficiency presented in Table 11.1.10 does not change with the collector area and type of food processing plants. Large areas ($\geq$ 3000 m^2) exhibit lower efficiency values because of the smaller size heat exchanger used in the simulation.

The percentage of the hot water load in a processing plant supplied by solar energy is presented in Table 11.1.11. The variation of the percentage among the different size solar systems is small. Collectors with large areas ($\geq$ 3000 m^2) exhibit lower percentage values because of the smaller size heat exchanger used in the simulation.

The variation of the percentage among the months in the year shown in Figure 11.1.14 follows the same change as the monthly average daily total radiation on a horizontal plane described in Figure 11.1.15. From Figures 11.1.14 and 11.1.15 can be concluded that the monthly collecor efficiency will vary within a relatively narrow range. The percentage of the hot water demand supplied by a solar system, hwoever, will depend to a large extent on the amount of solar radiation available.

Percentages for other type processing plants are tabulated in Appendices B7 through B10. Again, there is no considerable variation in percentage among the food processing plants. This is also illustrated in Table 11.1.12 where the yearly percentage of various size solar systems operating in different type food processing plantats is presented.

TABLE 11.1.10.--Yearly efficiency of various size solar collectors for food processing plants exhibiting different energy use profiles in East Lansing, Michigan.

Collector Area m^2	Efficiency, percent				
	Case A	Case B	Case C	Case D	Case E
150	45.5	45.5	45.6	45.6	45.6
250	45.9	45.5	45.5	--	--
500	45.9	45.9	46.0	46.2	46.0
1000	45.9	45.9	46.0	46.1	46.1
2000	45.3	45.3	45.3	--	--
3000	43.8	43.3	43.9	43.5	43.8
4000	43.6	43.0	43.6	--	--
5000	43.5	43.5	43.5	--	--
6000	42.6	42.1	42.6	42.2	42.6

TABLE 11.1.11.--Percentage of monthly load supplied by various size solar systems for food processing plants exhibiting energy use profiles as in Case A in East Lansing, Michigan.

Month	Percent of Load Delivered by Solar Collector Size, m^2								
	150	250	500	1000	2000	3000	4000	5000	6000
January	27.5	26.6	26.7	26.8	26.7	26.1	26.1	26.1	25.6
February	46.6	45.3	45.4	45.5	45.1	44.1	44.0	44.0	43.2
March	49.7	48.2	48.6	48.6	48.4	47.9	47.1	47.4	46.4
April	68.7	67.2	67.4	67.4	66.9	65.6	65.4	65.4	65.4
May	55.8	54.2	54.6	54.7	54.3	53.5	53.4	53.4	52.7
June	71.0	69.1	69.5	69.6	69.3	68.2	68.0	68.1	67.2
July	79.5	78.1	78.5	78.6	78.4	77.1	77.0	77.3	76.3
August	73.5	71.6	71.9	72.1	71.8	70.5	70.4	70.6	70.0
September	67.4	65.6	66.2	66.4	66.2	65.0	64.9	65.2	64.0
October	55.6	54.1	54.4	54.5	54.2	52.9	52.9	53.1	52.1
November	31.7	30.7	30.8	30.9	30.8	30.3	30.2	30.3	29.7
December	28.1	27.3	27.4	27.4	27.1	26.6	26.5	26.5	26.0

TABLE 11.1.12.--Percentage of yearly load delivered by various size solar systems for food processing plants with different energy use profile in East Lansing, Michigan.

Collector Area m^2	Percent of Load Supplied by Solar				
	Case A	Case B	Case C	Case D	Case E
150	54.8	55.2	55.7	56.9	56.2
250	53.3	55.6	56.1	--	--
500	53.6	54.1	54.5	55.6	54.9
1000	53.7	54.1	54.6	55.7	55.2
2000	53.4	53.9	54.3	--	--
3000	52.4	54.6	53.2	55.9	53.7
4000	52.3	54.4	53.1	--	--
5000	52.4	52.7	53.1	--	--
6000	51.6	52.6	52.2	56.8	52.7

The yearly performance and thermal output per collector unit area described in Table 11.1.13 indicate that the energy use profile in a food processing plant does not have a great effect on the thermal output of the solar system. The last four columns of Table 11.1.13 represent the collector incident energy, the energy absorbed by the collector, the energy delivered to the plant, and the energy lost from the tank, respectively. The difference between columns five and six is the amount of energy lost in the piping system, heat exchanger and storage tank. An average value of the losses is about nine percent.

In Table 11.1.13 Case D shows a better performance and higher thermal output. This was expected because in Case D about 50 percent of the daily hot water load is supplied around noon (see Figure 7.8) when the incident solar radiation reaches its maximum value. A hot water use schedule exhibiting its maximum around noon will result in large temperature rise across the solar collector.

11.2 Effect of Work Schedule and Operations on Solar System Performance

Changes in the work schedule and operations in food processing plants were introduced in TRNSYS as inputs by making the following assumptions:

1. The processing plants are assumed to operate five, six, and seven days per week;
2. The energy profiles of Figure 7.8 are moved backward. This means that a change in the daily work schedule

TABLE 11.1.13.--Yearly performance and thermal output per collector unit area of solar water heater in food processing plants with various energy use profiles.

Case	EFF	Percent by Solar	Incident Energy/m^2 10^6 KJ	Energy Gain/m^2 10^6 KJ	Energy Delivery/m^2 10^6 KJ	Tank Energy Loss/m^2 10^6 KJ
A	45.9	53.7	4.716	2.163	1.955	0.018
B	46.0	54.6	4.716	2.169	1.981	0.017
C	45.9	54.2	4.716	2.166	1.971	0.019
D	46.1	55.7	4.716	2.176	2.031	0.018
E	46.0	55.0	4.716	2.170	2.004	0.018

is assumed. For example, by moving the energy profile of Case A eight hours backward, the plant starts to operate at 10 a.m. instead of 2 a.m. as originally stated;

3. The system has to meet different requests for energy in the daily load of the processing plant; and
4. The size of the solar system does not change among the several runs.

In Figure 11.2.1 the temperature of the storage tank on a typical July Saturday, Sunday and Monday is shown. In the situation of five working days per week (5 D/W), the temperature is consistantly increasing during Saturday and Sunday when the plant is idle and drops on Monday when it resumes operation. The temperature on Sunday always exceeds 100°C. Under these circumstances a solar system must be protected from excessive pressure developed in the tank and the solar collector. A pressure relief valve or a pressurized tank is necessary to prevent damage to the system components. On Monday the temperature in the tank constantly decreases because the energy delivered from the tank to the processing plant is always higher than that absorbed by the solar collector.

In the case of six working days per week (6 D/W), the temperature in the tank increases constantly on Sunday, an idle day. For the seven working days per week scenario (7 D/W), the temperature in the tank remains considerably lower than for the 5 and 6 D/W values.

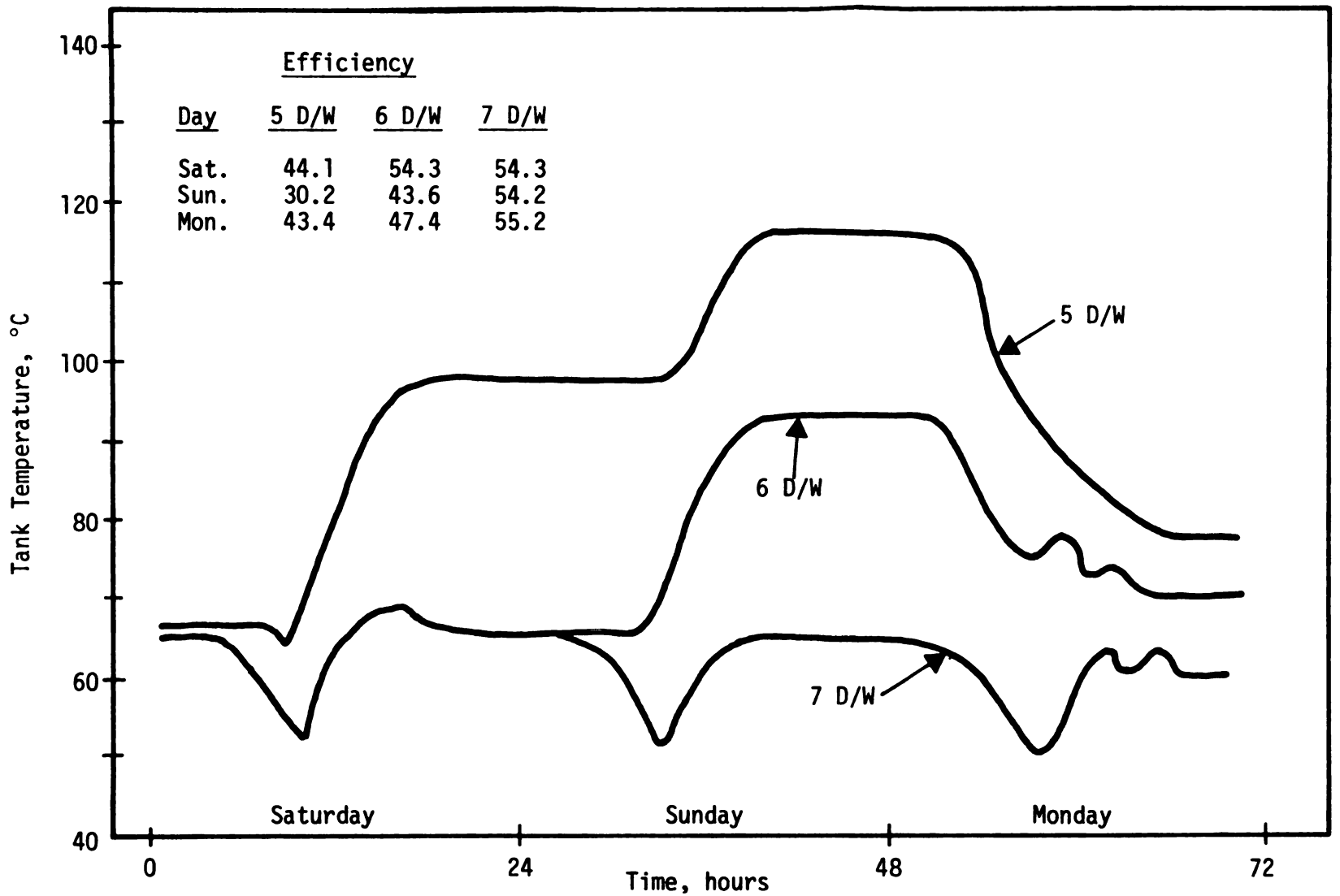

Figure 11.2.1.--Storage tank temperature during a typical weekend in July for solar systems in processing plants operating five, six or seven days per week.

The daily collector efficiency of the solar system corresponding to different operating days in the plant is tabulated in Figure 11.2.1. The variation of the efficiency among the three situations is obvious. On Sunday, for example, the 5 D/W and 7 D/W efficiencies are 30.2 and 54.2, respectively. The tank temperature difference between the two cases is about 50°C. The inlet tank temperature will differ by about the same magnitude. Therefore, a large difference between the efficiencies is to be expected (see Equations [5.19] and [5.25]).

In December the temperature behavior in the three tanks is shown in Figure 11.2.2. Because of lower insolation in December, large temperature differences as in July are not observed. The same can be said for the efficiency (see Figure 11.2.2).

The monthly efficiency and percent by solar for the three scenarios (5 D/W, 6 D/W, 7 D/W) are shown in Figures 11.2.3 and 11.2.4. From the figures is it clear that high efficiencies correspond to low percentages and vice versa.

The yearly thermal output and performance of the three systems is presented in Table 11.2.1.

In Table 11.2.2 the yearly and monthly collector efficiency of solar systems with the energy use profiles shifted backward in time is presented. From Tables 11.2.2, and 11.1.9 and Appendices B3 through B6 can be seen that the long-run performance is not affected by changes in the daily water use schedule in processing plants.

TABLE 11.2.1.--Yearly thermal output and performance of solar systems for food processing plants operating five, six or seven days per week in East Lansing, Michigan.

Day per Week	Collector Efficiency percent	Percent by Solar	Energy Gained/m^2 (10^6KJ)	Energy Delivered/m^2 (KJ)
5	46.0	54.9	2.17	1,998,360
6	48.5	50.5	2.31	2,187,517
7	51.1	45.2	2.41	2,269,040

TABLE 11.2.2.--Yearly and monthly collector efficiencies for solar systems in food processing plants exhibiting different energy use profiles and different processing schedules (500 m^2 collector) in East Lansing, Michigan.

Month	Efficiency, percent Processing Schedule Moved Forward, hours				
	Case A 8	Case B 4	Case C 9	Case D 6	Case E 4
January	41.8	41.4	41.8	41.6	42.0
February	43.0	43.1	42.8	42.9	43.1
March	42.7	42.8	42.2	42.5	42.9
April	45.8	45.7	45.5	46.1	45.9
May	45.5	45.5	44.9	45.6	45.8
June	47.6	47.5	47.6	48.2	47.7
July	46.3	46.3	46.1	46.7	46.7
August	48.4	48.3	48.2	48.9	48.9
September	46.8	46.5	46.9	47.0	47.0
October	47.1	47.1	47.0	47.4	47.3
November	46.5	46.4	46.5	46.8	46.6
December	42.3	42.6	42.0	42.1	42.6
Yearly	45.8	45.8	45.5	46.0	46.0

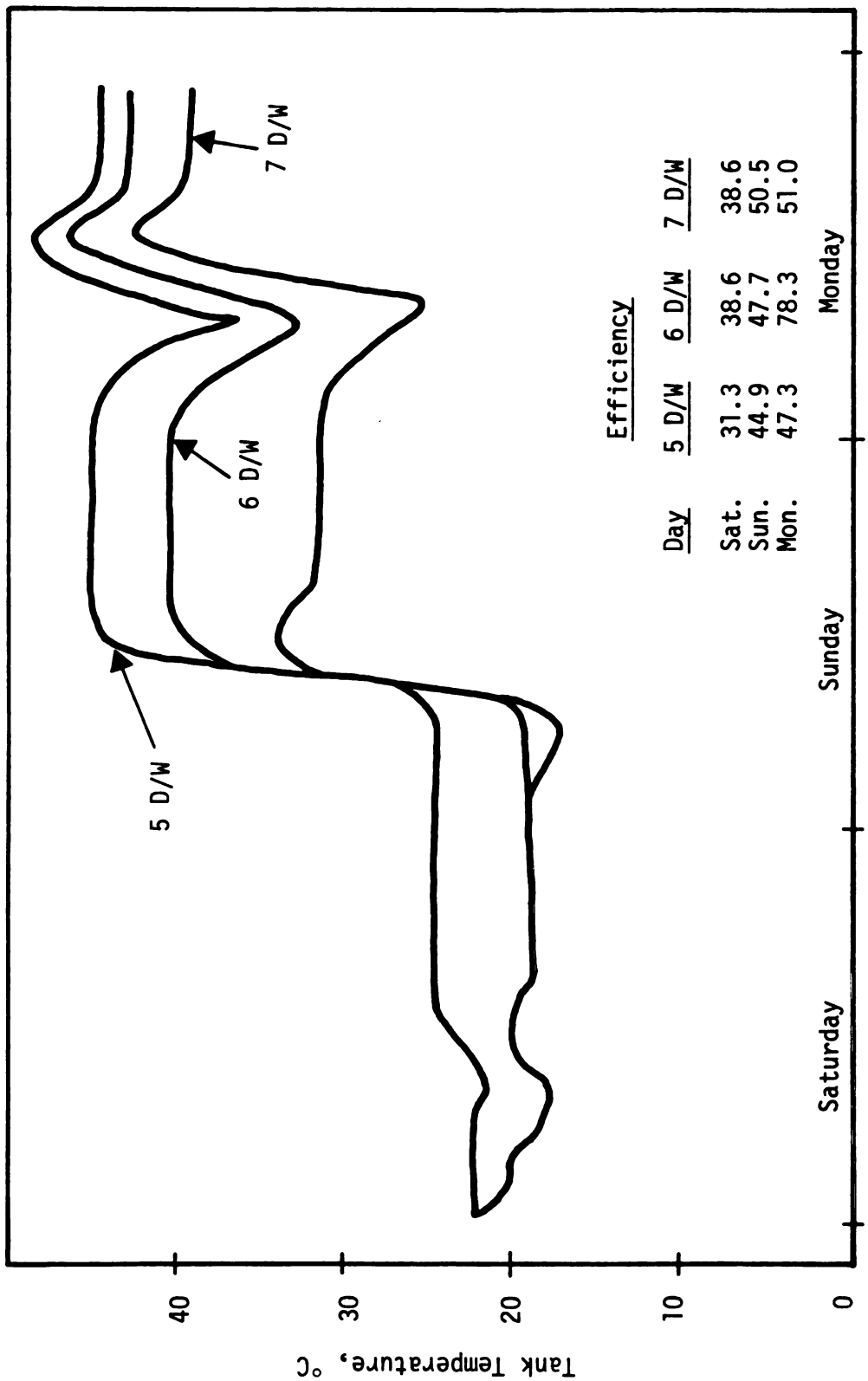

Figure 11.2.2.--Storage tank temperature during a typical weekend in December for solar systems in processing plants operating five, six or seven days per week.

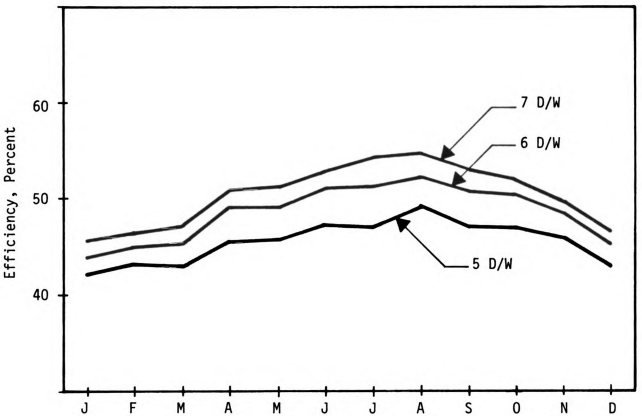

Figure 11.2.3.--Monthly collector efficiency of solar systems in processing plants operating five, six or seven days per week.

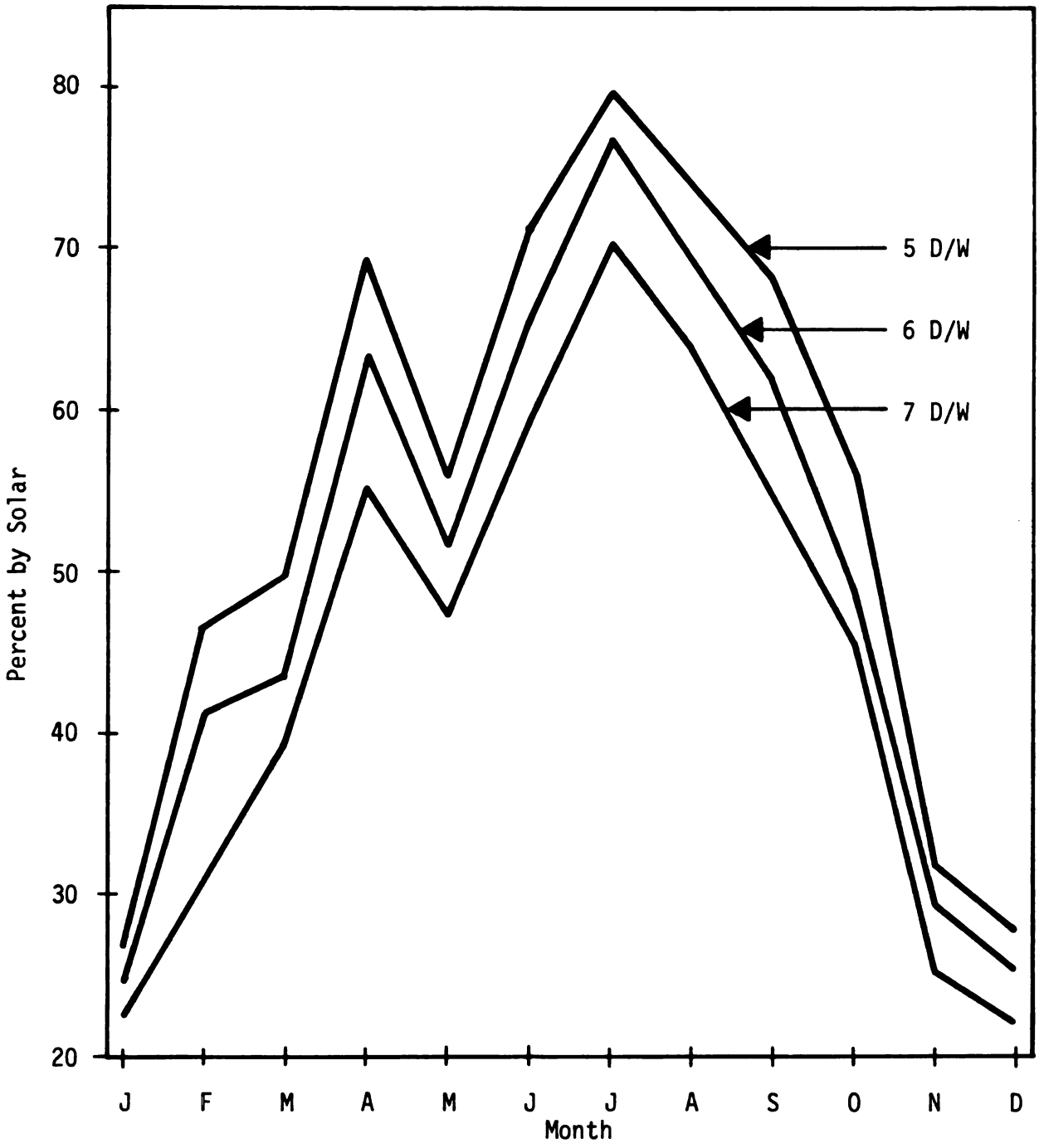

Figure 11.2.4.--Percent of monthly hot water supplied by solar in processing plants operating five, six or seven days per week.

The percentage of the monthly load supplied by solar systems delivering hot water at different temperatures is shown in Table 11.2.3. The percentage varies linearly with the temperature (Figure 11.2.5) since the hot water load is a linear function of temperature. The slope of the two parallel lines in Figure 11.2.5 is expected to remain constant for a certain location assuming the design parameters of the solar system do not change.

11.3 Load Quantity and Solar System Performance

In Chapter 9 a constant ratio (19.8) of collector area to the daily hot water load was assumed (see Table 9.1). For a constant collector area (1000 m^2) the performance of the solar system was observed by increasing or decreasing the amount of the daily load.

In Figures 11.3.1 and 11.3.2 the tank temperature and loss coefficient, respectively, for various loads is shown. The dashed line in the figures corresponds to a load determined by the ratio in Table 9.1. Smaller loads exhibit higher tank temperatures and loss coefficients.

The daily efficiency presented in Figure 11.3.2 increases with increasing loads because of lower loss coefficients and tank temperatures. The monthly efficiency presented in Figure 11.3.2 increases with increasing loads because of lower loss coefficients and tank temperatures. The monthly efficiency shown in Figure 11.3.3 changes according to the daily efficiency.

TABLE 11.2.3.--Percent of load supplied by solar under different hot water delivered temperatures in East Lansing, Michigan.

	Percent by Solar Hot Water Temperature, °C				
Month	50	60	70	74	80
January	44.4	35.4	29.3	27.4	25.0
February	71.9	59.4	49.6	46.6	42.5
March	73.5	62.5	52.8	49.6	45.4
April	91.1	83.4	73.2	69.1	63.4
May	81.1	69.4	59.2	55.8	51.1
June	95.7	87.1	75.6	71.2	62.3
July	89.3	93.o	83.9	80.0	74.5
August	96.4	88.2	77.7	73.7	68.2
September	92.5	83.1	72.0	68.1	62.7
October	84.3	70.7	59.7	56.1	51.4
November	51.8	41.2	34.1	31.9	29.1
December	45.3	36.0	29.8	27.9	25.4

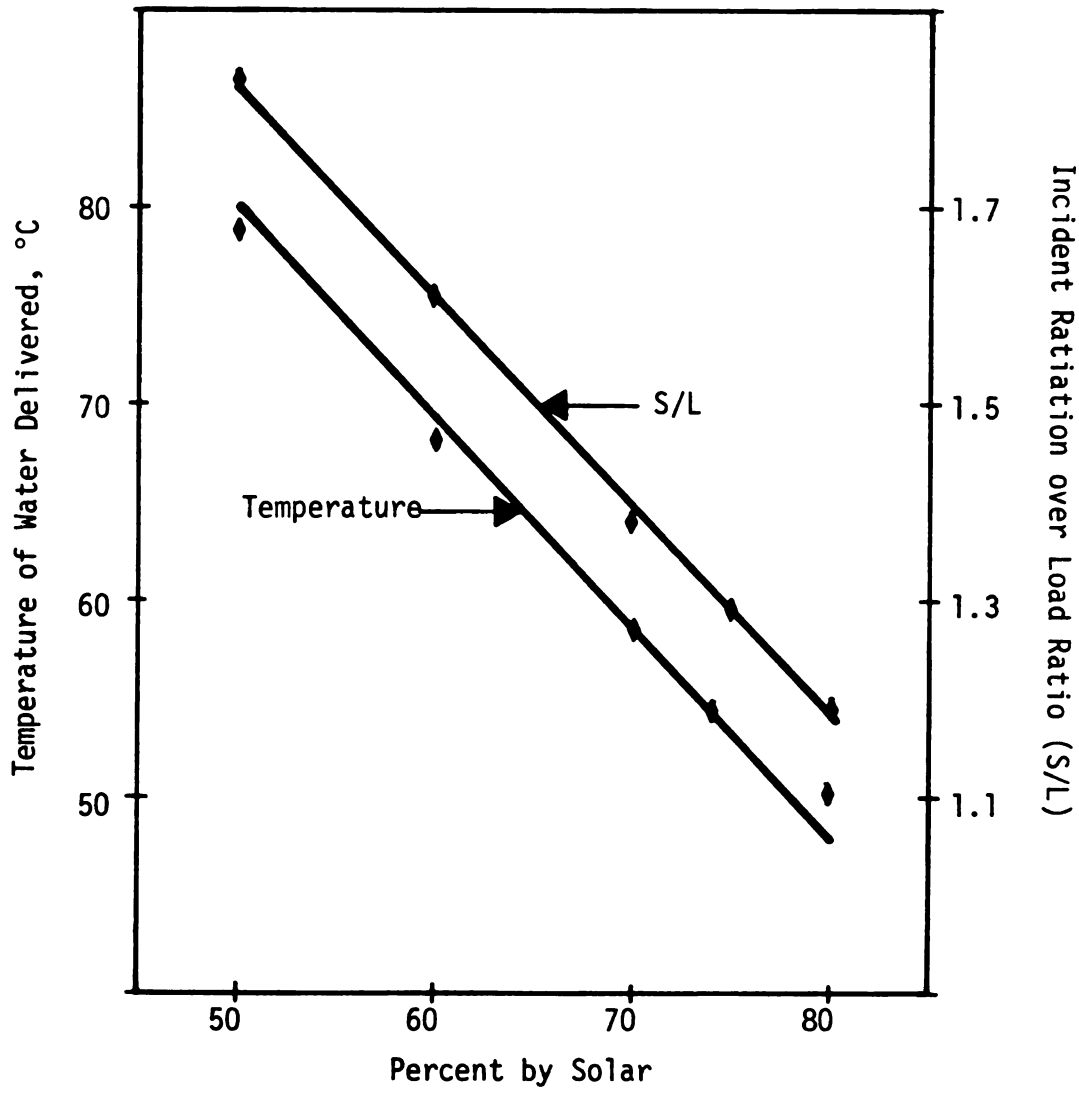

Figure 11.2.5.--Percentage of yearly load supplied by solar under different temperatures of hot water delivered.

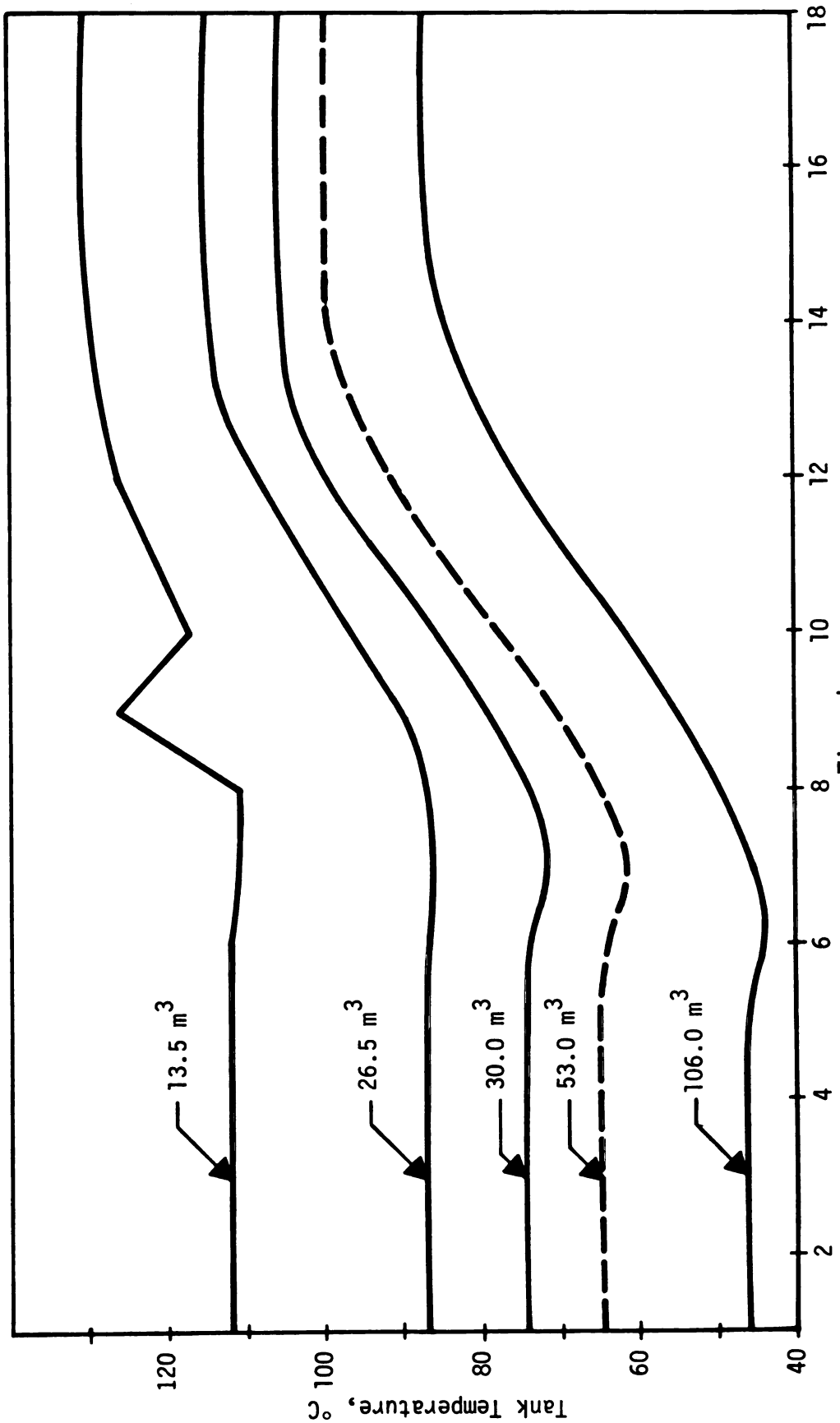

Figure 11.3.1.--Tank temperature of a 1000 m^2 collector system under different load quantities.

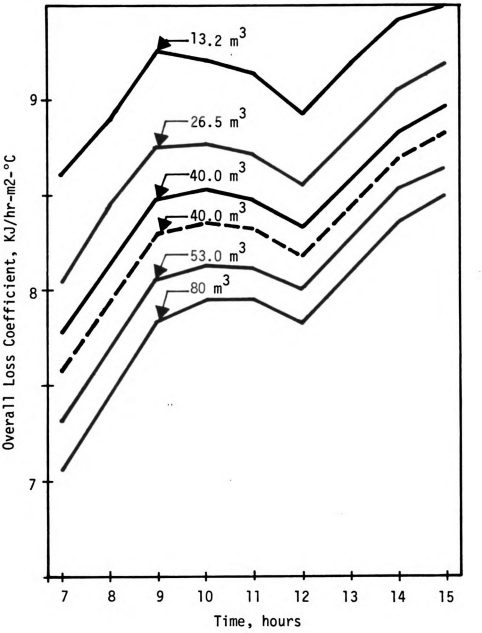

Figure 11.3.2.--Overall heat loss coefficient of a 1000 m^2 collector under various daily load conditions.

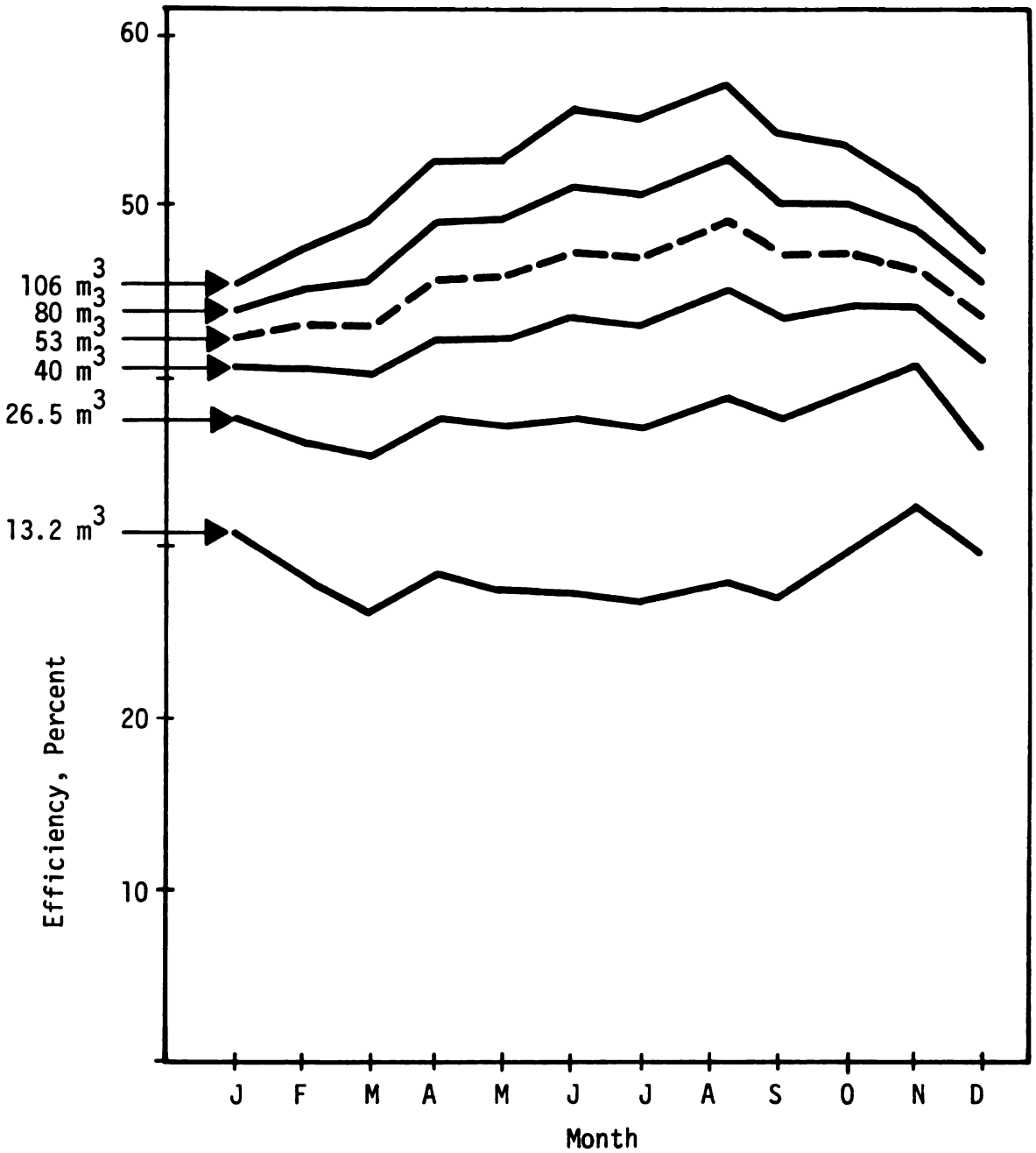

Figure 11.3.3.--Monthly efficiency of a 1000 m^2 solar collector under various daily load conditions.

The monthly percentage of the load supplied by solar decreases by increasing the load (Table 11.3.1). For small loads (12.6 m^3), the percentage is over 100 percent. The yearly performance and thermal output presented in Table 11.3.2 indicates that the thermal output and efficiency are improved by increasing the daily load. Since the percentage is decreasing under the same circumstances, higher efficiency and higher thermal output become a disadvantage above a certain value from a practical point of view.

11.4 Stratified Tank, Heat Exchanger, and Pump Requirements

In Chapter 4 the effect of tank stratification on the performance of the solar system was discussed. In a stratified tank the water temperature is not uniform over the vertical dimension of the tank. In this situation the tank is divided in sections or segments each one assumed to be at uniform temperature. A fully mixed or one section tank is assumed to be at uniform temperature over the vertical dimension.

For a solar system with 1000 m^2 collector three runs were made. In the first run, the tank temperature was assumed to be uniform. For the second and third runs two and three sections in the tank, respectively, were assumed.

The performance of the solar system under various tank stratification conditions is shown in Table 11.4.1. Under the tank stratification condition the fluid motion in the tank is due to density changes arising from the water heating process. As a result, the

TABLE 11.3.1.--Percentage of monthly load supplied by a solar system in processing plants with different hot water demand.

Month	Daily Hot Water Demand, m^3					
	12.6	26.5	39.7	53.0	79.5	106.0
January	69.6	46.0	34.5	27.5	22.3	15.5
February	96.3	73.5	57.3	46.6	37.9	26.9
March	96.0	77.3	61.0	49.7	40.4	28.8
April	98.3	92.0	80.8	69.2	58.3	42.3
May	97.9	82.1	67.1	55.8	55.8	33.0
June	100.0	95.7	83.8	71.2	60.0	43.4
July	100.0	99.3	91.5	80.1	63.6	50.8
August	100.0	97.8	86.4	73.8	61.8	44.9
September	100.0	94.8	81.1	68.2	56.3	40.3
October	99.8	86.2	68.3	56.2	46.2	32.9
November	86.2	54.7	40.1	32.0	25.6	17.9
December	72.3	45.6	34.8	27.9	22.5	15.6

TABLE 11.3.2.--Yearly performance and thermal output of a 1000 m^2 collector solar water heater for food processing plants with different daily hot water demand in East Lansing, Michigan.

Daily load, m^3	12.6	26.5	39.7	53.0	79.5	106.0
Collector Efficienty, percent	28.1	37.5	42.7	46.1	49.0	52.6
Percent by solar	94.4	79.9	66.0	55.1	45.6	32.7
Energy gained/m^2, KJ x 10^6	1.326	1.767	2.013	2.170	2.312	2.482
Yearly load, KJ x 10^9	1.124	1.949	2.770	3.642	4.776	7.210

TABLE 11.4.1.--Yearly and monthly collector efficiency and percent by solar of solar systems and stratified and fully mixed storage tanks (L/D = 2.16).

Month	Efficienty, Percent Tank Sections Assumed			Percent by Solar Tank Sections Assumed		
	1	2	3	1	2	3
January	40.3	42.2	43.0	26.0	27.3	27.8
February	40.4	42.9	46.7	44.2	46.4	47.1
March	40.4	43.0	43.9	47.4	49.5	50.5
April	42.8	45.5	46.5	64.4	67.8	69.0
May	42.7	45.7	46.7	52.7	54.8	55.6
June	44.4	47.2	48.2	66.7	69.3	70.2
July	43.6	46.9	48.0	76.1	77.7	78.4
August	46.0	49.2	50.3	70.6	72.2	73.0
September	44.1	47.0	48.0	64.9	47.2	47.9
October	44.5	47.2	48.1	53.4	55.5	56.3
November	44.1	46.0	46.6	30.5	31.8	32.3
December	41.0	43.3	44.5	26.6	28.1	28.7
Yearly	43.2	46.0	46.9	52.0	54.1	54.9

upper tank section is at a higher temperature than at the bottom of the tank (see Equations [4.7.3] and [4.7.5]). Thus, with a stratified tank water is supplied to the load at higher temperatures while the collector inlet temperature approaches that of the lower tank section. In a fully mixed tank the water temperature is uniform.

In Table 11.4.1 the difference in performance for various degrees of stratification is obvious. The difference is most pronounced when a fully mixed tank is compared to a two section tank. For example, the yearly collector efficiency of a three section tank is less than one percent higher than that of a two section tank.

The tank height over tank diameter ratio (L/D) and the tank inlet and outlet flow rates are the factors which affect the degree of stratification in the tank (Chapter 4). Below a certain L/D ratio the movement of the fluid in the tank due to buoyancy forces is disturbed by the inlet and outlet streams of the tank (see Figure 6.3.1) and the tank temperature would become uniform. A relationship between L/D, the flow rates in and out of the tank and the degree of stratification could not be found in the literature. For the Michigan State University solar system the L/D is 1.66 and the average flow rates in and out of the tank is about 7500 Kg/hr. Under these conditions the tank is at uniform temperature.

The monthly collector efficiency under reduced heat exchanger areas is presented in Table 11.4.2. In Chapter 9 it was stated that for solar systems with large collector areas, the heat exchanger was not scaled according to the ratio in Table 9.1. For a two to ten fold reduction in exchange area Table 11.4.2 shows the efficiency

TABLE 11.4.2.--Monthly collector efficiency at reduced heat exchanger areas.

Month	Efficiency Percent Reduction of Area			
	1	2	4	10
January	42.7	40.9	37.4	29.5
February	43.7	4.16	38.0	30.1
March	44.0	42.1	38.5	30.1
April	46.5	44.5	40.8	33.0
May	36.9	44.9	41.1	32.9
June	48.5	46.3	42.8	33.9
July	48.1	46.0	42.2	34.1
August	50.5	48.2	44.3	35.6
September	48.4	46.2	42.4	34.2
October	48.5	46.3	42.5	34.3
November	46.8	44.8	41.3	32.9
December	43.7	42.1	38.8	30.9
Yearly	47.1	45.0	41.3	33.1

TABLE 11.4.3.--Monthly and yearly pumping requirements of a solar water heater with a 1000 m^2 collector area.

Month	Pumping Requirements 10^7 KH	Energy Collected 10^7 KJ	Pumping Requirements Percent
January	1.1	9.5	11.5
February	1.2	14.2	8.8
March	1.6	16.3	9.9
April	1.7	22.1	7.6
May	1.8	19.3	9.6
June	2.1	24.1	9.0
July	2.2	27.2	8.0
August	2.2	26.0	8.4
September	1.8	21.2	8.6
October	1.6	19.1	8.7
November	1.0	10.1	10.1
December	1.1	8.6	13.0
Yearly	19.6	216.3	9.0

decreases according to the reduction. Column two indicates that a two fold reduction will reduce the yearly efficiency by about two percent. Since the heat exchanger is a relatively expensive component of the solar system its size can be reduced significantly without affecting the thermal performance of the solar system by a large margin.

The pumping requirements listed in Table 11.4.3 account for the electricity used to run the pump of the collector and that of the heat exchanger (see Figure 6.3.1). The last column of Table 11.4.3 is the percentage of the energy used by the pump with respect to the energy collected by the solar system. The yearly percentage is about nine and this indicates that the pumps of a solar system should be carefully selected and sized to avoid unnecessary electicity consumption.

11.5 Long-Term Solar Water Heater Performance in Selected Cities of the United States

The long-run performance and thermal output of a solar water heater in various locations of the United States has been investigated by the f-chart method. As was discussed in Chapter 10 the f-chart program was modified in order to be able to accept weekly instead of daily hot water loads. In addition to this change, a new "f-equation" was developed (see Equations [10.1] and (10.11]).

In Table 11.5.1 the monthly and yearly percent by solar for various size solar systems in East Lansing, Michigan is presented. The percentages were obtained by TRNSYS, the original f-chart program (F), the modified f-chart with Equation [10.1] unchanged (F1),

TABLE 11.5.1.--Percent of monthly and yearly load provided by solar calculated by TRNSYS, and the original and modified versions of f-chart.

	Collector area, m^2							
	150				500			
	TR	F	F1	F2	TR	F	F1	F2
January	27.5	18.6	25.1	29.8	26.7	17.8	24.0	28.5
February	46.6	32.7	43.1	45.2	45.4	31.3	41.4	42.8
March	49.9	36.7	48.1	49.8	48.6	35.2	46.3	47.2
April	68.7	54.5	69.8	71.4	67.4	52.4	67.5	68.3
May	55.8	45.5	59.5	60.8	54.6	43.9	57.3	57.6
June	71.0	57.6	74.0	74.0	69.5	55.4	71.3	71.1
July	79.5	66.0	83.5	78.8	78.5	63.6	80.9	77.4
August	73.5	60.0	76.5	74.8	71.9	57.6	74.0	72.1
September	67.4	51.1	66.0	65.6	66.2	49.1	63.7	62.3
October	55.6	43.6	56.9	56.2	54.4	41.9	54.8	53.2
November	31.6	17.9	24.2	28.1	30.8	17.1	23.2	26.9
December	28.1	14.8	20.1	26.2	27.3	14.1	19.2	25.1
Year	54.8	41.6	54.0	55.1	53.6	40.0	52.0	52.7

TABLE 11.5.1.--Continued.

Month	Collector area, m^2							
	1000				6000			
	TR	F	F1	F2	TR	F	F1	F2
January	26.8	17.8	24.0	28.5	25.6	18.6	25.1	29.8
February	45.5	31.3	41.4	42.8	43.7	32.7	43.1	45.2
March	48.6	35.2	46.3	47.2	46.6	36.7	48.1	49.8
April	67.5	52.4	67.5	68.3	64.6	54.6	69.8	71.4
May	54.7	43.9	57.3	57.6	52.8	45.7	59.5	60.8
June	69.3	55.4	71.3	71.1	68.1	57.6	73.8	74.0
July	78.6	63.6	80.9	77.4	77.0	66.0	83.5	78.4
August	72.1	57.6	74.0	72.1	70.5	59.9	76.5	74.8
September	66.4	49.1	63.7	62.3	64.0	51.1	66.0	65.6
October	54.5	41.9	43.8	53.2	52.2	43.6	56.9	56.2
November	30.9	17.1	23.2	26.9	29.8	17.9	24.2	28.1
December	27.3	14.0	19.2	25.1	26.5	14.8	20.1	26.2
Year	53.7	40.0	52.0	52.7	52.1	41.6	53.9	55.0

and the modified f-chart with Equation [10.1] being replaced by [10.11] (F2). The output from TRNSYS was assumed to be the criterion which established the degree of accuracy of the other models. The same weather data was used for both, TRNSYS and the f-chart method.

The values of column F are substantially lower than the ones obtained by TRNSYS because the water load for the run of column F was approximately 40 percent higher than for TRNSYS. The load in TRNSYS represents a processing plant operating five days per week. Since the original f-chart program accepts only daily loads as input, the weekly load will be seven times the daily load. Therefore, unless f-chart is modified to accept weekly instead of daily loads, the percentage by solar for plants operating less than seven days per week is substantially underestimated.

By modifying the program to accept weekly loads its accuracy has been considerably improved. The yearly values of column F1 for all solar systems on Table 11.5.1 are higher or lower by less than two percent than those of TRNSYS. The replacement of Equation [10.1] by Equation [10.11] has further improved the accuracy of f-chart (column F2). Except for the 6000 m^2 solar collector systems, the yearly percentages of column F2 show improvement over those of column F1.

In Table 11.5.1 it can be seen that the monthly percentages for F1 and F2 columns are not as close to TRNSYS as the yearly one. f-Chart cannot be as accurate as TRNSYS because the TRNSYS outputs are the result of physical simulation models which are far more accurate than the correlations f-chart is based upon. However, for

design purposes where the long-run performance of a solar water heater must be determined, the accuracy of f-chart is more than satisfactory.

Equation [10.11] has resulted in slightly more accurate results than Equation [10.1]. The error introduced by using Equation [10.1] is not substantial as can be seen from the data in Table 11.5.1.

The effect of location on solar system performance and thermal output was investigated by using f-chart to perform thermal analysis for selected cities in the United States. The locations of the cities investigated are shown in Figure 11.5.1 and Table 11.5.2.

In the modified version of f-chart used to investigate the effect of location on solar system performance and thermal output, Equation [10.1] was not replaced by Equation [10.11]. The data points used to estimate the parameters of Equation [10.11] were for East Lansing, Michigan. For cities with higher isolation than East Lansing, such as Phoenix, Arizona and Los Angeles, California, Equation [10.11] cannot be used because the values of X' and Y (see (see Chapter 10) are outside the range of X' and Y of East Lansing. The East Lansing range for both X' and Y was between 0.3 and 1.4. To make Equation [10.11] more general, the regression analysis discussed in Chapter 10 must be based on data points representing locations with various amounts of solar radiation. By not using Equation [10.11], however, the accuracy is not reduced significantly (see Table 11.5.1).

The yearly performance and thermal output of solar water heaters for twenty cities in the United States are presented in

TABLE 11.5.2.--Solar system yearly performance and thermal output for selected cities of the United States.

City	Yearly Incident Energy 10^6 KJ/m^2	Percent by Solar	Yearly Load 10^6 KJ	Energy Supplied/ Incident Energy	Energy Supplied$_2$ to Load/m^2 10^6 KJ
1. Atlanta, GA	5.92	71.6	3183.7	38.5	2.279
2. Bismarck, ND	5.99	65.3	3936.2	42.8	2.570
3. Buffalo, NY	4.45	49.0	3646.8	40.2	1.786
4. Charlotte, NC	6.15	72.4	3473.2	40.9	2.639
5. Chicago, IL	5.47	52.4	3588.9	40.9	2.239
6. Dallas, TX	6.49	78.7	3183.7	38.5	2.505
7. Denver, CO	8.24	91.0	3531.0	39.0	3.213
8. East Lansing, MI	5.41	50.9	3588.9	40.4	2.185
9. Great Falls, MT	6.05	67.4	3704.7	41.3	2.496
10. Houston, TX	5.83	72.1	3125.8	38.6	2.253
11. Jackson, MS	6.16	73.9	3299.5	39.6	2.437
12. Kansas City, MO	6.09	70.3	3531.0	49.8	2.482
13. Los Angeles, CA	7.24	85.7	3183.7	37.7	2.727
14. Memphis, TN	6.02	71.2	3415.3	40.4	2.431
15. Miami, FL	6.40	81.9	2836.4	36.3	2.322
16. Milwaukee, WI	5.37	60.5	3588.9	40.4	2.170
17. New Orleans, LA	6.25	75.3	3299.5	39.6	2.484
18. New York, NY	4.86	56.0	3588.9	41.3	2.009
19. Phoenix, AZ	8.54	94.3	3299.5	36.4	3.110
20. Portland, ME	4.72	52.9	3646.8	40.9	1.928
21. Portland, OR	4.67	52.7	3588.9	40.5	1.890
22. Salt Lake City, UT	7.49	82.6	3588.9	39.6	2.963

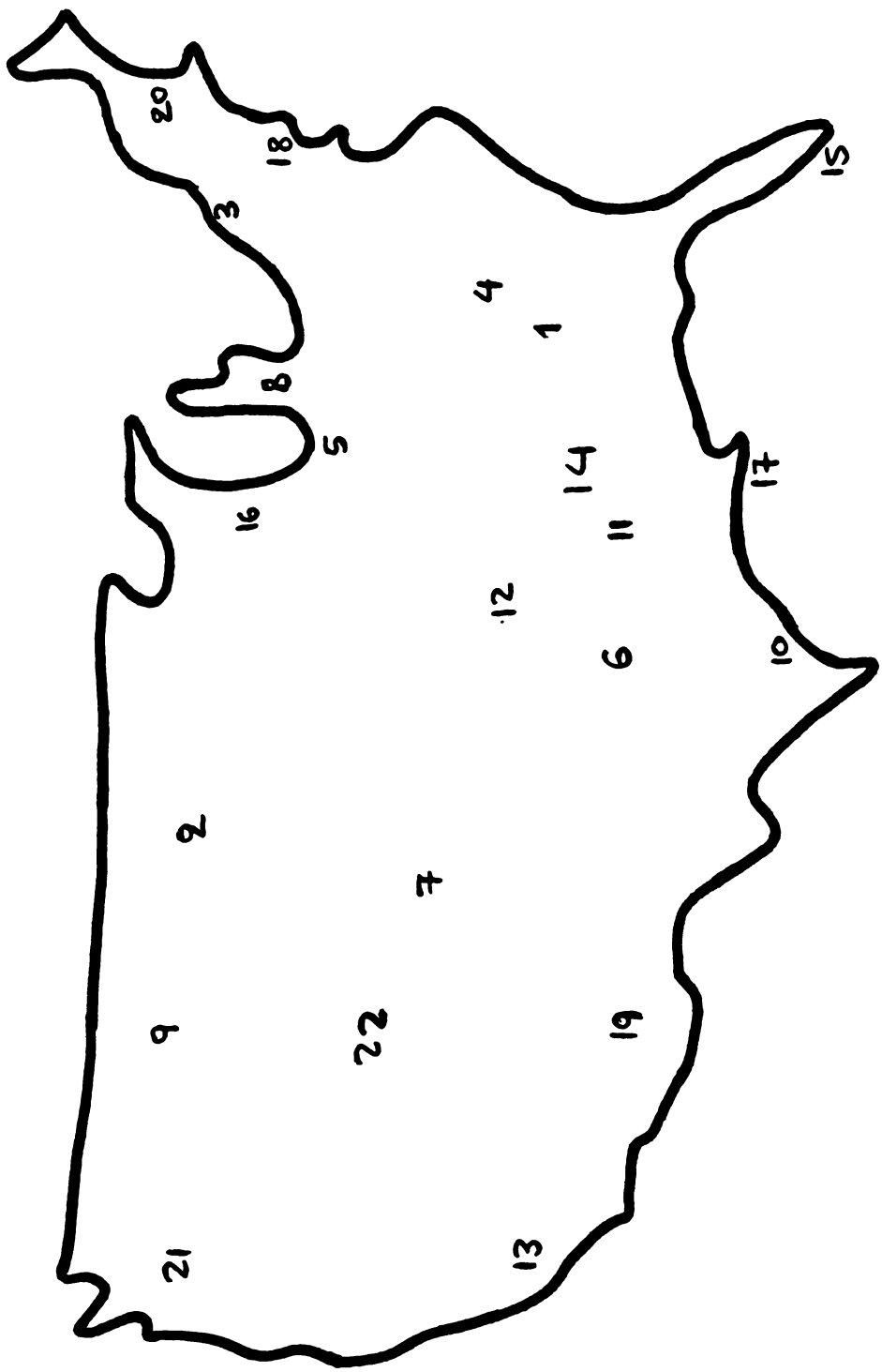

Figure 11.5.1.--Location of cities investigated in this study.

Table 11.5.2. A collector area of 1000 m^2 was assumed for the run. The weekly load and water set temperature were 264,960 Kg and 74°C, respectively. The water main temperatures was different for each city according to the values reported by Collins, 1925. The collector slope was assumed to be equal to the local latitude. The water use schedule was not taken into account because as was discussed previously it has no effect on the preformance of the system. The parameter values used for the runs are shown in Table 11.6.2.

The incident solar radiation, shown in the second column of Table 11.5.2, varies considerably among the cities. For example, in Denver, Colorado, the incident radiation is about twice as large as in Buffalo, New York. The percent by solar varies according to the incident radiation. In addition, cities with high insolation have higher water main temperatures. In spite of the same amount of hot water consumed by the processing plants in the various cities (264,960 Kg/week), the yearly energy load in Table 11.5.2 varies among the cities as a result of the different water main temperatures employed for each city.

The fifth column of Table 11.5.2 can be considered as an index of the efficiency of the solar collector. The values of the column are calculated by multiplying the yearly load by the percentage of solar. The result gives the amount of energy supplied by the solar system. The energy absorbed by a solar collector is partially lost from the pipes, the heat exchanger, and the tank and partially delivered to the load. Assuming the losses to be constant among the various cities, division of the energy supplied by the

incident solar radiation gives the values of Column 5 which can be considered as an indication of the efficiency of the solar collector. The index is relatively constant among the various cities in Table 11.5.2. The lower values for cities like Phoenix, Arizona and Los Angeles, California are because in cities of high insolation the solar system supplies more energy than is required by the load. Under such circumstances the percent by solar is higher than 100. f-Chart does not print values higher than 100 percent. As a result, in situations of 100 percent by solar the energy delivered to the load will be partially wasted and the efficiency index will be based on a fraction of the energy delivered. The relatively constant efficiency index values among the cities indicate that the yearly efficiency of a certain solar collector does not vary considerably from one location to the other.

The energy supplied to the load per m^2 shown in the last column varies also according to the incident radiation.

As was discussed previously, the overall loss coefficient is dependent on the design parameters of the solar system. The coefficient is an input for f-chart. The effect of the ambient temperature on the system's performance is taken into account by f-chart. The values of the efficiency index in Table 11.5.2 indicate that the different ambient temperatures among the various locations has minimal effect on the index. This is because for places with high ambient temperature the insolation is also high and this will result in higher tank temperature than in places with low insolation. Previously it was stated that high tank temperatures result in higher

collector inlet temperatures. As a consequence, the difference between the collector inlet and ambient temperature remains relatively constant among various locations. Therefore, the yearly collector efficiency does not depend to a large extent on the location. Design parameters such as the number of glass covers, transmittance of the glass, amount of insulation of the collector, emittance and absorbance of the absorber plate, storage capacity, effectiveness of the heat exchanger, collector fluid flow rate, and amount of hot water supplied by the solar system are the ones affecting the long-run solar system performance.

Table 11.5.3 presents the thermal output of a solar system under changing water set temperature conditions. The cities on Table 11.5.3 represent cases of high, low and medium insolation (see Table 11.5.2). By increasing the set temperature the percengage by solar decreases and vice versa. The relationship between set temperature and percent by solar is approximately linear (see Figure 11.2.5) because the thermal output of the solar system remains the same regardless of the set temperature while the load changes linearly with the set temperature. The non-linear relationship shown in Figure 11.5.2 is due to the wasted energy delivered by the system (discussed earlier) in situations where the solar system supplies more energy than that required by the load.

The yearly performance and thermal output of a solar system supplying hot water to food processing plants operating five, six or seven days per week is presented in Table 11.5.4. The cities in the table are of low, medium and high insolation. The effect of

TABLE 11.5.3.--Yearly thermal output of solar system in selected cities of the United States under various water set temperature conditions.

	Yearly Incident Radiation/m^2	Water Mains Temperature, °C	Water Set Temperature °C	Load 10^6 KJ	Percent by Solar	Energy Supplied to Loads/m^2 10^6 KJ
Bismark, ND	5.99	6.0	50.0	2546.9	86.6	2.204
	5.99	6.0	60.0	3125.8	78.1	2.440
	5.99	6.0	70.9	3704.7	68.7	2.544
	5.99	6.0	80.0	4283.7	60.8	2.604
	5.99	6.0	90.0	4862.4	54.3	2.640
Buffalo, NY	4.45	11.0	50.0	2257.5	71.6	1.616
	4.45	11.0	60.0	2836.4	60.9	1.727
	4.45	11.0	70.0	3415.3	52.0	1.775
	4.45	11.0	80.0	3994.1	45.1	1.801
	4.45	11.0	90.0	4573.0	39.5	1.806
Chicago, IL	5.47	12.0	50.0	2199.7	85.1	1.871
	5.47	12.0	60.0	2778.5	76.2	2.116
	5.47	12.0	70.0	3357.4	65.9	2.212
	5.47	12.0	80.0	3936.2	57.7	2.271
	5.47	12.0	90.0	4515.1	51.0	2.302
East Lansing, MI	5.41	12.0	50.0	2199.7	83.2	1.829
	5.41	12.0	60.0	2778.5	74.4	2.066
	5.41	12.0	70.0	3357.4	64.4	2.161
	5.41	12.0	80.0	3936.2	56.3	2.216
	5.41	12.0	90.0	4515.1	49.8	2.248

TABLE 11.5.3.--Continued.

City	Yearly Incident Radiation/m^2	Water Mains Temperature, °C	Water Set Temperature °C	Load 10^6 KJ	Percent by Solar	Energy Supplied to Loads/m^2 10^6 KJ
Kansas City, MO	6.09	13.0	50.0	2141.8	91.8	1.965
	6.09	13.0	60.0	2720.6	84.2	2.290
	6.09	13.0	70.0	3299.7	74.1	2.444
	6.09	13.0	80.0	3878.4	65.2	2.528
	6.09	13.0	90.0	4457.2	57.9	2.580
Miami, FL	6.02	25.0	50.0	1447.1	100.0	1.447
	6.02	25.0	60.0	2026.0	97.4	1.973
	6.02	25.0	70.0	2604.9	86.6	2.255
	6.02	25.0	80.0	3183.7	75.6	2.406
	6.02	25.0	90.9	3762.6	66.5	2.501
Phoenix, AZ	8.54	17.0	50.0	1910.2	100.0	1.910
	8.54	17.0	60.0	2489.1	98.7	2.456
	8.54	17.0	70.0	3068.0	95.7	2.936
	8.54	17.0	80.0	3646.8	91.1	3.321
	8.54	17.0	90.0	4225.7	82.8	3.498
Portland, ME	4.72	11.0	50.0	2257.6	77.8	1.756
	4.72	11.0	60.0	2836.4	65.6	1.860
	4.72	11.0	70.0	3415.3	56.1	1.915
	4.72	11.0	80.0	3994.1	48.7	1.945
	4.72	11.0	90.0	4573.0	42.8	1.957

TABLE 11.5.4.--Yearly thermal output of a solar system in selected cities of the United States under various operating days per week.

City	Operating Days per Week	Yearly Load 10^6 KJ	Percent by Solar	Energy Supplies to Load/m^2 10^6 KJ	Energy Supplied/ Incident Energy
Buffalo, NY	5	3646.8	49.0	1.786	40.2
	6	4376.2	42.6	1.864	41.9
	7	5105.5	37.6	1.919	43.1
Chicago, IL	5	3588.9	62.4	2.239	40.9
	6	4306.7	54.6	2.351	43.0
	7	5024.5	48.8	2.451	44.8
Kansas City, MO	5	3531.1	70.5	2.489	40.6
	6	4237.3	62.0	2.627	42.9
	7	4943.5	55.2	2.728	44.5
Phoenix, AZ	5	3299.5	94.3	3.110	36.4
	6	3959.4	88.0	3.483	40.8
	7	4619.0	79.8	3.686	43.2

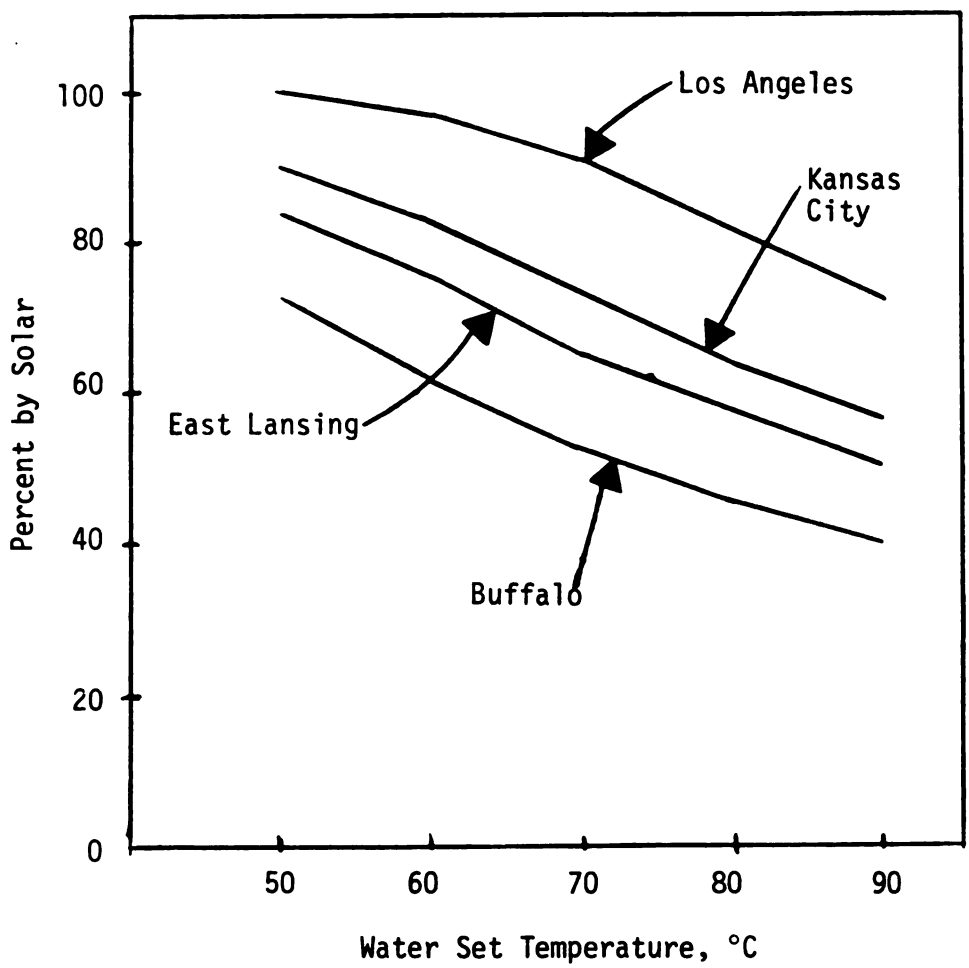

Figure 11.5.2.--Percent by solar for various cities under different water set temperatures.

location on system thermal output is obvious in Table 11.5.4. As was observed previously with TRNSYS results, by increasing the number of operating days per week the percent by solar decreases and the thermal output and the efficiency increases and vice versa.

11.6 Economics of Solar Water Heating

The economics of solar water heating was studied using the f-chart program. Subrouting ECON of f-chart performs on economic analysis of a solar system based on the life-cycle costing method discussed in Chapter 4. The life-cycle cost is found by discounting each case flow to its present value and finding the sum of these discounted cash flows. When two alternative systems are investigated in terms of their life-cycle costs, the system with the lowest cost is the most cost-effective.

The economics of solar water heating in selected cities of the United States is presented in Table 11.6.1. The size of the solar system, the values of the design parameters, the amount of hot water consumed in the processing plant and the economic scenario under which the values of Table 11.6.1 were obtained is presented in Table 11.6.2. In the discussion regarding the economics of solar water heating, unless specified othersiwe, the values shown in Talbe 11.6.2 are assumed. In Table 11.6.1 two economic scenarios are presented. In the first four columns the cost of the solar system is 200 $\$/m^2$ of collector area. In the last four columns the cost is 150 $\$/m^2$. The meaning of each column is illustrated at the end of the table.

TABLE 11.6.1.--Economics of a 1000 m^2 collector solar water heater in selected cities of the United States.

City	System Cost, $/m^2							
	200				150			
	1*	2	3	4	1	2	3	4
1. Atlanta, GA	7.7	11.0	18.0	-1.7	22.0	9.0	14.0	46.3
2. Bismarck, ND	13.7	10.0	16.0	18.2	29.3	8.0	13.0	75.0
3. Buffalo, NY	< 0	12.0	--	-58.7	9.5	11.0	17.0	-1.8
4. Charlotte, NC	12.6	10.0	16.0	12.5	27.9	9.0	13.0	69.4
5. Chicago, IL	6.8	11.0	18.0	-14.3	21.0	9.0	14.0	42.5
6. Dallas, TX	12.5	10.0	16.0	11.7	27.7	9.0	13.0	68.6
7. Denver, CO	25.9	9.0	13.0	81.2	46.5	7.0	10.0	138.1
8. East Lansing, MI	5.6	11.0	18.0	-19.6	19.5	9.0	15.0	37.3
9. Great Falls, MT	12.3	10.0	16.0	10.9	27.4	9.0	13.0	67.7
10. Huston, TX	7.2	11.0	18.0	-12.9	21.4	9.0	14.0	43.8
11. Jackson, MS	11.1	10.0	17.0	5.2	26.0	9.0	13.0	62.1
12. Kansas City, MO	12.0	10.0	17.0	9.5	27.1	9.0	13.0	66.4
13. Los Angeles, CA	16.8	10.0	15.0	33.7	33.4	8.0	12.0	90.6
14. Memphis, TN	10.9	10.0	17.0	4.4	25.8	9.0	13.0	61.2
15. Miami, FL	8.7	11.0	18.0	-6.1	23.1	9.0	14.0	50.7
16. Milwaukee, WI	5.2	11.0	19.0	-21.2	19.4	9.0	15.0	35.7
17. New Orleans, LA	12.0	10.0	17.0	9.6	27.1	9.0	13.0	66.4
18. New York, NY	1.0	12.0	20.0	-36.9	15.3	10.0	16.0	19.9
19. Phoenix, AZ	23.9	9.0	14.0	71.2	43.6	7.0	10.0	128.1
20. Portland, ME	< 0	12.0	20.0	-44.7	13.3	10.0	16.0	12.2
21. Portland, OR	< 0	12.0	--	-49.1	12.2	10.0	17.0	7.8
22. Salt Lake City, UT	21.2	9.0	14.0	56.9	39.6	8.0	11.0	113.7

*1 = Rate of return on the solar investment (percent).
2 = Years until undiscounted fuel saving = investment.
3 = Years until undiscounted solar saving = mortgage principal.
4 = Present worth of cumulative solar savings (10^3 $).

TABLE 11.6.2.--Economic scenario used in life-cycling costing analysis of various solar systems.

CODE	VARIABLE DESCRIPTION	VALUE	UNITS
1	AIR SH+WH=1, LIQ SH+WH=2, AIR OR LIQ WH ONLY=3	3.00	
2	IF 1, WHAT IS (FLOW RATE/COL AREA)(SPEC HEAT)?	12.23	W/C-M2
3	IF 2, WHAT IS (EPSILON)(CMIN)/(UA)?	2.00	
4	COLLECTOR AREA	1000.00	M2
5	FRPRIME-TAU-ALPHA PRODUCT(NORMAL INCIDENCE)	.68	
6	FRPRIME-UL PRODUCT	2.00	W/C-M2
7	INCIDENCE ANGLE MODIFIER (ZERO IF NOT AVAIL.)	0.00	
8	NUMBER OF TRANSPARENT COVERS	2.00	
9	COLLECTOR SLOPE	41.00	DEGREES
10	AZIMUTH ANGLE (E.G. SOUTH=0, WEST=90)	0.00	DEGREES
11	STORAGE CAPACITY	230.00	KJ/C-M2
12	EFFECTIVE BUILDING UA	24000.00	KJ/C-DAY
13	CONSTANT DAILY BLDG HEAT GENERATION	0.00	KJ/DAY
14	HOT WATER USAGE	264950.00	L/WEEK
15	WATER SET TEMP (TO VARY BY MONTH, INPUT NEG #)	74.00	C
16	WATER MAIN TEMP(TO VARY BY MONTH, INPUT NEG #)	12.00	C
17	CITY CALL NUMBER	207.00	
18	THERMAL PRINT OUT BY MONTH=1, BY YEAR=2	2.00	
19	ECONOMIC ANALYSIS ? YES=1, NO=2	1.00	
20	USE OPTMZD. COLLECTOR AREA=1, SPECFD. AREA=2	2.00	
21	SOLAR SYSTEM THERMAL PERFORMANCE DEGRADATION	0.00	PERCENT/YR
22	PERIOD OF THE ECONOMIC ANALYSIS	20.00	YEARS
23	COLLECTOR AREA DEPENDENT SYSTEM COSTS	150.00	$/M2 COLL.
24	CONSTANT SOLAR COSTS	6000.00	$
25	DOWN PAYMENT(PERCENT OF ORIGINAL INVESTMENT)	10.00	PERCENT
26	ANNUAL INTEREST RATE ON MORTGAGE	10.00	PERCENT
27	TERM OF MORTGAGE	20.00	YEARS
28	ANNUAL NOMINAL(MARKET) DISCOUNT RATE	10.00	PERCENT
29	EXTRA INSUR., MAINT. IN YEAR 1(PCT ORIG. INV.)	4.00	PERCENT
30	ANNUAL PERCENT INCREASE IN ABOVE EXPENSES	8.00	PERCENT
31	PRESENT COST OF SOLAR BACKUP FUEL (BF)	9.00	$/GJ
32	BF RISE: PERCENT/YR=1, SEQUENCE OF VALUES=2	1.00	
33	IF 1, WHAT IS THE ANNUAL RATE OF BF RISE	10.00	PERCENT
34	PRESENT COST OF CONVENTIONAL FUEL (CF)	9.00	$/GJ
35	CF RISE: PERCENT/YR=1, SEQUENCE OF VALUES=2	1.00	
36	IF 1, WHAT IS THE ANNUAL RATE OF CF RISE	10.00	PERCENT
37	ECONOMIC PRINT OUT BY YEAR=1, CUMULATIVE=2	2.00	
38	EFFECTIVE FEDERAL-STATE INCOME TAX RATE	40.00	PERCENT
39	TRUE PROP. TAX RATE PER $ OF ORIGINAL INVEST	2.00	PERCENT
40	ANNUAL PERCENT INCREASE IN PROPERTY TAX RATE	8.00	PERCENT
41	CALC. RT. OF RETURN ON SOLAR INVTMT?YES=1, NO=2	1.00	
42	RESALE VALUE (PERCENT OF ORIGINAL INVESTMENT)	1.00	PERCENT
43	INCOME PRODUCING BUILDING? YES=1, NO=2	1.00	
44	DPRC.: STR. LN=1, DC. BAL.=2, SM-YR-DGT=3, NONE=4	1.00	
45	IF 2, WHAT PCT OF STR. LN DPRC. RT. IS DESIRED?	150.00	PERCENT
46	USEFUL LIFE FOR DEPREC. PURPOSES	20.00	YEARS

TYPE IN CODE NUMBER AND NEW VALUE923,29900.

The second column of each scenario of Table 11.6.1 constitues the payback period of the solar system. The third column, a more meaningful index than payback, indicates the number of years until the undiscounted cumulative solar savings is equal to the remaining mrtgage. The present worth of cumulative solar savings shown in Column 4 indicates whether the solar system is a better investment than the conventional heater (which burns fuel costing 9.0 \$/GJ in this scenario) (see variable 34 of Table 11.6.2).

In Table 11.6.1 the 200 $\$/m^2$ scenario shows that for most cities the solar water heater is a less attractive alternative than conventional water heating because of the negative values of the present worth value of the solar savings. The economic indices of the table vary according to the amount of incident solar radiation (see Table 11.5.2). Denver and Los Angeles, which have the highest incidence of solar radiation, exhibit the best economic performance among the cities in Table 11.6.1.

Changing the cost from 200 to 150 $\$/m^2$ substantially improves the economics of solar water heating for all cities. Except for Buffalo, all of the cities show positive savings. Under this scenario solar water heating is a more attractive alternative than conventional water heating. The 50 $\$/m^2$ decrease represents a 25 percent reduction of the original cost of the solar system. At the present time the federal and most state governments allow taxpayers a deduction of 25 percent of all expenditures for solar systems from their taxable income during the year in which the investment is made.

In Table 11.6.3 the present worth of the solar savings of a solar water heater in selected cities of the United States for food processing plants operating five, six, or seven days per week is shown. The savings vary according to the available radiation among the cities. A solar system in a food processing plant operating seven days per week shows greater savings than the six and five work days per week processing plants. This is because the solar system in the seven day plant shows better performance and greater thermal output than the six and five day situations (see Table 11.5.4).

In Table 11.6.4 the present worth of the solar savings under various water set temperature is presented. The savings increase by increasing the set temperature. An important observation in Table 11.6.4 is that the savings increase faster from 50° to 60°C than from 80° to 90°C. For example, in Phoenix the savings from 50° to 60°C increase by $53,600 whereas from 80° to 90°C the increase is $17,300. The reason for this behavior is because at lower temperatures the solar system supplies more energy than is required in the processing plant. As was discussed previously the extra energy supplied is wasted. The small savings at lower temperatures regardless of the higher percentages by solar obtained (see Table 11.5.3) represent a penalty imposed by the wasted energy.

In Table 11.6.5 the thermal output performance and economics of an economically optimized collector area solar water heater is presented. Comparison of Tables 11.6.5 and 11.5.2 indicate that the optimized system showed better performance and higher thermal output than the fixed collector area system (1000 m^2). The cost of the

TABLE 11.6.3.--Present worth of cumulative solar savings (10^3 $) of a 1000 m^2 collector solar water heater in selected cities of the United States and food processing plants operating various days per week.

City	Work Days per Week		
	5	6	7
Buffalo, NY	-1.8	5.7	11.1
Chicago, IL	42.5	53.4	63.5
Kansas City, MO	66.9	80.5	90.6
Phoenix, AZ	128.1	164.8	184.7

TABLE 11.6.4.--Present worth of cumulative solar savings (10^3 \$) of a 1000 m^2 collector solar water heater in selected cities of the United States under various set temperatures.

	Set Temperature, °C				
City	50	60	70	80	90
Bismark, ND	39.2	62.6	72.3	78.1	81.6
Buffalo, NY	-18.6	-7.9	-3.0	-0.7	0.0
Chicago, IL	6.4	30.5	39.9	45.5	48.7
E. Lansing, MI	2.3	25.5	34.7	40.2	43.3
Kansas City, MO	15.5	47.6	62.7	70.8	75.8
Miami, FL	-35.3	16.9	43.9	58.8	68.3
Phoenix, AZ	10.2	63.8	110.7	148.9	166.2
Portland, ME	-4.9	5.2	10.8	13.6	14.6

TABLE 11.6.5.--Optimal collector area, and thermal output, performance economics of an optimized solar water heater in selected cities of the United States for a food processing plant.

City	1*	2	3	4	5	6	7	8	9
1. Atlanta, GA	822	62.6	40.9	2.424	25.1	9.0	13.0	48.6	0.63
2. Bismarck, ND	1076	68.8	42.0	2.517	28.1	9.0	13.0	75.4	0.75
3. Buffalo, NY	542	29.8	45.1	2.004	13.6	10.0	16.0	7.4	0.14
4. Charlotte, NC	976	71.2	41.2	2.53	28.3	8.0	13.0	69.4	0.76
5. Chicago, IL	870	56.4	42.5	2.326	22.8	9.0	14.0	43.5	0.53
6. Dallas, TX	890	73.0	40.2	2.610	30.0	8.0	12.0	69.6	0.83
7. Denver, CO	862	73.8	39.7	2.982	39.6	8.0	11.0	98.6	1.22
8. East Lansing, MI	834	53.3	42.4	2.293	22.0	9.0	14.0	38.9	0.50
9. Great Falls, MT	978	66.4	41.6	2.514	27.8	9.0	13.0	67.8	0.74
10. Houston, TX	810	62.4	41.3	2.407	24.7	9.0	13.0	46.4	0.61
11. Jackson, MS	902	69.0	41.0	2.523	27.0	9.0	13.0	62.8	0.74
12. Kansas City, MO	962	68.5	41.3	2.514	27.8	9.0	13.0	66.5	0.73
13. Los Angeles, CA	914	81.3	39.1	2.831	35.7	8.0	11.0	91.3	1.06
14. Memphis, TN	924	67.4	41.4	2.491	27.1	9.0	13.0	61.6	0.71
15. Miami, FL	772	69.5	39.9	2.553	28.2	9.0	13.0	55.1	0.76
16. Milwaukee, WI	828	52.6	42.4	2.279	21.7	9.0	14.0	37.4	0.48
17. New Orleans, LA	920	71.2	40.9	2.553	28.6	8.0	13.0	66.9	0.77
18. New York, NY	748	44.7	44.1	2.144	18.0	10.0	15.0	23.0	0.33
19. Phoenix, AZ	858	89.6	40.3	3.445	52.4	7.0	10.0	136.9	1.63
20. Portland, ME	686	39.2	44.1	2.083	16.4	10.0	15.0	16.7	0.26
21. Portland, OR	626	36.2	44.4	2.075	16.1	10.0	15.0	14.6	0.25
22. Salt Lake City, UT	964	81.2	40.3	3.022	40.9	8.0	11.0	114.7	1.27

* 1 = Optimized collector area at \$150/m^2
2 = Percent by solar.
3 = Energy supplied/energy incident.
4 = Energy supplied to load/m^2 (10^6 KJ)
5 = Rate of return on solar investment (percent)
6 = Years until undiscounted fuel savings = investment.
7 = Years until undiscounted solar savings = mortgage principal.
8 = Present worth of cumulative solar savings (10^3 \$).
9 = Savings/investment ratio.

systems in Table 11.6.5 is 150 $\$/m^2$. The collector area was optimized by the golden section search technique. The objective was to find the collector area which minimized the present value costs with the solar-assisted system over the period of analysis.

The years until undiscounted fuel savings equal the investment and the years until undiscounted solar savings equal the mortgage principal in Tables 11.6.1 and 11.6.5, are not reliable criteria of investment performance. They fail to consider the financial returns after the savings equal the investment and the mortgage principal. The present worth of cumulative solar savings is invalid when two systems of different size are compared.

To overcome the disadvantages of the above selection criteria the savings/investment ratio (SIR) is often used by researchers and economists as a measure of overall investment performance (see Chapter 4). The saving/investment ratio is not an f-chart output. It can be evaluated by dividing the present worth of cumulative solar savings by the present value of the solar systems investment. Savings/investment ratios greater than 1.0 indicate that the proposed investment is cost effective because it will return all capital funds at a rate greater than the discount rate.

The last column of Table 11.6.5 is the savings/investment ratio. Only four cities (Denver, Los Angeles, Phoenis and Salt Lake City) indicate SIR values greater than 1.0. In the remaining cities, a solar investment is not cost effective from a SIR point of view, despite the fact that the collector areas in Table 1.6.5 were optimized to obtain the highest savings.

The following illustration underscores the difference between the present worth of cumulative solar savings and SIR criteria. The cumulative solar savings criterion compares two energy alternatives. The alternative with the smaller cost (or higher savings) over the period of the analysis is the most cost effective. In Table 11.6.5 the solar energy alternative is more cost effective than a conventional water heater which utilizes fuel at 9.0 $/GJ (see parameters 31 and 34 in Table 11.6.2). The cumulative solar saving does not give an indication of the magnitude of the investment.

The SIR is considered a better measure of the overall expenditure performance of a solar water heating system because it accounts for both the magnitude of the investment and the savings over the period of analysis. Between two alternatives, the one with the higher SIR is the most cost effective even if both alternatives show SIR values less than 1.0.

The author recommends the SIR criterion whenever solar systems of various sizes are compared from an economic point of view. When systems of equal size are compared, the cumulative solar savings will give the same results at the SIR index.

The above observations are illustrated in Figure 11.6.1 where the relationship between the collector area and solar savings for Phoenix, Kansas City, Missouri, and Buffalo is presented. The highest point on the curves represents the optimum collector area under the economic scenario of Table 11.6.2. The effect of geographic location on present worth of solar savings is obvious. A solar system in Phoenix is a far more attractive investment for a

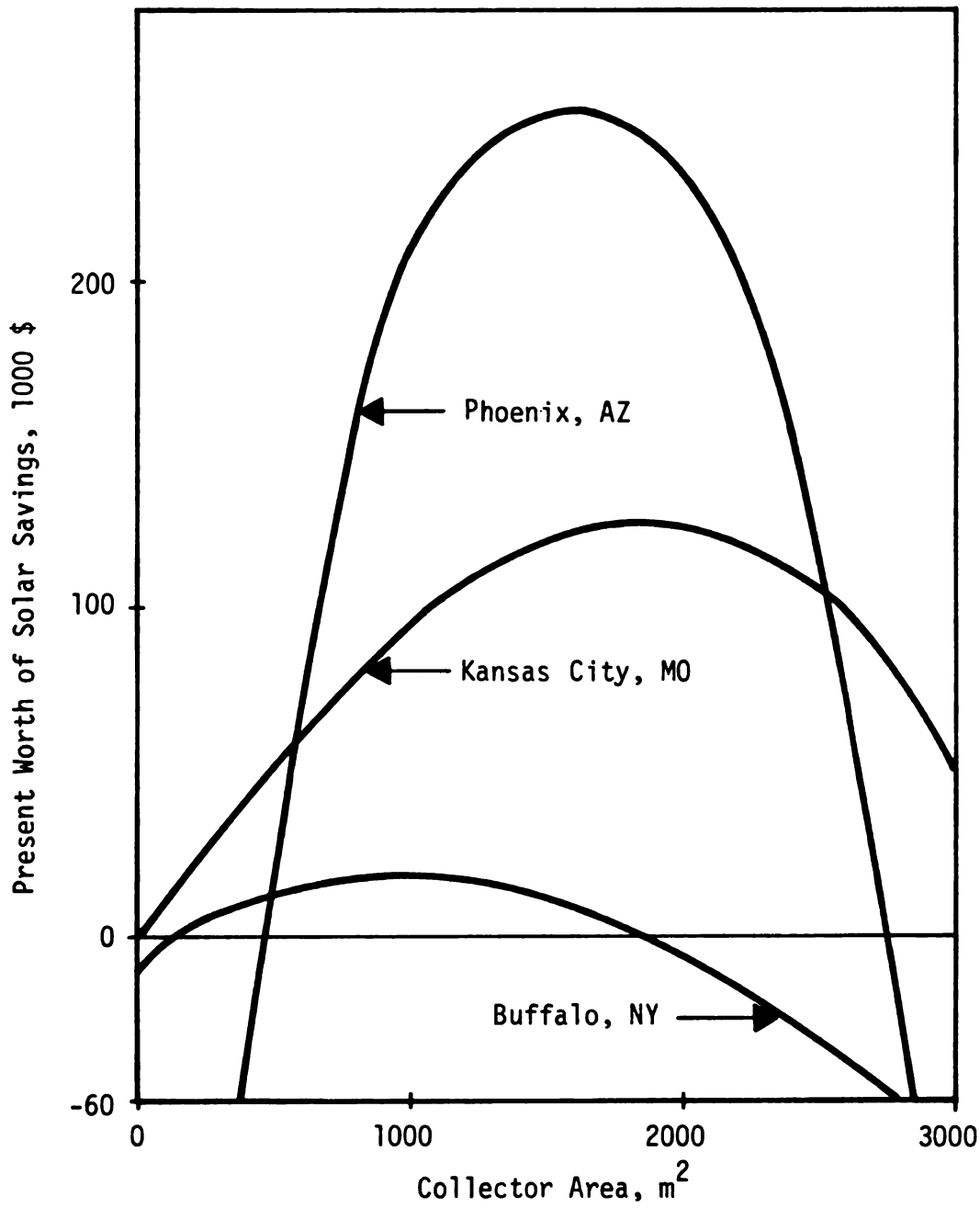

Figure 11.6.1.--Collector area and present worth of solar savings relationship.

food processing plant than in Buffalo. From Figure 11.6.1, two solar systems in Kansas City with collector areas of 1000 m^2 and 1500 m^2 are shown to save approximately 100,000 and 130,000 dollars, respectively. Which system is more cost effective is not obvious from the figure. The larger system supplies more energy to the load but it also requires a higher investment.

In Table 11.6.6 the percent by solar and savings/investment ratio for various collector areas in selected cities of the United States are presented. It can be seen that the larger the collector area and the percent by solar, the lower the SIR. Cities with an asterisk represent locations where more than 50 percent of the load can be supplied by solar and where the SIR ratio is greater than one. In general, cities in the Great Lakes states and in the Northeast do not show SIR values greater than 1.0 for the collector sizes investigated.

The economic output of the f-chart depends on various parameters (see Table 11.6.2). In addition to the large number of parameters involved in the economic analysis, the future value for a number of the parameters must be assumed in the analysis. Sensitivity tests have been performed in order to examine the significance of the various parameters on the economics of solar water heating.

In Figure 11.6.2 a linear relationship between the cost of the solar system and the solar savings is shown for Kansas City. A system costing more than 210 $\$/m^2$ of collector area will result in negative savings.

TABLE 11.6.6.--Percent by solar and savings/investment ratio (in parenthesis) for various collector areas in selected cities of the United States with constant hot water demand (1,514,000 Kg/week).

City	Collector Area, m^2				
	1000	3000	4000	7000	10000
Atlanta, GA	16.6 (1.314)	44.2 (0.959)	55.2 (0.792)	81.0 (0.338)	92.3 --
Bismarck, ND*	14.4 (1.450)	39.2 (1.172)	49.8 (1.085)	75.0 (0.665)	84.7 (0.190)
Buffalo, NY*	5.4 (0.481)	10.5 (0.333)	23.0 (0.256)	37.0 (0.156)	60.5 --
Charlotte, NC*	16.4 (1.573)	44.2 (1.217)	55.8 (1.049)	82.4 (0.587)	95.0 (0.103)
Chicago, IL	13.8 (1.124)	37.6 (0.840)	47.7 (0.703)	71.5 (0.328)	84.2 --
Dallas, TX*	18.6 (1.723)	49.3 (1.291)	61.7 (1.090)	87.6 (0.523)	95.6 --
Denver, CO*	22.5 (2.948)	58.4 (2.300)	72.4 (2.002)	96.5 (1.065)	99.8 (0.240)
East Lansing, MI	13.5 (1.056)	36.7 (0.775)	46.6 (0.642)	69.8 (0.274)	82.2 --
Great Falls, MT	15.2 (1.538)	41.0 (1.189)	51.8 (1.025)	76.4 (0.559)	87.5 (0.068)
Huston, TX	16.7 (1.276)	44.5 (0.476)	56.0 (0.763)	81.7 (0.315)	92.8 --

TABLE 11.6.6.--Continued.

City	Collector Area, m^2				
	1000	3000	4000	7000	1000
Jackson, MS*	17.1 (1.538)	45.7 (1.160)	57.4 (0.983)	83.7 (0.499)	93.2 --
Kansas City, MO*	15.9 (1.531)	42.9 (1.175)	54.2 (1.013)	80.1 (0.544)	90.9 (0.048)
Los Angeles, CA*	21.0 (2.193)	54.9 (1.652)	68.1 (1.404)	94.0 (0.701)	99.1 (0.014)
Memphis, TN*	16.2 (1.477)	43.6 (1.123)	54.9 (0.957)	80.9 (0.5000)	91.2 --
Miami, FL*	20.0 (1.565)	52.3 (1.113)	64.9 (0.905)	91.1 (0.341)	99.2 --
Milwaukee, WI	13.4 (1.025)	36.4 (0.750)	46.2 (0.632)	69.4 (0.259)	82.3 --
New Orleans, LA	17.4 (1.604)	46.5 (1.217)	58.4 (1.036)	85.2 (0.520)	94.8 --
New York, NY	12.1 (0.995)	33.2 (0.513)	42.3 (0.408)	64.7 (0.113)	80.4 --
Phoenix, AZ	25.0 (4.906)	64.1 (3.606)	78.8 (3.217)	97.4 (1.399)	100.0 (0.004)
Portland, ME	11.3 (0.611)	31.2 (0.407)	39.9 (0.310)	61.3 (3.012)	76.7 --

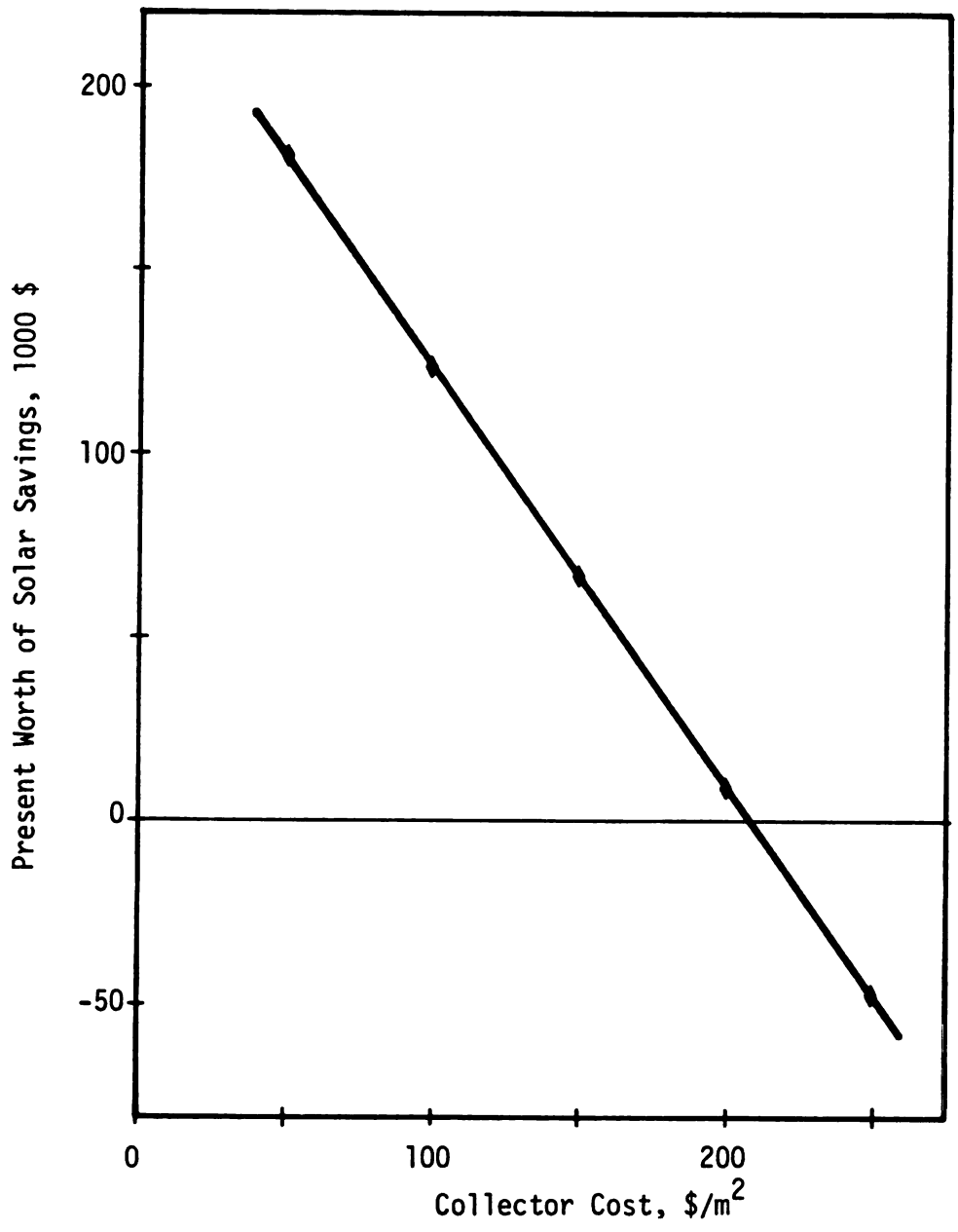

Figure 11.6.2.--Collector cost and solar savings relationship in Kansas City, MO.

A linear relationship between the life time of a solar system and solar savings for Kansas City is shown in Figure 11.6.3. A solar system with a life time of less than 12 years will result in negative savings under the assumed scenario values of Table 11.6.2.

The effect of the annual price escalation of the conventional and backup fuels is presented in Figure 11.6.4. The exponential relationship shown in Figure 11.6.4 indicates that fuel price escalation is a very sensitive parameter in the life-cycle costing analysis.

In Figure 11.6.5 the relationship between the annual discount rate and the savings for Kansas City is shown. The exponential relationship indicates that the annual discount rate is also a sensitive parameter in life-cycle costing analysis.

In Figure 11.6.6 the relationship between the inflation rate and the savings for Kansas City is shown. It can be seen that to obtain more than $100,000 savings the inflation must be negative (deflation). Thus, inflation is also a sensitive parameter in the life cycle costing analysis.

In Table 11.6.7 the economics of scale for East Lansing, Michigan is presented. Collector areas and water consumption rates in a processing plant are increased by the same order of magnitude. From Table 11.6.7 it can be seen that the solar savings are scaled up according to the collector area and water consumption. There is no change on the percent by solar and the other indices.

The effect of the conventional and back up fuel price on the savings investment ratio of a 1000 m^2 collector solar system in

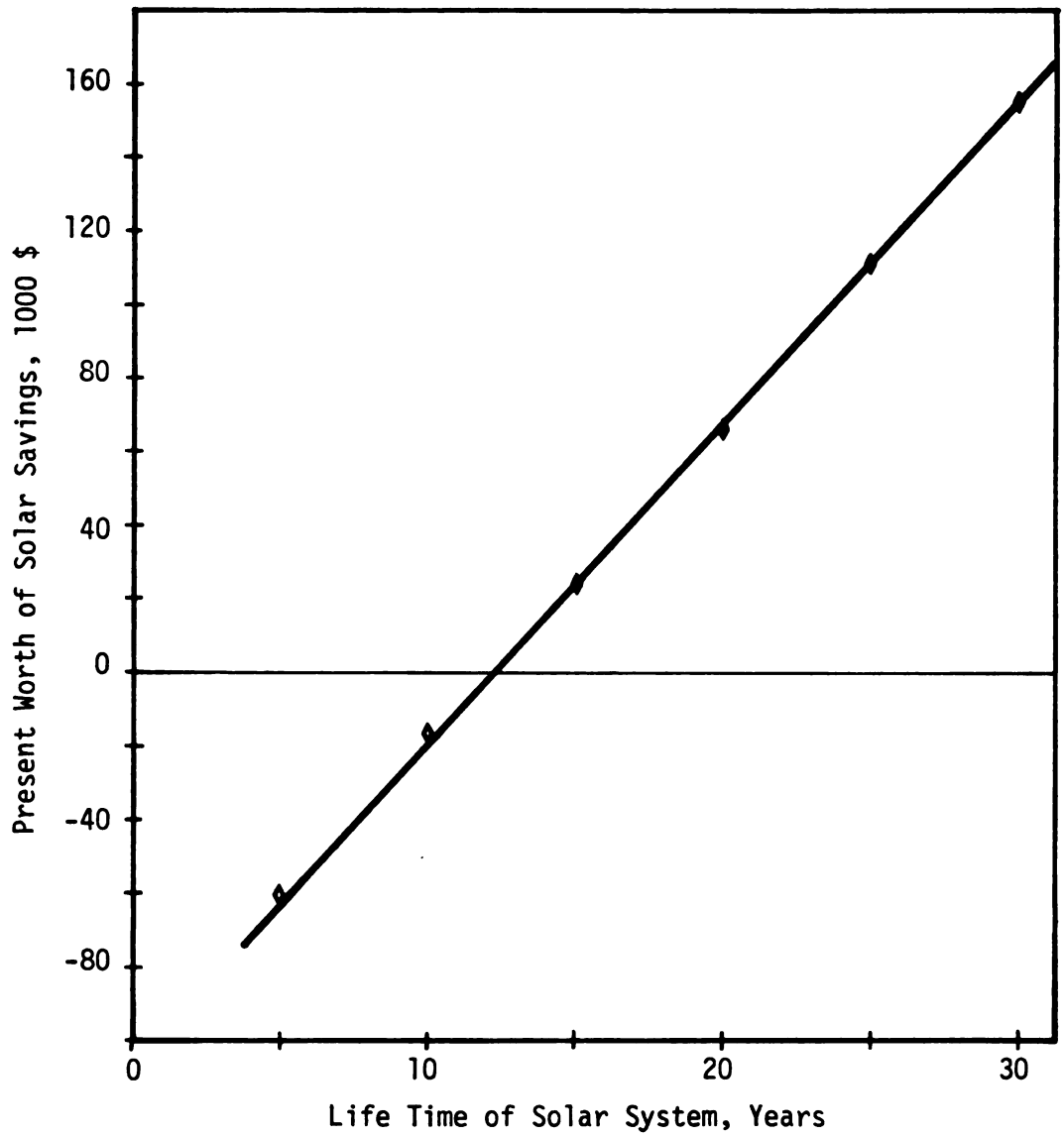

Figure 11.6.3.--Solar system life time and solar savings relationship in Kansas City, MO.

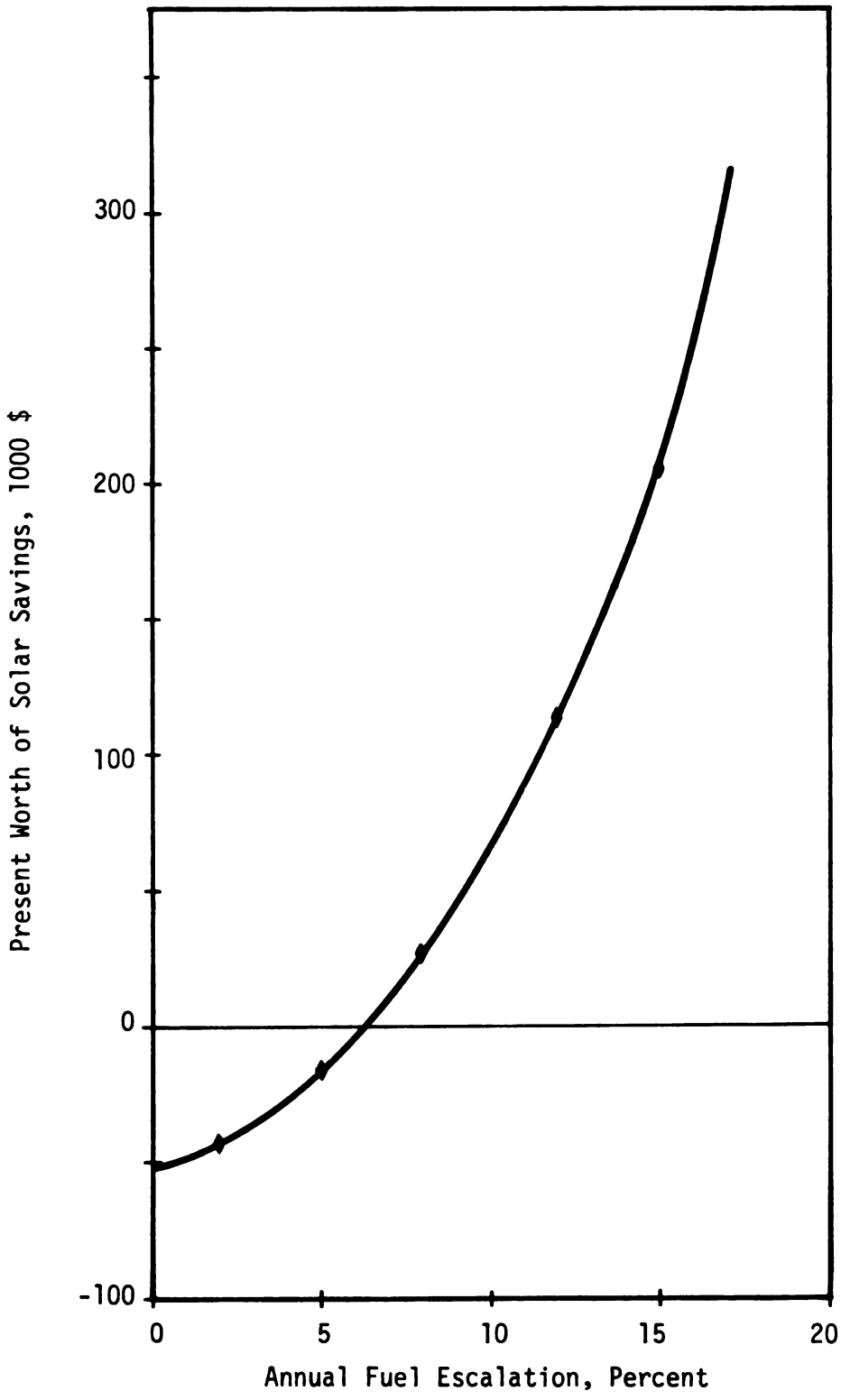

Figure 11.6.4.--Yearly fuel price escalation and solar savings relationship in Kansas City, MO.

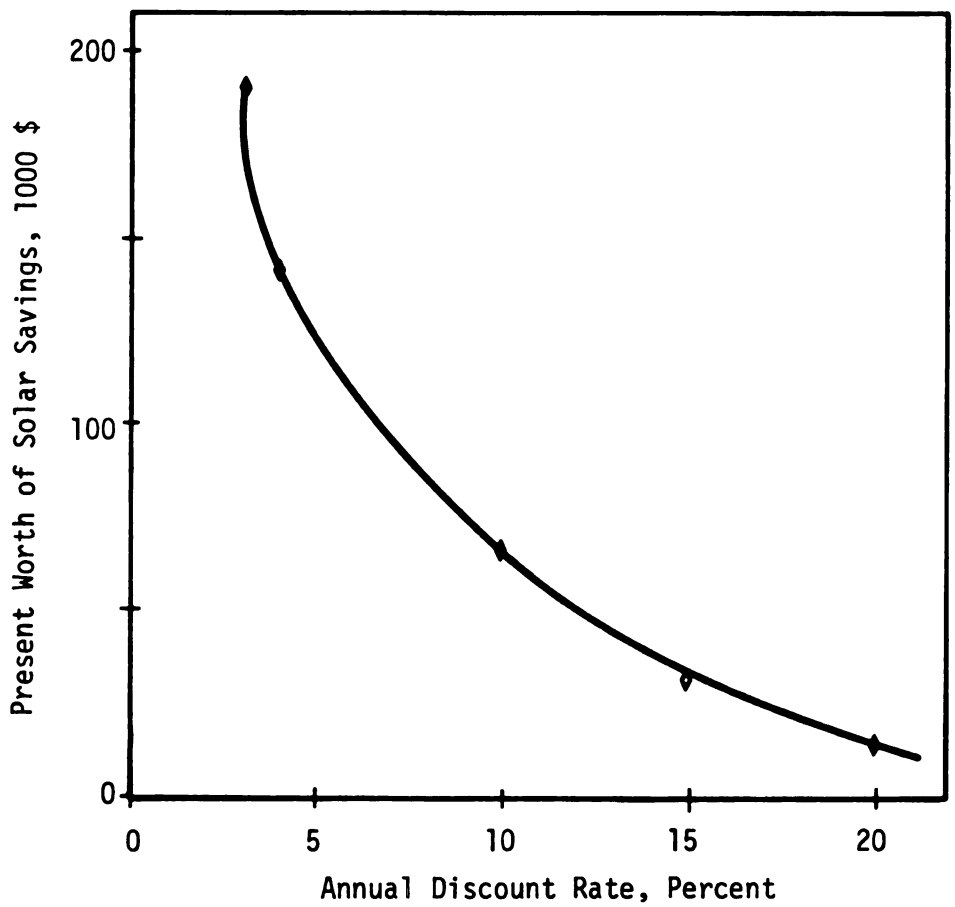

Figure 11.6.5.--Annual discount rate and solar savings relationship in Kansas City, MO.

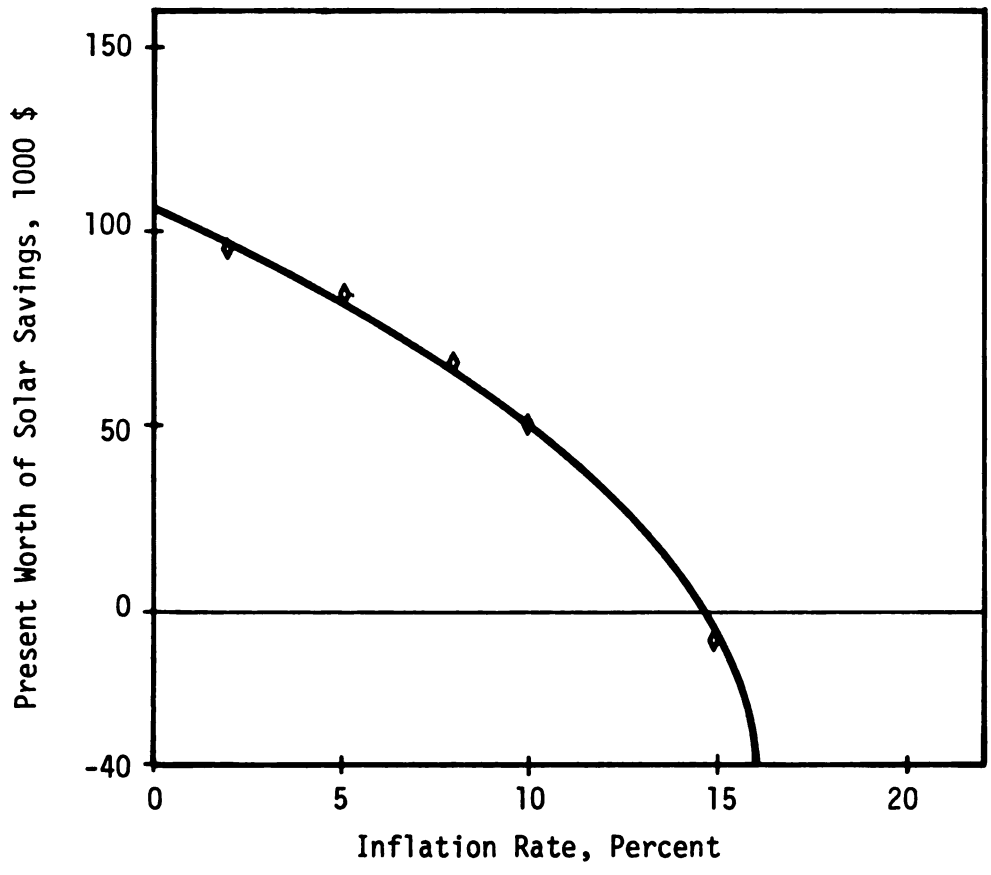

Figure 11.6.6--Inflation rate and solar savings relationship in Kansas City, MO.

TABLE 11.6.7.--Effect of scale up on solar system thermal output and economics in East Lansing, Michigan.

Collector Area, m^2	Water Use to load/m^2, GJ	Percent by Solar	1*	2	3	4	5
500	132,475	2.185	60.9	19.8	9	15	18.6	0.427
1000	264,950	2.185	60.9	19.8	9	15	37.3	0.427
2000	529,900	2.185	60.9	19.8	0	15	74.6	0.427
3000	794,850	2.185	60.9	19.8	9	15	111.9	0.427
4000	1,059,800	2.185	60.9	19.8	9	15	149.2	0.427

*1 = Rate of return on the solar investment, percent

2 = Years until undiscounted fuel savings = investment

3 = Years until undiscounted solar savings = mortgage principal

4 = Present worth of solar savins, 1000 $

5 = Savings/investment ratio

various cities of the United States is shown in Table 11.6.8. At the present, the prices for natural gas, oil and electricity are approximately 2.5, 9.0 and 15.0 $/GJ, respectively. Solar water heating is economical in all cities investigated when the conventional fuel is electricity. Under a natural gas scenario, the solar savings are negative in all cities studied. With oil the SIR index was higher or lower than 1.0 depending on the geographic location under consideration.

11.7 Discussion of the Results by Thomas and Singh et al.

The results by Thomas (1977) and Singh et al. (1978) are discussed here. In both studies TRNSYS was used to investigate the feasibility of solar water heating in food processing applications.

I. Thomas (1977) categorized dairy and meat processing plants according to size as shown in the chart on page 232.

This author disagrees with the procedure of classification shown because there is not consistancy among the sizes. For example, a medium meat plant is smaller than a medium dairy plant, while a small meat plant is larger than a small dairy plant. The energy audit on which Thomas based the classification of the processing plants is questionable. The large difference of the water temperature among the sizes is not clear. Since in all plants water is used for cleaning, the temperatures are expected to be approximately the same.

Geographic location was found by Thomas to have a definite effect on economic solar water heating feasibility for food

TABLE 11.6.8.--Savings/investment ratio at various fuel prices for solar systems in selected cities of the United States.

City	Fuel Cost, $/GJ		
	2.5	9.0	15.0
Buffalo, NY	-	-	1.248
Chicago, IL	-	0.460	2.049
Denver, CO	-	1.495	3.774
East Lansing, MI	-	0.404	1.955
Kansas City, MO	-	0.719	2.480
Los Angeles, CA	-	0.981	2.917
New York, NY	-	0.215	1.641
Phoenix, AZ	-	1.385	3.594

Plant Size	Water Use Kg/day	Operating days/week	Water Temperature, °C
DAIRY PLANTS			
Small	1,940	3	65
Medium	6,456	5	66
Large	25,000	6	79
MEAT PLANTS			
Small	3,026	5	60
Medium	5,410	5	71
Large	42,000	6	71

processing plants. Similar observations about the geographic location are made in this study (see Table 11.5.2).

The observation by Thomas that a plant operating six days per week showed better economic performance than a plant operating five days per week is confirmed by Table 11.6.3 of this study.

According to Thomas, a significant solar energy contribution can be made by replacing up to 90 percent of the fossil fuel energy consumption for most processing plants over a 20-year payback period. Whether the payback or the life time of a solar system is 20 years is not clear from the above statement. If the payback was 20 years, positive solar savings would have never been realized according to Table 11.6.1 of this study.

The conclusion of Thomas that solar energy can supply up to 90 to 100 percent of the annual energy demand is correct according to Table 11.5.2 of this study.

II. The principal results by Singh et al. (1978) are:

1. The more sensitive parameters for economic analysis in life cycle costing are:

   a. total yearly demand

   b. location

   c. conventional fuel cost

   d. annual discount rate

   e. collector area cost.

Similar observations about the above parameters have been made in this study (see Figures 11.6.1 through 11.6.7). In addition to the above parameters, annual fuel escalation price and inflation rate are found to be sensitive parameters.

2. The percent by solar in three cities found were identified as shown on page 234.

According to this study and results by Thomas (1977), the above figures are wrong. In East Lansing where the insolation is considerably lower than in Fresno, California, a solar system will supply approximately 50 percent of the energy needs, under approximately the same load as used by Singh et al. (1978) (see Tables 11.2.1 and 11.5.2).

According to the authors, "The contribution of solar energy in Fresno and Charleston was slightly greater than that in Madison

City	Collector Area, m^2	Load GJ	Percent by Solar
Madison, WI	1000	3,080	8.5
	4000	10,500	28.9
Fresno, CA	1000	2,580	71.0
	4000	7,960	34.1
Charleston, VA	1000	2,820	11.2
	4000	7,960	32.5

because both Fresno and Charleston have warmer climates than Madison and subsequently less heat loss in the collector system." This is not true. The higher contribution by solar in Fresno and Charleston is largely due to higher insolation in Fresno and Charleston than in Madison rather than to the warmer climates as the authors claim.

CHAPTER 12

CONCLUSIONS

1. The engineering behavior of a solar water heater for a food processing plant is accurately predicted by TRNSYS. Numerical results have been compared with experimental results obtained by the Michigan State University dairy plant solar water heater and the agreement was found to be more than satisfactory.

2. The f-chart program modified to accept weekly instead of daily water loads can be satisfactory used in the design of industrial type solar water heaters. Predicted values of solar system performance by the f-chart method were found to be in satisfactory agreement with the results obtained by TRNSYS.

3. Energy use profiles encountered in food processing plants have been identified and the effect of each on the performance of solar water heaters has been determined. The hourly and daily solar system performance have been found to be slightly effected by the daily process energy distribution in a food processing plant. The weekly, monthly, and yearly solar system performance, however are not effected as a result of the energy use pattern in a food processing plant.

4. The time a food processing plant assumes daily operation has been determined to have no effect on the performance and thermal output of a solar water heater.

5. The number of work days per week in a food processing plant has been found to have a significant effect on the engineering behavior and performance of a solar water heater. A solar water heater in a food processing plant operating seven days per week was found to have higher collector efficiency and thermal output per collector unit area than a solar system of equal size in a food processing plant operating five or six days per week. The solar water heater in a food processing plant operating five days per week contributed more to the yearly hot water load than in cases of six or seven operating days per week.

6. The yearly efficiency of a specified solar collector design was found to be relatively constant among the varius cities of the United States investigated by this study. The thermal output per collector unit area and consequently the fraction of the yearly hot water attributed to solar energy has been found to vary significantly among the various cities of the United States.

7. Depending on the yearly hot water load in a food processing plant and the geographic location, a solar water heater with storage tank capacity equal to the daily hot water load and the collector area sized according to the volume of the tank can supply up to 49 percent in Buffalo, New York and up to 94 percent in Phoeniz, Arizona of the yearly hot water needs.

8. A sensitivity analysis of the economic parameters has indicated that conventional fuel escalation costs over the period of the economic analysis, annual nominal discount rate and geographic location have the greatest effect on the economic performance of a solar water heater.

9. Solar water heating for food processing plants is economically feasible in most of the locations of the United States when oil and electricity is the alternative, the nominal discount rate is 10 percent, the solar system costs 159 $\$/m^2$ of collector area, the inflation rate is 8 percent, the fuel cost escalates at an annual rate of 10 percent and the economic life of the system is 20 years. In the Western states solar water heating is more cost effective than in the Eastern, Midwestern and Southern states.

CHAPTER 13

SUGGESTIONS FOR FUTURE RESEARCH

1. Investigate the engineering behavior of solar water heaters in food processing plants in geographic locations with different insolation.

2. Design an experiment to determine the validity of TRNSYS over a longer period of time.

3. Perform TRNSYS runs in selected geographic locations to modify the f-chart program under various amounts of solar radiation.

4. Study the potential of solar water heating in food processing plants by using parabolic and evacuated tube solar collectors.

BIBLIOGRAPHY

BIBLIOGRAPHY

Anonymous, 1978a. Solar energy research and development: Program Balance Annex, Vol. I HCP/M2693-01, Vol. II HCP/M2693-02. Available from NTIS.

Anonymous, 1978b. Fuel consumption in SIC-20. Food Engineering, Vol. 50, No. 5, pp. 43.

Anonymous, 1979. Lower frenzy, higher prices. Business Week, December 31, 1979.

Aplin, R. D. and Casler, G. L., 1973. Capital Investment Analysis: Using Discounted Cash Flows. Grid, Inc., Columbus, Ohio.

ASHRAE Application Handbook, 1974. American Society of Heating, Refrigeration and Air Conditioning. New York. New York.

Berry, R. E., Wagner, C. J. and Coleman, R. L., 1979. Solar drying of southeastern fruit, and vegetables. Presented at the Second International Conference of Energy Use Management. Los Angeles, October 22-26, 1979.

Beckman, W. A., Klein, S. A. and Duffie, J. A., 1977. Solar heating design. John Wiley and Sons, New York.

Beijdorff, A. F. 1979. Energy conservation: The prospects of improved energy efficiency. Presented at the Second International Conference of Energy Use Management. Los Angeles, October 22-26, 1979.

Biermant, H. and Smidt, S. 1970. The capital Budgeting Decision. The McMillon Co., 3rd ed., Ch. 2.

Boer, K. W., 1978. Payback of solar systems, Solar Energy, Vol. 20, pp. 225-232.

Bolin, H. R., Stafford, A. E. and Huxsole, C. C., 1977. Solar heated fruit dehydrator. Solar Energy, Vol. 20, pp. 289-296.

Buchberg, H. and Roulet, J. R., 1968. Simulation and optimization of solar collection and storage for hous heating. Solar Energy, Vol. 12, pp. 31-50.

Butt, S. H., 1976. Solar life cycle cash flow analysis. Presented at Western Regional Solar Heating and Cooling Workshops, January 28, 1976.

Butz, L. W., Beckman, W. A. and Duffie, J. A., 1974. Simulation of solar energy heating and cooling system. Solar Energy, Vol. 16, pp. 129-136.

Casper, M. E., 1977. Energy saving techniques for the food industry. Noyes Data Corporation.

Chen, C. S., Carter, R. D. and Buslig, B. S., 1979. Energy requirements for the taste citrus evaporators. Presented at the Second International Conference of Energy Use Management, Los Angeles, October 22-26, 1979.

Collings, W. D., 1925. Temperature of water available for industrial use in the United States. U.S. Geological survey water supply paper No. 520F.

Corradi, A. Q., 1979. Energy and the exercise of power. Foreign Affairs, Vol. 57, No. 5, pp. 1144-1166.

Corcoran, W. L., 1978. Economics of solar heating and cooling systems. ASHRAE Journal, July, 1978.

Dansburry, K. P., 1978. Determination of energy utilization and conservation potential in dairy plant operations. M.S. Thesis, Michigan State University, East Lansing.

Davis, D. C., Kranzler, G. A., Leung, H. K. and Swanson, B. G., 1979. Direct pasteurization of fruit juices utilizing solar energy. Presented at the Second International Conference of Energy Use Management, Los Angeles, October 22-26, 1979.

Deng, J. C. et al., 1979. Drying seafood products with solar energy. Presented at the Second International Conference of Energy Use Management, Los Angeles, October 22-26, 1979.

Decker, D. L., 1977. Energy management in industry. IEEE 1977 Energy Management Seminar Proceedings.

DeWinter, F., 1975. Heat exchanger penalties in double-loop solar water heating systems. Solar Energy, Vol. 17, pp. 335-337.

Dorf, R. C., 1978. Energy, Resources and Policy. Addison-Wesley Publishing Co., Reading, Mass.

Duffie, J. A. and Beckman, W. A., 1974. Solar Energy Thermal Processes. John Wiley and Sons, New York.

ERDA, 1976. An economic analysis of solar water and space heating. DSE-2322.

ERDA, 1977. Solar energy for agricultural and industrial processes. ERDA 77-72 UC-59.

Gilman, S. F., 1978. Solar energy: Present and future. ASHRAE Journal, Vol. 20, No. 11.

Graham, B. J., 1979. Evacuated tube collectors. Solar Age, November, 1979.

Graven, R. M., 1974. A comparison of computer programs used for modeling solar heating and air conditioning systems for buildings. Lawrence Berkeley Laboratory, University of California, Berkeley, LBL-3066.

Grimmer, D. P. and Moore, S. W., 1977. Cost effectiveness and durability: Two important factors in material choice. Solar Engineering, January, 1977.

Gustaferro, J. F., 1979. Preliminary forecast of lively U.S. consumption/production balances for 1985 and 2000 by States. Presented at the Second International Conference of Energy Use Management, Los Angeles, October 22-26, 1979.

Hayes, D., 1977. Energy: The solar prospect. Worldwatch Institute, Washington, D.C.

Hirst, E., 1973. Energy use for food in the U.S., Oak Ridge National Lab., U.S. Atomic Energy Commission, ORNL-NSF-EP-57, Oak Ridge, Tennessee.

Horwitz, B. A., 1980. The mathematics of discounted cash flow analysis. Chemical Engineering, Vol. 87, No. 10.

Hottel, H. C. and Woertz, B. B., 1974. Performance of flat-plate solar-heat collectors. Trans ASME, Vol. 64, 91.

Hottel, H. C. and Whillier, A., 1958. Evaluation of flat-plate solar collector performance, Trans. of Conference on the use of solar energy, pp. 74-104, University of Arizona.

Hughes, P. J., 1978. FCHART, Version 3.0. Users Manual, University of Wisconsin, EES Report 49-3.

Keynes, J. M., 1936. The general theory of employment, interest and money. New York, pp. 167.

Key, J. M., 1979. Computer simulation of a solar energy system. Sunworld, Vol. 3:(4), pp. 96-111. Pergamon Press, New York.

Keys, W. M. and London, A. L., 1958. Compact heat exchangers. The National Press, Palo Alto, California.

Klein, S. A., 1975. Calculation of flat-plate collector loss coefficients. Solar Energy, Vol. 17, pp. 79-80.

Klein, S. A., 1977. Calculation of monthly average insolation on tilted surfaces. Solar Energy, Vol. 19, pp. 325.

Klein, S. A., Cooper, P. I., Freeman, T. L., Beekman, D. M., Beckman, W. A. and Duffie, J. A., 1977. A method of simulation of solar processes and its application. Solar Energy, Vol. 17(1), pp. 29-37.

Klein, S. A. et al., 1979. TRNSYS: A transient simulation program. Report #38-10, University of Wisconsin, Engineering Experiment Station.

Kreith, F. and Kreider, J. F., 1978. Principles of Solar Engineering. McGraw-Hill Co., New York.

Knopf, F. C., Wilson, P. W. and Okos, M. R., 1978. Instrumentation for energy conservation. ASAE Paper No. 78-6513, St. Joseph, Missouri.

Lavai, Z. and Thomson, J., 1977. Experimental study of thermally stratified hot water storage tanks. Solar Energy, Vol. 19, pp. 519-524.

Lewis, R. A. and Muller, P. 1979. The future of coal synthetic fuels in the context of national and global energy futures and impacts. Presented at the Second International Conference of Energy Use Management, Los Angeles, October 22-26, 1979.

Liu, B. Y. H. and Jordan, R. C., 1962. Dairy insolation on surfaces tilted toward the equator. Transactions ASHRAE, 526-541.

Liu, B. Y. H. and Jordan, R. C., 1963. The long-term average performance of flat-plate solar energy collectors. Solar Energy, Vol. 7, pp. 53.

Lof, G. O. G., El-Wulki, M. M. and Chiou, J. P., 1964. Design and performance of domestic heating system employing solar heated air--The Colorado House. Proc. U.N. Conference on New Sources of Energy, 5 (185).

Lof, G. O. G. and Tybout, R. A., 1972. A model for optimizing solar heating design. ASME Paper 72-WA/Sol-8.

Lof, G. O. G. and Close, D. J., 1967. Solar water heaters. Low temperature engineering application of solar energy. Chapter VI ASHRAE. Edited by R. C. Jordan.

Loper, A., 1975. A complete course in canning. The Canning Trade, Inc., Baltimore, Maryland.

Louis, W. C. and Miller, D. C., 1978. Evacuated-tube solar collector: Effect of control on efficiency and high operating temperatures. ASHRAE Journal, May, 1978.

Lund, D. L., 1977. Compatibility of solar energy supply, collection and storage with food processing energy demands. University of Wisconsin, Department of Food Science, unpublished report.

Meador, R., 1978. Future energy alternatives. Ann Arbor Science Publishers, Inc., Ann Arbor, Michigan, pp. 176.

Miller, W. M., 1979. Fresh fruit drying potential with solar regenerated desicants. Presented at the Second International Conference of Energy Use Management, Los Angeles, October 22-26, 1979.

Morse, R. N. and Czarnecki, J. T., 1958. Flat-plate solar absorbers--The effect on incident radiation of inclimation and orientation. C.S.I.R.O. Engineering Section, August.

Mutch, J. J., 1977. Residential water heating: Fuel consumption, economics and public policy. RAND, Department R 1498, NSF.

Nelson, G. A., Lee, W. F. and Murray, W. G., 197e. Agricultural Finance, 6th Ed., The Iowa State University Press.

Newton, A. B., 1978. Controls: Reducing solar collector area by 35 to 40%. ASHRAE Journal, September.

Nwude, J. K., Brown, H. L. and Hamel, B. B., 1975. Utilization analysis of energy systems--Food processing industry, Campbell Sout Plant 2. NSF-RA-E-75-245.

Oonk, R. I., Beckman, W. A. and Duffie, J. A., 1975. Modeling of the CSU heating/cooling system. Solar Energy, Vol. 17(1), pp. 21-28.

Pierotti, A., Keeler, G. A. and Fritsch, A., 1977. Energy and food. Center for Science in the Public Interest.

Proctor, D. and Morse, R. N., 1977. Solar energy for the Australian food processing industry. Solar Energy, Vol. 19, pp. 63-72.

Puri, V. M., Okos, M. R. and Murks, J. S., 1979. Solar concentration of liquid foods. Presented at the Second International Conference of Energy Use Management, Los Angeles, October 22-26, 1979.

Quilman, B., 1977. Energy conservation techniques, IEEE 1977 Energy Management Seminar Proceedings.

Rabl, A., 1976. Optical and thermal properties of compound parabolic concentrators. Solar Energy, Vol. 18, pp. 497-511.

Rice, W., 1979. Federal policy on solar. Solar Age, November, 1979.

Rao, M. A. and Katz, J., 1976. Computer estimation of heat losses in food processing plants. Food Technology, March, 1976.

Rao, M. A., Katz, J. and Goel, V. K., 1978. Economic evaluation of measures to conserve thermal energy in food processing plants. Food Technology, April, 1978.

Reynolds, Smith and Hills, 1976. Life cycle costing emphasizing energy conservation, guidelines for investment analysis. ERDA-76/130 REV.

Ridker, R. G. and Cecelski, E. W., 1979. Resources, environment, and population: The nature of future limits. Population Bulletin, Vol. 34, No. 3, August, 1979. Population Reference Bureau, Inc., Washington, D.C.

Ridker, R. G. and Watson, W. D., 1980. To choose a future: Resource and environmental problems of the U.S. A long-term global outlook. John Hopkins Press for Resources for the Future, Baltimore, Maryland.

Rippen, A. L., 1977. Professor in the Department of Food Science and Human Nutrition, Michigan State University, East Lansing. Personal communications.

Rippen, A. L. and Mintzias, P., 1977. The mounting importance of energy conservation. Dairy and Ice Cream Field, Vol. 162, No. 11, pp. 36B.

Rippen, A. L., Bakker-Arkema, F. W., Coulter, D. and Mintzias, P. 1978. Design of a pilot scale solar water heater for dairy plants. Presented at the 1978 Annual Meeting of the Institute of Food Technologists, Paper No. 312.

The Rockefeller Foundation, 1978. International energy supply: A prospective from the industrial world, May, 1978.

Ruegg, R. T., 1975. Solar heating and cooling in buildings: Methods of economic evaluation. U.S. Department of Commerce, NBSIR 75-712.

Ruegg, R., 1978. Ins and outs of life cycle costing. Solar Engineering, July, 1978.

Schlesinger, R. J. 1977. Proportional controllers show gains for system efficiency. Solar Engineering, February, 1977.

Schreyer, J. M., 1979. TVA, Oak Ridge, Tennessee. Personal communications.

Schwartzberg, H. G. and Rosenau, J. R., 1979. Use of solar concentrated water absorbing brines to save energy in food processing. Presented at the Second International Conference of Energy Use Management, Los Angeled, October 22-26, 1979.

Siegel, R. and Howell, J. R., 1972. Thermal solar radiation heat transfer. McGraw-Hill Co., New York, Ch. 2.

Singh, R. K., Lund, D. B. and Buelow, F. H., 1978. Compatibility of solar energy with fluid milk processing energy demands. ASAE Paper No. 78-6526, St. Joseph, Michigan.

Singh, R. P., 1978. Energy accounting in food processing operations. Food Technology, December, 1978.

Singh, R., Buelow, F., Duffie, J. and Lund, D. L., 1979. Economic analysis of solar-assist in food dehydration. Presented at the Second International Conference of Energy Use Management, Los Angeles, October 22-26, 1979.

Singh, R. P., 1979. Process energy accounting in the canning industry. Presented at the Second International Conference of Energy Use Management, Los Angeles, October 22-26, 1979.

Smith, C. C., Anderson, G. and Chapman, J., 1979. Solar drying of potato products. Presented at the Second International Conference of Energy Use Manatement, Los Angeles, October 22-26, 1979.

Tabor, H., 1967. Selective surfaces for solar collectors. Low temperature engineering application of solar energy, Ch. VI, ASHRAE, edited by R. C. Jordan, 1967.

Telkes, M., 1974. Solar energy storage. ASHRAE Journal, May, 1974.

Thekaekara, M. P. and Drummond, A. J., 1971. Standard values for the solar constant and its spectral components. Nat. Phys. Sci., Vol. 6, pp. 229.

Thekaekara, M. P., 1974. Data on incident solar energy. Supplement to the proceedings, 20th Annual Meeting of Institute for Environmental Science, 21.

Thomas, S. M., 1977. Simulation and feasibility study of solar water heating for the food processing industry in the Midwestern United States. M.S. Thesis, Michigan State University, East Lansing.

Thomas, S. M., Bakker-Arkema, F. W. and Rippen, A. L. Feasibility of solar water heating in milk processing plants in the Midwestern United States, ASAE Paper No. 77-6519, St. Joseph, Michigan.

Trice, J. B., 1979. Industrial heat process. Solar Age, March, 1979.

Unger, S. G., 1975. Energy Utilization in the leading energy consuming food processing industries. Food Technology, December, 1975.

United Nations, Population Division. Unpublished data based on 1978 assessments.

U.S. Department of Commerce, 1976. Energy prospectives, 2

United States Department of Commerce, 1977. Solar heating and cooling of residential buildings. Sizing, installation and operation of systems. Stock No. 003-011-00085-2.

WASE, 1977. Energy: Global prospects 1985-2000. Report of the workshop on alternative energy strategies by MIT. McGraw-Hill Book Co., New York.

Whillier, A., 1967. Design factors influencing solar collector performance. Low temperature engineering application of solar energy. Ch. VI, ASHRAE, edited by R. C. Jordan, 1967.

Winston, R., 1975. Principles of cylindrical concentrators for solar energy. Solar Energy, Vol. 17, pp. 255-258.

Wilson, P. W., Knopf, F. C. and Okos, M. R., 1978. Energy utilization in meat processing plants. ASAE Paper No. 78-6507. St. Joseph, Michigan.

World Bank, 1979. Sober World Bank Report. INTERCOM: The international population news magazine. Vol. 7, Nos. 8 and 9. Population Reference Bureau, Inc., Washington, D.C.

Yellot, J. I., 1973. Utilization of sun sky radiation for heating and cooling of buildings. ASHRAE Journal, Vol. 15, No. 12, pp. 31-42.

Zapp, R. H., 1979. Solar water heating for the Ingham County Geriatric Medical Care Facility. Michigan Solar Energy Association Bulletin, August 10, 1979.

APPENDICES

```
                TRNSYS - A TRANSIENT SIMULATION PROGRAM
      FROM THE SOLAR ENERGY LAB AT THE UNIVERSITY OF WISCONSIN
                        VERSION  10.1  6/1/79


*SIMULATION FOR IND HEAT 2000  GAL LOAD
 SIMULATION          1.000E+00     8.760E+03     2.500E-01
 TOLERANCES          1.000E-02     1.000E-02
 LIMITS  200  200
 WIDTH   132
 UNIT  9     TYPE  9       CARD  READER
       PARAMETERS 11
       1.000E+01     1.000E+00     7.000E+00     5.560E-01    -1.770E+01     9.000E+00     4.470E-01     0.            1.000E+01
       4.187E+01     0.
 UNIT 16     TYPE 16       RADIATION PROCESSOR
       PARAMETERS  5
       1.000E+00     1.000E+00     4.270E+01     4.871E+03     0.
       INPUTS  6
        9,10          9,19          9,20          0, 0          0, 0          0, 0
       0.            0.            0.            0.            4.380E+01     0.
 UNIT  1     TYPE  1       SOLAR  COLLECTOR
       PARAMETERS 10
       2.000E+00     1.500E+02     9.500E-01     3.640E+00     9.000E-01     2.000E+00     1.000E-01     4.500E-01     4.380E+01
       8.200E-01
       INPUTS  5
        3, 1          3, 2          9, 7         16, 6          9, 9
       1.000E+01     0.            0.            0.
 UNIT  2     TYPE  2       PUMP   CONTROLLER
       PARAMETERS  3
       4.000E+00     1.000E+01     3.000E+00
       INPUTS  3
        1, 1         13, 1          2, 1
       1.000E+01     1.000E+01     0.
 UNIT  3     TYPE  3       COLLECTOR  PUMP
       PARAMETERS  1
       9.600E+03
       INPUTS  3
        5, 1          3, 2          2, 1
       1.000E+01     0.            0.
 UNIT  5     TYPE  5       HEAT EXCHANGER
       PARAMETERS  4
       2.000E+00     2.000E+04     3.640E+00     4.186E+00
       INPUTS  4
        1, 1          1, 2         13, 1         13, 2
       1.000E+01     0.            1.000E+01     0.
 UNIT 13     TYPE 13       HEAT EXCHANGER  PUMP
       PARAMETERS  1
       5.000E+03
       INPUTS  3
        4, 1          4, 2          2, 1
       1.000E+01     0.            0.
 UNIT  4     TYPE  4       STORAGE  TANK
       PARAMETERS  5
       7.600E+00     5.400E+00     4.186E+00     1.000E+03     1.000E+00
       INPUTS  5
        5, 3          5, 4          0, 0         14, 1          0, 0
       1.500E+01     0.            1.200E+01     0.            2.100E+01
       DERIVATIVES  2
       2.000E+01     2.000E+01
 UNIT  6     TYPE  6       AUXILIARY  HEATER
       PARAMETERS  3
       1.000E+07     7.400E+01     4.186E+00
       INPUTS  3
        4, 3          4, 4          0, 0
       1.000E+01     0.            1.000E+00
```

```
UNIT 14     TYPE 14          LOAD  ONE
*TOTAL LOAD DISTRIBUTION
     PARAMETERS 44
     0.              0.              3.000E+00       0.              3.000E+00       6.300E+02       1.500E+01       6.300E+02       1.500E+01
     0.              2.700E+01       0.              2.700E+01       6.300E+02       3.900E+01       6.300E+02       3.900E+01       0.
     5.100E+01       0.              5.100E+01       6.300E+02       6.300E+01       6.300E+02       6.300E+01       0.              7.500E+01
     0.              7.500E+01       6.300E+02       6.700E+01       6.300E+02       6.700E+01       0.              3.900E+01       0.
     9.900E+01       6.300E+02       1.110E+02       6.300E+02       1.110E+02       0.              1.680E+02       0.

UNIT 24     TYPE 24          INTEGRATOR.
     INPUTS  4
     16, 6           1, 3            4, 6            6, 3
     0.              0.              0.              0.

UNIT 25     TYPE 25          PRINTER.
     PARAMETERS  4
     1.200E+01       1.000E+00       9.760E+03       6.000E+00
     INPUTS  8
     1, 1            1, 3            24, 1           24, 2           24, 3           24, 4           1, 4            1, 2
     TCOL            RANK            FRAC            QCOL            QTAN            QMOX            UL              MCOL

UNIT 28     TYPE 28          DAILY SIMUL SUMMARY
     PARAMETERS 19
     2.400E+01       1.000E+00       9.760E+03       0.              0.              -3.000E+00      0.              -1.000E+00      1.500E+02
     1.000E+00       -3.000E+00      2.000E+00       -4.000E+00      0.              -2.000E+00      2.000E+00       -4.000E+00      0.
    -4.000E+00
     INPUTS  4
     1, 3            16, 6           9, 7            4, 7
     LABELS  5
     QCOL            MCOL            EFFD            TAMAV           DELTM

UNIT 29     TYPE 28          WEEKLY SIMUL SUMMARY
     PARAMETERS 26
     1.680E+02       1.000E+00       9.736E+03       0.              0.              -3.000E+00      0.              -1.000E+00      1.500E+02
     1.000E+00       -3.000E+00      2.000E+00       -4.000E+00      0.              0.              3.000E+00       -3.000E+00      -1.300E+01
     2.000E+00       -4.000E+00      0.              -2.000E+00      2.000E+00       -4.000E+00      0.              -4.000E+00
     INPUTS  6
     1, 3            16, 6           4, 6            6, 3            9, 7            4, 5
     LABELS  7
     QCOL            MCOL            EFFW            QLOAD           PERSOL          TAMAV           QTENV

UNIT 30     TYPE 28          MONTHLY SIMUL SUMMARY
     PARAMETERS 38
    -1.000E+00       1.000E+00       9.760E+03       0.              0.              -3.000E+00      0.              -1.000E+00      1.500E+02
     1.000E+00       -3.000E+00      2.000E+00       -4.000E+00      0.              0.              3.000E+00       -3.000E+00      -1.300E+01
     2.000E+00       -4.000E+00      0.              -2.000E+00      2.000E+00       -4.000E+00      -1.300E+01      -4.000E+00      0.
    -4.000E+00       0.              -4.000E+00
     INPUTS  7
     1, 3            16, 6           4, 6            6, 3            9, 7            4, 5            9,10
     LABELS  9
     QCOL            MCOL            EFFM            QLOAD           PERSOL          TAMAV           QTANK           QTENV           TRADHR

END

        TRANSIENT SIMULATION      STARTING AT TIME =  1.000E+00
                                  STOPPING AT TIME =  9.760E+03
                                          TIMESTEP =    1/4
            DIFFERENTIAL EQUATION ERROR TOLERANCE =  1.000E-02
                  ALGEBRAIC CONVERGENCE TOLERANCE =  1.000E-02
```

APPENDIX A2.--Hourly and daily simulation output.

Time	Tool	TTank	UL	MCOL
4922.0000	1.436E+01	9.002E+01	7.584E+00	0.
4923.0000	1.436E+01	8.963E+01	7.584E+00	0.
4924.0000	1.436E+01	8.910E+01	7.554E+00	0.
4925.0000	2.151E+01	8.849E+01	7.703E+00	0.
4926.0000	3.220E+01	8.781E+01	7.947E+00	0.
4927.0000	7.144E+01	8.602E+01	8.648E+00	0.
4928.0000	6.711E+01	8.378E+01	8.228E+00	6.400E+04
4929.0000	6.520E+01	8.269E+01	8.146E+00	6.400E+04
4930.0000	6.761E+01	8.174E+01	8.190E+00	6.400E+04
4931.0000	7.739E+01	8.080E+01	8.490E+00	6.400E+04
4932.0000	7.275E+01	7.995E+01	8.400E+00	6.400E+04
4933.0000	5.415E+01	7.851E+01	7.967E+00	0.
4934.0000	4.224E+01	7.661E+01	7.667E+00	0.
4935.0000	7.046E+01	7.572E+01	8.220E+00	0.
4936.0000	5.737E+01	7.500E+01	7.664E+00	6.400E+04
4937.0000	5.757E+01	7.349E+01	7.518E+00	0.
4938.0000	4.073E+01	7.175E+01	7.151E+00	0.
4939.0000	2.641E+01	7.151E+01	6.738E+00	0.
4940.0000	2.337E+01	7.149E+01	6.666E+00	0.
4941.0000	2.170E+01	7.147E+01	6.656E+00	0.
4942.0000	2.003E+01	7.145E+01	6.650E+00	0.
4943.0000	1.964E+01	7.144E+01	6.630E+00	0.
4944.0000	1.931E+01	7.142E+01	6.601E+00	0.
4945.0000	1.892E+01	7.140E+01	6.579E+00	0.

```
**********************************************************************
*        SIMULATION SUMMARY FOR TIME = 4921.000  TO  4945.000        *
*                                                                    *
*    GCOL          HCOL          EFFD          TAMAV         DELTN   *
* 2.390E+06     8.581E+06     2.785E-01     2.206E+01     2.654E+08   *
*                                                                    *
**********************************************************************
```

APPENDIX A3.--Daily and weekly TRNSYS simulation output.

```
*****************************************************************
*       SIMULATION SUMMARY FOR TIME = 2689.000  TO  2713.000
*
*    QCOL          HCOL          EFFD          TAMAV         QELTN
* 8.194E+06     2.354E+07     3.480E-01     4.323E+00     3.619E+08
*
*****************************************************************

*****************************************************************
*       SIMULATION SUMMARY FOR TIME = 2713.000  TO  2737.000
*
*    QCOL          HCOL          EFFD          TAMAV         QELTN
* 6.339E+06     1.780E+07     3.562E-01     5.817E+00     3.091E+08
*
*****************************************************************

*****************************************************************
*       SIMULATION SUMMARY FOR TIME = 2737.000  TO  2761.000
*
*    QCOL          HCOL          EFFD          TAMAV         QELTN
* 6.170E+06     1.641E+07     3.761E-01     8.180E+00     2.695E+08
*
*****************************************************************

*****************************************************************
*       SIMULATION SUMMARY FOR TIME = 2761.000  TO  2785.000
*
*    QCOL          HCOL          EFFD          TAMAV         QELTN
* 1.157E+07     2.456E+07     4.710E-01     1.232E+01     2.912E+08
*
*****************************************************************

*****************************************************************
*       SIMULATION SUMMARY FOR TIME = 2785.000  TO  2809.000
*
*    QCOL          HCOL          EFFD          TAMAV         QELTN
* 6.937E+06     1.704E+07     4.062E-01     1.979E+01     2.933E+08
*
*****************************************************************

*****************************************************************
*       SIMULATION SUMMARY FOR TIME = 2809.000  TO  2833.000
*
*    QCOL          HCOL          EFFD          TAMAV         QELTN
* 8.394E+05     6.408E+06     1.311E-01     1.975E+01     2.921E+08
*
*****************************************************************

*****************************************************************
*       SIMULATION SUMMARY FOR TIME = 2833.000  TO  2857.000
*
*    QCOL          HCOL          EFFD          TAMAV         QELTN
* 3.975E+06     1.271E+07     3.127E-01     1.861E+01     3.453E+08
*
*****************************************************************

*****************************************************************************************
*       SIMULATION SUMMARY FOR TIME = 2689.000  TO  2857.000
*
*    QCOL          HCOL          EFFD          QLOAD         PERSOL        TAMAV         GTENV
* 4.402E+07     1.185E+08     3.715E-01     3.944E+07     1.004E+00     1.268E+01     7.584E+05
*
*****************************************************************************************
```

APPENDIX A4.--Monthly and yearly TRNSYS simulation output.

SIMULATION SUMMARY FOR TIME = 1.000 TO 744.000 JAN

QCOL	HCOL	EFFM	QLOAD	PERSOL	TAMAV	QTANK	QTENV	TRADMN
1.096E+08	4.540E+08	4.176E-01	6.323E+08	3.580E+00	-2.126E+00	1.718E+08	9.~55E+05	1.~25E+05

SIMULATION SUMMARY FOR TIME = 744.000 TO 1416.000 FEB

QCOL	HCOL	EFFM	QLOAD	PERSOL	TAMAV	QTANK	QTENV	TRADMN
2.729E+08	6.468E+08	4.220E-01	5.526E+08	2.170E+00	-3.242E+00	2.546E+08	1.683E+06	2.146E+05

SIMULATION SUMMARY FOR TIME = 1416.000 TO 2160.000 MAR

QCOL	HCOL	EFFM	QLOAD	PERSOL	TAMAV	QTANK	QTENV	TRADMN
3.164E+08	7.475E+08	4.233E-01	6.050E+08	2.024E+00	1.235E+00	3.009E+08	1.979E+05	3.116E+05

SIMULATION SUMMARY FOR TIME = 2160.000 TO 2880.000 APR

QCOL	HCOL	EFFM	QLOAD	PERSOL	TAMAV	QTANK	QTENV	TRADMN
4.386E+08	9.799E+08	4.476E-01	7.931E+08	1.~63E+00	9.170E+00	3.931E+08	5.226E+05	4.799E+05

SIMULATION SUMMARY FOR TIME = 2880.000 TO 3624.000 MAY

QCOL	HCOL	EFFM	QLOAD	PERSOL	TAMAV	QTANK	QTENV	TRADMN
3.786E+08	8.401E+08	4.507E-01	6.395E+08	1.627E+00	1.240E+01	3.508E+08	2.627E+05	4.~0E+05

SIMULATION SUMMARY FOR TIME = 3624.000 TO 4344.000 JUN

QCOL	HCOL	EFFM	QLOAD	PERSOL	TAMAV	QTANK	QTENV	TRADMN
4.673E+08	1.004E+09	4.654E-01	5.931E+08	1.452E+00	1.823E+01	4.015E+08	3.336E+05	5.906E+05

SIMULATION SUMMARY FOR TIME = 4344.000 TO 5088.000 JUL

QCOL	HCOL	EFFM	QLOAD	PERSOL	TAMAV	QTANK	QTENV	TRADMN
5.435E+08	1.177E+09	4.619E-01	6.435E+08	1.290E+00	2.239E+01	4.~09E+08	4.607E+05	6.737E+05

SIMULATION SUMMARY FOR TIME = 5088.000 TO 5832.000 AUG

QCOL	MCOL	EFFM	QLOAD	PERSOL	TAMAV	QTANK	QTENV	TRADMR
5.130E+08	1.059E+09	4.843E-01	6.496E+08	1.367E+00	2.079E+01	4.682E+08	3.705E+06	5.525E+05

SIMULATION SUMMARY FOR TIME = 5832.000 TO 6552.000 SEP

QCOL	MCOL	EFFM	QLOAD	PERSOL	TAMAV	QTANK	QTENV	TRADMR
4.070E+08	8.792E+08	4.629E-01	5.643E+08	1.491E+00	1.452E+01	3.754E+08	3.331E+06	3.962E+05

SIMULATION SUMMARY FOR TIME = 6552.000 TO 7296.000 OCT

QCOL	MCOL	EFFM	QLOAD	PERSOL	TAMAV	QTANK	QTENV	TRADMR
3.764E+08	8.093E+08	4.651E-01	6.593E+08	1.585E+00	9.334E+00	3.541E+08	2.579E+06	2.944E+05

SIMULATION SUMMARY FOR TIME = 7296.000 TO 8016.000 NOV

QCOL	MCOL	EFFM	QLOAD	PERSOL	TAMAV	QTANK	QTENV	TRADMR
1.940E+08	4.350E+08	4.552E-01	6.048E+08	3.163E+00	4.294E+00	1.912E+08	1.116E+06	1.393E+05

SIMULATION SUMMARY FOR TIME = 8016.000 TO 8760.000 DEC

QCOL	MCOL	EFFM	QLOAD	PERSOL	TAMAV	QTANK	QTENV	TRADMR
1.711E+08	3.996E+08	4.280E-01	5.772E+08	3.390E+00	-1.059E+00	1.688E+08	6.052E+05	1.201E+05

FINAL SIMULATION SUMMARY, TIME = 8760.000

QCOL	MCOL	EFFM	QLOAD	PERSOL	TAMAV	QTANK	QTENV	TRADMR
4.272E+09	9.431E+09	4.530E-01	7.270E+09	1.551E+00	9.596E+00	3.923E+09	2.954E+07	4.597E+06

APPENDIX B1.--Collector inlet and outlet temperatures (°C) during a typical day in July for various food processing plants.

	Case A		Case B		Case C		Case D		Case E	
Hour	Ti	To	Ti	To	Ti	To	Ti	To	Ti	To
7- 8	31.5	33.3	33.0	34.7	34.6	36.3	39.2	40.8	34.8	36.5
8- 9	38.3	42.0	39.6	43.2	40.2	43.8	44.1	47.5	39.8	43.4
9-10	44.2	49.7	45.6	51.1	46.0	54.5	49.2	54.6	46.7	52.2
10-11	50.4	57.5	52.1	59.1	51.9	59.0	51.6	58.6	53.9	60.8
11-12	58.8	66.9	58.7	66.7	57.9	65.9	59.2	67.2	60.4	68.4
12-13	65.9	74.1	63.7	71.9	61.9	70.2	65.2	73.4	65.6	73.7
13-14	70.3	77.8	66.4	74.0	64.9	72.6	62.6	70.4	65.6	73.3
14-15	73.1	79.3	67.2	73.6	64.9	71.4	57.4	64.2	65.6	72.1
15-16	73.9	78.6	67.8	72.8	64.9	69.9	59.7	64.9	66.4	71.4
16-17	72.4	75.3	67.8	71.0	64.9	68.1	61.0	64.4	66.4	69.6
17-18	67.5	68.8	66.3	67.7	64.9	66.3	61.0	62.6	63.3	64.7

APPENDIX B2.--Collector inlet and outlet temperatures (°C) during a typical day in July for various food processing plants.

	Case A		Case B		Case C		Case D		Case E	
Hour	Ti	To	Ti	To	Ti	To	Ti	To	Ti	To
8- 9	27.0	31.7	28.2	32.8	28.7	33.3	30.6	35.2	27.8	32.4
9-10	25.2	28.2	26.6	29.5	26.7	29.6	28.6	31.3	26.9	29.4
10-11	30.4	34.9	31.8	36.2	31.7	36.1	31.7	36.2	32.3	36.7
11-12	39.0	45.3	39.2	45.5	38.9	45.1	39.4	46.0	39.5	45.7
12-13	42.4	47.9	41.4	47.0	41.0	46.6	42.7	48.2	41.8	47.3
13-14	50.4	57.2	48.5	55.4	47.3	54.2	46.0	53.0	47.9	54.8
14-16	49.4	53.7	47.5	51.9	46.4	50.8	40.0	45.1	46.9	51.3
16-17	47.7	49.0	44.5	45.0	42.7	44.2	37.6	39.3	43.1	44.6

APPENDIX B3.--Monthly efficiency for various size solar collectors for food processing plants exhibiting energy use profiles as in Case B.

Month	Efficiency, Percent Collector Size, m^2				
	150	500	1000	3000	6000
January	41.9	42.2	42.2	40.2	39.2
February	42.7	43.0	43.0	40.9	39.7
March	42.5	43.0	42.9	40.8	39.7
April	45.3	45.8	45.8	43.6	42.4
May	45.3	45.8	45.8	43.6	42.4
June	47.0	47.5	47.3	45.2	44.0
July	46.3	46.9	46.9	44.6	43.3
August	48.7	49.1	48.9	46.7	45.4
September	46.7	47.2	47.2	45.0	43.7
October	46.9	47.3	47.3	45.1	43.9
November	46.1	46.3	46.3	44.4	43.0
December	42.6	42.6	43.0	41.2	40.1

APPENDIX B4.--Monthly efficiency for various size solar collectors for food processing plants exhibiting energy use profile as in Case C.

Month	Efficiency, Percent Collector Size, m^2				
	150	500	1000	3000	6000
January	41.9	42.2	42.2	39.9	38.8
February	42.6	42.9	42.9	40.3	39.2
March	42.6	43.0	43.0	40.5	39.3
April	45.0	45.5	45.5	42.8	41.5
May	45.3	45.7	45.7	43.1	41.9
June	46.8	47.2	47.2	44.5	43.2
July	46.5	46.9	46.8	44.0	42.6
August	48.7	49.2	49.2	46.3	44.9
September	46.4	47.0	46.9	44.3	43.0
October	46.6	47.2	46.9	44.5	43.4
November	45.8	46.0	46.0	43.7	42.4
December	43.0	43.3	43.3	41.1	40.0

APPENDIX B5.--Monthly efficiency for various size solar collectors for food processing plants exhibiting energy use profile as in Case D.

Month	Efficiency, Percent Collector Size, m^2				
	150	500	1000	3000	6000
January	42.0	42.5	42.5	40.2	39.1
February	42.7	43.2	43.1	40.6	39.4
March	42.5	43.1	43.1	40.5	39.2
April	45.1	45.6	45.6	42.9	41.5
May	45.5	46.0	46.0	43.4	42.1
June	46.8	47.4	47.4	44.7	43.3
July	46.3	47.1	47.0	44.3	43.0
August	48.5	49.2	49.2	46.3	44.9
September	46.5	47.2	47.1	44.6	43.0
October	47.0	47.5	47.5	44.8	43.5
November	46.1	46.6	46.6	44.1	42.8
December	42.8	43.3	43.3	41.1	40.0

APPENDIX B6.--Monthly efficiency for various size solar collectors for food processing plants exhibiting energy use profile as in Case E.

Month	Efficiency, Percent Collector Size, m^2				
	150	500	1000	3000	6000
January	42.0	42.2	42.1	40.3	39.2
February	42.6	43.1	43.0	40.8	39.6
March	42.5	43.0	42.9	40.9	39.7
April	45.3	45.6	45.6	43.4	42.2
May	45.4	45.8	45.7	43.6	42.4
June	46.9	47.4	47.4	45.2	44.1
July	46.3	47.0	46.9	44.6	43.4
August	48.6	49.1	49.1	48.8	45.5
September	46.6	47.2	47.1	45.0	43.6
October	46.8	47.3	47.2	45.0	43.8
November	45.8	46.2	46.2	44.2	43.0
December	42.7	43.1	43.0	41.3	40.2

APPENDIX B7.--Monthly percent by solar for various size solar collectors for food processing plants exhibiting energy use profile as in Case B.

Month	Efficiency, Percent Collector Size, m^2				
	150	500	1000	3000	6000
January	28.0	27.3	27.3	27.6	26.9
February	47.5	46.4	46.5	46.1	45.5
March	50.7	49.5	49.6	50.1	48.8
April	68.9	67.8	67.8	68.0	66.7
May	56.0	54.9	54.9	55.6	54.7
June	70.8	69.3	69.4	69.9	68.6
July	78.9	77.7	77.8	78.5	77.5
August	73.6	72.2	72.2	73.2	71.9
September	68.4	67.3	67.3	67.7	66.6
October	56.8	55.5	55.4	55.6	54.5
November	32.6	31.8	31.8	32.1	31.4
December	28.9	28.1	28.1	28.4	27.8

APPENDIX B8.--Monthly percent by solar for various size solar collectors for food processing plants exhibiting energy use profile as in Case C.

	Efficiency, Percent Collector Size, m^2				
Month	150	500	1000	3000	6000
January	28.3	27.4	27.5	26.7	26.2
February	47.6	46.5	46.6	45.1	44.1
March	50.4	49.2	49.3	47.9	46.9
April	70.2	68.3	68.9	66.9	65.4
May	56.2	55.2	55.4	54.0	53.2
June	72.0	70.3	70.4	68.7	67.3
July	80.6	79.6	79.7	78.2	76.9
August	74.3	72.8	72.9	71.2	70.0
September	68.8	67.4	67.5	65.9	64.8
October	57.0	55.7	55.8	54.4	53.2
November	32.6	31.7	31.8	30.9	30.2
December	28.5	27.7	27.7	27.0	26.4

APPENDIX B9.--Monthly percent by solar for various size solar collectors for food processing plants exhibiting energy use profile as in Case D.

Month	Efficiency, Percent Collector Size, m^2				
	150	500	1000	3000	6000
January	28.9	28.1	28.1	28.3	31.1
February	49.2	47.8	47.9	48.0	48.5
March	51.8	50.4	50.6	51.0	52.7
April	71.7	70.2	70.6	70.3	69.5
May	57.7	56.4	56.6	56.9	57.0
June	73.0	71.5	71.6	71.3	70.1
July	81.3	80.0	80.1	80.2	79.1
August	75.5	74.0	74.2	74.1	73.0
September	70.1	68.7	68.8	69.2	68.2
October	58.6	57.3	57.4	57.3	56.8
November	33.4	32.3	32.6	32.9	35.0
December	29.5	28.7	28.7	29.0	31.6

APPENDIX B10.--Monthly percent by solar for various size solar collectors for food processing plants exhibiting energy use profile as in Case E.

Month	Efficiency, Percent Collector Size, m^2				
	150	500	1000	3000	6000
January	28.3	27.4	27.4	26.7	26.1
February	47.9	46.6	46.9	45.3	44.3
March	50.8	49.6	50.0	48.3	47.3
April	70.6	69.1	69.1	67.7	66.1
May	56.9	55.8	55.9	54.8	53.9
June	72.8	71.2	71.3	69.7	68.3
July	81.1	80.0	80.3	78.8	77.6
August	75.2	73.7	73.7	72.3	71.1
September	69.4	68.1	68.3	66.6	65.5
October	57.5	56.1	56.0	54.7	53.5
November	32.8	31.9	32.0	31.0	30.4
December	28.7	27.9	28.1	27.2	26.5